Universidade de Aveiro Departamento de Química
2019

Belinda Isabel Gomes Soares

Desenvolvimento de uma tecnologia inovadora para a deslenhificação da madeira usando solventes eutécticos

Development of an innovative technology for wood delignification with eutectic solvents

Universidade de Aveiro Departamento de Química
2019

Belinda Isabel Gomes Soares

Desenvolvimento de uma tecnologia inovadora para a deslenhificação da madeira usando solventes eutécticos

Development of an innovative technology for wood delignification with eutectic solvents

Tese apresentada à Universidade de Aveiro para cumprimento dos requisitos necessários à obtenção do grau de Doutor em Engenharia Química, realizada sob a orientação científica do Doutor João Manuel da Costa e Araújo Pereira Coutinho, Pró-reitor e Professor Catedrático do Departamento de Química da Universidade de Aveiro, da Doutora Carmen Sofia da Rocha Freire Barros, Investigador Principal do CICECO da Universidade de Aveiro e da Doutora Paula Cristina de Oliveira Rodrigues Pinto, Coordenadora de I&D tecnológico do RAIZ – Instituto de Investigação da Floresta e Papel.

Apoio financeiro do POCI no âmbito do projecto MultiBiorefinery (POCI-01-0145-FEDER-016403) e no âmbito do projecto CICECO – Aveiro Institue of Materials, FCT (UID/CTM/5001/2019), financiado por fundos nacionais através da FCT/MCTES.

O doutorando agradece o apoio financeiro da FCT, da The Navigator Co. e do FSE no âmbito do III Quadro Comunitário de Apoio (SFRH/BDE/103257/2014).

Aos meus pais e irmãos
Ao **RUI** e a **LUANA**

o júri

presidente

Prof.ª Dr.ª Anabela Botelho Veloso
Professora Catedrática do Departamento de Economia, Gestão, Engenharia Industrial e Turismo da Universidade de Aveiro,

Prof. Dr. Boelo Schuur
Professor Associado da Universidade de Twente, Holanda.

Prof.ª Dr.ª Isabel Maria Delgado Jana Marrucho Ferreira
Professora Associada com Agregação do Departamento de Engenharia Química do Instituto Superior Técnico de Lisboa.

Doutor Nuno Oliveira
Direcção Técnica de Produtos, The Navigator Company.

Doutor André Miguel da Costa Lopes
Estagiário de Pós-Doutoramento, Universidade de Aveiro.

Prof. Dr. João Manuel da Costa e Araújo Pereira Coutinho
Professor Catedrático do Departamento de Química da Universidade de Aveiro.

agradecimentos

Gostaría de agradecer ao professor João Coutinho, pela oportunidade que me deu em fazer parte deste projecto. Agradecer a sua orientação científica, o seu rigor na análise e discussão dos resultados, apoio e constantes incentivos, e por me ter permitido fazer parte de um grupo de trabalho excepcional. Obrigado pelos conhecimentos transmitidos e por ter contribuido para o meu crescimento profissional.

Aos meus coorientadores, Dra. Carmen Freire e Dra. Paula Pinto. Obrigado pela vossa orientação e disponibilidade na correção desta tese. O meu agradecimento especial ao Eng. José Luis Amaral do RAIZ (descanse em paz) pelo incentivo e carinho com que me orientou por parte da empresa até 2017. Recordarei com carinho todo o seu apoio e dedicação para levar até bom porto este trabalho.

Um agradecimento especial ao professor Armando Silvestre, que juntamente com o professor João Coutinho formaram uma dupla de orientação científica que se revelou muito importante na definição, contrução e finalização de todo o trabalho desenvolvido e apresentado nesta tese. Obrigada pelo incentivo e apoio contante, e por ter acreditado nas minhas capacidades para a realização dos trabalhos propostos.

Não posso deixar de agradecer ao CICECO pelos equipamentos e espaço de trabalho. Em particular, à Engenheira Ana Caço pelo espaço cedido no laboratório das aulas; ao doutor Hilário Tavares, à doutora Paula Santos e à técnica Maria Manuela Marques pelo apoio na parte técnica das caracterizações às lenhinas; ao professor Dmitry Evtyguin pela generosa partilha de conhecimento. Ao RAIZ pelas matérias-primas e pelas análises realizadas as fibras. A todos o meu muito obrigado!.

À toda a familia PATH, o meu muito OBRIGADO!, por me terem acolhido com muito carinho nesta familia científica, por toda a partilha de conhecimento, conversas, rizadas e convívios. Dentro desta famílía existem para mim estrelinhas muito especiais que não devem ser ignoradas, Tânia Sintra, Pedro Carvalho, Helena Passos, Margarida Martins, Liliana Silva, Catarina Neves, Mónia Martins, João Santos, Carlos Mendonça, Vanessa Vieira e Filipa Vicente, que de alguma forma tornaram este caminho muito mais agradável e feliz.

As minhas meninas, Sandra Magina e Marina Matos OBRIGADO por estes dez anos de amizade e companheirismo, por serem o meu porto de abrigo nos bons e maus momentos, por rirem e chorarem comigo, por TUDO (vocês sabem!). Acrescento, Ana Caço e Inês Mendes, obrigada pela amizade e ajuda em momentos importantes deste trabalho. À Felisbela e Luis por todo o carinho e apoio transmitido.

Por fim, à minha família!, o meu pilar. Mãe e pai obrigada pelo amor, por me terem ensinado a lutar pelos meus sonhos e fazerem de mim a pessoa feliz que sou. Aos meus irmãos, Vita e Joca pelo carinho, amizade e apoio incondicional. Ao RUI agradeço por todo os dias de felicidade, apoio incondicional e amizade. Por útimo agradeço ao meu tesouro, LUANA, por me ensinar todos os dias o que é ser feliz com pouco e a amar sem limites.

palavras-chave

Solventes eutécticos, solubilidade, hidrotropia, co-solvência, compostos modelo de monómeros de lenhina, lenhinas técnicas, deslenhificação de madeira, lenhina, fibras de celulose, madeira de *Eucalyptus globulus*, biorefineria.

resumo

Este trabalho teve como objectivo estudar o uso de solventes eutécticos (SEs) no fraccionamento de madeira, com vista à sua aplicação em processos de produção de pasta, no âmbito de uma biorrefineria. Nesse sentido, foi desenvolvido um estudo fundamental que permitisse compreender a solubilidade de lenhinas técnicas (kraft e organosolv) e dos seus monómeros (siringaldeído e ácidos siríngico, vanílico e ferúlico) nos SEs puros e respetivas soluções aquosas. Mostrou-se que, soluções aquosas de ácido propiónico:ureia (2:1) com concentrações de 50 ou 75 % m/m a 353.15 K aumentam a solubilidade da lenhina em duas ordens de grandeza relativamente à sua solubilidade em água pura ou solventes orgânicos convencionais usados normalmente para a solubilização de lenhina [aumento de solubilidade de (228.3 ± 8.2)- e (474.7 ± 2.7)-vezes para as lenhinas kraft e organosolv, respectivamente]. Além disso, foi possível obter uma solubilização máxima dos monómeros de lenhina usando uma solução aquosa de etileno glicol:cloreto de tetrabutilfosfónio (2:1) com concentrações de 50 ou 75 % m/m a 323.15 K [(34.9 ± 6.7)-, (116.6 ± 1.6)-, (58.6 ± 0.4)- e (202.5 ± 16.9)-vezes, respectivamente]. É de salientar o papel fundamental da água que permite o efeito hidrotrópico na solubilização da lenhina e seus monómeros nas soluções aquosas dos SEs estudados. De seguida, os melhores SEs foram usados no processo de deslenhificação de madeira de *Eucalyptus globulus* como prova de conceito. O efeito da adição de catalizadores ácidos foi igualmente estudado. Os resultados obtidos confirmaram que a adição de um catalizador ácido às soluções aquosas de SEs promovem a extração de lenhina. Neste estudo, dois sistemas aquosos de SEs (50 % m/m) apresentaram resultados excelentes na deslenhificação da madeira de *E. globulus*: (i) ácido propiónico:ureia (2:1) na presença de 25 % m/m de catalisador ácido *p*-toluenosulfónico (8 h, 363.15 K e pressão atmosférica). Este sistema resultou num rendimento de fração sólida de 59.50 ± 0.51 % m/m, contendo 3.86 ± 0.10 % m/m de lenhina Klason residual. A análise da pasta resultante permitiu concluir que as fibras de celulose foram preservadas quando comparadas com a pasta kraft de *E. globulus*; e (ii) mixtura ternária (*p*-toluensulfonato de sódio: ácido *p*-toluenosulfónico:cloreto de colina) numa razão molar óptima de (0.393:0.376:0.232) nas condições óptimas de operação de 3 h, 363.15 K e pressão atmosférica. Este sistema resultou num rendimento de fração sólida de 46.60 ± 2.70 % m/m, contendo 2.74 ± 0.08 % m/m de lenhina Klason residual. As análises químicas estruturais realizadas às lenhinas isoladas revelaram menos modificações induzidas pelos sistemas propostos, quando comparados com a lenhina kraft de *E. globulus* ou outros sistemas SEs reportados na literatura. Por fim, estudos preliminares de aumento de escala usando os SEs propostos revelaram-se promissores.

keywords

Eutectic solvents, solubility, hydrotropy, cosolvency, lignin monomer compounds, technical lignins, wood delignification, lignin, cellulose fibers, *Eucalyptus globulus* wood, biorefinery.

abstract

The goal of this work was to study the use of Eutectic Solvents (ESs) for wood fractionation aiming at their application on pulping processes, in the biorefinery framework. To achieve this purpose, fundamental studies were performed to better understand the solubility of lignin monomer model compounds (syringaldehyde and syringic, vanillic and ferulic acids) and technical lignins (kraft and organosolv) in ESs and their aqueous solutions. Particularly, aqueous solutions of propionic acid:urea (2:1) at 50 or 75 wt % of concentration and 353.15 K improved lignin solubility by two orders of magnitude in comparison to water and conventional lignin solvents [solubility enhancement of (228.3 ± 8.2)- and (474.7 ± 2.7)-fold for kraft and organosolv lignin, respectively]. Furthermore, maximum solubilization of lignin monomer model compounds was achieved using ethylene glycol:tetrabutylphosphonium chloride (2:1) aqueous solutions at 50 or 75 wt % of concentration and 323.15 K [(34.9 ± 6.7)-, (116.6 ± 1.6)-, (58.6 ± 0.4)- and (202.5 ± 16.9)-fold, respectively]. It should be highlighted the fundamental role of water, which allows a hydrotropic effect on lignin (and their monomers) solubility in these ESs aqueous solutions. The best ESs to enhance the solubility of lignin in water was used to develop a new wood delignification process. Therefore, delignification of *Eucalyptus globulus* wood catalyzed by mineral or organic acids in ESs aqueous solutions was studied. The results obtained confirmed that the wood delignification using ESs aqueous solutions requires the addition of acid catalyst in order to enhance lignin removal. Two different ESs aqueous systems were identified as the best to delignify *E. globulus* wood under mild conditions: (i) the 50 wt % aqueous solution of propionic acid:urea (2:1) in the presence of 25 wt % of *p*-toluenesulfonic acid as catalyst (8 h, 363.15 K and atmospheric pressure). This system led to the production of a solid fraction yield of 59.50 ± 0.51 wt %, containing a residual Klason lignin of 3.86 ± 0.10 wt % with preserved cellulose fibers, when compared to conventional *E. globulus* kraft pulp; and (ii) the 50 wt % aqueous solution of ternary-ESs mixture (sodium *p*-toluenesulfonate:*p*-toluenesulfonic acid:choline chloride) at optimal molar ratio of (0.393:0.376:0.232) that allowed producing 46.60 ± 2.70 wt % of solid fraction yield, containing a residual Klason lignin of 2.74 ± 0.08 wt % under milder conditions (3 h, 363.15 K and atmospheric pressure). Moreover, the chemical structural analysis of both isolated lignins revealed that fewer transformations are induced by these systems, when compared to *E. globulus* kraft, and other ESs reported in literature. Finally, promising preliminary results show the feasibility for scaling the ES wood delignification process using both ESs.

CONTENTS

NOMENCLATURE

Abbreviations

C_6	Aromatic ring
C_9	Phenylpropane unit
^{13}C	Carbon 13
$CDCl_3$	Deuterated chloroform
DMSO-d_6	Deuterated dimethyl sulfoxide
^{1}H	Hydrogen 1
ANOVA	Analysis of variance
BBD	Box-Behnken design
CO_2	Carbon dioxide
CP	Central point
CEPI	Confederation of European Paper Industries
DES	Deep eutectic solvents
DC	Degree of condensation
DLS	Dynamic light scattering
ES	Eutectic solvent
FTIR	Fourier-transform infrared
GA	Gravimetric analysis
G	Guaiacyl propane unit of lignin
H	*p*-Hydroxyphenyl propane unit of lignin
HBD	Hydrogen bond donor
HBA	Hydrogen bond acceptor
LMM	Lignin monomer model compound
LCC	Lignin-carbohydrate complex
MHC	Minimum hydrotrope concentration
ND	Not detected
NMR	Nuclear magnetic resonance
OP	Optimal point
ppu	Phenylpropane unit
S	Syringyl propane unit of lignin

Eutectic solvent components

Hydrogen bond donors

AA	Acetic acid
BA	Butyric acid
EG	Ethylene glycol

FA	Formic acid
Fru	Fructose
G	Glycerol
Glu	Glucose
GlyA	Glycolic acid
LA	Lactic acid
Lev	Levulinic acid
MA	Malic acid
OA	Oxalic acid
OAA	Oxalic acid anhydrous
PA	Propionic acid
PTSA	*p*-Toluenesulfonic acid
U	Urea
Xyl	Xylose

Hydrogen bond acceptors

Al	Alanine
Bet	Betaine
[Ch]Cl	Choline Chloride
Hist	Histidine
Glyc	Glycine
Pro	Proline
NaPTS	Sodium *p*-toluenesulfonate
$[N_{1111}]Cl$	Tetramethylammonium Chloride
$[N_{2222}]Cl$	Tetraethylammonium Chloride
$[N_{3333}]Cl$	Tetrapropylammonium Chloride
$[N_{4444}]Cl$	Tetrabutylammonium Chloride
$[P_{4444}]Cl$	Tetrabutylphosphonium Chloride
U	Urea

Symbols

$\Delta_{Sol}G_m$	Molar Gibbs energy of solution
$\Delta_{Sol}H_m$	Molar Enthalpy of solution
$\Delta_{Sol}S_m$	Molar Entropy of solution
ζ_H	Relative contributions to the Gibbs energy by enthalpy

ζ_{TS}	Relative contributions to the Gibbs energy by entropy
σ	Standard deviation
S	Solubility of compounds in eutectic solvents
S_0	Solubility of compounds in water

Subscripts

Sol	Solution
m	Molar
x_{LMMC}	Molar fraction solubilities of lignin monomer model compounds

SCOPE AND OBJECTIVES

The concerns about global climate change have been driving academic researchers, companies and governments to establish long-term policies in order to reduce greenhouse gas emissions to mitigate global warming.[1] In the framework of the fight against climate change, the European Commission presented a Roadmap for possible actions to reduce 80 % of CO_2 emissions (compared to 1990) by 2050, helping the European Union become a competitive low-carbon economy.[2] In this context, the European pulp and paper industry faces a great challenge due to their energy-intensive wood delignification processes. In 2007, 5 % of total global industrial energy consumption and 2 % of global direct CO_2 emissions were attributed to this sector.[3]

Kraft and sulfite chemical pulping are currently the most used industrial processes for pulp production.[4] The aim of the chemical pulping processes is to delignify the wood matrix by chemically degrading and/or sulfonating the lignin into water-soluble fragments to liberate the cellulose fibers.[5] However, to achieve a successful wood delignification, strong alkaline or acidic media at high temperatures and pressures are required.[5] Although the kraft process led to the production of cellulose fibers with excellent properties, its main disadvantages comprises the use of strong alkaline conditions resulting in metal corrosion problems, malodorous gases emissions and high consumption of bleaching chemicals. The production of lower strength pulp is the main disadvantage of the sulfite process.[6] Furthermore, several modifications on the chemical structure of isolated lignins are induced by these delignification processes, particularly the incorporation of sulfur, which might preclude their subsequent valorization in biorefinery processes.[5,6]

In 2011, the Confederation of European Paper Industries (CEPI) presented the Forest Fiber Industry 2050 Roadmap for a low-carbon economy. It evaluated alternatives to achieve an 80 % reduction of CO_2 emissions and at the same time create 50 % more value for the sector and concluded that breakthrough technologies would be needed to achieve these targets.[7] In 2012, Deep Eutectic Solvents (DES) were elected by CEPI as one of the most revolutionary and promising mild pulping technologies, to produce cellulose fibers at lower temperatures and pressures, while simultaneously produce high-quality lignin and hemicelluloses fractions for high-volume applications.[8] It is expected that DES delignification technology would help reducing the process energy intensity by at least 40

% and the investment cost by 50 % when compared to current pulping processes, due to pressure-free layout and simplified chemical recovery.[9]

The high importance of the pulp and paper sector in our economy, associated with the unexplored potential of DES in pulp production, motivated the realization of this work, focused on the development of a new wood delignification technology based on DES that allowed the production of cellulose fibers and lignin, at mild conditions.

In order to achieve this goal, the following objectives were drawn:

- Screening and design DES for the selective extraction of lignin from *Eucalyptus globulus* wood.
- Optimization of the DES delignification process.
- Development of methodologies for the isolation of lignin from liquid fraction as well as for DES recovery.

The present thesis is thus organized in four sections. The first section presents a brief state-of-the-art of: (i) wood and their biopolymers; (ii) a description of conventional and alternative wood delignification processes, as well as the general aspect of delignification are addressed; (iii) the definition and properties of 'deep' eutectic solvents, and the topics: eutectic solvents in wood biopolymers solubilization, and eutectic solvents in wood delignification processes, are also discussed.

The experimental work is presented in the second section, where the preparation of eutectic solvents, lignin solubility assays, wood delignification process, optimization methodologies and analytical techniques applied to characterize the final products, are described.

The obtained results and their discussion are presented in the third section. This section was organized in two parts, part A – the fundamental study, focused on to study of the solubility of technical lignins (and their monomers) in several eutectic solvents (Chapter I and II) and the part B – the proof of concept, where the best eutectic solvents to solubilize lignin were selected to perform the wood delignification process (Chapter III and Chapter IV). Finally, the fourth section comprises the most relevant conclusions obtained in this thesis, as well as suggestions for future work.

STATE-OF-THE-ART

The Portuguese pulp and paper industry is one of the most important industrial sector in our economy. Portugal is the 3rd largest European producer of pulp, and of chemical pulps.[10] The vast use of *Eucalyptus globulus* wood for pulp production derives from its peculiar characteristics which results in a great performance in cooking and bleaching processes, as well as in pulps with excellent papermaking properties, which are an international benchmark in this sector.[11–13]

1. Wood and their principal biopolymers

Wood quality is critically important to the pulp and paper industry, because many aspects such as pulp yield, consumption of cooking liquor, and potential for bleaching, are dependent on the chemical composition of wood.[11,14] This is determined by the relative proportions of their principal biopolymers: cellulose, hemicelluloses and lignin, in the wood cell wall (Figure 1). According to literature,[11] the pulp yield is primarily influenced by the lignin and cellulose contents on wood while hemicelluloses determine the technical properties of resulting pulps (e.g. high hemicelluloses content improves tensile strength but reduces pulp opacity).

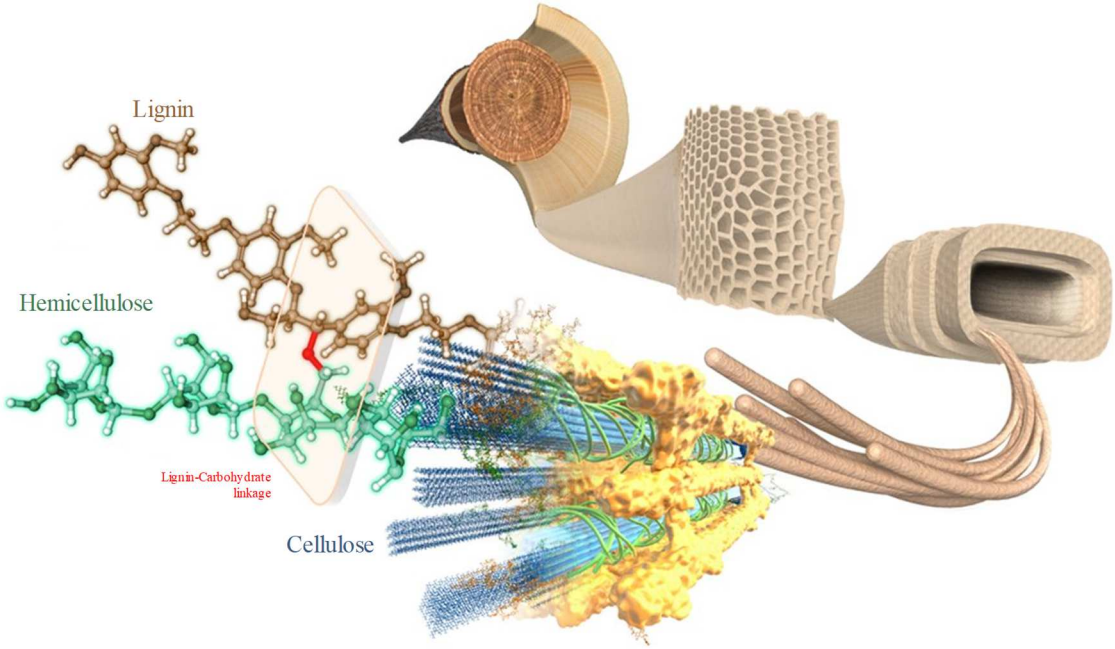

Figure 1. Illustration of the wood cell walls and their ultrastructure. Reproduced and adapted from Nishimura *et al.*[15], (https://rdcu.be/bKQyI, http://creativecommons.org/licenses/by/4.0/).

Therefore, the information about the chemical composition and structure of wood components is essential for the optimization of the technological processes and pulp and paper quality control.[13] The typical chemical composition of different wood species is summarized in Table 1**.**

Table 1. Chemical composition of softwoods and hardwoods.[11,13,16–18]

Components / wt %	**Softwood**	**Hardwood**
Cellulose	35 – 50	40 – 55
Hemicelluloses	25 – 35	20 – 40
Lignin	25 – 35	18 – 28
Extractives	3 – 8	1 – 5
Ash	0.2 – 0.5	0.2 – 0.8

1.1 Cellulose

Cellulose is the main constituent of wood (Table 1) independently of the wood species and it is located predominantly in the secondary cell wall.[6] Regarding its molecular structure, cellulose is a homopolysaccharide composed of β-$_D$-glucopyranose units which are linked by (1→ 4)-glycosidic bonds in a $^4C_1$ conformation (Figure 2).[6] The repeating unit in cellulose consists in two consecutive glucopyranose units, known as cellobiose unit, and every glucose unit is hence turned around the C1-C4 axis by 180° with respect to its neighbors, giving to cellulose a 2-fold screw axis.[6] The molecular weight of cellulose varies widely depending on the origin and on the isolation and purification procedures.[5,19,20] As cellulose is a linear polymer, the size of the molecule chain is usually specified as degree of polymerization.[20] The degree of polymerization, which is the number of glucose units that make up the polymer, is above 10000 in native cellulose wood but less than 1000 in highly bleached kraft pulps and around 600 – 1200 for dissolving pulp.[17]

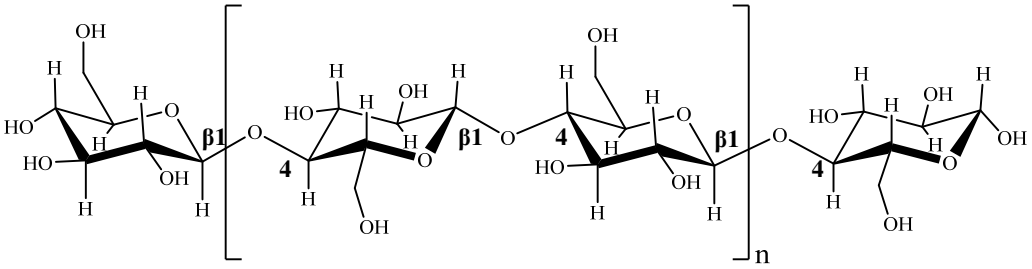

Figure 2. Molecular structure of cellulose. Reproduced from Sjöström *et al.*[6]

The supramolecular structure of cellulose is responsible for many of the cellulose chemical and physical properties.[19,21] According to literature,[6,20] the hydroxyl groups of cellulose macromolecules are able to form two types of hydrogen bonds depending on their site at the glucose units. There are hydrogen bonds between hydroxyl groups of adjacent glucose units in the same cellulose molecule (intramolecular linkages). These linkages give a certain stiffness to the single chains. There are also hydrogen bonds between hydroxyl groups of adjacent cellulose molecules (intermolecular linkages). These linkages are responsible for the formation of supramolecular structures.

According to several authors,[6,19] bundles of cellulose molecules are aggregated together in the form of microfibrils, in which highly ordered (crystalline) regions, difficult to penetrate by solvents or reagents, alternate with less ordered (amorphous) regions, readily penetrated and therefore more susceptible to hydrolysis reactions.[5] Microfibrils build up fibrils and finally cellulose fibers. The hierarchical morphology of natural cellulose fibers is illustrated in Figure 3. As a consequence of its fibrous structure and strong hydrogen bonds, cellulose has a high tensile strength and it is insoluble in most solvents.[6]

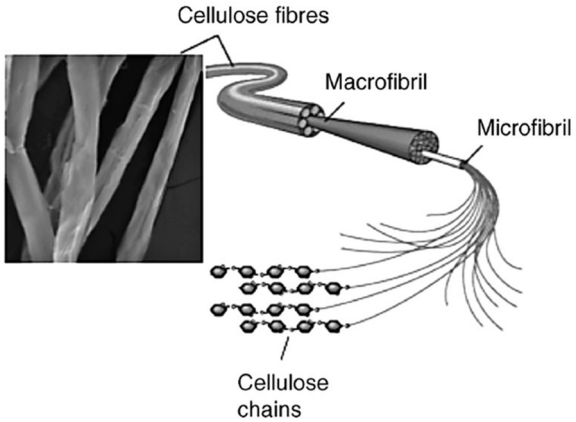

Figure 3. Hierarchical morphology of natural cellulose fibers. Reproduced from Belgacem *et al.*[19]

1.2 Hemicelluloses

Hemicelluloses are the second most abundant source of polysaccharides on wood.[22] Concerning their molecular structure, hemicelluloses are heteropolysaccharides composed of various monosaccharides, such as pentoses (β-D-xylose, α-L-arabinose), hexoses (β-D-mannose, β-D-glucose, α-D-galactose), as well as uronic acids (D-glucuronic acid, 4-*O*-methyl-D-glucuronic acid and D-galacturonic acid).[6,22] Other sugars such as α-L-rhamnose and α-L-fucose may also be present in small amounts and the hydroxyl groups of sugar can be partially substituted with acetyl groups.[23] The composition and structure of the hemicelluloses of softwoods differ in a characteristic way from those of hardwoods (Table 1).[6]

Softwood hemicelluloses. The principal hemicelluloses present in softwoods comprise galactoglucomannans, arabinoglucuronoxylans and arabinogalactans.[6]

Galactoglucomannans (O-acetyl-galactoglucomannans) are the main hemicelluloses in softwoods, accounting for about 10 – 25 % of their dry mass, with a degree of polymerization within the range of 40 – 100.[23] Their backbone is a linear or possibly slightly branched chain built up of (1→ 4)-linked β-D-glucopyranose and β-D-mannopyranose units. The α-D-galactopyranose residues are linked as a single-unit side chains to the backbone by (1→ 6)-bonds (Figure 4). An important structural feature is that the hydroxyl groups at C-2 and C-3 positions in the main chain units are partially substituted by *O*-acetyl groups, on the average one group per 3 – 4 hexose units. According to literature,[6] galactoglucomannans are easily depolymerized by acids, in particular the bond between galactose and the main chain. The acetyl groups are much more easily cleaved under alkali than acid conditions.

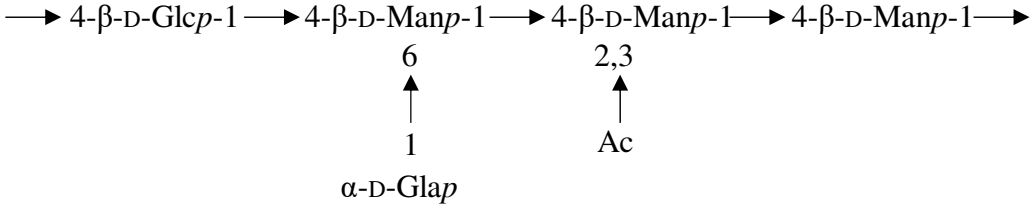

Figure 4. Abbreviated formula of galactoglucomannans. Sugar units: glucopyranose (Glc*p*); mannopyranose (Man*p*); galactopyranose (Gal*p*); *O*-acetyl group (Ac). Reproduced from Sjöström *et al*.[6]

Arabinoglucuronoxylans (arabino-4-*O*-methylglucuronoxylan) are composed of a backbone containing (1→ 4)-linked β-D-xylopyranose units which are partially substituted at C-2 by 4-*O*-methyl-D-glucuronic acid groups, on the average of two residues per ten xylose units. In addition, these hemicelluloses contain α-L-arabinofuranose units, on the average of 1.3 residues per ten xylose units (Figure 5). Because of their furanosidic structure, the arabinose side chains are easily hydrolyzed by acids. Both the arabinose and uronic acid substituents stabilize the xylan chain against alkali-catalyzed degradation.[6] The arabinoglucuronoxylan have a degree of polymerization within the range of 50 – 185.[20,23]

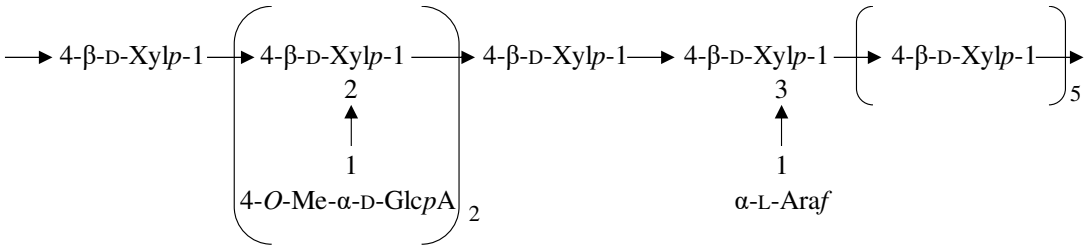

Figure 5. Abbreviated formula of arabinoglucuronoxylans. Sugar units: xylopyranose (Xyl*p*); 4-*O*-methyl-α-D-glucopyranosyluronic acid (Glc*p*A); arabinofuranose (Ara*f*). Reproduced from Sjöström *et al*.[6]

Arabinogalactans backbone is built up by (1→ 3)-linked β-D-galactopyranose units. Almost every units carries a branch attached to position 6, largely (1→ 6)-linked β-D-galactopyranose residues but also L-arabinose (Figure 6). There are also few glucuronic acid residues present in the molecule. The highly branched structure is responsible for its low viscosity and high solubility in water.[6] This polysaccharide present a degree of polymerization within the range of 100 – 600.[23]

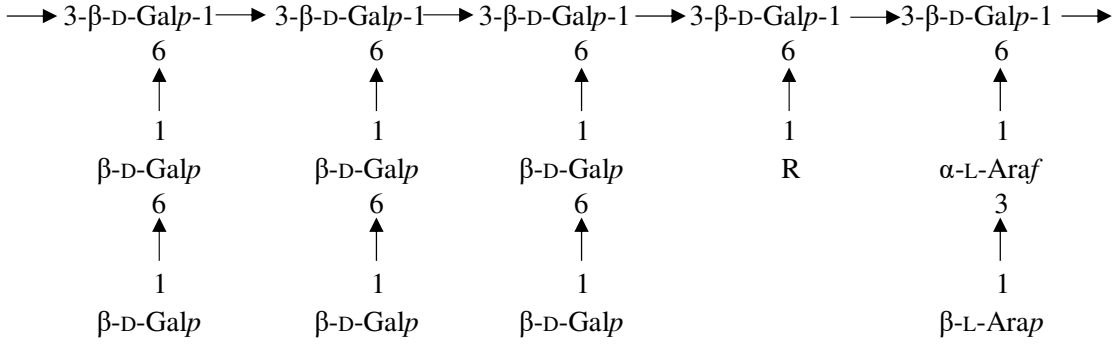

Figure 6. Abbreviated formula of arabinogalactans. Sugar units: galactopyranose (Gal*p*); arabinopyranose (Ara*p*); arabinofuranose (Ara*f*), and R is β-D-galactopyranose or less frequently, α-L-arabinofuranose, or β-D-glucopyranosyluronic acid residue. Reproduced from Sjöström *et al*.[6]

Hardwood hemicelluloses. Glucuronoxylans and glucomannans are the main hemicelluloses presents in hardwoods.[6]

Glucuronoxylans (*O*-acetyl-4-*O*-methylglucurono-β-D-xylan or simply xylan) are the most abundant hemicelluloses in hardwoods. Depending on the hardwood species, the xylan content varies within the limits of 15 – 30 % of the dry wood. As illustrated in Figure 7, their backbone consists of β-D-xylopyranose units, linked by (1→ 4)-bonds. Most of the xylose residues contain an *O*-acetyl group at C-2 or C-3 (about seven acetyl residues per ten xylose units). Additionally, the xylose units in the xylan chain contain (1→ 2)-linked 4-*O*-methyl-α-D-glucuronic acid residues, on the average of about one uronic acid per ten xylose residues. According to literature,[6] the xylosidic bonds between the xylose units are easily hydrolyzed by acids, whereas the linkages between the uronic acid groups and xylose are very resistant. Furthermore, acetyl groups are easily cleaved under alkaline conditions. Xylans present a degree of polymerization around 100 – 218.[20,23]

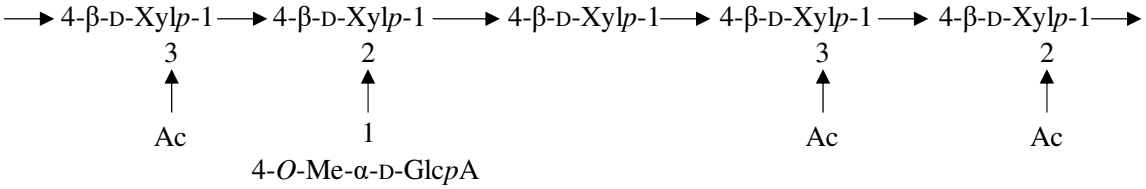

Figure 7. Abbreviated formula of xylans. Sugar units: xylopyranose (Xyl*p*); 4-*O*-methyl-α-D-glucopyranosyluronic acid (Glc*p*A); *O*-acetyl group (Ac). Reproduced from Fengel *et al*.[20]

Glucomannans are composed of β-D-glucopyranose and β-D-mannopyranose units linked by (1→ 4)-bonds (Figure 8). The glucose:mannose ratio varies between 1:2 and 1:1, depending on the wood species. According to literature,[6] the mannosidic bonds between the mannose units are more rapidly hydrolyzed by acids than the corresponding glucosidic bonds, and glucomannans are easily depolymerized under acidic conditions. The degree of polymerization of glucomannans varies between 40 and 70.[23]

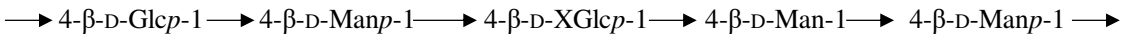

Figure 8. Abbreviated formula of glucomannans. Sugar units: glucopyranose (Glc*p*); mannopyranose (Man*p*). Reproduced from Sjöström *et al*.[6]

1.3 Lignin

Lignin is a three-dimensional amorphous biopolymer.[5,6] Its principal role in cell walls is to form the middle lamella, the intercellular material which cements the cellulose fibers together. Additional, lignin is also contained within the remaining cross-section of the fiber.[5] It is bounded to matrix hemicelluloses through covalent bonds and the hemicelluloses from their part are associated with cellulose microfibrils by hydrogen bonds and other intermolecular forces.[22] Lignin also performs various biological functions in wood, acting as hydrophobic barriers which protect wood from biological attack by various enzymatic systems, which are commonly effective in aqueous solutions. They also assist water transport by sealing wood cell walls against water losses.[22]

Its structure is composed of three major subunit types, *p*-hydroxyphenyl, guaiacyl and syringyl derived from *trans*-*p*-coumaryl, *trans*-coniferyl and *trans*-sinapyl alcohols, respectively (Figure 9). The amount of phenylpropane units and chemical bonds depend on wood species. Almost all the phenylpropane units in softwood lignins (e.g. lignin from *Pinus* and *Spruce* woods) are of the guaiacyl type (G) with small proportions of *p*-hydroxyphenyl units (H), hardwood lignins (e.g. lignin from *Birch*, *Eucalyptus*, *Beech* and *Aspen* woods) contains also additional syringyl units (S) with a very small proportion of H units.[6]

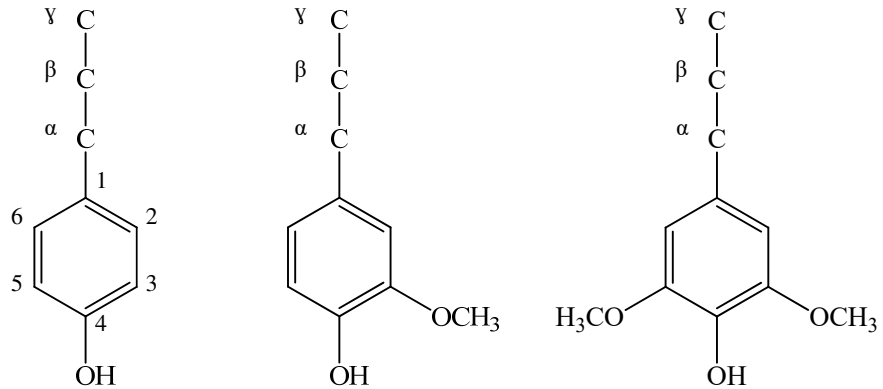

p-hydroxyphenyl propane (H) | guaiacyl propane (G) | syringyl propane (S)

Figure 9. The phenylpropane structural units of lignin. Reproduced and adapted from Sjöström *et al*.[6]

Intermolecular linkages. The phenylpropane units of lignin are linked together through aryl ether (β–*O*–4, α–*O*–4, 4–*O*–5') and carbon–carbon bonds (5–5', β–5, β–1, β–β) either in aliphatic and/or

aromatic moieties.[6] The structures most frequently found in softwood and hardwood lignins are depicted in Figure 10 and their proportions in lignin are summarized in Table 2. The main bond between phenylpropane units in native lignin are β–*O*–4 alkyl-aryl ether bonds, contributing to between 40 and 60 % of all types of substructures in lignin. Higher abundance of β–*O*–4 substructures are reported in hardwood lignin than in softwood lignin.[6] Another substructure also containing an alkyl-aryl ether is α–*O*–4.[6,22] These alkyl-aryl ether bonds are crucial on most depolymerization mechanisms used in delignification process.[6,22,24] The substructures containing carbon–carbon bonds such as in biphenyl substructures (5–5'), or in β–1 linked substructure or in pinoresinol β–β linked substructures or ether bonds C–O–C in diaryl ether substructures, such as those containing 4–*O*–5' diaryl-ether bonds (Figure 10), are essentially stable under typical pulping conditions.[6,22]

The degree of lignin condensation is an important characteristic as it is often negatively correlated with the lignin reactivity.[25] Most commonly, condensed lignin structures are lignin moieties linked to other lignin units via 2, 5 or 6 positions of the aromatic ring (in H units also C–3 positions). The most common condensed structures are 5–5', β–5 and 4–*O*–5'structures. Since the C–5 position of the syringyl aromatic ring is occupied by a methoxyl group and therefore it cannot be involved in condensation, hardwood lignins are less condensed than softwood lignins.[25]

Table 2. Type and frequencies of linkages in softwood and hardwood lignins.[6,16,22,26–30]

Linkages	**Number / 100 *ppu***	
	Softwood	**Hardwood**
β–*O*–4 (**1**)	43 – 50	50 – 65
β–5, α–*O*–4 (**2**)	9 – 12	4 – 6
α–*O*–4 (**2'**)	6 – 8	4 – 8
β–β (**3**)	2 – 4	3 – 7
5–5' (**4**)	10 – 25	4 – 10
4–*O*–5' (**5**)	4	6 – 7
β–1 (**6**)	3 – 7	5 – 7

The numbers refer to Figure 10; *ppu* – phenylpropane unit.

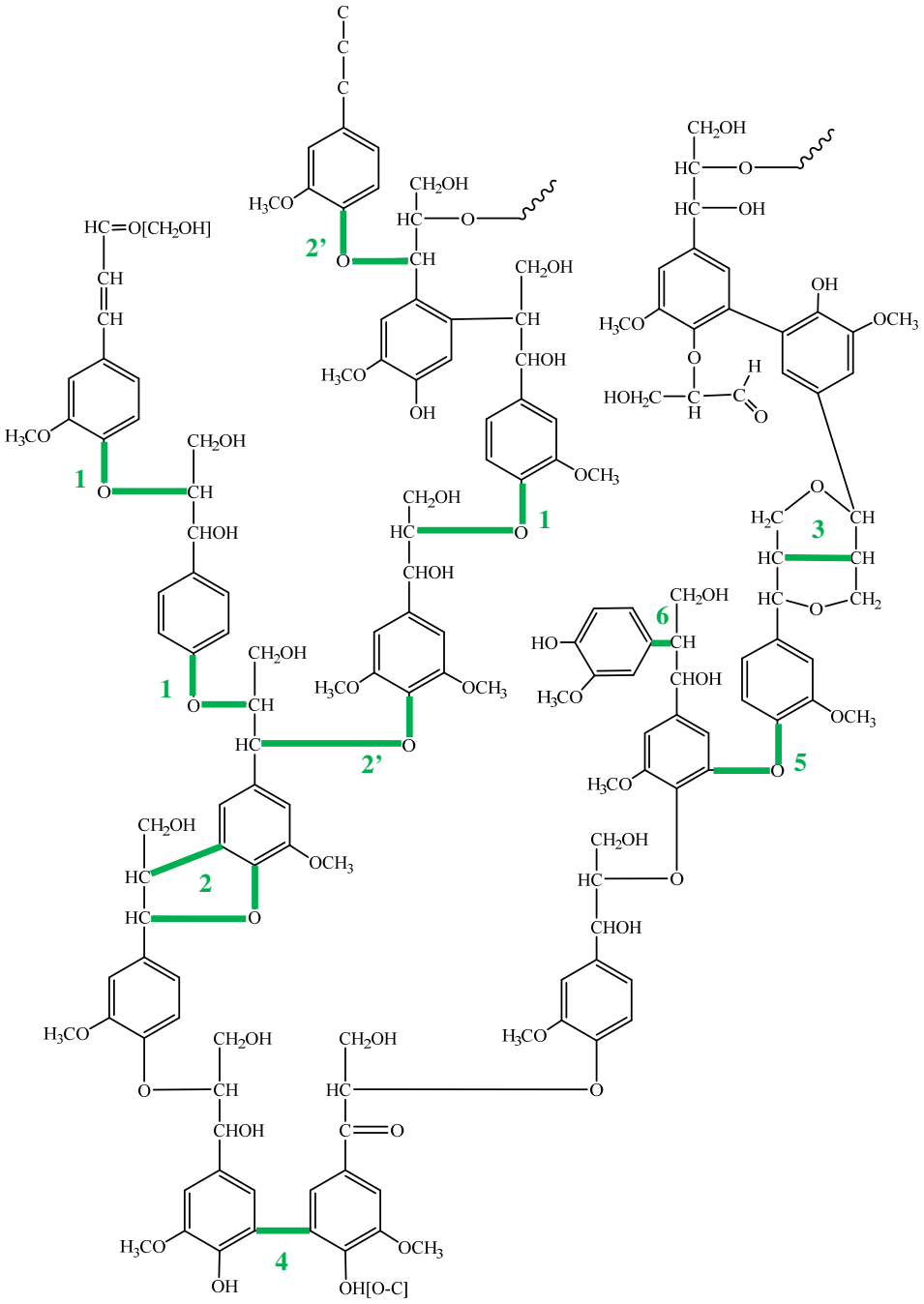

Figure 10. A structural segment of softwood lignin proposed by Adler (1977), representing the common linkages between the phenylpropane units. The numbers are identified in Table 2. Reproduced and adapted from Sjöström *et al.*[6]

The possible existence of covalent bonds between lignin and polysaccharides so-called the lignin-carbohydrates complexes (LCC), has been a subject of much debate and intensive studies.[6,15,24,31] Besides fundamental interest, studies on the structures of LCC in wood are of great importance, as LCCs influence many chemical properties of wood and consequently the

delignification performance.[32] Three types of lignin-carbohydrate bonds, generated under the conditions of lignin biosynthesis,[6,26] are suggested in the literature namely benzyl ether, benzyl ester and phenyl glycosidic linkages.[6,31] Figure 11 shows some typical LCC structures commonly believed to be present in the wood matrix. Benzyl ester bonds connect lignin and carbohydrates moieties through uronic acid of sugars and hydroxyl group of lignin.[24,31] These ester linkages are easily cleaved in alkaline conditions.[6] Benzyl ether and phenyl glycosidic link glycosyl or mannosyl residues of carbohydrates and phenolic or hydroxyl groups of lignin.[31] These linkages are more stable in alkaline than acidic conditions. Glycosidic bonds link carbohydrates and side chain hydroxyl groups of lignin.[31] These linkages are easily cleaved in acidic conditions.[6] Furthermore, the literature[6,24,31] suggests that LCC content depends of wood species, *i.e.* the benzyl ether bonds are dominant in softwood LCC with two different structures of lignin, namely lignin-xylan and lignin-glucomannan, while the phenyl glycosidic linkages are prevalent in hardwood LCC containing xylan–lignin and cellulose–lignin complexes.[31]

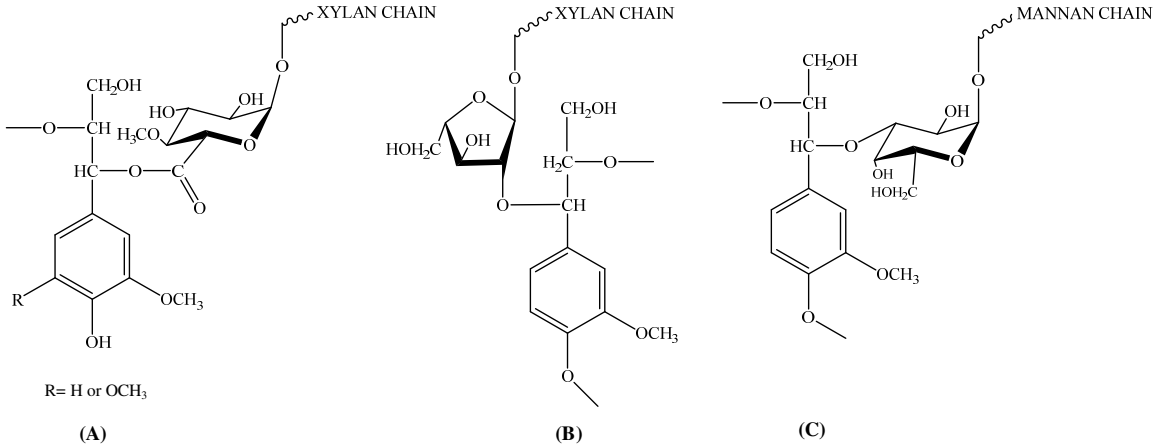

Figure 11. Typical lignin-carbohydrates linkages: benzyl ester (A); benzyl ether (B) and phenyl glycoside (C). Reproduced and adapted from Sjöström *et al*.[6]

Functional groups. The phenylpropane units of lignin contain different functional groups (Table 3). The most common ones are aromatic methoxyl and phenolic hydroxyl, primary and secondary aliphatic hydroxyl, ether groups and, small amounts of carbonyl groups (of the aldehyde and ketone types) and carboxyl groups. Depending on the wood species, the phenylpropane units may contain one methoxyl group on the C–3 position (softwood lignin) or on both the C–3 and C–5 positions (hardwood lignin). Figure 12 outlines the main functional groups present in wood lignin.

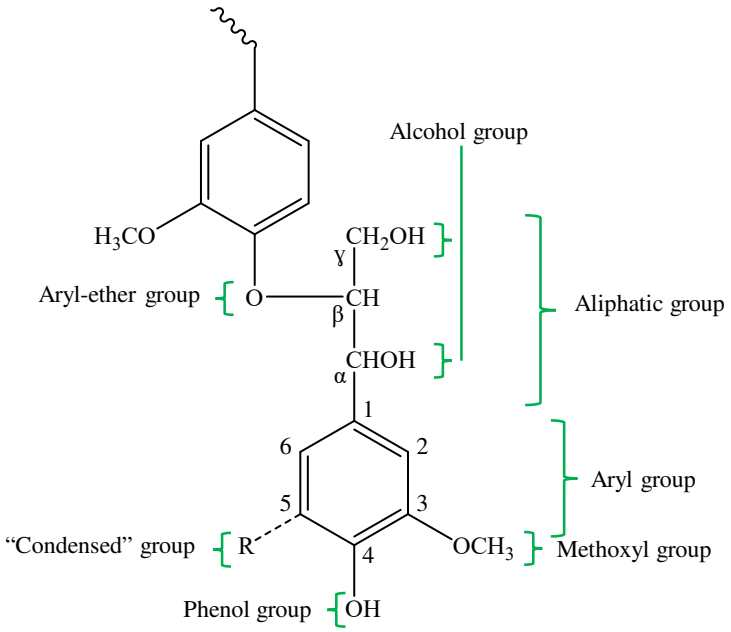

Figure 12. Functional groups of lignin. Reproduced and adapted from Heitner *et al*.[26]

Table 3. Functional groups of lignin.[6,27,28,30]

Functional group	Number / 100 *ppu*	
	Softwood	Hardwood
Methoxyl	92 – 97	139 – 164[b]
Phenolic hydroxyl	20 – 30	10 – 29[b]
Aliphatic hydroxyl	16	-
Benzylic hydroxyl	120[a]	16[b]
Total Carbonyl	10 – 15	3[b] – 24
Carboxyl (cinnamic acid)	-	4 – 13[b]

ppu – phenylpropane unit; (a) Milled wood lignin; (b) dioxane lignin.

The detail knowledge about the characteristics of the linkages and functional groups are of great interest and necessary for a detailed understanding of the depolymerization mechanism of lignin in conventional and new pulping processes.[6]

2. Conventional pulping processes

The aim of the pulping processes, in particular chemical pulping processes, is to delignify the wood matrix by chemically degrading and/or sulfonating the lignin into water-soluble fragments to liberate the cellulose fibers.[5,22] However, to achieve a successful wood delignification, strong alkaline or acidic media at high temperatures and pressures are required.[5]

2.1 Kraft pulping process

Kraft process is currently the most used industrially process for pulp production, accounting for more than 90 % of world pulp production.[4] The main active chemical agents in the kraft process are hydroxide and hydrosulfide anions (OH^- and HS^-) which are present in the kraft cooking liquor, an aqueous solution of sodium hydroxide and sodium sulfide, denoted as white liquor.[4,5] The alkaline attack causes fragmentation of the lignin macromolecule into smaller fragments that are then dissolved as phenolate or carboxylate ions.[5] The hydrosulfide ion plays an important role in kraft pulping by accelerating delignification (because of their strong nucleophilicity when compared with hydroxyl ions), rendering nonselective soda cooking into a selective delignifying process and reducing condensation reactions by blocking reactive groups.[4,5]

Delignification during kraft process proceeds in three distinct phases.[4,5] In the initial phase, rapid delignification is caused by the cleavage of β–aryl and α–aryl ether bonds in the phenolic units of lignin and it is characterized as an extraction process. In this initial phase, the predominant loss of carbohydrates is observed. The removal of lignin in bulk delignification phase follows a first order reaction. Main part of the lignin is removed in this phase while at the same time only minor carbohydrate losses occur. The cleavage of β–aryl bonds in nonphenolic units of lignin requires more drastic conditions (temperature and alkalinity) and is assumed to be the main delignification reaction. Kraft cooking is typically completed at a lignin content of 4 – 5 % for softwoods and about 3 % for hardwoods. At this final stage (residual phase), condensation reactions can occur leading to the formation of stable carbon-carbon bonds between lignin units that lead to the formation of lignin structures which are more difficult to cleave.[4] Furthermore, with continuous delignification, the dissolution of carbohydrates extensively increases. The hemicelluloses content is reduced by approximately 40 %.[5] The loss is caused by dissolution of

low-molecular-weight carbohydrates, removal of acid groups, and degradation by the so-called, peeling reaction. The relatively low loss of cellulose, about 10 %,[5] is explained by the accessibility of hydroxyl ions into the crystalline region of the cellulose. During delignification, there is also a corresponding reduction in pulp viscosity (a measure of cellulose weighted-average molecular weight). If pulp viscosity is allowed to fall below a critical level, the pulp strength drops dramatically. Thus, in order to maintain high yields and to preserve the high quality of the pulp, delignification is limited to a certain degree of delignification, targeting kappa numbers of about 20 – 30 for softwood and 15 – 20 for hardwood kraft pulps. The conventional kraft conditions, pulp yields and kappa number for softwood and hardwood are summarized in Table 4.

Although the kraft process allows the production of fibers with excellent properties for paper-grade pulp, its main disadvantages comprise the use of strong alkaline conditions resulting in metal corrosion problems, malodorous gases emission and high consumption of bleaching chemicals. Regarding the main structural changes during pulping process (Table 5, Table 6 and Table 7),[6,33] hardwood kraft lignin presents lower molecular weight than the respective wood lignin and softwood kraft lignin. Furthermore, kraft lignin contains a lower amount of residual aliphatic hydroxyl groups and β–*O*–4, and higher content of phenolic hydroxyl and carboxylic acid groups than the respective wood lignin. This technical lignin is characterized by the incorporation of sulfur into its chemical structure, particularly located on the aromatic ring, which might preclude its subsequent valorization within biorefinery processes.[5,6]

2.2 Sulfite pulping process

Sulfite pulping is the second most important chemical pulping process. Although the sulfite pulps account for less than 6 % of the total chemical pulp production, this process has received renewed attention as a prospective approach for the biorefinery concept, where the cellulosic pulp is shipped essentially as a chemical feedstock (e.g., dissolving pulp).[34] The acid sulfite process is the dominant technology for the production of dissolving pulps and accounts for approximately 70 % of the total world production.[4] On the other hand, the sulfite liquors are processed to produce fuels (e.g., bioethanol),[35] food additives (proteins, flavors, xylitol, etc.)[36] and lignin-based chemicals.[34]

It can be performed in a large range of pH, between 1 and 12, which is regulated by the ratio of SO_2 (free and bonded) and basic components of the pulping liquor (Table 4).[22] Typical bases used in sulfite pulping comprise the cations: Ca^{2+}, Mg^{2+}, NH_4^+ and Na^+, which could change the behavior of the lignin product.[6,34] Nowadays, the most common industrial process to produce chemical pulps are the acid sulfite and bisulfite process using magnesium hydroxide as base.[34] Higher pH sulfite pulping is mainly performed with sodium or ammonium hydroxide cations as bases, which are considered chemical agents for semi-chemical pulps.[22] However, due to the nature of this pulping process it will be not considered within the scope of the present thesis.

In the particular case of acid pulping (acid sulfite and bisulfite) there are two types of reaction that are responsible for the delignification: sulfonation and hydrolysis.[34] The sulfonation allows the incorporation of hydrophilic groups into lignin macromolecules, while hydrolysis cleave particularly α–*O*–4 ether bonds between lignin phenylpropane units and between them and polysaccharides, LCC.[5,6] The introduction of sulfonic groups in C_α and C_γ of C-3-alkyl lateral chain of phenylpropane units of lignin is the main reaction.[33] Sulfonic groups increase the hydrophilicity of the lignin fragments (lignosulphonate), confering them water solubility and, allowing their removal from the wood.[33] The cleavage of α–aryl ether bond takes place regardless of whether the phenolic hydroxyl of the phenylpropane units are etherified or free.[6] The sulfonation of lignin and condensation reactions are strongly affected by the acidity of the pulping solution being increased while pH value decrease.[6,34]

The production of lower strength pulp and the dependence of the process from the wood species are the main disadvantages of the sulfite process, compared to kraft process.[6] The main advantages of sulfite over the kraft pulps are their higher flexibility of the cooking process, covering the entire pH range and its easier bleaching.[34] Regarding the main structural changes of lignin during acid sulfite pulping, lignosulfonates present higher content of sulfonic groups, molecular weight, methoxyl groups and β–*O*–4 structures and have fewer phenolic hydroxyl groups than kraft lignin.[33,37,38] Furthermore, it often contains considerable amounts of carbohydrates, either dissolved in the liquor or still attached to the lignin polymer.[4] The principal changes on lignosulphonates induced by acid sulfite pulping process are summarized in Table 5, Table 6 and Table 7.

3. Organosolv pulping process

The organosolv process uses a mixture of organic solvents with water (30 to 70 % of organic solvent in water) to dissolve lignin by hydrolytic cleavage at elevated temperatures.[39] Various solvents have been studied including, acetone, methanol, ethanol, butanol, acetic acid, formic acid, ethylene glycol, glycerol, etc.[40] Low-boiling solvents, like methanol and ethanol, are used to reduce the energy requirement for their recovery by distillation and high-boiling solvents like ethylene glycol and glycerol are useful for high-temperature treatment without the need for pressure vessels.[18] To improve the delignification performance and allow to operate at lower temperature and pressures, some mineral or organic acids as catalysts have been studied.[39,40] The principal solvents/catalyst and conditions applied in organosolv pulping process, as well as the corresponding pulp yields and kappa number for softwood and hardwood are summarized in Table 4.

The cleavage of β-ether linkages seems to be the most important reaction in the lignin depolymerization during organosolv pulping.[22,41] In noncatalyzed organosolv pulping, the cleavage of β-aryl ether bonds is believed to occur in lignin after its dissolution in the pulping liquor. This type of reaction takes place in the so-called autohydrolysis processes, where acid is provided by the splitting of acetyl groups from hemicelluloses.[22] In acidic systems, easily hydrolysable α-ether linkages and β-aryl ether bonds are most readily cleaved. In general, β-ether cleavages appear to be more important in strongly acidic media. Furthermore, the hydrolysis of ether linkages between lignin and carbohydrates (LCC) takes place also in acidic systems.[41] On the other hand, α-ether linkages are readily cleaved in alkaline systems if they occur in phenylpropane units containing free phenolic groups. Alkaline cleavage of β-aryl ether bonds occurs, especially in the presence of nucleophilic additives such as hydrosulfide ion or an anthraquinone derivative.[41] As for other pulping processes, hardwoods are more readily delignified than softwoods.[33] Finally, lignin condensation reactions are important side reactions in both acidic and alkaline systems, that can be minimized by the appropriate choice of solvent.[41]

The main advantages of organosolv processes over the conventional pulping processes including a smaller environmental footprint, simple solvent recovery and in some cases, it is possible to operate at low temperatures and atmospheric pressure.[42] However, the most significant advantage is the isolation of high-quality sulfur-free lignin fraction, less degraded hemicelluloses

and cellulose fractions, for further valorization. The organosolv lignins undergo fewer transformations as compared to kraft and sulfite pulping (Table 5, Table 6 and Table 7). This technical lignin presents a lower content of hydroxyl groups, higher molecular weight and lower condensation degree compared to lignin coming from more drastic delignification processes.[33] Furthermore, the absence of organic sulfur (either as thiol groups, as in kraft lignin, or as sulfonic groups, as in lignosulfonates) is an advantage from the point of view of lignin valorization.[33]

Even though the organosolv processes have not seen real developments towards industrial scale (only at pilot and demonstration plant scale), they remain an interesting alternative for pulp production, offering simultaneous lignin and hemicelluloses streams, and therefore a true biorefinery approach for wood processing.[22]

Table 4. Summary of wood pulping processes: chemicals, conditions, pulp yield and kappa number.

Pulping processes	Chemicals	Conditions	Pulp yield / wt %	kappa number	References
Kraft (pH 10 – 14)	NaOH, Na_2S	(428.15 – 448.19 K), (1 – 3 h), (7 – 10 bar)	(40 – 55),[a] (39 – 56)[b]	(13 – 30),[a] (9 – 20)[b]	Sixta *et al.*[4] Costa *et al.*[43] Neiva *et al.*[44] Mendes *et al.*[45] Sjöström *et al.*[6] Smook *et al.*[5]
Sulfite					
acid sulfite (pH 1 – 2)	H^+, HSO_3^- with Na^+, Ca^{2+}, Mg^{2+}, NH_4^+ bases	(403.15 – 413.15 K), (3 – 7 h), (5 – 7 bar)	(48 – 54),[a] 53[b]	15,[a] 8[b]	Sixta *et al.*[4] Evtuguin *et al.*[34]
bisulfite (pH 3 – 5)	(H^+), HSO_3^- with Na^+, Mg^{2+} and NH_4^+ bases	(423.15 – 443.15 K), (1 – 3 h), (7 – 10 bar)	(50 – 55)[a]	-	Sjöström *et al.*[6] Smook *et al.*[5] Pinto *et al.*[33]
Organosolv	Methanol, ethanol, acetone, formic acid, butanol, acetic acid, ethylene glycol, glycerol, tetrahydrofurfuryl alcohol, etc. and mineral acids (hydrochloric, sulfuric and phosphoric acids) or organic acids (formic, oxalic and salicylic acids) have been used as acid catalyst	(373.15 – 523.15 K), (10 – 30 bar)	(53 – 58),[a,*] (48 – 52)[b,*]	(27 – 36),[a,*] (29 – 44)[b,*]	Johansson *et al.*[40] Pinto *et al.*[33]

(a) Softwood; (b) Hardwood; (*) Ethanol as solvent (40 – 60 %).[40]

Table 5. Assignments and quantification (number/C_9) of the linkages and functional groups of technical lignins identified by ^{1}H NMR.[27,28,43]

Assignment (spectroscopy range) / ppm	**Amount / (number/ C_9)**		
	Native lignin[a,b]	Kraft lignin[b]	Organosolv lignin[b]
aliphatic -CH_2 and -CH_3 (δ_H, 0.7-1.5)	0.29	0.23	0.44
aliphatic OH, -$OCOH_3$ aliphatic (δ_H, 1.5-2.2)	**1.05**	**0.45**	**0.61**
phenolic OH, -$OCOH_3$ phenolic (δ_H, 2.2-2.5)	**0.28 – 0.52**	**0.42 – 0.78**	**0.71**
H_β in β-β structures (δ_H, 3.0-3.2)	0.19	0.07	0.23
H_α in β-5 structure (phenilcoumaran) and H_α in α-O-4 structures (δ_H, 4.9-5.6)	0.13 – 0.22	0.15	0.18
H_α in β-O-4 structures without C_α=O and H_α in β-1structures (δ_H, 5.7-6.2)	**0.47 – 0.52**	**0.19**	**0.25**
H in aromatic ring (δ_H, 6.2-8.0)	**3.20**	**2.11**	**2.04**

(a) dioxane lignin; (b) *Eucalyptus globulus* wood.

Table 6. Assignments and quantification (number/aromatic group C_6) of the linkages and functional groups of technical lignins by ^{13}C NMR.[27,28,37,38,43]

Assignment (spectroscopy range) / ppm	**Amount / (number/aromatic group C_6)**			
	Native lignin[a,b]	Kraft lignin[b]	Lignosulfonate[b]	Organosolv lignin[b]
C_β in β-5 and β-β structures (δ_C, 52.5-54)	0.06, 0.13	0.07	-	0.10
aromatic -OCH_3 (δ_C, 54-57)	**1.47 – 1.75**	**1.38**	**1.36 – 1.45**	**1.40**
C_γ in β-*O*-4 structures without C_α=O (δ_C, 58.5-60.8)	**0.46 – 0.52**	**0.10**	**0.34**	**0.26**
C_γ in β-5 and β-*O*-4 structures with C_α=O; C_γ in β-1 (δ_C, 61.6-64.2)	0.04 – 0.07	0.03	0.03 – 0.06	0.07
C_α in β-*O*-4 structures; C_γ in pinoresinol and β-β structures (δ_C, 69-77)	0.71	0.17	-	0.34
C_β in β-*O*-4 structures; C_α in β-5 and β-β structures (δ_C, 79-90)	0.82	0.16	-	0.44
aromatic C_{Ar}-H (δ_C, 100-120)	2.05 – 2.17	1.83	2.10 – 2.11	1.95
aromatic C_{Ar}-C (δ_C, 120-135)	1.27 – 1.29	1.86	1.20 – 1.38	1.75
aromatic C_{Ar}-O (δ_C, 135-160)	2.54 – 2.68	2.30	2.51 – 2.70	2.30
CHO in benzaldehyde-type structures (δ_C, 190-191.8)	0.02 – 0.03	0.02	-	0.04
CHO in cinnamaldehyde-type structures (δ_C, 193-194.6)	0.03 – 0.04	0.02	-	0.04
CO in aldehyde and ketones, C_α=O/C_β=O (δ_C, 196.5-203.5)	0.47	0.30	-	0.47
CO C_α=O, carboxyl (δ_C, 207-209.5)	0.15	0.13[c]	-	-
S:G:H ratio	**84:14:2**[b] / **80:20:0**[a,b]	**0:97:3**[c] / **82:12:0**[b] / **74:26:0**[b]	**0:95:5**[c] / **72:28:0**[b]	**72:28:0**[e] / **70:30:0**[b]
Condensation degree	**15**[a,b]	**43**[b]	**-**	**35**[b]

(a) dioxane lignin; (b) *Eucalyptus globulus* wood; (c) softwood; (e) other hardwoods.

Table 7. Characteristics of some technical lignins obtained from different pulping processes: molecular weight, sulfur content and purity.[5,6,28,30,33,37,38]

Characteristics	**Native lignin**	**Kraft lignin**	**Lignosulfonate**	**Organosolv lignin**
Molecular weight ($\overline{M_n}$, g/mol)	(8000 – 10000)[a] / (2360)[b]	(2350 – 5000)[a] / (1820)[b]	(10000 – 60000)[a] / (2350 – 12000)[b]	1745[a] / 2000[b]
Sulfur content	Free	Moderate	High	Free
Purity	High	Moderate	Low	High

(a) softwood; (b) hardwood.

In the search for sustainable wood delignification processes deep eutectic solvents (DES) have emerged as promising alternatives.[7,8,46]

4. ‘Deep’ eutectic solvents

4.1 Definition and properties

Abbott and co-workers,[47] coined the term ‘deep eutectic solvents’, to describe mixtures of amides with quaternary ammonium salts with melting points lower than those of their pure components, allegedly due to hydrogen bonding interactions between the two components in a well-defined stoichiometric proportion as represented in Figure 13 (a). Later, the term was extended to other mixtures, defining DES as eutectic mixtures of Lewis or Brønsted acids and bases which can contain a variety of anionic and/or cationic species.[48] Recently, an alternative definition of DES was proposed by Martins *et al*.[49] as the mixture of two or more pure compounds for which the eutectic point temperature is below that of an ideal liquid mixture, presenting significant negative deviations from ideality. Additionally, the temperature depression should be such that the mixture is liquid at operating temperatures for a certain composition range. Furthermore, the authors[49] suggest that ‘eutectic solvent (ES)’ could be used as a generic term to describe mixtures that do not fulfill these criteria. Due to the absence of information about the solid-liquid phase diagram of the solvents investigated in this work, we decide to adopt the term ‘eutectic solvent’ (ES) to define them.

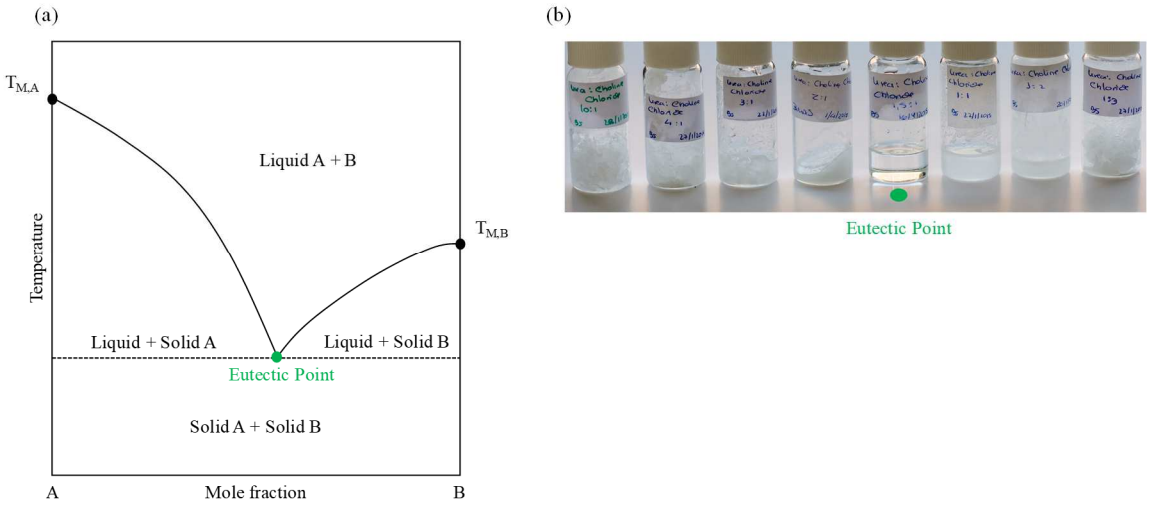

Figure 13. Schematic representation of a simple eutectic phase diagram of two components (a). Example of U:[Ch]Cl (1.5:1) eutectic mixture at room temperature. Adapted from Smith *et al.*[48]

The first reported ES (composed of urea and choline chloride ([Ch]Cl))[47] remains the most widely investigated (Figure 13, b). However, ES can be prepared by mixing other salts, such as tetraalkylammonium or phosphonium, with a hydrogen bond donor, such as amines, polyols, carboxylic acids, and carbohydrates, among others.[46,49–54] Figure 14 illustrates common examples of hydrogen bond donors (HBDs) and hydrogen bond acceptors (HBAs) that can be combined in order to prepare an ES. Even though the complete characterization of ESs, in terms of the solid-liquid phase diagram and the melting properties of their pure components is often missing, they exhibit a wide range of physicochemical properties that have been characterized by several authors.[48,55] In general, ES exhibit low freezing points, relatively high viscosity, poor ionic conductivities, higher densities than water, higher surface tension than molecular solvents, wide range of pH and excellent dissolution properties, which can be tuned by the combination of different HBDs with HBAs. Their simplicity of preparation and the possibility to tune their properties make them an attractive class of solvents for several applications such as, electrochemistry, catalysis, organic synthesis, dissolution and separation processes, and material chemistry[55,56] Recently, ES emerged as potential solvents for wood processing.[57]

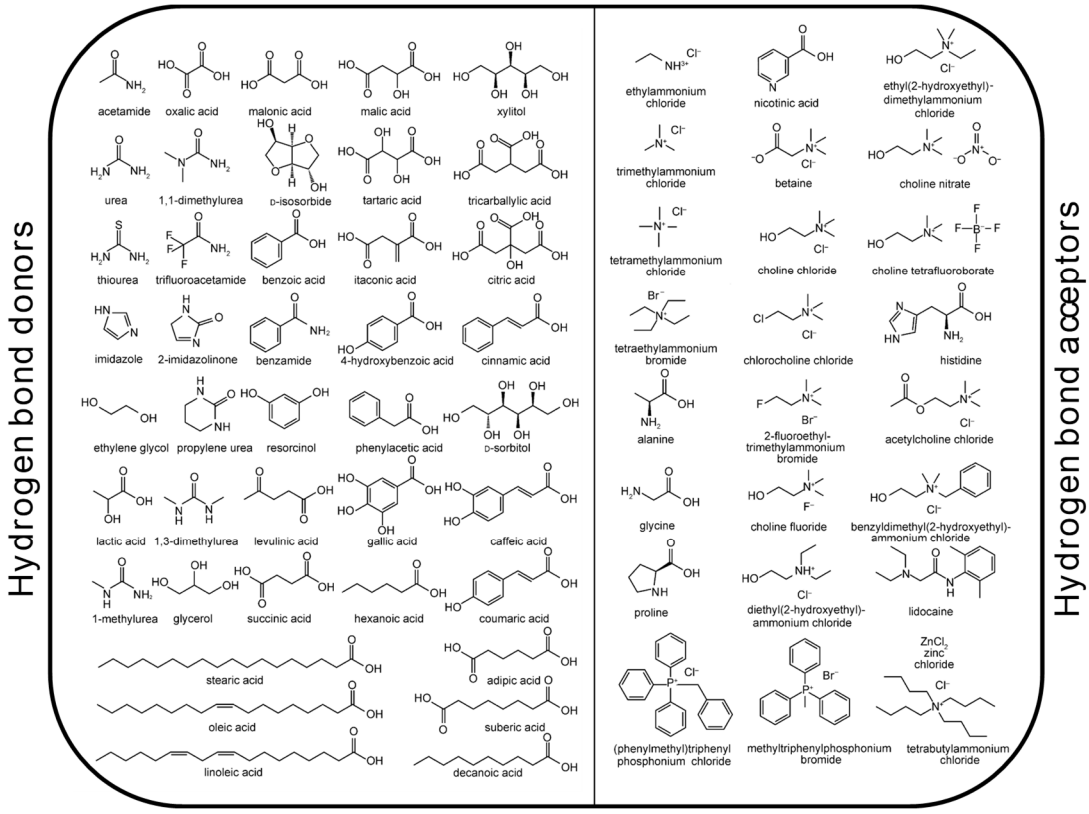

Figure 14. Chemical structures of hydrogen bond donors and hydrogen bond acceptors commonly used in eutectic solvents preparation. Reproduced and adapted from Francisco *et al.*[58]

4.2 Eutectic solvents in cellulose, hemicelluloses and lignin solubilization

Several research groups have been studying the potential of neat ESs on lignin, hemicelluloses and cellulose solubilization (Table 8).[46,59–62] Francisco *et al*.[46] was the first to report the solubility of alkali lignin, cellulose and starch, in several ESs combining carboxylic acids with [Ch]Cl and amino acids. The authors[46] concluded that most of the selected combinations (HBs:HBAs) show high lignin solubility and very poor or negligible cellulose solubility. Kumar *et al.*[59] also performed a similar study and both authors[46,59] selected LA:[Ch]Cl (10:1[46] or 9:1[59]) as the best ES to solubilize alkali lignin. However, different results were reported by Lynam *et al*.[60] where FA:[Ch]Cl (2:1) seems to be the best ES, instead of LA:[Ch]Cl (10:1). Recently, the great performance of U:[Ch]Cl (2:1) on xylan solubilization was reported by Morais *et al.*[62] These results suggest that ESs could be used to achieve selective extraction of biopolymers from lignocellulosic biomass.

Despite the demonstrated huge potential as solvent for lignin solubilization, an obvious disadvantage of neat ES is their high viscosity. To overcome this disadvantage, the effect of the addition of water to ES in lignin solubilization was also investigated by Kumar *et al.*[59] The authors[59] observed that an increase to 50 wt % of water affected negatively the lignin solubility in LA:[Ch]Cl (10:1) decreasing its solubility in 95 wt %. Although, the possibility of using ESs to improve lignin solubilization in aqueous media is very attractive, it is still poorly investigated. It is thus important to achieve a deeper understanding of the role of ESs and their aqueous solutions on the selective solubilization of lignins.

There are several methods to enhance the aqueous solubility of hydrophobic compounds, including cosolvency, hydrotropy, complexation, ionization, and use of surface-active agents.[63] In this thesis, we are interested not only to study the solubility of technical lignins (and their monomers) in several ESs (neat and aqueous solutions), but also to understand the main mechanisms responsible for the solubility. Thus, to better understand the solubilization mechanisms, the concepts behind the hydrotropy and cosolvency phenomena are here addressed.

Table 8. Solubility of wood biopolymers in several neat eutectic solvents.

ESs (HBDs:HBAs molar ratio)	Conditions	Cellulose / wt %	Hemicelluloses / wt %	Lignin / wt %	References
LA:Pro (3.3:1)	333.15 K, 20 – 40 min	<1[d]	<1[b]	9[c]	Lynam *et al.*[60]
LA:Pro (2:1)	333.15 K	0.00[a]	-	7.56[c]	Francisco *et al.*[46]
LA:Bet (5:1)	333.15 K, 12 h	0.0[e]	0.0[b]	38 ± 3.7[c]	Kumar *et al.*[64]
LA:Bet (2:1)	333.15 K	0.00[a]	-	12.03[c]	Francisco *et al.*[46]
	333.15 K, 12 h	0.0[e]	0.0[b]	12 ± 1.3[e]	Kumar *et al.*[64]
	333.15 K, 20 – 40 min	<1[d]	<1[b]	9[c]	Lynam *et al.*[60]
LA:[Ch]Cl (10:1)	333.15 K	0.00[a]	-	11.82[c]	Francisco *et al.*[46]
	333.15 K, 20 – 40 min	<3[d]	<5[b]	13[c]	Lynam *et al.*[60]
LA:[Ch]Cl (9:1)	333.15 K, 12 h	0.0[e]	-	100[e]	Kumar *et al.*[64]
LA:[Ch]Cl (5:1)	333.15 K	0.00[a]	-	7.77[c]	Francisco *et al.*[46]
	333.15 K, 12 h	0.0[e]	0.0[b]	100[e]	Kumar *et al.*[64]
LA:[Ch]Cl (3:1)	333.15 K	0.00[a]	-	4.55[c]	Francisco *et al.*[46]
LA:[Ch]Cl (2:1)	333.15 K	0.00[a]	-	5.38[c]	Francisco *et al.*[46]
	333.15 K, 12 h	0.0[e]	0.0[b]	100[e]	Kumar *et al.*[64]
LA:Hist (9:1)	333.15 K	0.00[a]	-	11.88[c]	Francisco *et al.*[46]
LA:Glyc (9:1)	333.15 K	0.00[a]	-	8.77[c]	Francisco *et al.*[46]
LA:Al (9:1)	333.15 K	0.00[a]	-	8.47[c]	Francisco *et al.*[46]
MA:Al (1:1)	373.15 K	0.11[a]	-	1.75[c]	Francisco *et al.*[46]
MA:[Ch]Cl (1:1)	373.15 K	0.00[a]	-	3.47[c]	Francisco *et al.*[46]
MA:Glyc (1:1)	373.15 K	0.14[a]	-	1.46[c]	Francisco *et al.*[46]
MA:Pro (1:2)	373.15 K	0.24[a]	-	6.09[c]	Francisco *et al.*[46]
MA:Pro (1:3)	373.15 K	0.78[a]	-	14.90[c]	Francisco *et al.*[46]
OA:Bet (1:1)	333.15 K	0.00[a]	-	0.66[c]	Francisco *et al.*[46]

OA:Pro (1:1)	333.15 K	0.00[a]	-	1.25[c]	Francisco *et al.*[46]
OA:[Ch]Cl (1:1)	333.15 K	0.00[a]	-	3.62[c]	Francisco *et al.*[46]
OA:Glyc (3:1)	358.15 K	0.00[a]	-	0.28[c]	Francisco *et al.*[46]
OA:Hist (9:1)	333.15 K	0.25[a]	-	0.00[c]	Francisco *et al.*[46]
OAA:Pro (1:1)	333.15 K	0.15[a]	-	0.00[c]	Francisco *et al.*[46]
FA:[Ch]Cl (2:1)	333.15 K, 20 – 40 min	<1[d]	<1[b]	14[c]	Lynam *et al.*[60]
AA:[Ch]Cl (2:1)	333.15 K, 20 – 40 min	<1[d]	<1[b]	12[c]	Lynam *et al.*[60]
U:[Ch]Cl (2:1)	363.15 K	-	24.35 ± 2.37[b]	-	Morais *et al.*[62]
U:[Ch]Cl (1:1)	363.15 K	-	17.24 ± 0.93[b]	-	Morais *et al.*[62]
U:[Ch]Cl (1:2)	363.15 K	-	14.85 ± 2.06[b]	-	Morais *et al.*[62]

Sources: (a) cellulose (90%); (b) xylan; (c) alkali lignin; (d) medium fibrous cellulose; (e) no information; (-) not performed.

Hydrotropy is the phenomenon of increasing the solubility of water-insoluble or sparingly water-soluble organic compounds in aqueous solutions in the presence of hydrotropes,[65] which are a class of water-soluble compounds characterized by an amphiphilic structure, yet unable to form micelles.[65] Some examples of hydrotropes are sodium salts such as benzoate, citrate, salicylate, *p*-toluenesulfonate, xylenesulfonate, and urea.[65] Their signature characteristic is a sigmoidal solubilization profile (Figure 15). In some cases where the entire concentration range can be explored, they even display a maximum of solubility, suggestive of cooperative intermolecular interactions involved in the solubilization process.[65] Recent studies[66] showed the coaggregation of the solute with the hydrotropes, above a minimum hydrotrope concentration (MHC), to be the main mechanism behind the enhanced solubilization. The MHC of a hydrotrope is considered as a measure of the stability of its aggregation form relative to its monomeric form. Thus, the lower the MHC, the greater the hydrotrope's stability.[67] The main advantage of hydrotropes is the quick recovery of the solute from hydrotropic solutions by simple dilution with water, followed by filtration.

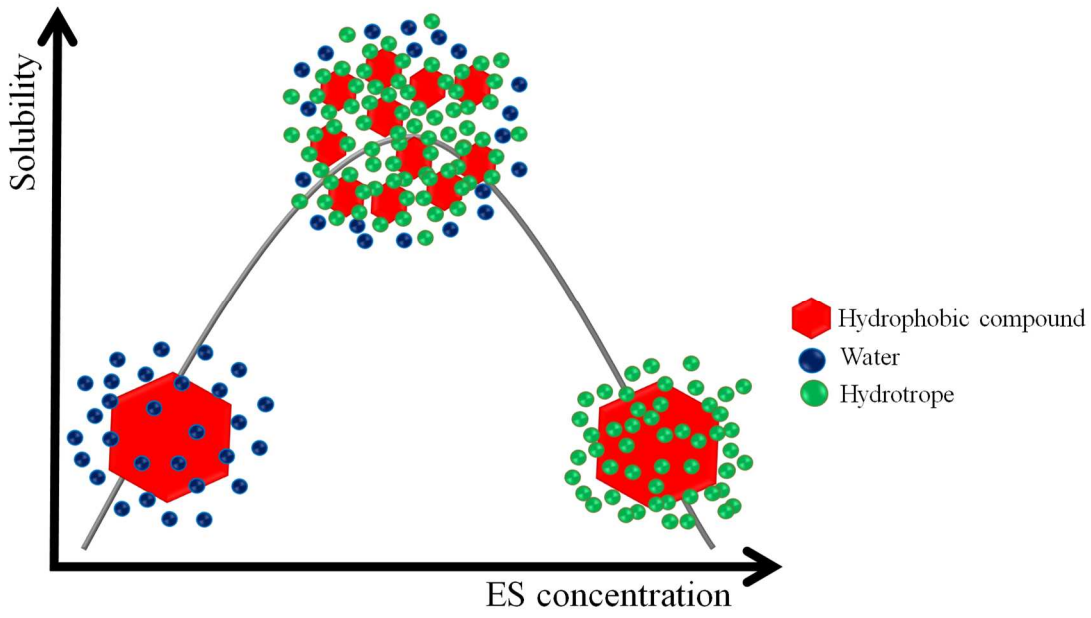

Figure 15. Schematic representation of hydrotropy solubilization mechanism.

Cosolvents are water-soluble compounds that can enhance the solubility of poorly aqueous, soluble hydrophobic compounds. This solubilization process, unlike that of hydrotropes, is not

based on the formation of aggregates but on the solvation of the solute by a mixed solvent (water + cosolvent) with physical properties and a solvation ability that are intermediate to those of neat water and cosolvent.[68] Depending on the nature of the solute, many different compounds may be used as cosolvents in aqueous solutions, but for poorly soluble hydrophobic compounds, ethanol, propylene glycol, glycerol, and polyethylene glycols are widely used.[69] Most cosolvents have HBD and/or HBA groups as well as small nonpolar regions. Their hydrophilic hydrogen-bonding groups ensure water miscibility, while their nonpolar regions may create dispersive interactions with the solute and interfere with the water hydrogen-bonding network, reducing the overall intermolecular attraction of water molecules. By disrupting water self-association, cosolvents reduce the ability of water to squeeze out nonpolar, hydrophobic compounds, thus increasing their solubility.[68] The solubilization effected by cosolvent is a linear or monotonic function of its concentration (Figure 16).[65] Contrary to a hydrotropic system, the solute recovery is achieved by cosolvent evaporation.

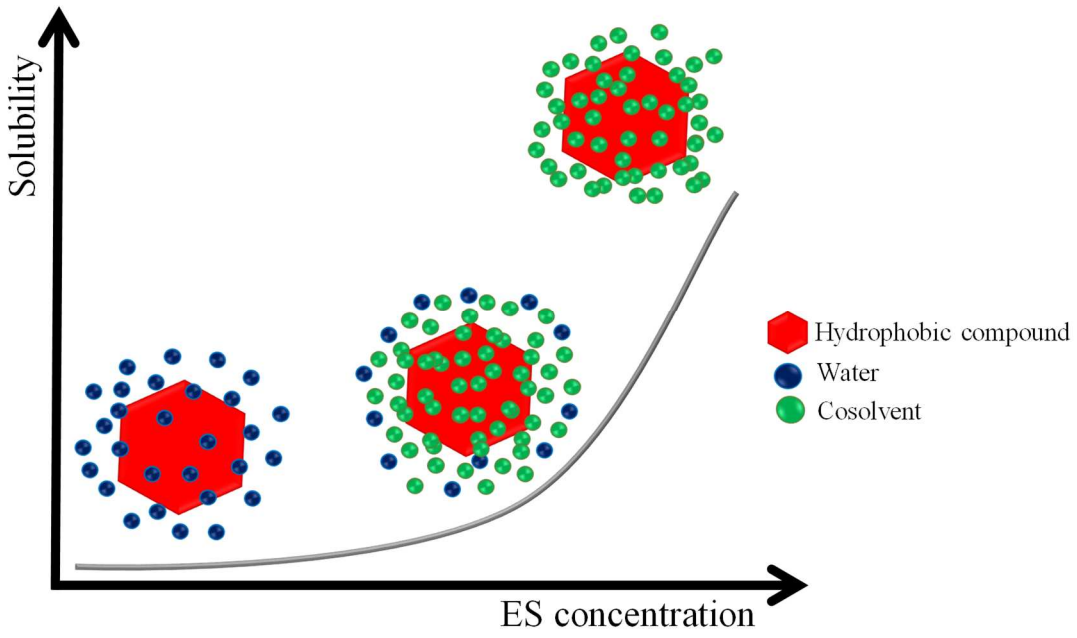

Figure 16. Schematic representation of cosolvency solubilization mechanism.

Hydrotropes and cosolvents have been used for a long time in several drug formulations, cleaning agents, and personal care products.[69] However, in biomass processing, studies on the application of hydrotropes have been scarce[70] when compared with the extensive use of cosolvents.[71] Yet, ESs with hydrotropic or cosolvent behavior in aqueous media seem to hold a lot

of potential to be applied in this field, where novel, greener, and more performant solvents are in great demand.

4.3 Eutectic solvents in wood delignification processes

Since 2012, ESs have been rapidly emerging as a new solvents for biomass processing, particularly for the fractionation of lignocellulosic biomass[72] and the extraction/separation of bioactive compounds from biomass.[73] However, increasing demands for deep cuts in CO_2 emission and to improve the added value are impelling the pulp and paper industry to develop innovative technologies based on ESs. It is expected that this new pulping technology led the production of cellulose fibers at lower temperatures and pressures, while simultaneously producing lignin and hemicelluloses fractions for high-volume applications.[9] In this context, some researchers have been focused on investigating the potential of ESs on wood delignification processes.[74–78] More details regarding wood delignification using ESs (type of wood, ESs used, delignification conditions, as well as solid fraction, removal lignin and recovery lignin yields) are summarized in Table 9.

The wood species are one of the process variables in pulping technology with high impact on the final product quality, due to their compositional differences. In that sense, to assess the potential of ESs on wood delignification processes, both hardwoods (*Populus sp.*,[74,76] *Eucalyptus camaldulensis*[75] and *Fagus sylvatica*[77,78]) and softwoods (*Pseudotsuga menziesii*)[74] were reported in literature. Among the studied ESs, LA:[Ch]Cl (10:1) appears to be the more selective solvent for wood delignification at mild conditions (363.15 K, 6 h). This ES system led to a lignin removal of 24 and 10 wt % for hardwood and softwood, respectively. However, a higher lignin removal yield of 66 wt % for hardwood was reported by Mamilla *et al.*[77] using OA:[Ch]Cl (1:1) at 353.15 K and 8 h. These works[46,74,76,77] agree that hemicelluloses are partly co-extracted with lignin and cellulose fibers are not dissolved. At this point, it is important to highlight that different separation methods to isolate lignin from ES liquid fraction were applied by these authors, making comparative analysis difficult.

Table 9. Wood delignification processes mediated by eutectic solvents.

Woods	ESs	Conditions	Solid fraction / wt %	Lignin removal / wt %	Recovery lignin from ESLF[b] / wt %	References
HARDWOODS						
Populus spp.	AA:[Ch]Cl	363.15 – 418.15 K, 0.5 – 9 h	100 – 60	31 – 73	10 – 22	Vasco *et al.*[74]
	LA:[Ch]Cl	363.15 – 418.15 K, 0.5 – 9 h	90 – 60	24 – 81	10 – 40[a]	Vasco *et al.*[74]
	Lev:[Ch]Cl	363.15 – 418.15 K, 0.5 – 9 h	100 – 60	19 – 81	10 – 20	Vasco *et al.*[74]
	OA:[Ch]Cl (1:1)	353.15 – 373.15 K, 9 h	75 – 64	5 – 90	*	Chen *et al.*[76]
Eucalyptus camaldulensis	LA:[Ch]Cl (10:1)	363.15 – 403.15 K, 6 h	78 – 40	18 – 84	6 – 60	Mei *et al.*[75]
	OA:[Ch]Cl (1:1)	353.15 K, 8 h	50	66	*	Mamilla *et al.*[77]
	GlyA:[Ch]Cl (3:1)	333.15 K, 24 h	*	17	*	Jablonsky *et al.*[78]
Fagus sylvatica	LA:Ala (9:1)	333.15 K, 24 h	*	15	*	Jablonsky *et al.*[78]
(Beech wood sawdust)	LA:Bet (2:1)	333.15 K, 24 h	*	12	*	Jablonsky *et al.*[78]
	LA:Glyc (9:1)	333.15 K, 24 h	*	6	*	Jablonsky *et al.*[78]
	EG:[Ch]Cl (2:1)	333.15 K, 24 h	*	5	*	Jablonsky *et al.*[78]
SOFTWOODS						
Pseudotsuga menziesii	AA:[Ch]Cl	363.15 – 418.15 K, 0.5 – 9 h	95 – 70	10 – 28	10 – 30	Vasco *et al.*[74]
	LA:[Ch]Cl	363.15 – 418.15 K, 0.5 – 9 h	90 – 65	10 – 64	10 – 50[a]	Vasco *et al.*[74]
	Lev:[Ch]Cl	363.15 – 418.15 K, 0.5 – 9 h	95 – 70	10 – 28	10 – 20	Vasco *et al.*[74]

(a) contaminated lignin; (b) ESLF – ES liquid fraction; (*) no information.

Regarding the main structural changes in isolated lignins induced by ESs, some authors,[74,75,79] using different techniques, showed that under mild conditions the amount of β-*O*-4 structures of the isolated lignin was lower than native lignin and higher than those observed on organosolv processes.[75] However, the extensive cleavage of these structures was reported when the ES delignification took place under harsh conditions [(393.15 K and 6 – 24 h)[74] or (393.15 – 453.15 K and 3 h)[79]]. Furthermore, the isolated lignins[74,79] presented lower molecular weight than the native lignin, and high purity when compared with kraft and lignosulfonate lignins. Table 10 presents more details regarding the main changes in isolated lignin induced by LA:[Ch]Cl, comparatively to native lignin.[74] These changes were assessed by (^{1}H and quantitative ^{13}C) NMR and GPC analysis. However, it is worth mentioning that Lyu *et al.*[79] and Mei *et al.*[75] resorted to 2D-HSQC NMR analysis to characterize the isolated lignin. Their results cannot be directly compared with the characterization applied within the scope of this thesis.

Table 10. Principal changes in lignin induced by eutectic solvents system.

Structural element[a]	**number/aromatic group C$_6$**	
	Native lignin[d]	**LA:[Ch]Cl-lignin**
aliphatic -CH_2 and -CH_3	1.83	1.97
aromatic -OCH_3	0.97	0.90
C_γ in β-5 and β-*O*-4 structures with C_α=O	0.65	0.09
C_α in β-*O*-4 structures	0.57	ND[c]
C_β in β-*O*-4 structures	0.42	ND[c]
aromatic C_{Ar}-H	2.75	3.09
aromatic C_{Ar}-C	1.66	1.69
aromatic C_{Ar}-O	1.59	1.22
Functional groups[b]	**number/aromatic group C$_9$**	
	Native lignin[d]	**LA:[Ch]Cl-lignin**
aliphatic OH	1.62	1.54
phenolic OH	0.05	0.49
Molecular weight[e] **/ g mol^{-1}**	**Native lignin**[d]	**LA:[Ch]Cl-lignin**
	890	2950

(a) Quantitative ^{13}C NMR analysis; (b) ^{1}H NMR analysis of acetylated lignin; (c) ND, not detected; (d) Milled wood lignin isolated from *Pseudotsuga menziesii* (softwood); (e) Gel permeation chromatography (GPC) analysis of acetylated lignins

EXPERIMENTAL SECTION

One of the main objectives of this work was to develop a new wood delignification process using eutectic solvents (ESs), to produce high-quality cellulose fibers and precipitated lignin for further valorization. Two strategies were outlined to accomplish this purpose (Figure 17): a fundamental study (Part A) followed by the proof of concept (Part B). The fundamental study is focused on the solubility of technical lignins (and their monomers) in several ESs, where the influence of ES components, their concentration and the solubilization mechanisms were investigated (Chapters I and II). Based on these results, the best ES system to solubilize lignin was them used to perform *Eucalyptus globulus* wood delignification at mild conditions, as proof of concept (Chapters III and IV). Furthermore, the final products (solid fraction and precipitated lignin) were characterized in order to evaluate the feasibility of this ES based wood delignification process.

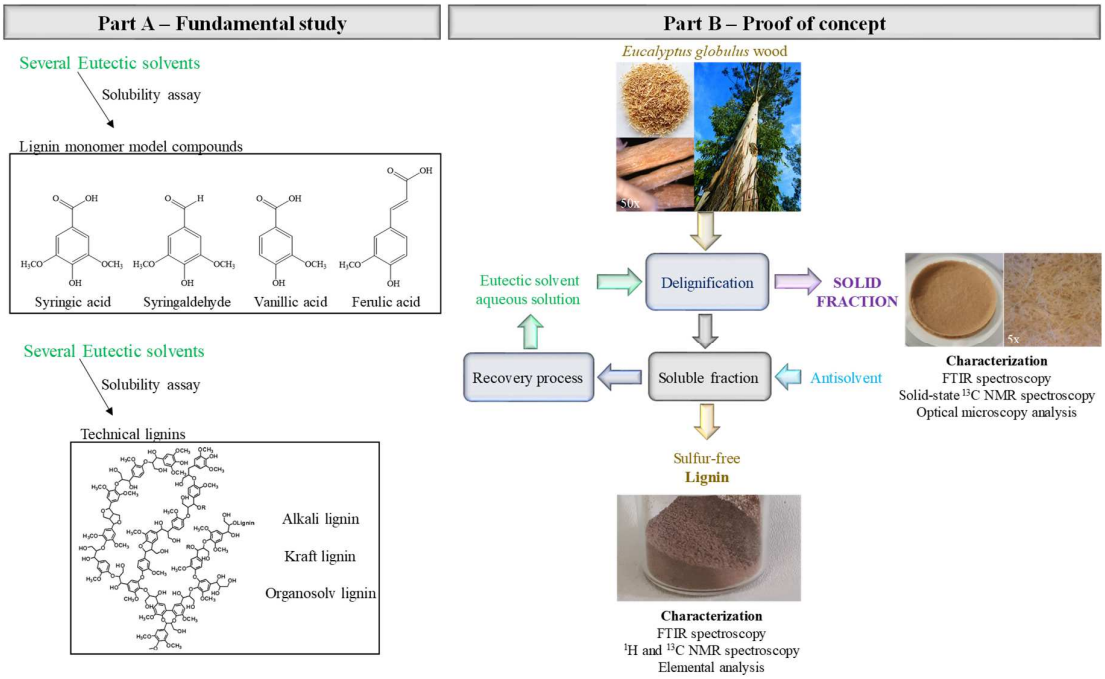

Figure 17. Schematic representation of the experimental methodology.

The experimental section is composed by four subsections. The first subsection describes all the chemicals (ES components and lignin monomer model compounds) and samples (technical lignins, wood and kraft pulp) used in this thesis. The second subsection

presents the methodologies used for ES preparation, solubility assay (technical lignins and their monomers) and wood delignification process. The optimization methodologies are presented in the third subsection and, finally the fourth subsection present the analytical techniques used to characterize the solid fraction and precipitated lignin.

1. Chemicals and samples

1.1 Chemicals

Starting materials for preparation of ESs were used as received. Several hydrogen bond donors (HBDs) such as carboxylic acids, polyols, sugars and urea, and hydrogen bond acceptors (HBAs) like choline chloride, proline, betaine, urea, ammoniums and phosphoniums, were combined to prepare ESs. These several ESs were used in this thesis to cover the effects of the HBDs and HBAs chemical structures on the solubilization of technical lignins (and their monomers). Urea was used as both HBD and HBA, as demonstrated by Ashworth *et al*.[80] To ensure the correct molar proportion in the ES preparation, the water content of all starting materials was measured using a Metrohm 831 Karl Fischer coulometer. The key information about the studied HBDs and HBAs is summarized in Table 11, and their structures shown in Figure 18. Hydrochloric acid (37 % of purity, supplied by Riedel-de Haën), sulfuric acid (>95 % of purity, supplied by Fisher Scientific) and *p*-toluenesulfonic acid monohydrate (>98 of purity, supplied by TCI Chemicals) were used as acid catalyst on ES wood delignification processes presented in the Chapter III of this thesis.

Table 11. Compounds descriptions, CAS number, molecular weight, mass fraction purity, water content and supplier of the investigated ES components.

Compounds	CAS number	Mw / g mol^{-1}	Purity[a] / wt %	Water Content / wt %	Supplier
Hydrogen Bond Donors					
Formic acid (FA)	64-18-6	46.03	98	1.08 ± 0.08	Panreac
Acetic acid (AA)	64-19-7	60.05	99	0.12 ± 0.01	Fisher Scientific
Propionic acid (PA)	79-09-4	74.08	>99	0.09 ± 0.01	Merk Chemicals
Butyric acid (BA)	107-92-6	88.11	99	0.14 ± 0.05	Riedel de Häen
DL-Lactic acid (LA)	50-21-5	90.08	85	14.45 ± 0.27	Acros Organics
Glycolic acid (GlyA)	79-14-1	76.05	99	0.11 ± 0.01	Acros Organics
DL-Malic acid (MA)	617-48-1	134.09	99.5	0.01 ± 0.00	Panreac
p-Toluenesulfonic acid monohydrate (PTSA)	6192-52-5	190.22	>98	9.63 ± 0.25	TCI Chemicals
Urea (U)	57-13-6	60.06	>99	0.003 ± 0.00	Panreac
Glycerol (G)	56-81-5	92.09	99.8	0.13 ± 0.04	Fisher Scientific
Ethylene glycol (EG)	107-21-1	62.07	>99.5	0.12 ± 0.02	Sigma-Aldrich
α-D(+)-Glucose (Glu)	492-62-6	180.16	96	anhydrous	Sigma-Aldrich
D(+)-Xylose (Xyl)	58-86-6	150.13	99	0.01 ± 0.00	Sigma-Aldrich
D(-)-Fructose (Fru)	57-48-7	180.16	98	0.25 ± 0.04	Panreac
Hydrogen Bond Acceptors					
Choline Chloride ([Ch]Cl)	67-48-1	139.62	99	2.17 ± 0.45	Acros Organics
L(-)-Proline (Pro)	609-36-9	115.13	99	3.95 ± 0.61	Acros Organics
Betaine (Bet)	107-43-7	117.15	98	1.27 ± 0.11	Acros Organics
Tetramethylammonium chloride ([N_{1111}]Cl)	75-57-0	109.6	97	1.14 ± 0.15	Sigma-Aldrich
Tetraethylammonium chloride ([N_{2222}]Cl)	56-34-8	165.71	>98	1.15 ± 0.002	Sigma-Aldrich
Tetrapropylammonium chloride ([N_{3333}]Cl)	5810-42-4	221.81	98	1.79 ± 0.11	Sigma-Aldrich
Tetrabutylammonium chloride ([N_{4444}]Cl)	1112-67-0	277.92	97	2.70 ± 0.03	Sigma-Aldrich
Tetrabutylphosphonium chloride ([P_{4444}]Cl)	2304-30-5	294.88	>95	-	Io-li-tec
Sodium *p*-toluenesulfonate (NaPTS)	657-84-1	194.18	>90	2.04 ± 0.15	TCI Chemicals
Urea (U)	57-13-6	60.06	>99	0.003 ± 0.00	Panreac

[a] As reported by the supplier.

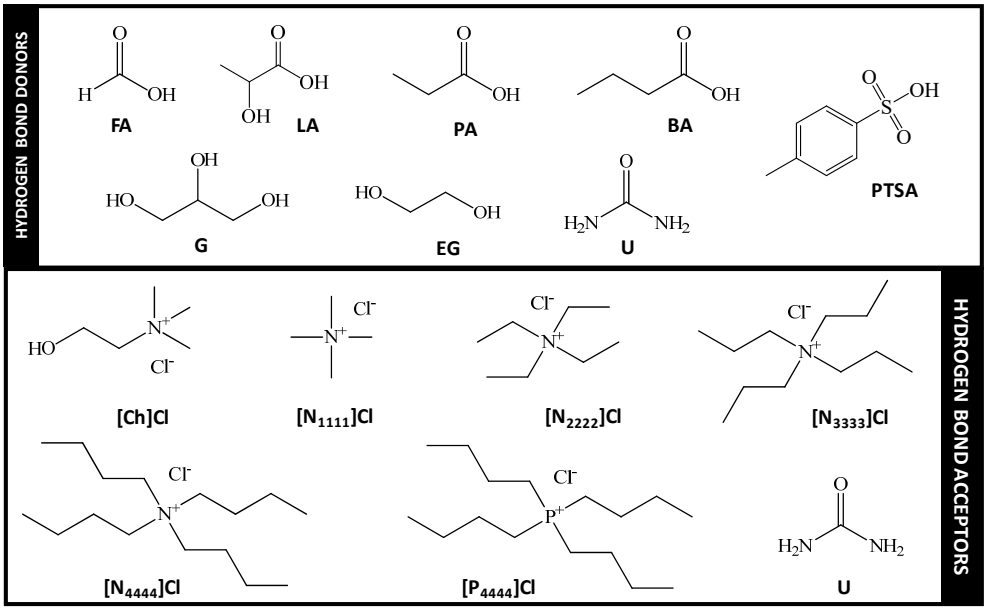

Figure 18. Chemical structures of investigated HBDs and HBAs.

Lignin monomer model compounds (LMMCs), such as syringaldehyde, and vanillic, syringic and ferulic acids were selected for the fundamental studies to evaluate the potential of ES (neat or in aqueous solutions) for lignin solubilization, taking into account that syringaldehyde, syringic and vanillic acids are lignin depolymerization products, e.g. by thermochemical processes.[33,81,82] Ferulic acid was here selected as LMMCs to evaluate the influence of aliphatic alkyl chain (similar to *trans*-coniferyl alcohol chemical structure, Figure 9) on their solubilization in ES. All the LMMCs were used as received. The key information about these compounds is summarized in Table 12, and their structures are shown in Figure 19.

Table 12. Lignin monomer model compounds information: name, CAS, molecular weight, mass fraction purity and supplier.

LMMCs	CAS number	Mw / g mol^{-1}	Purity[a] / wt %	Supplier
Syringic acid	530-57-4	198.17	>98	Acros Organics
Syringaldehyde	134-96-3	182.17	98	Acros Organics
Vanillic acid	121-34-6	168.15	97	Acros Organics
Ferulic acid	1135-24-6	194.18	>99	Acros Organics

[a] As reported by the supplier.

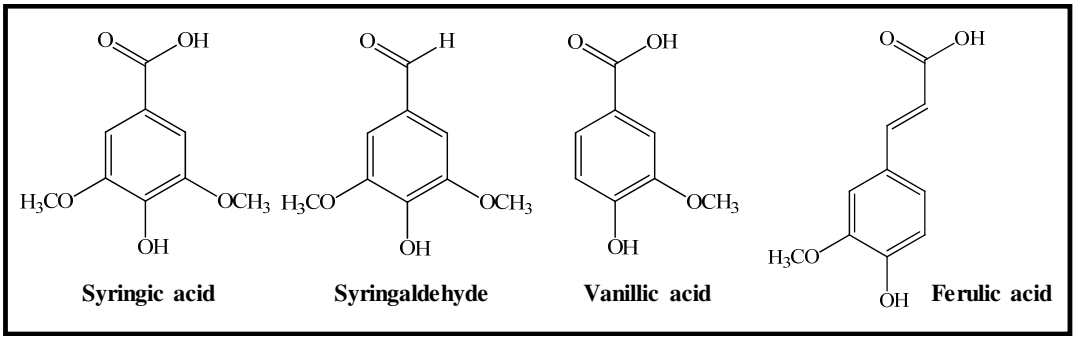

Figure 19. Chemical structures of investigated LMMCs.

1.2 Samples

Four samples of technical lignins (kraft, organosolv, alkali and dioxane lignins) were used in this thesis. Kraft, organosolv and alkali lignins samples were selected for the fundamental studies to investigate the solubilization of lignin in aqueous solution of ESs. The kraft and dioxane lignins were used as benchmark in the proof of concept studies. *Eucalyptus globulus* wood sample, fraction 40 – 60 mesh, air dried, with 8.37 ± 0.02 wt % of moisture and 19.94 ± 0.35 wt % of Klason lignin content, was used to investigate the performance of ESs as delignification solvent and a kraft pulp sample was used for comparative purpose. *E. globulus* wood (40 – 60 mesh) was kindly supplied by The Navigator Company. The kraft pulp with kappa number 14.4 was kindly supplied by The Navigator Company.

Organosolv lignin was produced by ethanol organosolv processing of *E. globulus* wood (kindly supplied by Lignol Innovations Inc., Canada) and the commercially available alkali lignin was kindly supplied by Sigma-Aldrich. The kraft lignin was isolated from *E. globulus* industrial kraft liquor kindly supplied by The Navigator Company, following the procedure described by Pinto *et al*.[83] The dioxane lignin was extracted from *E. globulus* wood by mild acidolysis using dioxane and HCl as described by Evtuguin *et al*.[27]

2. Methodologies

2.1 Eutectic solvents preparation

The two-component mixtures (HBD and HBA), were placed in sealed glass vials with a stirring bar and heated in an oil bath at 323.15 ± 0.01 K, with constant stirring until transparent liquids were formed. After the liquid formation, the mixtures were kept at this temperature for one hour before being allowed to return to room temperature.[84] All experiments were carried out with ESs liquid at room temperature (see in Table 13 the list of ESs investigated in Part A - Fundamental study). The aqueous solutions of ESs (25, 50, 75 and 95 wt %) were prepared by diluting the neat ESs in deionized water. The water content of the ES components was checked using a Metrohm 831 Karl Fisher coulometer and the value was taken into account in the preparation of the ESs aqueous solutions. The pH of ESs aqueous solutions was measured at 298.15 ± 0.01 K using a Mettler Toledo S47 SevenMulti^{TM} dual meter pH and conductivity equipment with an uncertainty of ± 0.01. The calibration of the pH meter was carried out with two buffers (pH of 4.00 and 7.00).

Table 13. List of ESs families investigated.

ESs families	Molar ratio
Carboxylic acids	
FA:[Ch]Cl	2:1
AA:[Ch]Cl	2:1
AA:Pro	2:1
AA:Bet	2:1
AA:U	4:1
PA:[Ch]Cl	4:1; 3:1; 2:1; 1:1; 1:2; 1:3; 1:4
PA:Pro	2:1
PA:Bet	2:1
PA:U	4:1; 2:1; 1:1; 1:2; 1:4
BA:U	2:1
LA:[Ch]Cl	2:1; 1:2; 10:1
LA:Pro	2:1
LA:Bet	2:1
LA:U	2:1
GlyA:[Ch]Cl	3:1
GlyA:Pro	3:1; 2:1; 1:1
MA:[Ch]Cl	1:1
PTSA:[Ch]Cl	1:1
Polyols	
G:[Ch]Cl	2:1
EG:[Ch]Cl	2:1

EG:[N_{1111}]Cl	2:1
EG:[N_{2222}]Cl	2:1
EG:[N_{3333}]Cl	2:1
EG:[N_{4444}]Cl	2:1
EG:[P_{4444}]Cl	2:1
Sugars	
Glu:[Ch]Cl	1:1
Xyl:[Ch]Cl	2:1
Fru:[Ch]Cl	1:1
Reference [47]	
U:[Ch]Cl	2:1

2.2 Solubility of lignin monomer model compounds in eutectic solvents

Each LMMCs (syringaldehyde, and syringic, vanillic and ferulic acids) was added in excess amount to 2.0 ± 0.1 g of each ES aqueous solution, pure water and neat ES. They were then equilibrated at a given temperature (303.15, 313.15 and 323.15 K) under constant agitation (300 rpm) using a stirring plate with heat control Pt1000, H03D series from LBX Instruments and a specific aluminum disk to support the sealed glass vials with a stirring bar (Figure 20, left). After the saturation was reached, the samples were filtered with 0.45 μm PTFE filters from Whatman to separate the macroscopic solid from the liquid phase. After the filtration, all samples were collected and put into an air oven at the same equilibrium temperature for 2 hours. Then, the samples of the liquid phase were diluted in distillated water, and the amount of LMMCs was quantified by Ultraviolet-visible (UV-vis) spectroscopy. For the results presented in the fundamental study (Chapter I), the Pharma-Spec spectrometer (SHIMADZU UV-1700), was used. The respective calibration curves are presented in Figure S1.1 and Table S1.1, at Supporting Information (SI). The results presented in Chapter II were obtained using the T60UV-Visible spectrometer (PG Instruments Ltd). See calibration curves in Figure S1.2 and Table S1.2 (SI). Note that, in some cases, the maximum absorbance of these compounds was shifted, due to the strong interaction between model compounds and ESs. At least three individual samples were quantified for each mixture and temperature.

Figure 20. Solubility assay of LMMCs (left) and technical lignins (right).

2.3 Solubility of technical lignins in eutectic solvents

Similar to the procedure described above for the study of the solubility of LMMCs, technical lignins (kraft and organosolv lignins) were added in excess amount to 2.0 ± 0.1 g of ESs aqueous solutions, pure water or neat ESs (Figure 20, right). To quantify the dissolved lignin in saturated ESs solutions, a new method based on Fourier-transform infrared (FTIR) spectroscopy was implemented (for more details see S2 in SI, the method and the calibration curve are presented in Figure S2.3 and Table S2.1). When pure water was used, due to the low solubility of lignin, the amount of dissolved lignin in samples was quantified by UV-vis spectroscopy, following the above reported methodology, at a wavelength of 280 nm using the calibration curve of alkali lignin (see Figure S1.2 and Table S1.2, SI).

2.4 Wood delignification process

Wood delignification assays were performed in a glass reaction tube heated in an oil bath at mild conditions (363.15 K, 8 h, wood/liquid ratio of 0.5/10 w/w and 300 rpm, at atmospheric pressure). After the delignification step, the reaction mixture was cooled overnight. The solid residue (pulp fibers or partially delignified wood) was separated from the reaction mixture by filtration, then the solid fraction was washed with ethanol and water until neutral pH and dried overnight in an oven with a vacuum system at 303.15 K, before gravimetric analysis. The solid fraction yield was calculated by the ratio between the dry weight of obtained solid fraction and the dry weight of the initial wood sample.

The dissolved lignin was precipitated from the ES liquor by the addition of cold distilled water. The solution was allowed to stand overnight, to promote their precipitation. The precipitated lignin was filtrated and washed with distilled water until a pH value of 4 – 5, and finally dried overnight in an oven with a vacuum system at 303.15 K, before gravimetric analysis. The precipitated lignin yield was calculated by the ratio between the dry weight of precipitated lignin and the dry weight of the initial wood sample. All experiments were performed in duplicate (for more details see Figure 21).

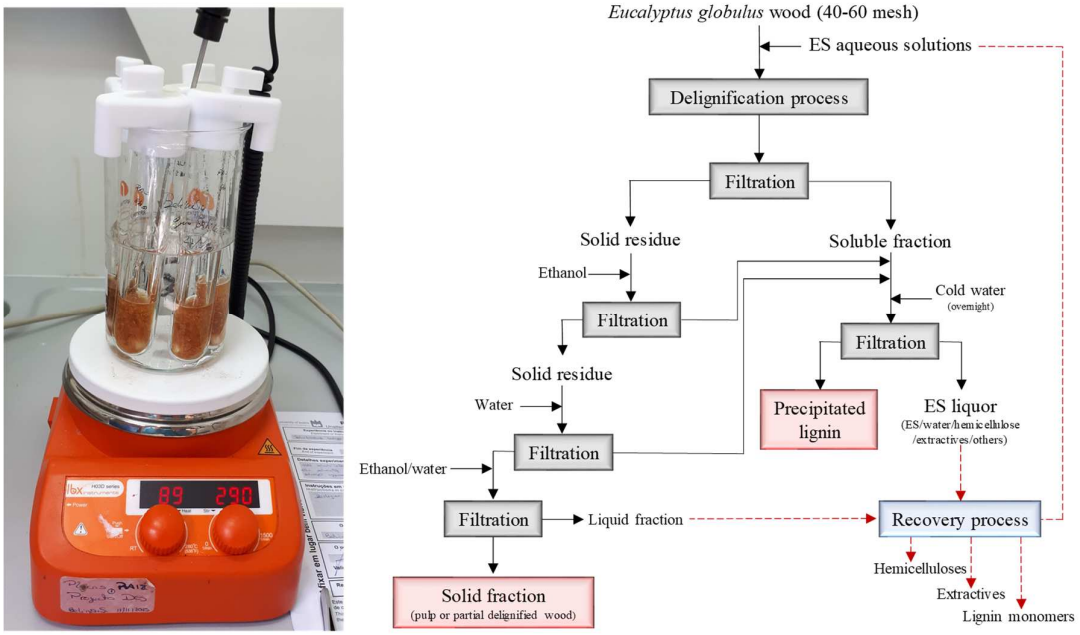

Figure 21. Wood delignification experimental setup (left) and flowchart of experimental methodology used to obtain the solid fraction and precipitated lignin (right). The recovery process (red dashed line) was not performed in this thesis.

Toward scaling the ES wood delignification process, preliminary tests were performed using a 300 ml PARR Stirred reactor 4843 (Figure 22) at mild conditions (363.15 K, 3 or 8 h, wood/liquid ratio of 6/120 w/w and 238 rpm, at atmospheric pressure). The final products (solid fraction and precipitated lignin) were obtained following the same methodology described in Figure 21.

Figure 22. PARR Stirred reactor 4843 (300 ml of capacity).

3. Optimization methodologies

Two optimization methodologies were adopted in this thesis. The Box-Behnken design for process variables optimization, such as temperature, time and ES concentration, was performed in Chapter III. The Simplex-Centroid design was implemented in Chapter IV to achieve the optimization of ternary ES aqueous solution used as solvent for wood delignification.

3.1 Box-Behnken design

The wood delignification conditions, such as temperature, time and ES concentration were optimized using the Box-Behnken design (BBD), a widely used form of the Response Surface Methodology.[85] The total number of experimental runs were determined using Design-Expert 11.0 software. The number of experiments (N) required for development of BBD is defined as: N = 2 x k x (k-1) + C_0 (where k is the number of factors and C_0 is the number of central points). A second order polynomial regression model equation was used to express the predicted responses (yields of solid fraction and precipitated lignin) as a function of independent variables:

$$Solid\ fraction\ or\ Precipitated\ lignin\ yields = \beta_0 + \sum_{i=1}^{k} \beta_i x_i + \sum_{i=1}^{k} \beta_{ii} (x_i)^2 + \sum_{i<j}^{k} \sum_{j}^{k} \beta_{ij} x_i x_j \quad (1)$$

where β_0, β_i, β_{ii} and β_{ij} are the regression coefficients. β_0 is a constant term which corresponds to the response when the value of x_i is zero for each parameter, β_i is the linear effect term, β_{ii} is the square effect term, β_{ij} is the interactive effect term and x_i, x_j are the variables that represent the important parameters affecting the characteristic of the process being carried out. Analysis of variance (ANOVA) was used to estimate the statistical significance of the main effects and interactions, coefficients and residues that provide an overall summary for the full model. The experimental BBD was performed at 3-factors and 3-level factorials to evaluate the effects and interactions of process variables [temperature (323.15, 343.15 and 363.15 K), time (1, 4.5 and 8 h) and ES concentration (50, 75 and 100 wt %)] on *E. globulus* wood delignification (see experimental design matrix in Table 14). BBD was performed in Chapter III, in order to find the optimal conditions for *E. globulus* wood delignification, where the responses precipitated lignin yield was desired to be maximum and the solid fraction yield close to 50 wt %. Once the maximized value of overall desirability is found, the optimal conditions are obtained.

Table 14. Experimental matrix of Box-Behnken design for process variable optimization of wood delignification process with ES aqueous solutions (Chapter III).

runs	Temperature / K	Time / h	ES concentration / wt %
1	343.15	4.5	75
2	363.15	1	75
3	343.15	8	100
4	343.15	4.5	75
5	343.15	1	50
6	343.15	8	50
7	343.15	4.5	75
8	323.15	4.5	50
9	323.15	8	75
10	363.15	8	75
11	343.15	4.5	75
12	323.15	4.5	100
13	323.15	1	75
14	363.15	4.5	50
15	343.15	4.5	75
16	343.15	1	100
17	363.15	4.5	100

3.2 Simplex-Centroid design

Mixture design is defined as special type of Response Surface Methodology in which the factors are the components of a mixture and the response is a function of the proportions of each components.[86] A simplex-centroid design was performed in Chapter IV to assess the effect of the three components of the ternary ES aqueous solution (NaPTS, PTSA and [Ch]Cl), as solvent for *E. globulus* wood delignification at mild conditions. Figure 23 shown the simplex-centroid design for three components, studied in Chapter IV. Each of the three vertices in the equilateral triangle corresponds to a pure blend (mixture that is made up to 100 % of a single component), and each of the three sides of the triangle represents a binary blend mixture that has none of one of the three components (the component labeled on the opposite vertex). Interior points in the triangle represent mixtures in which all three components are present at nonzero proportionate amounts. The centroid of the triangle corresponds to the mixture with equal proportions of all components.[85] Aqueous solutions of each design points at 50 wt % of water were prepared placing at the same time, the mixture components at the corresponding molar ratio and distilled water, in a glass beaker with a stirring bar and heated in an oil bath at 353.15 ± 0.01 K, with constant stirring until a transparent liquid was formed. After the liquid formation, the solvents were kept at this temperature for thirty minutes before use. The water content in ternary mixtures components was taken into account in the preparation of these aqueous solutions. All experiments were performed in duplicate.

Experimental results were fitted according to *Quadratic* model for solid fraction yield response and *Special Cubic* model for precipitated lignin yield response, in simplex-centroid design:

$$Solid\ fraction\ yield = \beta_1 x_1 + \beta_2 x_2 + \beta_3 x_3 + \beta_{12} x_1 x_2 + \beta_{13} x_1 x_3 + \beta_{23} x_2 x_3 \quad (2)$$

$$Precipitated\ lignin\ yield = \beta_1 x_1 + \beta_2 x_2 + \beta_3 x_3 + \beta_{12} x_1 x_2 + \beta_{13} x_1 x_3 + \beta_{23} x_2 x_3 + \beta_{123} x_1 x_2 x_3 \quad (3)$$

where, x_1, x_2 and x_3 are independent variables and correspond to the molar proportion of NaPTS, PTSA and [Ch]Cl in the mixture, respectively; and β comprises the estimated parameters.

The obtained results were statistically analyzed with a 95 % confidence level. Student's *t*-test was used to check the statistical significance of the adjusted data. The adequacy of the model was determined by evaluating the lack of fit, the regression coefficient (R^2) and the *F*-value obtained from the ANOVA that was generated. The Design-Expert 11.0 software was used for the statistical analysis and for representing the contour plots.

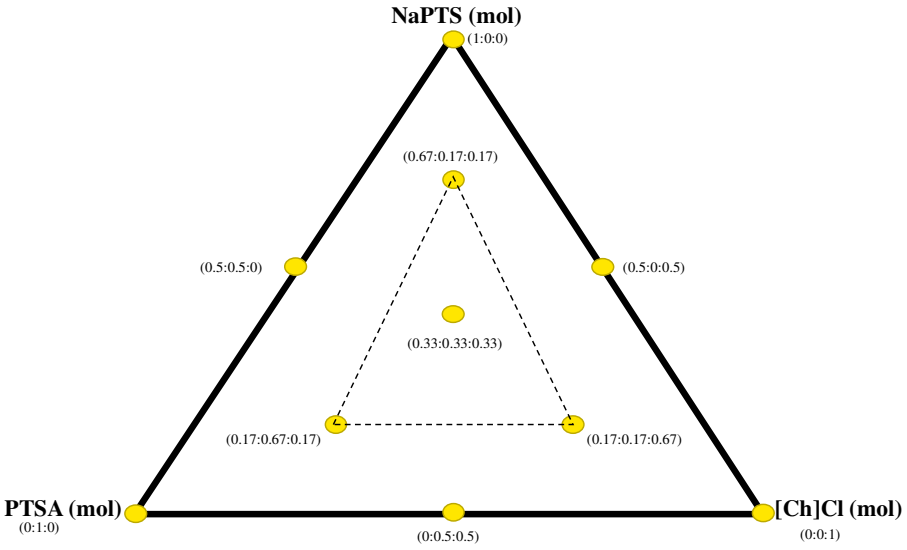

Figure 23. Simplex-Centroid design of ternary mixture NaPTS:PTSA:[Ch]Cl used to improve the wood delignification (Chapter IV).

4. Samples characterization

All the analytical techniques used to characterize the different samples in this thesis are summarized in Table 15. The detailed description of each techniques is presented below.

Table 15. Samples characterization.

Samples	**Analytical Techniques**
Saturated technical lignins (kraft and organosolv) and LMMCs in ES	Fourier-transform infrared (FTIR) spectroscopy Ultraviolet-visible (UV-vis) spectroscopy Dynamic light scattering (DLS)

E. globulus wood	FTIR spectroscopy Ash content Klason lignin
Solid fraction obtained from ES system or pulp from kraft process	FTIR spectroscopy Light-Polarized Optical Microscopy Solid-state ^{13}C Nuclear Magnetic Resonance (NMR) spectroscopy Klason lignin
Lignin (from conventional kraft or dioxane processes or ES system)	FTIR spectroscopy ^{1}H NMR spectroscopy (acetylated lignin) ^{13}C quantitative NMR spectroscopy Elemental analysis

Fourier-transform infrared (FTIR) spectroscopy. The FTIR spectra of solid fraction, kraft pulp, technical lignins and precipitated lignin were recorded using a FTIR System Spectrum BX (PerkinElmer), coupled with a universal ATR sampling accessory, in transmittance (%) mode from 4000 to 600 cm^{-1} with resolution of 4 cm^{-1} and interval of 2 cm^{-1}. Each spectrum corresponded to the average of 32 scans. All spectra were baseline corrected for further analysis.

Dynamic light scattering (DLS). To evaluate the presence of ES-solute nanoaggregates, as well as to determine their size, saturated solutions of LMMCs and technical lignins (organosolv and kraft) in aqueous solution of PA:U (2:1) at 50 wt % and 323.15 K were analyzed by dynamic light scattering using a Malvern Zetasizer Nano-ZS from Malvern Instruments (zetasizer software version 7.12). Samples were measured in disposable glass cuvettes at temperature of 323.15 K. Data were then acquired in the automatic mode, ensuring that enough photons were accumulated for the result to be statistically relevant. At least two individual samples were analyzed in triplicated for each sample and before the measurements, all samples were filtered with 0.45 μm PTFE filters from Whatman. The aqueous solution of PA:U (2:1) at 50 wt % viscosity and refractive index at 323.15 K were previously measured.

Ash content. Ash content in wood was determined gravimetrically by calcination at 798.15 ± 298.15 K according to Tappi standard T 211 om-12.[87]

Klason lignin. Klason lignin content in wood and solid fractions were determined by the Klason method according to Tappi standard T 222 om-98.[88]

Light-polarized optical microscopy. The cellulose fibers images of the kraft pulp and solid fraction were acquired using an Olympus BX-51 light polarized microscope (Olympus Co., Tokyo, Japan).

Solid-state ^{13}C Nuclear Magnetic Resonance (NMR) spectroscopy. Solid state ^{13}C NMR spectra of kraft pulp and solid fractions were recorded using a Bruker AVANCE III 400 MHz spectrometer, with CP/MAS probe and operating at 75 MHz.

^{13}C NMR spectroscopy. Quantitative ^{13}C NMR spectra were recorded using a Bruker ASCENDTM 500 spectrometer operating at 125.77 MHz. About 500 mg of dried lignins samples were dissolved in 2.2 mL of deuterated dimethyl sulfoxide (DMSO-d_6). The mixture was placed into 10 mm dimeter tubes and the spectra were recorded at 303.15 K with TMS as internal reference. The relaxation delay was 10 s and about 1800 scans were collected (90° pulse).

^{1}H NMR spectroscopy. Prior to ^{1}H NMR analysis, lignins were acetylated following known procedure.[89] The acetylated lignins were dissolved in deuterated chloroform ($CDCl_3$) (10-12 mg/0.7 mL solvent), placed into 5 mm diameter tubes, and the spectra were recorded using a Bruker ASCENDTM 500 spectrometer operating at 500.16 MHz, at room temperature. Sodium 3-(trimethylsilyl) propionate-d_4 (TMS) was used as an internal standard ($\delta = 0.00$). The relaxation delay was 3 s and about 200 scans were collected (90° pulse).

Elemental analysis. Carbon, hydrogen, sulfur and nitrogen contents in lignin samples were determined using a Truspec 630-200-200 equipment. The carbon, hydrogen, sulfur contents were detected by infrared absorption and the nitrogen content by thermal conductivity. The combustion furnace temperature was 1348.15 K and the afterburner temperature was 1123.15 K. The oxygen content was calculated by subtracting the carbon, hydrogen, sulfur and nitrogen percentages from 100 %.

PART A

FUNDAMENTAL STUDY

Chapter I

Enhanced solubility of Lignin monomer model compounds and Technical lignins in aqueous solutions of Eutectic Solvents

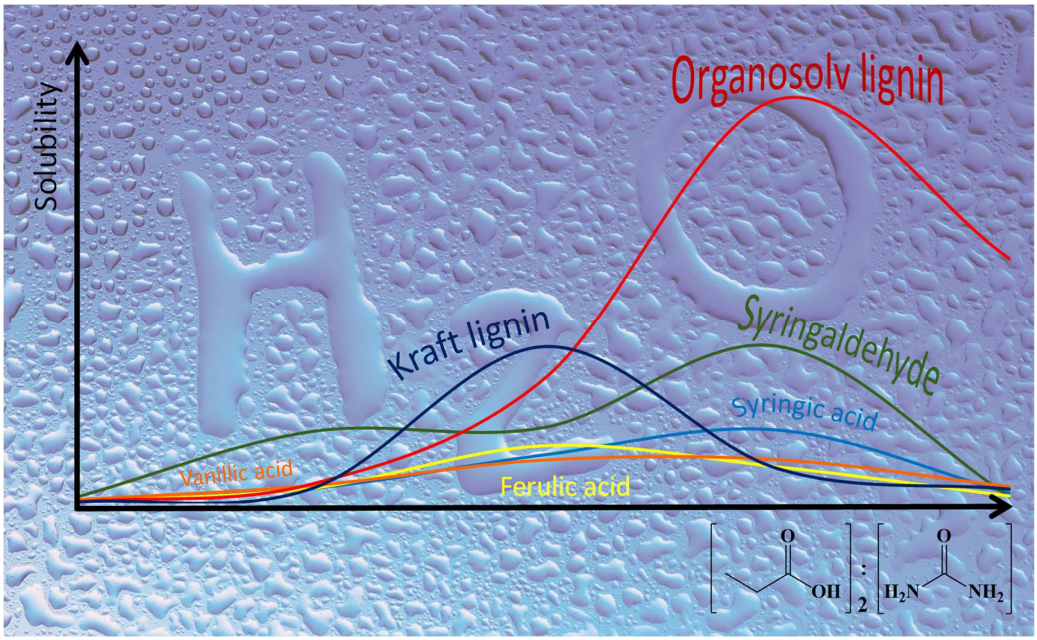

Aqueous solutions of eutectic solvents enhance the solubility of technical lignins more than 200 times opening the possibility for new lignin extraction and conversion processes

Adapted from:

Belinda Soares; Daniel J. P. Tavares; José Luis Amaral[†]; Armando J. D. Silvestre; Carmen S. R. Freire and João A. P. Coutinho. *ACS Sustainable Chem. Eng.* **2017**, 5 (5), pp. 4056 – 4065. DOI: 10.101021/acssuschemeng.7b00053.

[†] in memory of José Luis Amaral who passed away in January 2018

ABSTRACT

The solubilities of lignin monomer model compounds and technical lignins (organosolv and kraft) in aqueous solutions of several eutectic solvents were here investigated. The effects of eutectic solvents components, temperature and concentration, were evaluated. The results show aqueous solutions of eutectic solvents to be a new class of powerful solvents where both the hydrogen bond donor and the hydrogen bond acceptor synergistically contribute to increase the solubility of the lignin model compounds, being the dispersive interactions with lignin the driving force behind the good performance of eutectic solvents. The solubility of the model compounds is shown to be a good guide for the selection of the best eutectic solvents for technical lignin solubility, leading to identifying an aqueous solution of eutectic solvents allowing a solubility enhancement of (322 ± 12)- and (473 ± 28)-fold times for kraft and organosolv lignin, respectively. The results indicate that the solubility of the technical lignins and their monomers in eutectic solvents aqueous solutions is driven by a hydrotropic mechanism, confirmed by dynamic light scattering, that is here observed for the first with eutectic solvents as hydrotropes.

MAIN GOAL & STRATEGY

To assess the potential of eutectic solvents as new solvents for delignification process, and subsequent use of lignin, it is important to study the dissolution of lignin in neat eutectic solvents and their aqueous solutions. Aiming at select the best eutectic solvent to be used as delignification medium, the solubility of lignin monomer model compounds in aqueous solutions of eutectic solvents was investigated. The effects of eutectic solvents components (chemical structure and HBD:HBA molar ratio), temperature and concentration, were investigated. This study was used to assess the transferability of the information based on these studies with lignin monomers to real lignin samples and to identify the best eutectic solvents for the dissolution of technical lignins (organosolv and kraft). This work intends to contribute to the achievement of a deeper and sounder knowledge about the solubility of lignin in aqueous solutions of eutectic solvents opening new perspectives for wood delignification and lignin conversion processes.

RESULTS & DISCUSSION

1. Solubility of lignin monomer model compounds in eutectic solvents

Aiming at investigating the potential of ESs aqueous solutions for delignification processes, and bearing in mind the complexity of lignin, the solubilities of some LMMCs, such as syringaldehyde, and vanillic, syringic and ferulic acids, in aqueous solutions of ESs were determined. It is well known that the solubility of a substance fundamentally depends on the physical and chemical properties of the solute and solvent as well as on the temperature, pressure and on the pH of the solution. Considering that the ESs properties depend on the HBD and HBA structures, it is crucial to evaluate the effects of HBDs and HBAs, their molar ratio, concentration in the aqueous solution, and temperature on the solubility of LMMCs. In order to achieve this goal, the lignin model compound selected to develop this preliminary study was syringic acid, one of the main components of oxidatively depolymerized technical lignin.[43] The solubilities of these LMMCs in pure water at 303.15, 313.15 and 323.15 K, were also measured for comparative purposes and are reported in Table 16.

Table 16. Experimental solubilities of LMMCs and technical lignins in pure water.

	Solubility ± σ^a / mg g^{-1}		
T / K	**303.15**	**313.15**	**323.15**
LMMCs			
syringic acid	1.28 ± 0.01	1.60 ± 0.03	1.87 ± 0.08
syringaldehyde	2.92 ± 0.01	4.41 ± 0.10	7.91 ± 0.76
vanillic acid	1.81 ± 0.06	2.93 ± 0.06	3.24 ± 0.11
ferulic acid	0.63 ± 0.06	0.82 ± 0.03	1.53 ± 0.05
Technical lignins			
organosolv lignin	-	0.93 ± 0.17	1.07 ± 0.24
kraft lignin	-	0.64 ± 0.002	0.79 ± 0.009

[a] σ, standard deviation.

1.1 Effect of eutectic solvents components

Several families of ESs were prepared combining HBDs (carboxylic acids, polyols, sugars and urea (U)) with HBAs ([Ch]Cl, Pro, Bet and U) at a molar ratio that results in a liquid ESs at room temperature, aiming at studying the effects of HBDs and HBAs on

syringic acid solubility. Therefore, in order to study the impact of the HBD on syringic acid solubility a series of ESs with common HBA were used. Based on the well-known U:[Ch]Cl system,[47,84] the favorable properties of [Ch]Cl, its low price and "green" characteristics overall,[90] this compound was adopted as the HBA for this study. Syringic acid solubility was studied in 25 wt % aqueous solution of ESs (HBD:[Ch]Cl) at 303.15 K. The influence of HBD on the solubility enhancement of syringic acid and the respective pH of the ESs aqueous solutions are depicted in Figure 24. The detailed values of solubility and pH, and the respective standard deviations, are reported in Table S3.1 (SI). On this figure the *S* and S_0 represent the solubility (mg g^{-1}) of syringic acid in the aqueous solutions of the ES and in pure water, respectively. Therefore, the S/S_0 ratio represents the solubility enhancement by the use of ES as solvent.

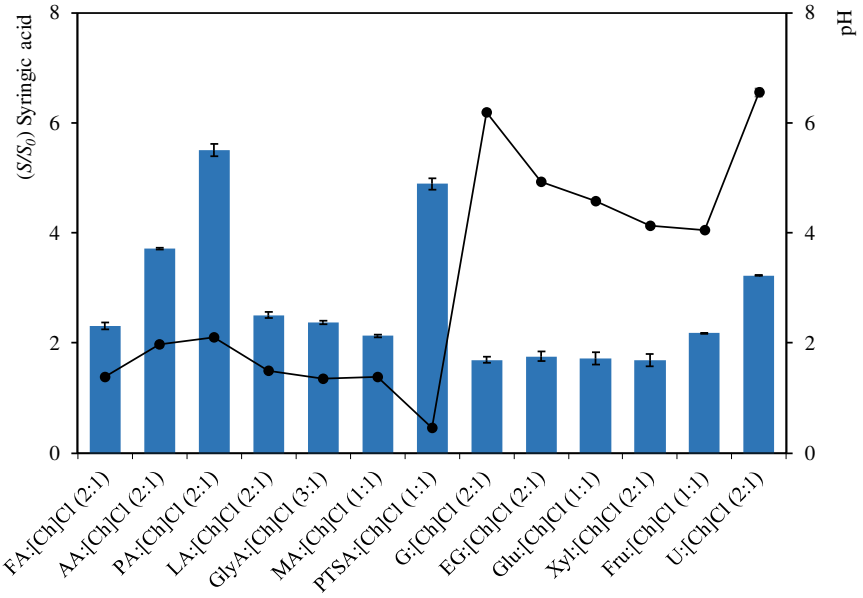

Figure 24. Influence of HBDs on the solubility enhancement of syringic acid in aqueous solutions with 25 wt % of ES, at 303.15 K. The pH values of the respective ES aqueous solutions are presented in black dots.

The results reported in Figure 24, show that the HBD chemical structure has a significant influence on the syringic acid solubility. Sugars and polyols-based ESs exhibited a low ability to solubilize syringic acid, leading to a lower solubility enhancement (around 2-fold) than the U:[Ch]Cl reference ES (3-fold). A large number of hydroxyl groups on these HBDs makes them too polar and they probably form a network of hydrogen bonds that becomes a hindrance to syringic acid solubilization.[91] A positive influence of carboxylic

acids-based ESs on syringic acid solubility was observed, with solubility enhancements that nearly reach 6-fold. Among the carboxylic acids-based ESs, those with PTSA and PA provided the best results (4.9- and 5.5-fold, respectively). Furthermore, it is perceptible that the alkyl side chain length has an impact over the syringic acid solubility as well as the presence or absence of functional groups on the acids chemical structure. As depicted in Figure 25, an increasing alkyl side chain length (from FA, to AA and PA) results in an increased solubility of the solute. The presence of hydroxyl groups in the acid alkyl chain of LA and GlyA was observed to have a negative impact in syringic acid solubility when compared with PA and AA, respectively. In fact, an increase in syringic acid solubility was observed when decreasing the polarity of the carboxylic acids (*i.e.* from LA, to AA and PA). Similarly, LA demonstrated to have a better performance than MA. The presence of a second carboxylic group may be the reason for the lower solubilization performance of MA. Moreover, an enhanced performance of PTSA was expected due to the presence of the aromatic group and the possibility to establish π···π interactions with the aromatic ring of syringic acid. Although PTSA was one of the best HBD, its performance was worse than that of the linear carboxylic acids.

In general, it seems that an increase in syringic acid solubility is achieved by decreasing the polarity of the carboxylic acids. These results suggest that the dispersive interactions between the organic acid alkyl chain and the syringic acid structure are the main reason for the good performance of PA, instead of the hydrogen bond interactions, π···π interactions and the polar character of polyols, sugars and some organic acids (LA, GlyA and MA). Furthermore, the pH value of ESs aqueous solutions seems to have no significant effect in the solubility of syringic acid. Overall PA:[Ch]Cl with a molar ratio of 2:1 presented the best solubility enhancement.

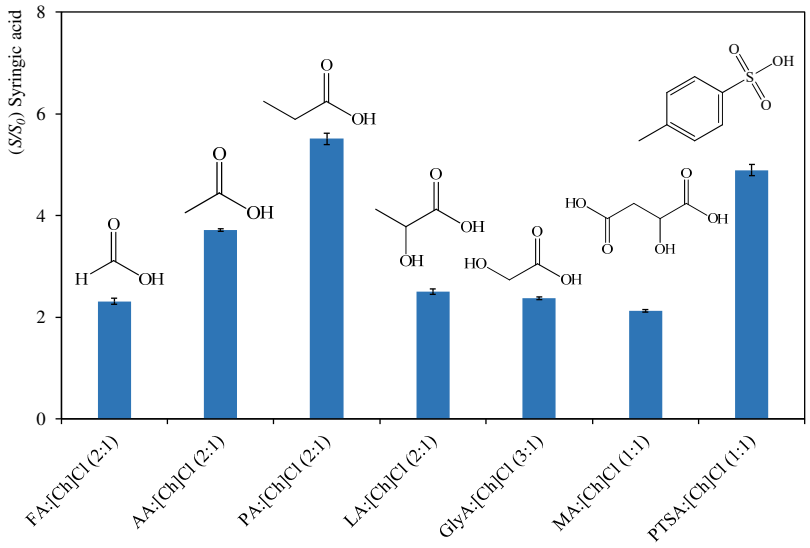

Figure 25. Influence of carboxylic acids HBDs chemical structure on the solubility enhancement of syringic acid in aqueous solutions with 25 wt % of ES, at 303.15 K.

Considering the advantageous performance of the carboxylic acids-based ES, three different carboxylic acids (LA, AA and PA) were combined with four HBAs ([Ch]Cl, Pro, Bet and U) in order to evaluate the effect of HBAs on syringic acid solubility. The solubility enhancement of syringic acid was again studied in 25 wt % aqueous solutions of ESs at 303.15 K. The influence of HBA on the solubility enhancement of syringic acid and the pH of each ES aqueous solution are depicted in Figure 26. The detailed values of solubility and pH, and the respective standard deviations are reported in Table S3.1 (SI).

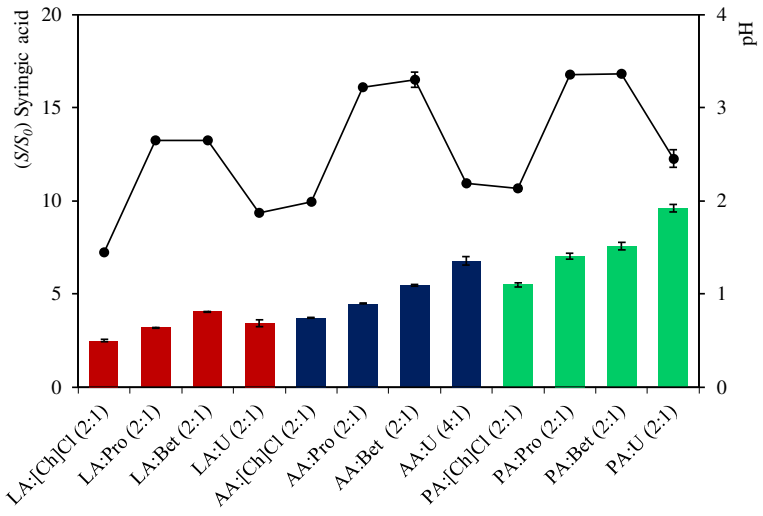

Figure 26. Influence of HBAs on the solubility enhancement of syringic acid in aqueous solutions with 25 wt % of ES, at 303.15 K. The pH value of the respective ES aqueous solutions is presented in black dots.

The results reported in Figure 26 show that the solubility of syringic acid is also affected by the HBAs, increasing in the sequence of [Ch]Cl < Pro < Bet < U, independently of the carboxylic acids studied, with the exception of LA. In this case, Bet showed a somewhat better syringic acid solubility enhancement (4-fold) than U (3.4-fold) as HBA. In general, the ESs prepared with PA as HBD displayed the best solubility enhancements, being PA:U the best ES in terms of solubility enhancement (around 10-fold). Furthermore, the replacement of [Ch]Cl by U lead to an increase of 4-fold on the solubility of syringic acid, explained by the increase of dispersive interactions associated with U. Once again, no effects of the pH in the syringic acid solubility in ESs aqueous solutions were perceived (see Figure 26).

1.2 Effect of eutectic solvent molar ratio

The composition of ES (HBD:HBA ratio) plays an important role on its physico-chemical properties. By changing the HBD:HBA molar ratio it is possible to obtain, at room temperature, a solid, a liquid or a combination of both.[57,92] It is thus important to understand if the solubility enhancement added by using ES resulted of a possible synergetic effect between HBD and HBA. For this purpose, four carboxylic acids-based ESs (PA:[Ch]Cl, LA:[Ch]Cl, GlyA:Pro and PA:U) with different molar ratios were studied in aqueous solutions with 25 wt % at 303.15 K. The detailed values of solubility and the respective standard deviations, are reported in Table S3.1 (SI).

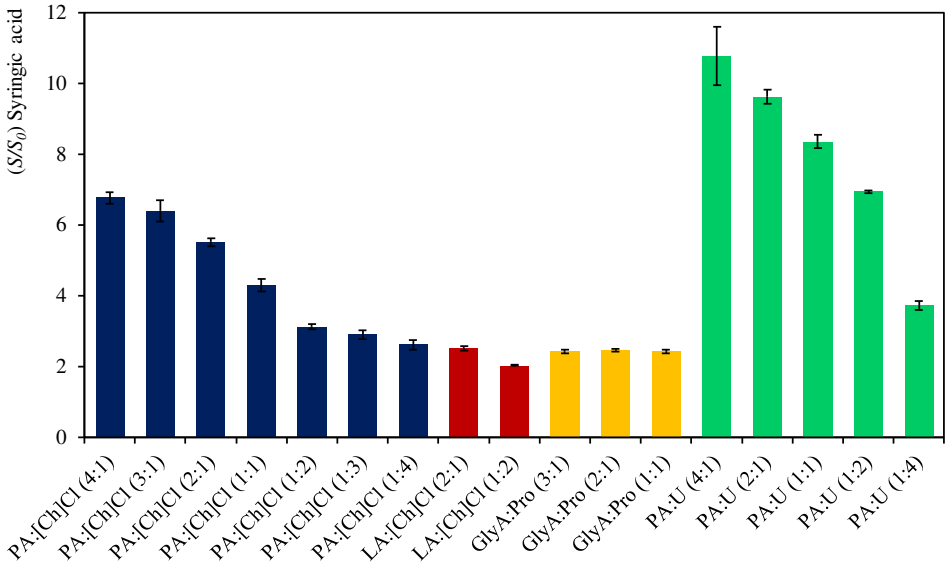

Figure 27. Influence of HBD:HBA molar ratio on the solubility enhancement of syringic acid in aqueous solutions with 25 wt % of ES, at 303.15 K.

According to the results shown in Figure 27 the molar ratio has a significant impact in the syringic acid solubility enhancement. Indeed, the solubility increased with the increase of HBD molar ratio, suggesting that the increase of dispersive interactions between the HBD and syringic acid promotes the good performance of ES aqueous solutions. Again, better results can be obtained by using PA:U rather than PA:[Ch]Cl, which can be explained by the contribution of both components (HBD and HBA) to establish dispersive interactions with the lignin model compound.

The results here reported show the potential of PA:U aqueous solutions at 303.15 K to enhance the solubility of syringic acid. However, the focus of this work it is not the evaluation of the performance of ESs to solubilize syringic acid but the selection of the best ES to enhance the solubility of technical lignins. For a more complete evaluation of the ESs potential, the solubility of other monomer aromatics compounds such as syringaldehyde, vanillic and ferulic acids in aqueous solution with 25 wt % of PA:U at different molar ratio and 303.15 K were also studied and the results are reported in Figure 28. The detailed values of solubility and the respective standard deviations, are reported in Table S3.1 and S3.2 (SI).

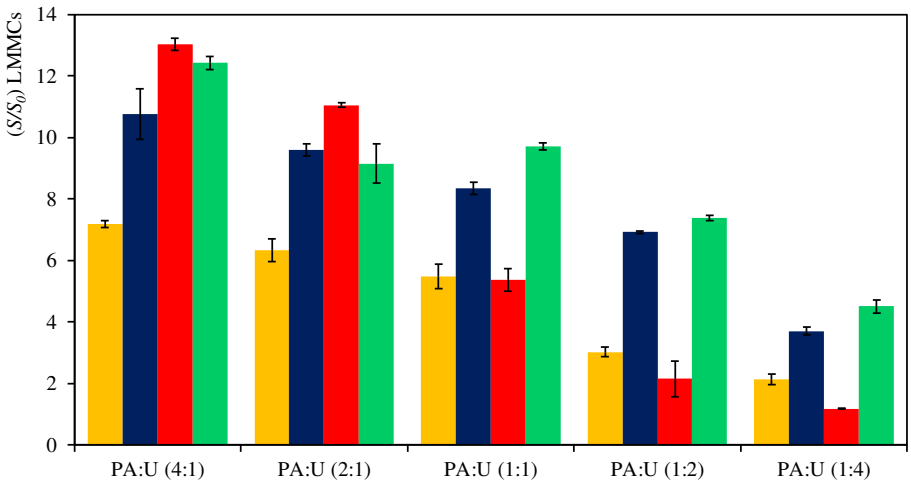

Figure 28. Influence of HBD:HBA molar ratio a on the solubility enhancement of LMMCs (syringaldehyde (green), syringic (blue), vanillic (yellow) and ferulic (red) acids), in aqueous solutions with 25 wt % of ES, at 303.15 K.

The results reported in Figure 28 show a clear impact of the HBD:HBA molar ratio on the solubility enhancement of all LMMCs investigated. The increase of molar ratio improved the LMMCs solubility, as previously shown in Figure 27 for syringic acid at the same conditions. Considering the solubility enhancement of each LMMCs in PA:U aqueous solutions, it is possible to observe that PA:U with molar ratio 4:1 and 2:1 show similar solubilities in the case of vanillic and syringic acids and a slight increase of solubility was observed for syringaldehyde and ferulic acid using PA:U (4:1). These results suggest that the enhanced solubilization observed in ESs aqueous solutions resulted from a possible synergistic effect between HBD and HBA. Taking into account the similar solubility enhancement obtained for most of the LMMCs using PA:U (4:1) and (2:1) aqueous solutions at 303.15 K, the PA:U (2:1) was selected to study the impact of the ES concentration and temperature upon its ability to enhance the solubility of the LMMCs investigated. The PA:U (2:1) has also the advantage over the PA:U (4:1) because of having a lower vapor pressure as result of a lower concentration in PA, and being closer to the eutectic point of the mixture thus having a larger liquidus range.

1.3 Effect of eutectic solvent concentration and temperature

The effect of ES concentration in aqueous solution was studied in the entire concentration range, from pure water to neat ES at three different temperatures (303.15, 313.15 and 323.15 K). The impact of PA:U (2:1) concentration and temperature on the solubility enhancement of LMMCs are presented in Figure 29. The detailed solubility values and the respective standard deviations, are reported in Table S3.3 (SI).

As expected, the solubilities of LMMCs in the studied concentrations range increased with the temperature. This trend may not be clear in Figure 29 due to the fact that the plot is represented in S/S_0 for each temperature, but it can be confirmed in the detailed data represented in Table S3.3 (SI). Furthermore, it is clear the influence of PA:U (2:1) concentration on the solubility enhancement of each LMMCs as depicted in Figure 29. Aqueous solutions of PA:U (2:1) at concentrations of 50 and 75 wt % seem to allow the best solubility enhancement of LMMCs. Considering the combination of concentration and temperature effects, at 323.15 K and a concentration of 75 wt % the PA:U (2:1) enhanced the syringic and vanillic acids solubilities by 47- and 16-fold, respectively, while syringaldehyde achieved a 42-fold increase at 313.15 K and a ES concentration of 50 wt % at this temperature potentiated the solubility enhancement of ferulic acid of 51-fold at the same temperature. The shape of these curves, with strong maxima at intermediate compositions between pure water and the neat ES suggest that the solubility of these monomer model compounds is being driven by a hydrotropic mechanism, previously described for ionic liquids,[93] and confirmed by the presence of small aggregates typical from the density fluctuations[66] of the hydrotropic solubilization, using dynamic light scattering analyses as described below. A hydrotropic solubilization driven by ES is here observed for the first time since, to the best of our knowledge, this has never been previously reported.

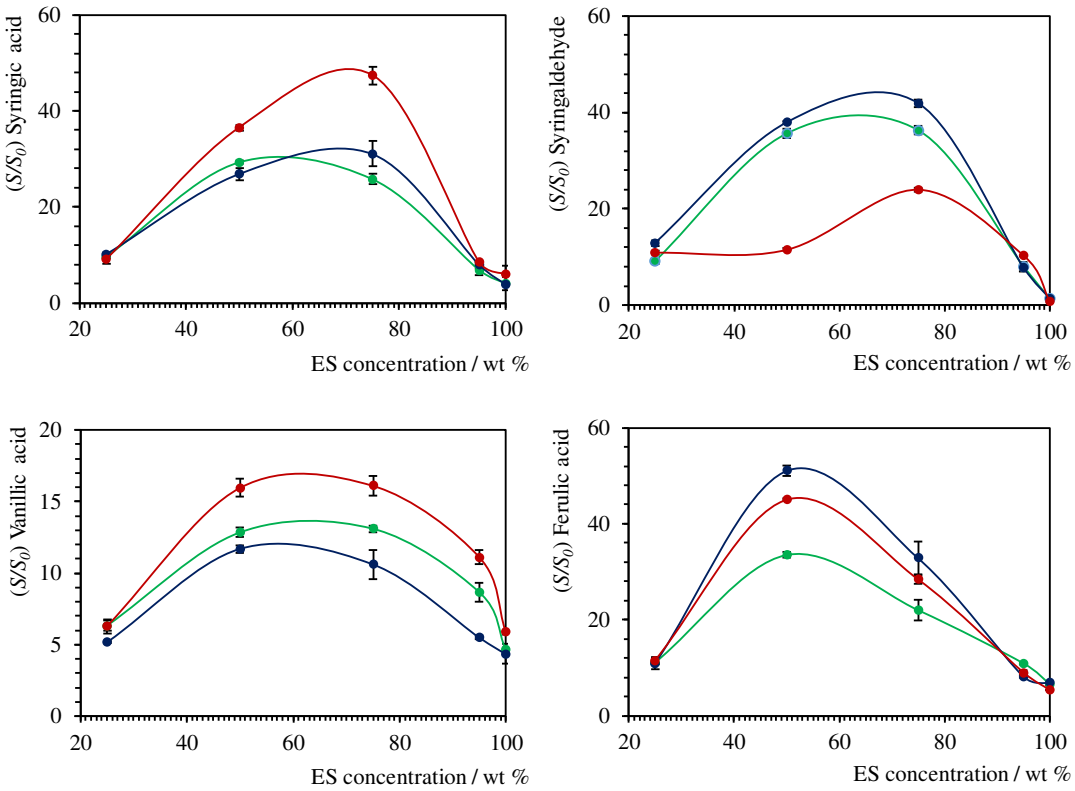

Figure 29. Influence of PA:U (2:1) concentration and temperature on the solubility enhancement of LMMCs (syringaldehyde, and syringic, vanillic and ferulic acids). The different temperatures studied were 303.15 K (green), 313.15 K (blue) and 323.15 K (red).

The results hitherto reported reveal that PA:U (2:1) aqueous solutions, have an impressive potential to solubilize LMMCs, specially ferulic acid and syringaldehyde at low temperature and syringic acid at high temperature. Its ability to solubilize vanillic acid seems to be weaker. The selectivity demonstrated here by PA:U (2:1) aqueous solution to solubilize aromatic aldehydes and acids, can open new pathways for the fractionation of phenolic compounds from complex mixtures obtained, for example, by lignin depolymerization, e.g. from black liquors in pulp and paper industry, where the selective recovery and separation of these aromatic compounds is still an important goal in the biorefinery context aiming at their future valorization.[94] Finally, these results also suggest that aqueous solutions of PA:U (2:1) at 50 wt % could be a good candidate to solubilize technical lignin. This subject will be investigated below.

2. Solubility of technical lignins in eutectic solvents

Based on the results of LMMCs solubility in ES aqueous solutions reported above and keeping in mind the importance of dissolving lignin in aqueous media, the solubility of organosolv and kraft lignin using PA:U (2:1) was evaluated in aqueous solutions with the ES concentrations of 25, 50, 75 and 100 wt % at two temperatures (313.15 and 323.15 K). The detailed values of solubility and the respective standard deviations, are reported in Table S3.4 (SI). The solubility of technical lignins (organosolv and kraft) in pure water at 313.15 and 323.15 K were also measured aiming to determine the solubility enhancement added by using this ES. These values are reported in Table 16.

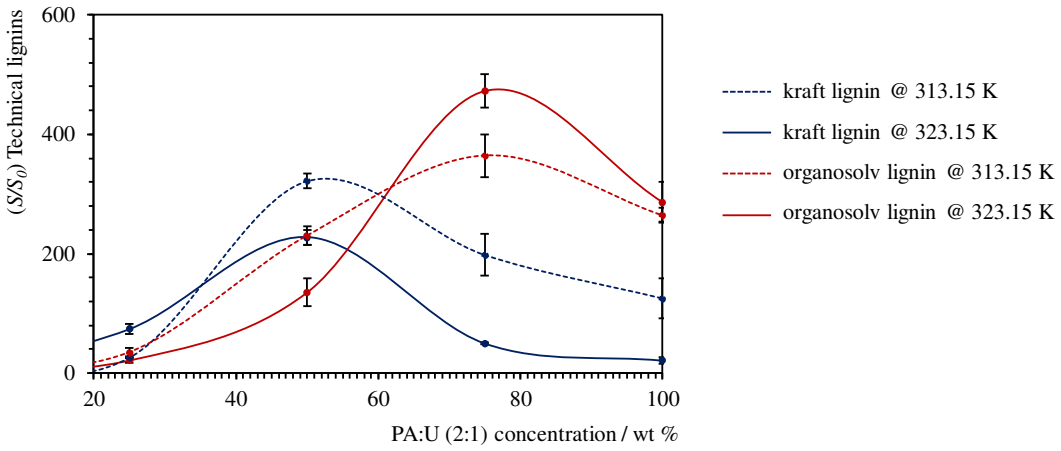

Figure 30. Influence of PA:U (2:1) concentrations on the solubility of organosolv and kraft lignins at 313.15 and 323.15 K.

The ability of this ES (neat or in aqueous solutions) to enhance organosolv and kraft lignins solubility is depicted in Figure 30. The similarity of the solubility trend here reported with those previously observed for LMMCs under the same conditions, is remarkable suggesting that the organosolv and kraft lignins solubilities in the ES aqueous solutions are also driven by an hydrotropic mechanism, what is confirmed below by the presence of nanometric aggregates resulting from density fluctuations[66] typical of these solubilization mechanisms.[95] The organosolv and kraft lignins solubility enhancement depends on both the ES concentration and temperature, being the best results obtained at 313.15 and 323.15 K for kraft and organosolv lignins, respectively. Concerning the ES concentration, it is possible to observe that aqueous solutions at 50 wt % of PA:U (2:1) achieved an kraft lignin solubility

enhancement of (322 ± 12)-fold and organosolv lignin solubility enhancement of (473 ± 28)-fold. This is a remarkable performance of ES aqueous solution taking into account the low solubility of kraft and organosolv lignins in pure water (Table 16). Considering the ability of alkali aqueous solutions (e.g. NaOH, pH 10) to solubilize lignin and aromatic and phenolic acids derived from lignin (e.g. vanillic, syringic acids, etc.) reported by Evstigneev,[96] some experiments were also carried out in order to compare the results achieved with the potential of NaOH aqueous solution (at pH 10) to enhance the solubility of kraft lignin and LMMCs as show in Figure 31. The detailed values of solubility and the respective standard deviations, are reported in Table S3.5 (SI). Albeit aqueous NaOH shows an effective solubility enhancement of about 127-fold in kraft lignin and 1.3-fold in LMMCs, these values are much lower than those achieved with ES aqueous solutions, further supporting their huge potential to solubilize technical lignins and LMMCs.

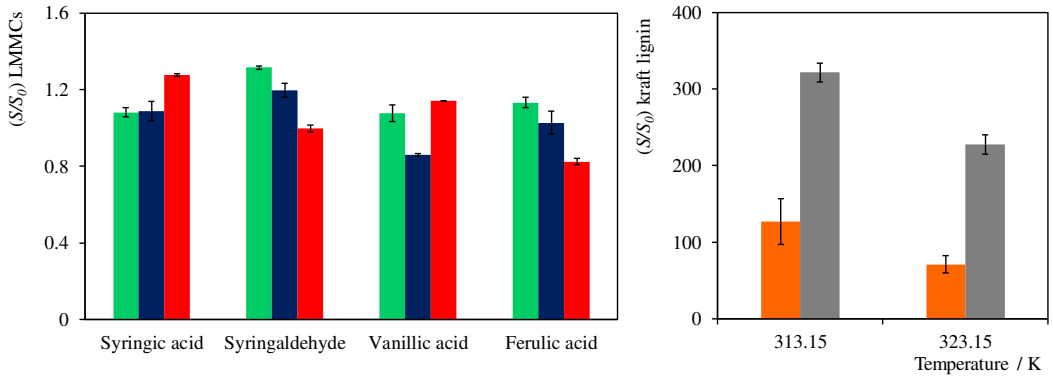

Figure 31. Solubility of LMMCs (left) in NaOH aqueous solution, at 303.15 (green), 313.15 (blue) and 323.15 K (red). Solubility of kraft lignin (right) in NaOH aqueous solution (orange) and PA:U (2:1) 50 wt % aqueous solution (grey), at 313.15 and 323.15 K.

In this work, the evaluation of the ES potential to enhance the solubility of lignin was carried out using a kraft lignin isolated from *E. globulus* industrial kraft liquor and organosolv lignin from *E. globulus* wood (a more preserved lignin when compared with the kraft lignin[43]). Taking into account the chemical structure of the lignin it seems to be possible to anticipate the performance of ES aqueous solution on the lignin solubilization through the evaluation of LMMCs, as demonstrated in this work.

3. Dynamic light scattering

In order to probe the mechanism of hydrotropy, suggested above to be driving the enhanced solubilization of the technical lignins and their monomeric precursors, the presence of nanoaggregates, resulting from the density fluctuation[66] associated to the formation of hydrotrope-solute aggregates, was assessed by dynamic light scattering (DLS) in aqueous solutions (aqueous solution of PA:U (2:1) at 50 wt % and 323.15 K) of technical lignins and LMMCs. The size of the nanoaggregates detected in these solutions and the respective standard deviations, are reported in Figure 32 and Table S3.6 (SI).

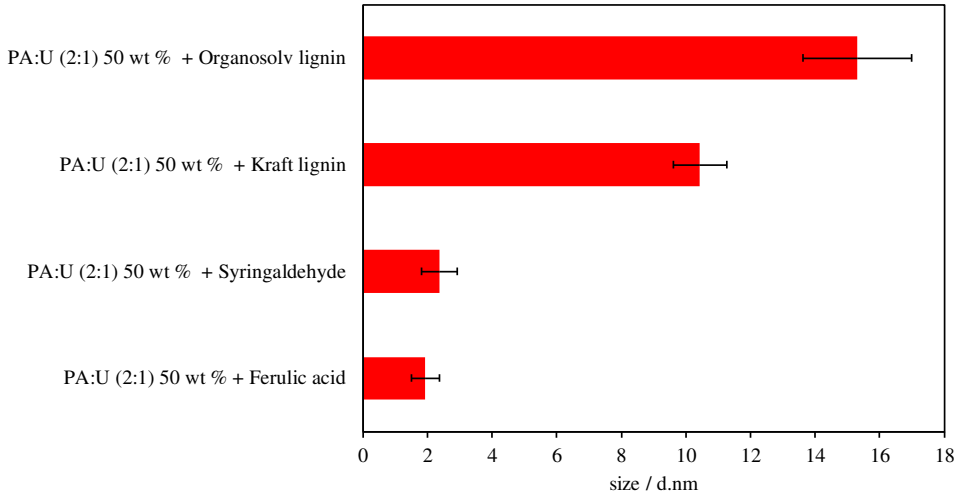

Figure 32. Nanoaggregate size present in saturated aqueous solutions of technical lignin and LMMCs in PA:U (2:1) at 50 wt % and 323.15 K, analyzed by DLS.

While no aggregates were observed in the aqueous solutions of PA:U (2:1) at 50 wt %, the DLS results confirm the presence of nanoaggregates on the saturated aqueous solutions of technical lignins (kraft and organosolv) and LMMCs (syringaldehyde and ferulic acid) with sizes above 2 nm. These observations are in good agreement with the results previously reported by our research team for the solubility of phenolic compounds in aqueous solutions of ionic liquids.[95] The presence of nanoaggregates in the solutions of syringic and vanillic acids were also probed by DLS, but the size of the aggregates observed were below the equipment resolution and thus cannot be trusted. The presence of these nanoaggregates is expected in hydrotropic solutions and supports the previous suggestion that the mechanism of hydrotropic solubilization of lignin and the aromatic and phenolic

acids derived from lignin depolymerization is dominated by the hydrotrope-solute aggregation, as previously described for ionic liquids and others hydrotropes.[66,95]

CONCLUSIONS

In this work, a comprehensive study on the solubility of lignin monomer model compounds in neat eutectic solvents and their aqueous solutions was performed. It was here disclosed, for the first time, the ability of eutectic solvents to enhance the solubility of poorly soluble lignin derived compounds such as syringaldehyde, and syringic, vanillic and ferulic acids and technical lignins itself in aqueous solutions of eutectic solvents through an hydrotropic mechanism, with the dispersive interactions being the main reason for the good performance of eutectic solvents dissolution ability. The influence of hydrogen bond donors and hydrogen bond acceptors chemical structure, molar ratio, concentration and temperature on lignin monomer model compounds solubility were investigated and the results show that both hydrogen bond donors and hydrogen bond acceptors play a significant role in the solubilization of these compounds with a possible synergistic effect between the two eutectic solvents starting materials. Maximum solubilization of model compounds (ferulic, syringic and vanillic acids, and syringaldehyde) in PA:U (2:1) aqueous solution [(51.1 ± 1.1)-, (47.4 ± 1.9)- and (16.1 ± 0.7)-fold, and (41.9 ± 0.8)-fold, respectively] were achieved at 50 or 75 wt % of PA:U (2:1) and 313.15 or 323.15 K.

Regarding the kraft and organosolv lignins solubilities in eutectic solvents, a remarkably similar behavior to that obtained for lignin monomer model compounds was observed. These results suggest that the lignin solubility in aqueous solution of eutectic solvents results from a hydrotropic mechanism, confirmed by dynamic light scattering analysis and that it is possible to anticipate the lignin solubility in eutectic solvents aqueous solution and select the best eutectic solvent by studying the solubility of lignin monomer model compounds. Maximum solubilization of kraft and organosolv lignins in PA:U (2:1) aqueous solution [(322 ± 12)- and (473 ± 28)-fold, respectively] were achieved at 50 wt % of PA:U (2:1).This work provides a new understanding of lignin solubilization using eutectic solvents aqueous solutions, and demonstrates the potential of eutectic solvents to be used in new delignification and lignin conversion processes, as well as novel solvents to achieve the fractionation/purification of aromatic components present in black liquor.

Chapter II

Hydrotropy and Cosolvency in Lignin Solubilization with Eutectic Solvents

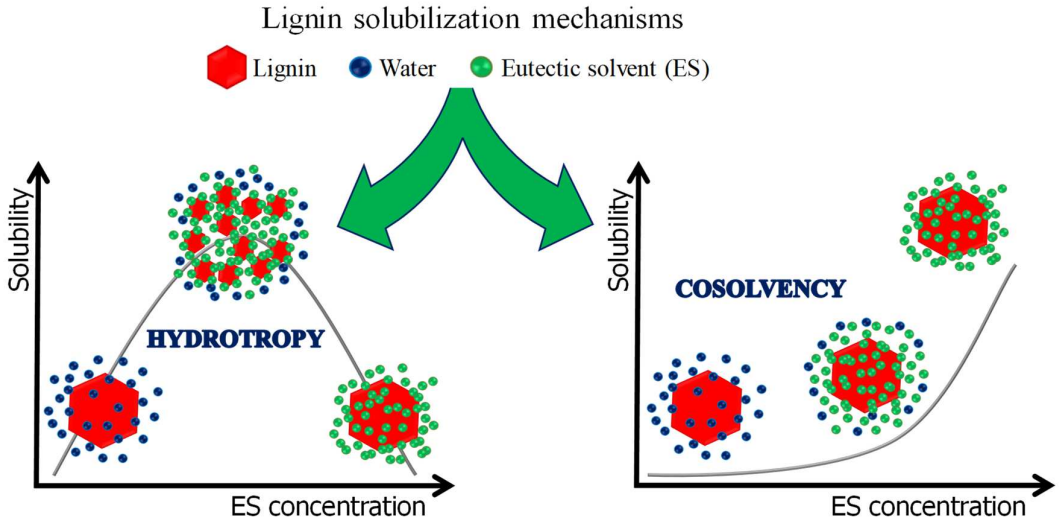

Two mechanisms are shown to be responsible for the remarkable solubilization of lignin in aqueous solutions of eutectic solvents.

Adapted from:

Belinda Soares; Armando J. D. Silvestre; Paula C. R. Pinto; Carmen S. R. Freire and João A. P. Coutinho. *ACS Sustainable Chem. Eng.* **2019,** 7 (14), pp. 12485 – 12493. DOI: 10.1021/acssuschemeng.9b02109.

ABSTRACT

The mechanisms responsible for the good solubility of lignin in aqueous solutions of eutectic solvents are here investigated in more detail using both monomer model compounds and technical lignins (kraft and organosolv lignins). The results show the ability of eutectic solvents to act either as hydrotropes or cosolvents, enhancing the solubility of these poorly soluble solutes (technical lignins or their monomers). Hydrotropy was shown to lead to a remarkable enhancement of organosolv lignin solubility of (474.7 ± 2.7)-fold times using an aqueous solution of propionic acid:urea (2:1) while for the systems where the solubilization mechanism was cosolvency, the best solubility enhancement was (194.2 ± 4.1)-fold times using ethylene glycol:tetrabutylphosphonium chloride (2:1). The solubility of kraft lignin was also enhanced with aqueous solution of propionic acid:urea (2:1) (228.3 ± 8.2)-fold times and ethylene glycol:tetraethylammonium chloride (2:1) (163.0 ± 16.1)-fold times by the same mechanisms.

MAIN GOAL & STRATEGY

Encouraged by our previous work (Chapter I), the current study attempts at further expand the solubility studies of technical lignins and their monomers in eutectic solvents, in order to assess the solubilization mechanisms responsible for the high solubility of lignin in eutectic solvents aqueous solutions. To achieve this purpose, the solubilities of lignin monomer model compounds and technical lignins in eutectic solvents aqueous solutions, were investigated, and the effect of the eutectic solvents components and their concentration were studied. It is expected that the results here reported will open new perspectives for the development of wood delignification and lignin conversion processes, as well as processes for the fractionation/purification of aromatic compounds present in black liquor.

RESULTS & DISCUSSION

To investigate the solubilization mechanisms responsible for the good performance of ESs aqueous solutions in lignin solubilization, the solubilities of LMMCs and technical lignins were evaluated, and the effect of the ES components and their concentration studied.

1. Effect of eutectic solvent components and concentration on lignin monomer model compounds solubilization

Several families of ESs were prepared by combining HBDs (carboxylic acids, polyols and U) with HBAs ([Ch]Cl, [P_{4444}]Cl and U) at a molar ratio that results in a liquid ES at room temperature, aiming to study the effects of HBDs and HBAs on the solubilization mechanism of LMMCs. Due to the good performance of LA:[Ch]Cl (10:1) to solubilize lignin, reported by some authors,[60,97] this mixture was also studied for comparative purposes instead of the LA:[Ch]Cl (2:1) reported in our previous work (Chapter I). The HBA [P_{4444}]Cl was here selected due to the recognized capacity of phosphonium-based ionic liquids to dissolve lignin.[98] The effect of ES concentration in aqueous solution was studied in the entire concentration range, from pure water to neat ES, at 323.15 K. The influence of ES components and concentration on the LMMC solubility are illustrated in Figure 33 andFigure 34. The detailed solubility values and the respective standard deviations, are reported in Table S4.1 (SI). On Figure 33 and Figure 34, the S and S_0 represent the solubility (mg g^{-1}) of LMMC in the aqueous solutions of ESs and in pure water, respectively. Therefore, the S/S_0 ratio represents the solubility enhancement due to the use of ESs. The solubilities of the LMMC were measured to be used as benchmark and previously reported in Chapter I.

Two different solubility behaviors of the LMMCs can be observed on these figures. While the results grouped on Figure 33 for the ESs (PA:[Ch]Cl (2:1), U:[Ch]Cl (2:1), PTSA:[Ch]Cl (1:1) and EG:[P_{4444}]Cl (2:1)) present a non-monotonic solubility enhancement with the ES concentration, with a maximum at intermediate ES concentrations, those in Figure 34 present a monotonic increase on solubility from the water to the neat ES.

Figure 33, shows that aqueous solutions of PA:[Ch]Cl (2:1), U:[Ch]Cl (2:1), PTSA:[Ch]Cl (2:1) and EG:[P_{4444}]Cl (2:1), at concentrations of 50 and 75 wt % seem to

allow the best solubility enhancement of the LMMCs. The shape of these curves, with a maxima at intermediate ES concentration, suggests that the solubility of these monomer model compounds is being driven by a hydrotropic mechanism.[99] A similar behavior was previously reported in Chapter I, for the solubility of these compounds in aqueous solutions of PA:U (2:1) as well as for the solubility of phenolic compounds in aqueous solutions of ionic liquids, reported by Claudio *et al*.[95] Furthermore, the sigmoidal profile of hydrotropy observed in Figure 33 for vanillic acid solubility in aqueous solutions of EG:[P_{4444}]Cl (2:1) and ferulic acid in aqueous solutions of PTSA:[Ch]Cl (1:1) is suggestive of a cooperative intermolecular interaction involved in the solubilization process, as reported by Balasubramanian *et al*.[65]

This group of ESs demonstrated to have higher ability to enhance the solubility of the most hydrophobic compounds, *i.e.* ferulic acid, considering the chemical structures of these LMMCs and their poor solubility in water. The hydrophobicity of the phenolic acids follows the sequence: ferulic acid (increase the alkyl chain length) > syringic acid (presence of two methoxyl groups) > vanillic acid (one methoxyl group). Regarding the ES components, it is possible to observe that EG:[P_{4444}]Cl (2:1) has the highest ability to increase the solubility of LMMCs, followed by PA:[Ch]Cl (2:1), PTSA:[Ch]Cl (1:1) and U:[Ch]Cl (2:1). The aqueous solution of EG:[P_{4444}]Cl (2:1) at 50 or 75 wt %, enhanced the ferulic, syringic and vanillic acids and syringaldehyde solubilities by (202.5 ± 16.9)-, (116.6 ± 1.6)-, (59.3 ± 2.5)- and (34.9 ± 6.7)-fold, respectively. This pattern reflects the effects of the HBDs and HBAs chemical structure in ESs through their ability to act as hydrotropes. These results suggest that the dispersive interactions between the nonpolar moiety of the HBDs and the lignin monomer structure are the main reason for the good performance of PA, instead of the hydrogen bond interactions, $\pi\cdots\pi$ interactions from the aromatic moiety in PTSA and the polar character of polyols, as previously reported in Chapter I. As for the HBA, the higher ability of [P_{4444}]Cl to act as hydrotrope when compared with [Ch]Cl, was previously demonstrated by Claudio *et al*.[95] Bauduin *et al.*[100] suggested that the volume fraction of the nonpolar moiety of the hydrotrope in water, positively correlates with the ability to enhance the solubility of poorly water-soluble compounds. This seems to be in accordance with the results observed in this work.

The EG:[P_{4444}]Cl (2:1) aqueous solutions, demonstrated an impressive ability to solubilize LMMCs. However the ability of U:[Ch]Cl (2:1) to solubilize syringaldehyde,

syringic and vanillic acids seems to be weaker. Finally, PA:[Ch]Cl (2:1) and PTSA:[Ch]Cl (1:1), only showed hydrotropic capability to solubilize syringaldehyde and ferulic acid, respectively. This suggest that ESs can be chosen to selectively dissolve target groups of compounds from complex mixtures.

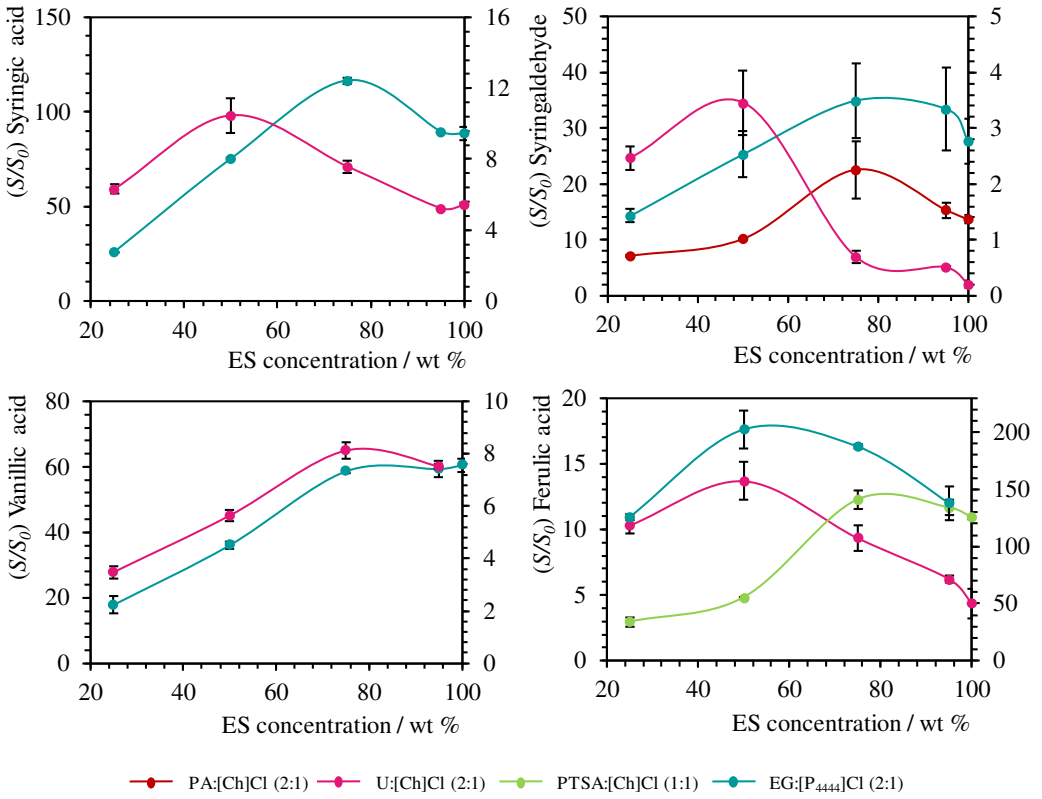

Figure 33. Hydrotropic behavior of ESs in aqueous solutions on LMMCs solubilization at 323.15 K. See secondary axis for EG:[P_{4444}]Cl (2:1) in ferulic acid and U:[Ch]Cl (2:1) in syringaldehyde, and syringic and vanillic acids.

A different solubility behavior is observed for the ESs systems reported in Figure 34. Again, the solubility of syringaldehyde and, syringic, ferulic and vanillic acids is shown to depend not only on the ES components but also on their concentration. The most important point that emerges from Figure 34 is that the solubilization induced by these ESs (LA:[Ch]Cl (10:1), FA:[Ch]Cl (2:1), PA:[Ch]Cl (2:1), PTSA:[Ch]Cl (1:1) and EG:[Ch]Cl (2:1)) is a monotonic function of their concentration, being maximal for the neat ES, as typically observed in the cosolvency mechanism.[101] The solubilization of LMMCs by these five ESs with cosolvents behavior, could be ranked in the following order: PA:[Ch]Cl (2:1) > EG:[Ch]Cl (2:1) > PTSA:[Ch]Cl (1:1) > FA:[Ch]Cl (2:1) > LA:[Ch]Cl (10:1). This pattern

reflects the effects of the HBDs chemical structure on their ability to act as cosolvents and the interactions with the LMMCs. The neat PA:[Ch]Cl (2:1) and EG:[Ch]Cl (2:1), enhanced the ferulic solubility by (85.4 ± 0.8)- and (82.0 ± 2.1)-fold, respectively. The studied ESs demonstrated a much lower ability to solubilize syringaldehyde, even if PA:[Ch]Cl (2:1) could enhance its solubility by more than 20 times by hydrotropy, as discussed above. The same behavior was observed for PTSA:[Ch]Cl (1:1), where hydrotropy seems to be the favored mechanism in the solubilization of ferulic acid.

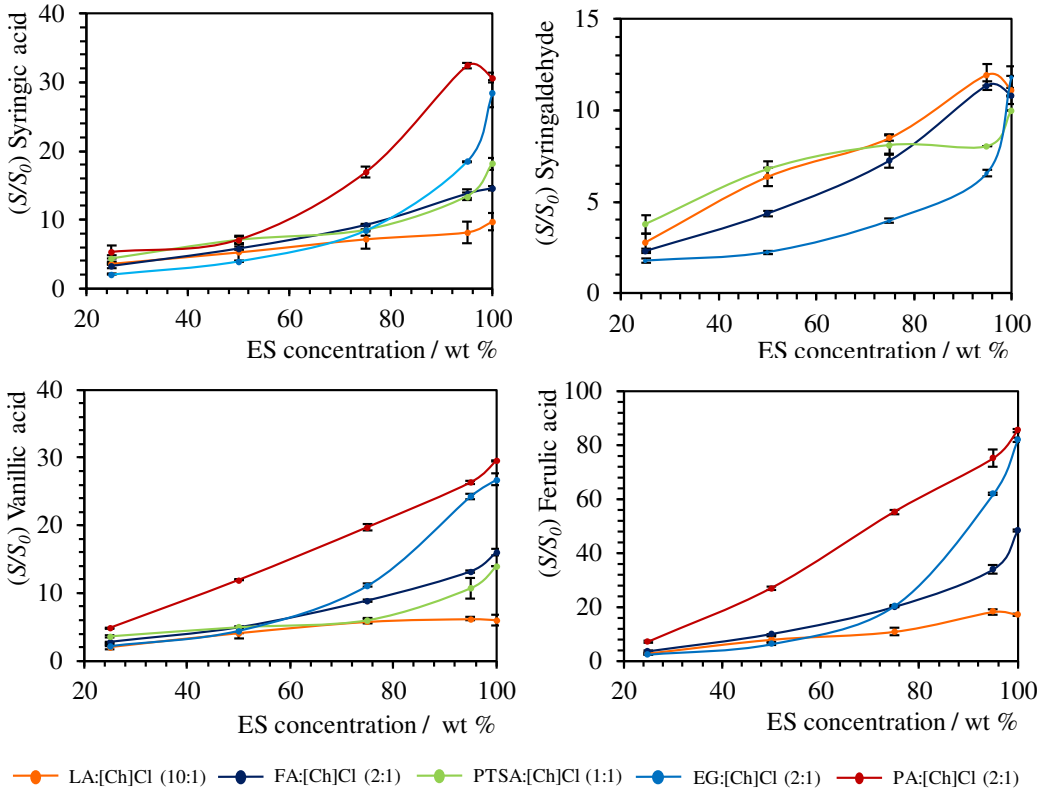

Figure 34. Cosolvent behavior of ESs in aqueous solutions on LMMCs solubilization at 323.15 K.

The results hitherto reported reveal that two different solubilization behaviors, here interpreted as, hydrotropy or cosolvency, are responsible for the good solubility of LMMCs on ESs. The solubility behaviors observed are independent of temperature, as shown in Figure 35 and Figure 36, and Tables S4.2 and S4.3 (SI), in agreement with our previous studies (Figure 29).

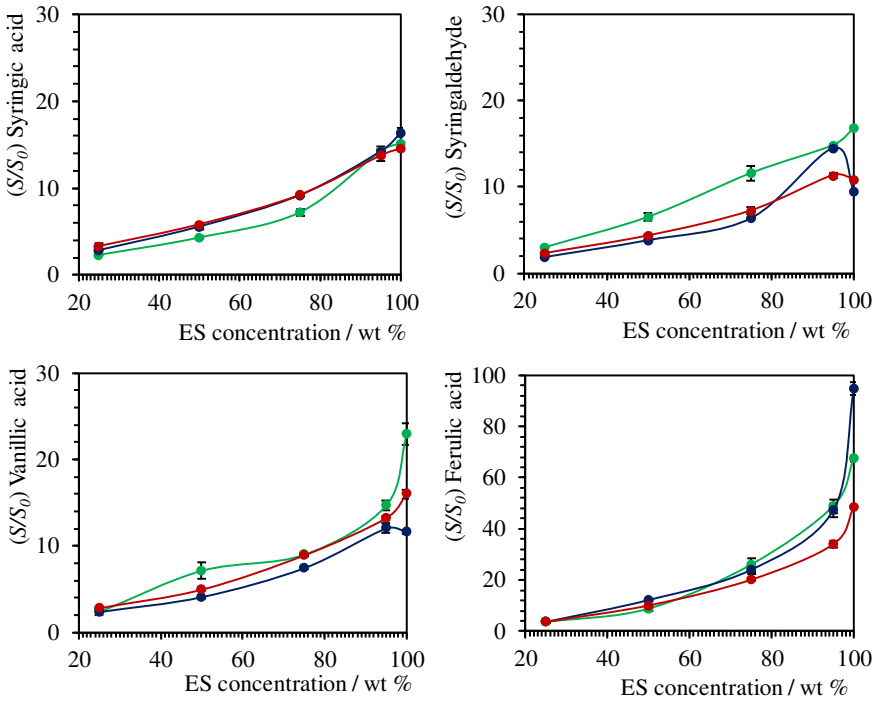

Figure 35. Influence of FA:[Ch]Cl (2:1) concentration and temperature on the solubility enhancement of LMMCs. The different temperatures studied were 303.15 K (green), 313.15 K (blue) and 323.15 K (red).

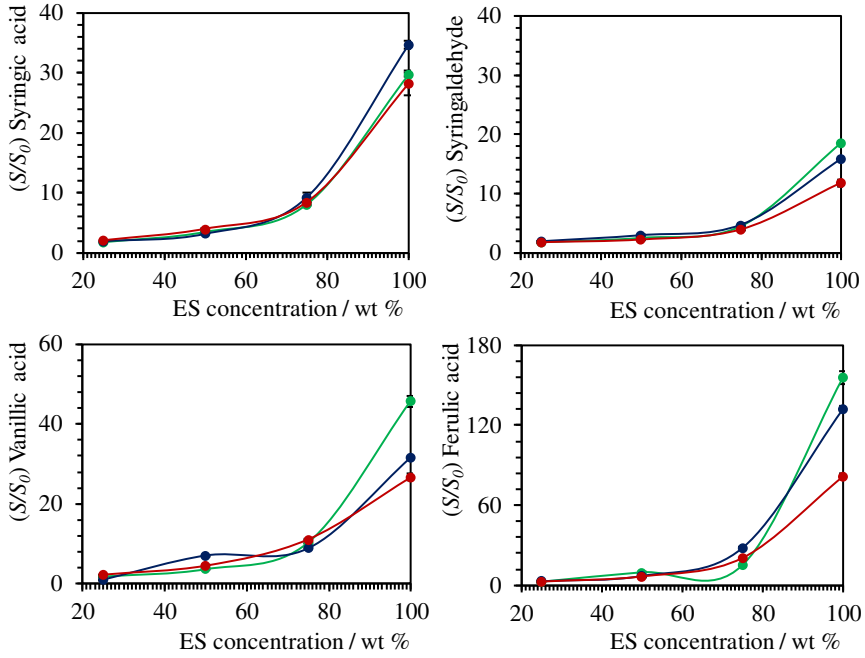

Figure 36. Influence of EG:[Ch]Cl (2:1) concentration and temperature on the solubility enhancement of LMMCs. The different temperatures studied were 303.15 K (green), 313.15 K (blue) and 323.15 K (red).

Additionally, it is important to highlight the excellent performance of ESs aqueous solutions in the solubilization of LMMCs by hydrotropy mechanism that may improve the solubility of these model compounds by two orders of magnitude when compared with water. On the other hand, given the selective character of ESs to solubilize aromatic aldehydes and acids (by hydrotropy or cosolvency solubilization mechanisms), and the possibility to recover these compounds by using water as antisolvent, these results open new promising pathways for the fractionation of phenolic compounds from pulp and industry black liquors, where the selective recovery and separation of these compounds is an important challenge in the biorefinery framework.[102]

2. Thermodynamic functions of solution

The evaluation of thermodynamic functions of solutions was performed to explore the molecular mechanisms behind the solvation phenomena of LMMCs in ESs systems. When LMMCs are solubilizes in ES concentration range, the process is followed by a change in the thermodynamic functions of the system, in particular the molar Gibbs energy [$\Delta_{sol}G_m(T)$], molar enthalpy [$\Delta_{sol}H_m(T)$], and molar entropy [$\Delta_{sol}S_m(T)$] of solution.[103] These thermodynamic functions can be estimated by means of the van't Hoff equation and derived from the temperature dependence of the experimental solubility data (see Table S4.8, SI) for those systems with small deviations from ideal behavior, according to the following equations:[103]

$$\Delta_{Sol}G_m(T) = -RT(\ln x_{LMMCS})_p \quad (4)$$

$$\frac{\Delta_{Sol}H_m(T)}{RT^2} = \left(\frac{\partial \ln x_{LMMCs}}{\partial T}\right)_p \quad (5)$$

$$\Delta_{Sol}S_m(T) = \frac{\Delta_{Sol}H^{\circ}{}_m(T) - \Delta_{Sol}G^{\circ}{}_m(T)}{T} \quad (6)$$

where x_{LMMCs} is the mole fraction solubility of LMMCs, R is the gas constant (8.134 J mol^{-1} K^{-1}, and T is the temperature at a constant pressure p. These thermodynamic parameters

regard the transference of the solute molecules to a "hypothetical" ideal-dilute solution where solute-solute interactions can be neglected.

Assuming that in the temperature studied range (303.15, 313.15 and 323.15 K) the molar enthalpy of each LMMCs in ES concentration can be considered temperature independent (as observed above Figure 29, Figure **35** and Figure **36**), the temperature behavior of the measured data was fitted using the following equation (7):

$$\ln x_{LMMCs} = A + \frac{B}{T} \quad (7)$$

where T is the temperature (K) and A and B are the regression constants, which are related to $\Delta_{sol}S_m(T)$, $\Delta_{sol}H_m(T)$, and R. Based on the correlation parameters A and B it was possible to determine the thermodynamic functions of solution of LMMCs in different ES concentrations at 303.15 K, as reported in Table S4.9.

It is evident from the Figure 37 that the molar Gibbs energy of solutions are positive in all of the studied cases, meaning that the LMMCs solution processes are not spontaneous. Moreover, the molar enthalpy of solution is positive in all of the studied cases, showing that the solution processes are endothermic. The molar enthalpies of solution for syringic acid in ESs were lower than for vanillic acid, ferulic acid or syringaldehyde, indicating that ESs has higher capability to solubilize syringic acid. Furthermore, it was possible to observe that PA:U (2:1) presented lower molar enthalpies of solutions for syringic acid and syringaldehyde (in all ES concentration range), meaning that the enthalpic energetic balance involved in the dissolution of syringic acid and syringaldehyde in PA:U (2:1) is more favorable. In the case of EG:[Ch]Cl (2:1) the dissolution of ferulic acid is more favorable and the dissolution of vanillic acid appear to be more favorable in FA:[Ch]Cl (2:1) and EG:[Ch]Cl (2:1) than PA:U (2:1). Regarding the molar entropy of solution, a negative value was obtained for syringic acid at 25 wt % of PA:U (2:1), and positive for all other LMMCs solubilized in ES (neat and their aqueous solutions). In general, the positive values of molar entropy of solution indicate that the entropy of solubilizing LMMCs is unfavorable in all the ESs examined. Furthermore, the high values of the enthalpy suggest that more energy is needed for overcoming the cohesive force between the solute and the solvent.[104]

The relative contributions to the Gibbs energy by enthalpy (ζ_H) and entropy (ζ_{TS}) toward the dissolution process, was determined by the equations (8) and (9), according to literature[105] and are reported in Table S4.9 (SI).

$$\zeta_H = \frac{|\Delta_{Sol}H_m|}{|\Delta_{Sol}H_m| + |303.15\ K \times \Delta_{Sol}S_m|} \times 100 \quad (8)$$

$$\zeta_{TS} = \frac{|303.15 \times \Delta_{Sol}S_m|}{|\Delta_{Sol}H_m| + |303.15\ K \times \Delta_{Sol}S_m|} \times 100 \quad (9)$$

The results show that molar enthalpy (ζ_H values up to 58 %) is the main contributor to the positive molar Gibbs energy of solution of LMMCs in ESs. These results indicate that energy factor have more impact on LMMCs solubility variation.

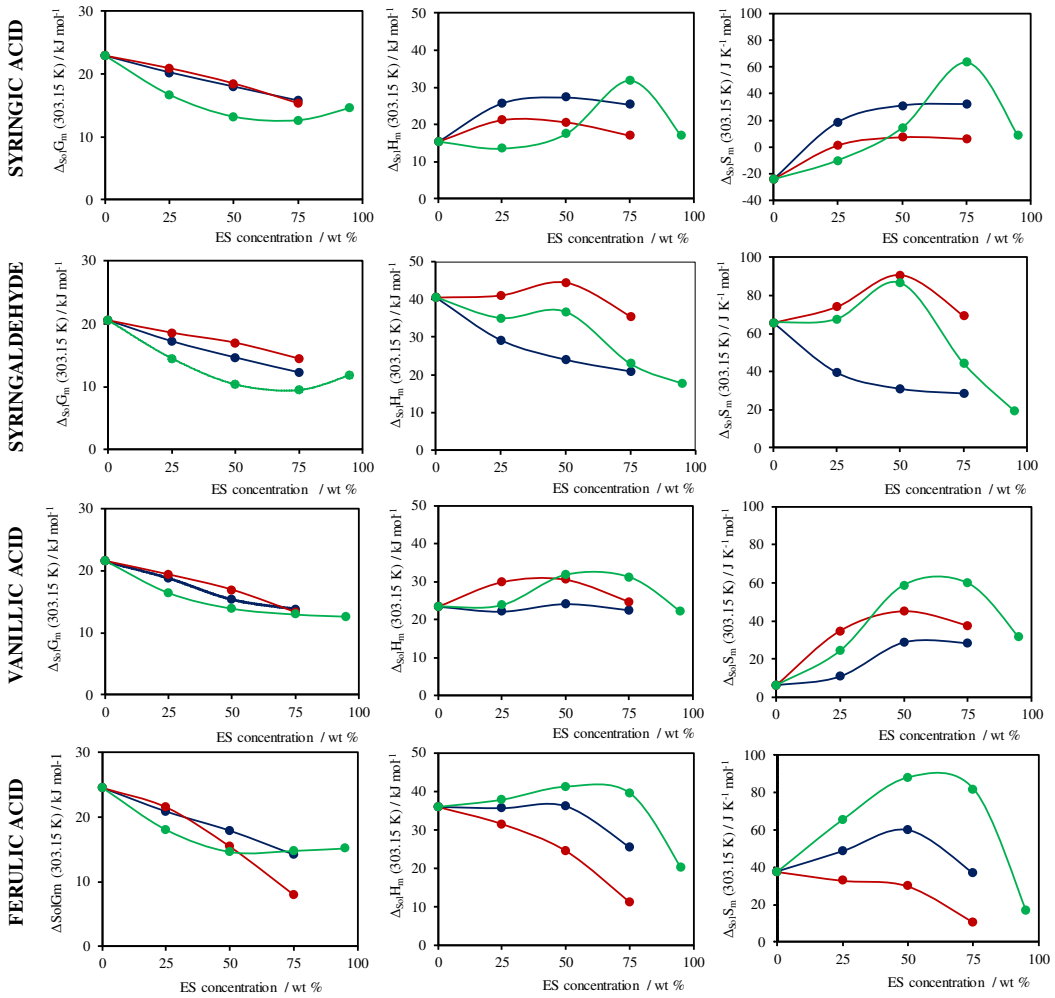

Figure 37. Molar thermodynamic functions of solution for LMMCs in ESs [FA:[Ch]Cl (2:1) – blue, EG:[Ch]Cl (2:1) – red and PA:U (2:1) – green] at 303.15 K.

3. Effect of eutectic solvent components and concentration on technical lignins solubilization

Based on the results of LMMCs solubility in ESs aqueous solutions reported above, the solubility of kraft and organosolv lignins in ESs aqueous solutions was investigated at 353.15 K. Several ESs were prepared combining HBDs (carboxylic acids, polyols and U) with HBAs ([Ch]Cl, [N_{3333}]Cl, [P_{4444}]Cl and U) at a molar ratio that results in a liquid ES at room temperature, aiming at studying the effects of HBDs and HBAs on the solubilization of technical lignins. In this study, it was decided to include also ammonium-based ESs to compare with phosphonium- and choline-based ESs. Based on the preliminary study of technical lignins solubility in neat ESs at 353.15 K (Figure 38), the [N_{3333}]Cl was selected to assess the solubilization mechanism induced by this HBA combined with EG to enhance the solubility of technical lignins (for more details see Table S4.4, SI). The detailed values of technical lignins solubility and the respective standard deviations, are reported in Table S4.5 (SI). The solubility of technical lignins (kraft and organosolv lignin) in pure water at 303.15, 313.15, 323.15 and 353.15 K and at atmospheric pressure, were measured to be used as benchmark and are reported in Table 17.

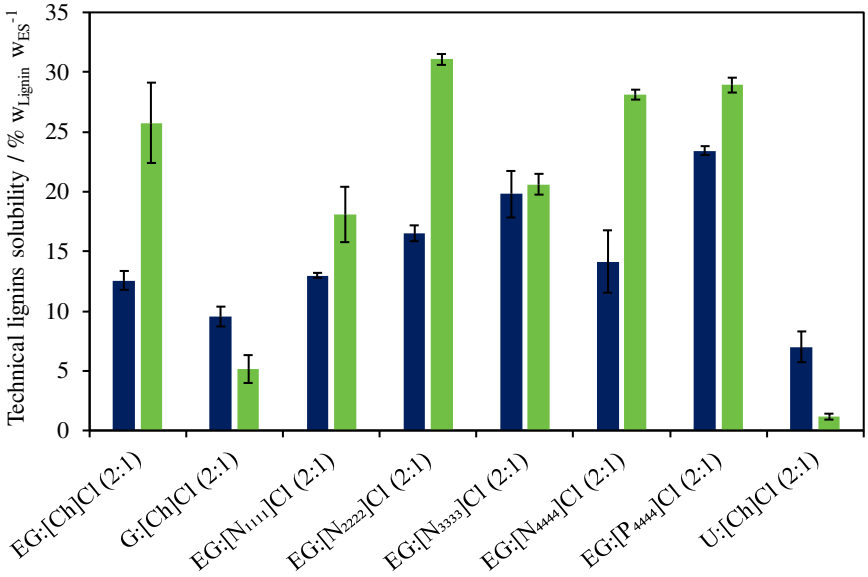

Figure 38. Solubilities of technical lignins in neat polyols-based ESs at 353.15 K, obtained from FTIR spectroscopy at 1510 cm^{-1}. Kraft lignin (blue) and organosolv lignin (green).

Table 17. Experimental solubility of technical lignins in pure water.

	Solubility ± σ / mg g^{-1}			
T/K	**303.15**	**313.15**	**323.15**	**353.15**
Technical lignins				
kraft lignin	0.48 ± 0.03	0.63 ± 0.02	0.77 ± 0.03	1.21 ± 0.09
organosolv lignin	0.41 ± 0.03	0.87 ± 0.04	1.03 ± 0.02	1.49 ± 0.25

σ, standard deviation.

As expected, the solubilization of technical lignins in ESs (neat or in aqueous solution) followed the same trend previously observed for LMMCs. Two different behaviors were observed in Figure 39 and Figure 40 showing the effects of ES components and concentrations on technical lignins. As for the model compounds, the solubility of technical lignins presents either a non-monotonical increase with ESs, with a solubility maximum at intermediate concentrations, or a monotonical increase with ESs. According to our previous discussion for the model compounds these results suggest that technical lignins can be solubilized in ESs aqueous solutions, by hydrotropy or cosolvency mechanisms. The differences in solubilization mechanisms can be associated to the synergetic contribution of both HBDs and HBAs to enhance the technical lignin solubility, previously discussed.

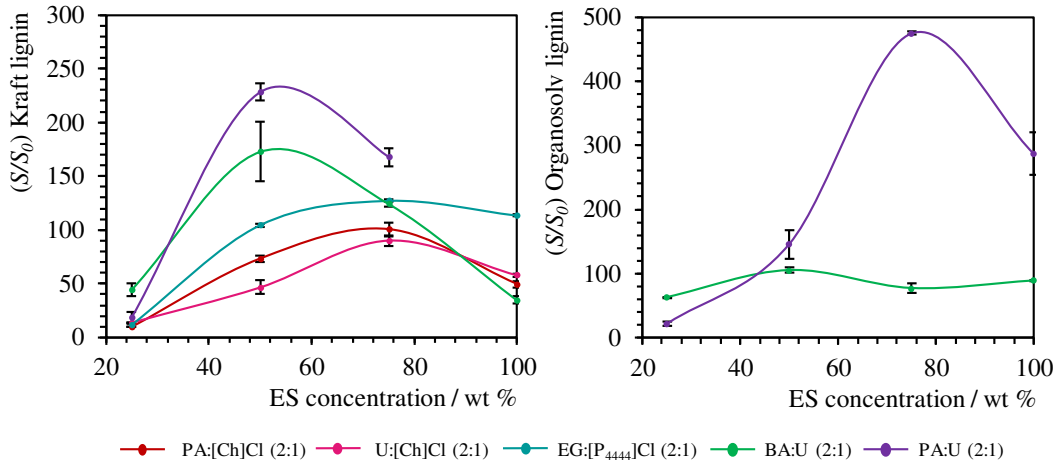

Figure 39. Hydrotropic behavior of ESs in aqueous solutions on technical lignins solubilization at 353.15 K.

The aqueous solutions of PA:[Ch]Cl (2:1), U:[ChCl (2:1), EG:[P_{4444}]Cl (2:1), BA:U (2:1) and PA:U (2:1) exhibited hydrotropic solubility for kraft lignin while only BA:U (2:1) and PA:U (2:1) showed the same effect for the organosolv lignin solubilization, as shown in Figure 39. Concerning the ES concentration, remarkable improvements on technical lignin

solubilization were observed from (105.5 ± 3.5)- to (474.7 ± 2.7)-fold times using ESs aqueous solutions at 50 or 75 wt %, when compared with their solubility in water. Furthermore, as suggested by the results with model compounds, the solubility of the technical lignins confirm that PA:U (2:1) aqueous solution are the best, followed by BA:U (2:1), EG:[P_{4444}]Cl (2:1), PA:[Ch]Cl (2:1) and U:[ChCl (2:1).

Another group of ESs, LA:[Ch]Cl (10:1), FA:[Ch]Cl (2:1), PTSA:[Ch]Cl (1:1), EG:[Ch]Cl (2:1), EG:[N_{3333}]Cl (2:1) and EG:[P_{4444}]Cl (2:1), exhibited a cosolvent-type behavior, as shown in Figure 40, with the neat ESs being the best solvents overall. Although the solubility of technical lignins on the best performing ES is significantly higher than in water by 100 – 200 times, the solubility enhancement by this mechanism is lower than that achieved with hydrotropy.

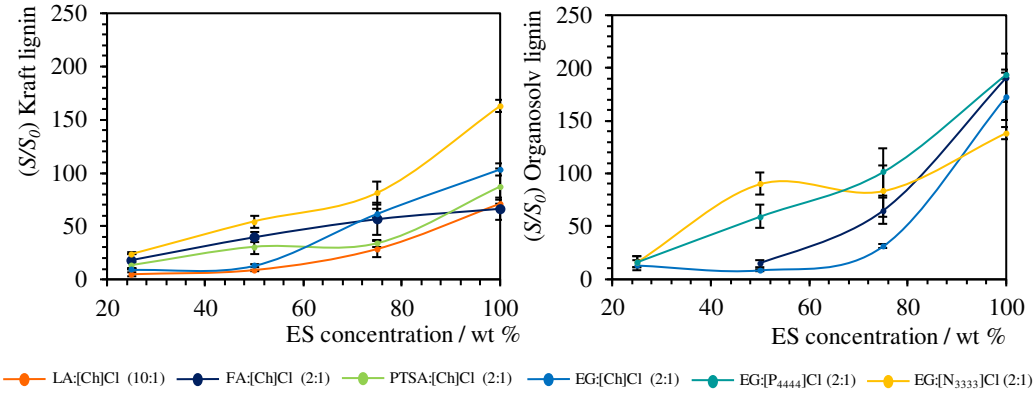

Figure 40. Cosolvent behavior of ESs in aqueous solutions on technical lignins solubilization at 353.15 K.

Regarding the solubilization of kraft lignin by cosolvency, the neat EG:[N_{3333}]Cl (2:1) appear to be the best solvent [(163.0 ± 16.1)-fold], followed by EG:[Ch]Cl (2:1), PTSA:[Ch]Cl (2:1), FA:[Ch]Cl (2:1) and LA:[Ch]Cl (10:1). These results show the important effect of HBDs and HBAs on the kraft lignin solubilization mechanisms. Indeed, when EG is combined with [Ch]Cl or even [N_{3333}]Cl, the predominant solubilization mechanism was cosolvency. However, if EG is combined with [P_{4444}]Cl, a more hydrophobic component, the kraft lignin solubilization is driven by hydrotropy. On the other hand, when EG:[P_{4444}]Cl (2:1) and EG:[N_{3333}]Cl (2:1) where used to solubilize organosolv lignin, both ESs presented a cosolvent behavior. These results suggest, that the ES hydrotropic or cosolvent character not only depend of the ES components and their

hydrophobic/hydrophilic properties, but also on the chemical structure of the solute. It is important to remark that the delignification processes and the recovery from pulping liquors have a remarkable influence on the structure of the technical lignins (kraft and organosolv lignins). This is certainly the reason why the same ES enhances the solubility of kraft and organosolv lignins by different solubility mechanisms. Furthermore, FA:[Ch]Cl (2:1) and EG:[Ch]Cl (2:1) also present good performances to enhance the solubility of organosolv lignin by (190.8 ± 23.0)- and (172.9 ± 22.4)-fold, respectively. Finally, we again observe that the profiles of the hydrotropy and cosolvency mechanisms are independent of temperature (Figure 41 and Figure 42, and Tables S4.6 and S4.7, SI), and the results reported in Chapter I.

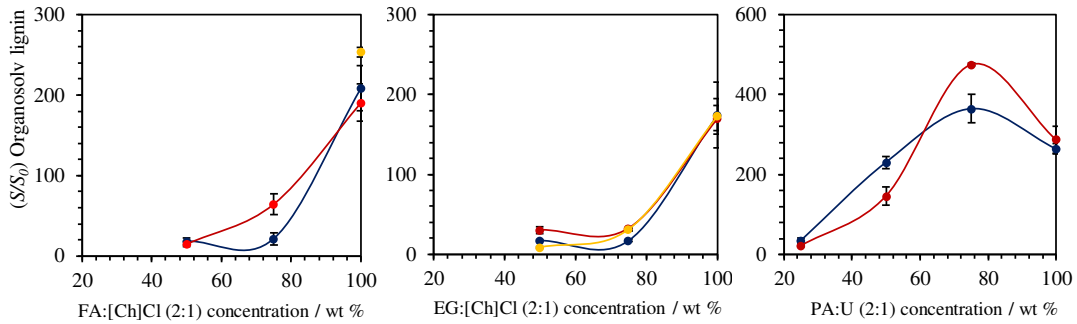

Figure 41. Influence of FA:[Ch]Cl (2:1), EG:[Ch]Cl (2:1) and PA:U (2:1) concentration and temperature on the solubility enhancement of organosolv lignin. The different temperatures studied were 313.15 K (blue), 323.15 K (red) and 353.15 K (yellow).

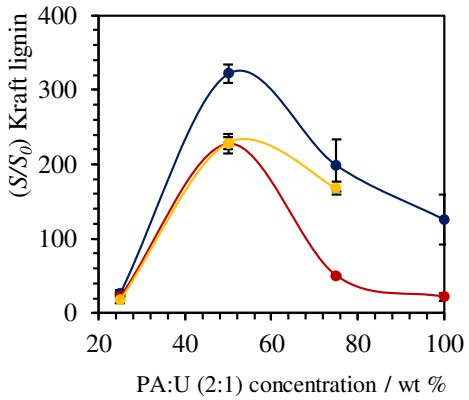

Figure 42. Influence of PA:U (2:1) concentration and temperature on the solubility enhancement of kraft lignin. The different temperatures studied were 313.15 K (blue), 323.15 K (red) and 353.15 K (yellow).

CONCLUSIONS

This work attempts to know the solubilization mechanisms responsible for the good performance of eutectic solvent aqueous solutions on lignin solubilization using lignin monomer model compounds and technical lignins. Considering the complex chemical structure of the lignin, it seems to be possible, through the evaluation of lignin monomer model compounds, not only to predict the performance of eutectic solvents (neat or in aqueous solution) on the lignin solubilization but also to demonstrate the mechanisms that rule their solubilization.

Regarding the lignin monomer model compounds (syringaldehyde, and syringic, vanillic and ferulic acids), a maximum solubilization was achieved using EG:[P_{4444}]Cl (2:1) aqueous solution at 50 or 75 wt % of concentration and 323.15 K [(34.9 ± 6.7)-, (116.6 ± 1.6)-, (58.6 ± 0.4)- and (202.5 ± 16.9)-fold, respectively] driven by hydrotropy mechanism. From the dependence of the solubility on temperature, the molar thermodynamic functions (Gibbs energy, enthalpy and entropy) of solution of lignin monomer model compounds in three different eutectic solvents [PA:U (2:1), FA:[Ch]Cl (2:1) and EG:[Ch]Cl (2:1)], where ideal solution can be considered at 303.15 K, were determined. The results allowed to better understand the solubilization of lignin monomer model compounds in eutectic solvents (neat and their aqueous solutions). The determination of molar enthalpies of solution allowed to conclude that PA:U (2:1) has great ability to solubilize syringic acid and syringaldehyde. The dissolution of ferulic acid is more favorable in EG:[Ch]Cl (2:1) and vanillic acid in FA:[Ch]Cl (2:1) and EG:[Ch]Cl (2:1). Furthermore, the impressive ability of PA:U (2:1) aqueous solution at 50 wt % and neat EG:[N_{3333}]Cl (2:1) to solubilize kraft lignin at 353.15 K, driven by different solubilization mechanisms, hydrotropy and cosolvency, respectively [(228.3 ± 8.2)- and (163.0 ± 16.1)-fold, respectively], were here identified. Additionally, the remarkable improvement of organosolv lignin solubility achieved by the PA:U (2:1) aqueous solutions at 75 wt % of (474.7 ± 2.7)-fold, by hydrotropy and (194.2 ± 4.1)-fold using the neat EG:[P_{4444}]Cl (2:1), by cosolvency.

In summary, these results show the capability of eutectic solvents to act as hydrotropes or cosolvents, selectively enhancing the solubility of poorly soluble solute depending on the eutectic solvents components and solute hydrophobicity. These studies provide a new understanding of lignin solubilization mechanisms in eutectic solvent aqueous

solutions, and demonstrate that eutectic solvents are promising solvents to apply in biomass processing, as well as, novel solvent for the selective extraction of aromatic compounds present in black liquor, aiming at their future valorization.

PART B

PROOF OF CONCEPT

Chapter III

Wood Delignification with Eutectic Solvents

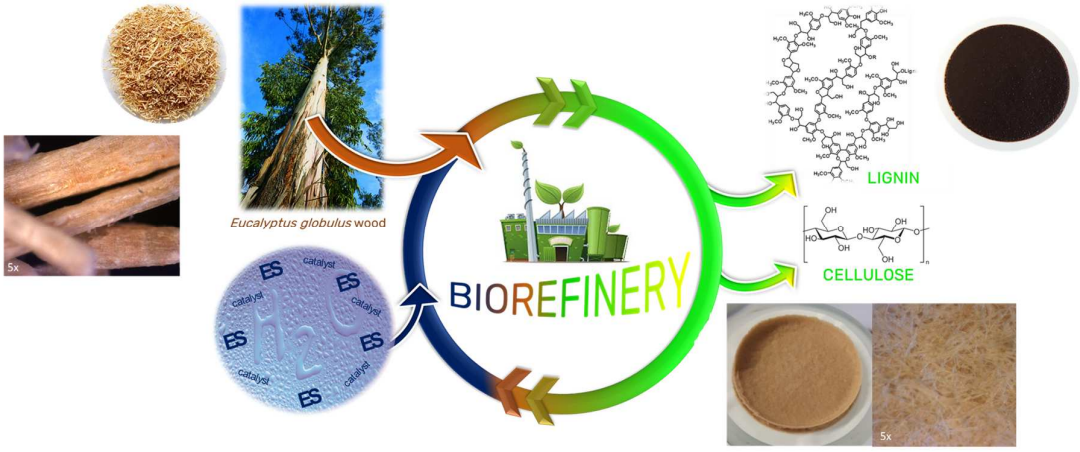

Improvements on wood delignification process mediated by eutectic solvents aqueous solutions in the presence of acids as catalyst, at mild conditions

Adapted from:

Belinda Soares; André M. da Costa Lopes; Armando J. D. Silvestre; Paula C. R. Pinto; Carmen S. R. Freire and João A. P. Coutinho. **2019.** *Wood delignification with eutectic solvents.* Under preparation.

ABSTRACT

The potential of eutectic solvents aqueous solutions for *Eucalyptus globulus* wood delignification, assisted by mineral or organic acids as catalysts, was here investigated. The obtained solid fractions and precipitated lignins were characterized in order to evaluate the effect of this new process on the cellulose fibers and on the structure of the precipitated lignins. Specifically, aqueous solutions of propionic acid:urea (2:1), urea:choline chloride (2:1), lactic acid:choline chloride (10:1) and *p*-toluenesulfonic acid:choline chloride (1:1) were investigated. The best eutectic solvent system, preserving the cellulose fibers as compared with kraft pulp and lignin structure after wood delignification, at mild conditions (8 h, 363.15 K and atmospheric pressure) was an aqueous solution of propionic acid:urea (2:1) 50 wt %, catalyzed with 25 wt % of *p*-toluenesulfonic acid, producing 59.50 ± 0.51 wt % of cellulose pulp containing a residual Klason lignin of 3.86 ± 0.10 wt %. This new approach led to a lignin removal of 80.64 wt % from *Eucalyptus globulus* wood. Furthermore, it was possible to recover 40.73 wt % of lignin from eutectic solvents liquor by simple precipitation with water.

MAIN GOAL & STRATEGY

The main objective of the present work is to develop eutectic solvent wood delignification processes at mild conditions able to induce minor structural changes to extracted lignin (regarding β-*O*-4 structures, aliphatic and phenolic hydroxyl groups contents) while preserving cellulose fibers. To achieve this purpose, aqueous solutions of different eutectic solvents, namely propionic acid:urea (2:1), *p*-toluenesulfonic acid:[Ch]Cl (1:1), lactic acid:[Ch]Cl (10:1) and urea:[Ch]Cl (2:1), previously shown to be able to selectively dissolve lignin (see Part A – Fundamental study), assisted by mineral or organic acids as catalysts, were investigated for *Eucalyptus globulus* wood delignification. The feasibility of these systems for wood delignification was evaluated based on the characterization of the final products, viz precipitated lignin and cellulose fibers.

RESULTS & DISCUSSION

Based on our previous results, where the potential of ESs aqueous solutions to enhance the solubility of technical lignins was demonstrated, ESs aqueous solutions of PA:U (2:1), PTSA:[Ch]Cl (1:1), LA:[Ch]Cl (10:1) and U:[Ch]Cl (2:1) at 50 wt % were used to develop a new wood delignification process under mild conditions (8 h, solid/liquid ratio of 0.5/10 w/w, 300 rpm and 363.15 K). The success of this wood delignification process was assessed by determining the solid fraction and precipitated lignin yields. Considering the negligible cellulose solubilization in ESs,[74,106] wood delignification was conducted by adjusting experimental conditions to maximize the amount of the precipitated lignin (19.94 ± 0.35 wt % is the lignin content in *E. globulus* wood) and to preserve the cellulose fraction, *i.e.* to obtain a solid fraction yield close to 50 wt % (assuming a 50 wt % cellulose content in *E. globulus* wood).[13]

1. Screening of eutectic solvents aqueous solutions for wood delignification

Due to the good performance of LA:[Ch]Cl (10:1) in wood delignification, reported by some authors,[64,74,75,106–108] this mixture was used for comparative purposes instead of LA:[Ch]Cl (2:1) reported in Chapter I. The yield of obtained solid fraction and precipitated lignin are depicted in Figure 43 (the detailed solid fraction and precipitated lignin yields and the respective standard deviations, are reported in Table S5.1, SI).

The high solid fraction yield (above 70 wt %) and the low precipitated lignin yield (below 3 wt %) observed in Figure 43 using PA:U (2:1), LA:[Ch]Cl (10:1) and U:[Ch]Cl (2:1) aqueous solutions, indicated that wood delignification was inefficient on these systems. The successful delignification of *E. globulus* wood was only achieved using the PTSA:[Ch]Cl (1:1) aqueous solution, with a solid fraction yield of 46.41 ± 0.88 wt %, containing a residual Klason lignin of 10.69 ± 0.16 wt %. Furthermore, after the lignin isolation from ES liquor, 15.38 ± 0.59 wt % of precipitated lignin was attained. These results suggest that other wood constituents, such as hemicelluloses, dissolved in ES liquor are also precipitated with lignin from PTSA:[Ch]Cl (1:1) system contributing to the slight misleading precipitated lignin yield, considering the native lignin content in wood (19.94 ± 0.35 wt %)

and the residual Klason lignin in solid fraction. A detailed characterization of the solid fraction and precipitated lignin will be presented below.

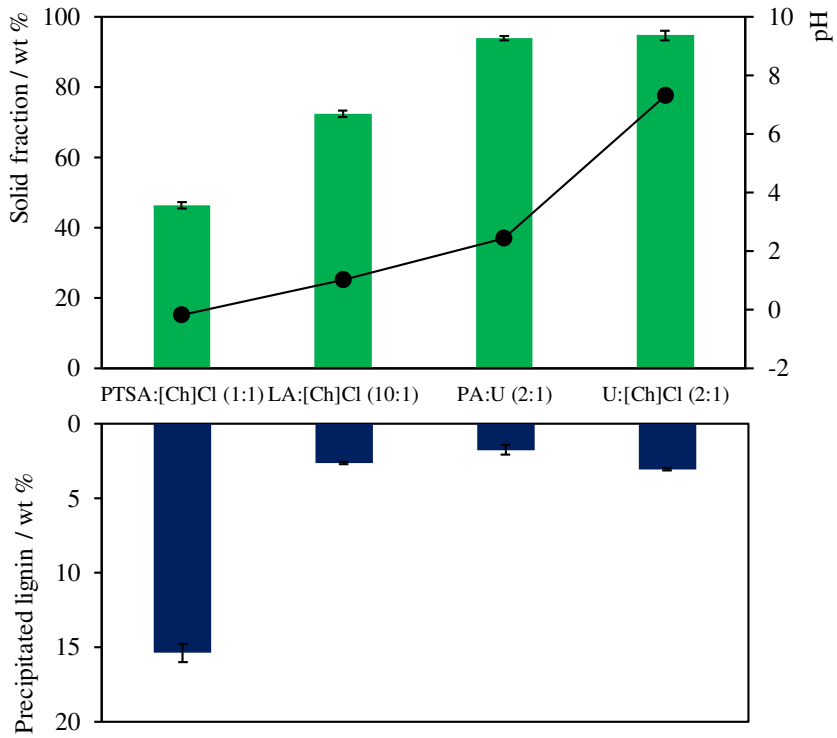

Figure 43. Screening of ESs aqueous solutions at 50 wt % for *E. globulus* wood delignification (8 h, wood/liquid ratio of 0.5/10 w/w, 300 rpm and 363.15 K) based on solid fraction (green) and precipitated lignin (blue) yields. The pH values of ESs aqueous solutions are represented in black dots.

The need for an acidic media to promote delignification through cleavage of ether bonds between lignin phenylpropane units, particularly α-*O*-4 and β-*O*-4 ether linkages, and between them and polysaccharides,[4–6] may explain the weak performance of PA:U (2:1) aqueous solution for wood delignification due to the low acid strength of PA (pKa of 4.87).[109]

On the other hand, the LA:[Ch]Cl (10:1) aqueous solution system in particular, produced a solid fraction yield of 72.35 ± 0.89 wt % and precipitated lignin yield of 2.62 ± 0.09 wt %. These values are substantially lower than the previously reported lignin removal yields (see Table 9),[74,75] which despite the fact that different species were used, namely *Pseudotsuga menziesii,*[74] *Populus sp.*[74] and *E. camaldulensis,*[75] should be related to the ES concentration and therefore to pH. Indeed, Kumar *et al.*[59] demonstrated that an increase of water content up to 50 wt % affected negatively the lignin solubility in ESs decreasing its

solubility in 95 wt %. These results are in line with our previous work (presented in Part A – Fundamental study), regarding the study of lignin solubilization in ESs, where the cosolvent character of LA:[Ch]Cl (10:1) in aqueous solution to solubilize technical lignin is demonstrated. To confirm the effect of LA:[Ch]Cl (10:1) concentration on *E. globulus* wood delignification performance, neat LA:[Ch]Cl (10:1) was also tested (see Table S5.1, SI). The results showed an improved wood delignification with neat LA:[Ch]Cl (10:1) (solid fraction of 62.51 ± 1.37 wt % containing a residual Klason lignin of 12.05 ± 1.26 wt % and a precipitated lignin of 4.42 ± 0.37 wt %) in comparison to its aqueous solution. These results demonstrate the negative effect of water on wood delignification when using this particular system.

Given the good performance of PTSA:[Ch]Cl (1:1) aqueous solution in *E. globulus* wood delignification under mild conditions, it is important to evaluate the resulting fibers and the lignin structural features induced by this new ES based process.

The FTIR spectrum of the solid fraction-PTSA:[Ch]Cl showed a spectroscopic profile similar to a standard kraft pulp, indicating that this fraction is mainly composed of cellulose (Figure 44). The absorption bands were assigned following the literature[117–119] and details are presented in Table S5.2 (SI).

However, the optical microscopy images of fibers in solid fraction-PTSA:[Ch]Cl revealed substantial morphological differences when compared with kraft pulp fibers (Figure 45). The fibers in solid fraction-PTSA:[Ch]Cl are fragmented, possibly due to the strong acidic media combined with the long time used in this delignification process (8 h). Moreover, the brownish color observed in the surface of the fibers can be associated with the presence of residual lignin, as consequence of existing lignin condensation reactions, which are promoted by acidic conditions and long reaction times.[5,6] In summary, these results suggest that the process conditions (363.15 K and 8 h) in PTSA:[Ch]Cl (1:1) delignification process, although inducing delignification, compromised the fibers quality when compared with kraft pulp fibers.

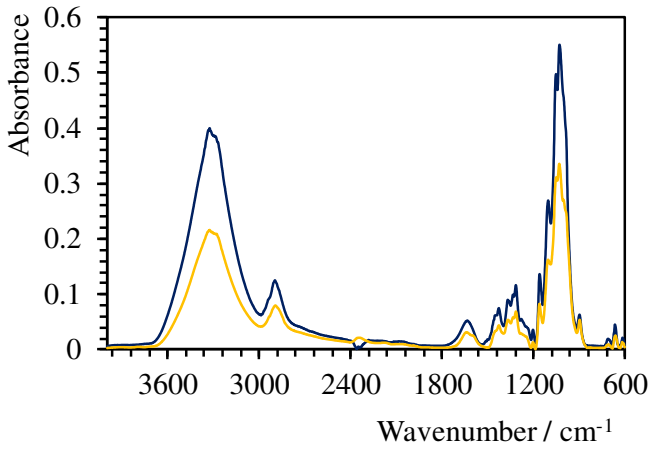

Figure 44. Normalized FTIR spectra of solid fraction-PTSA:[Ch]Cl (blue) and the conventional kraft pulp from *E. globulus* wood with kappa number 14.4 (yellow).

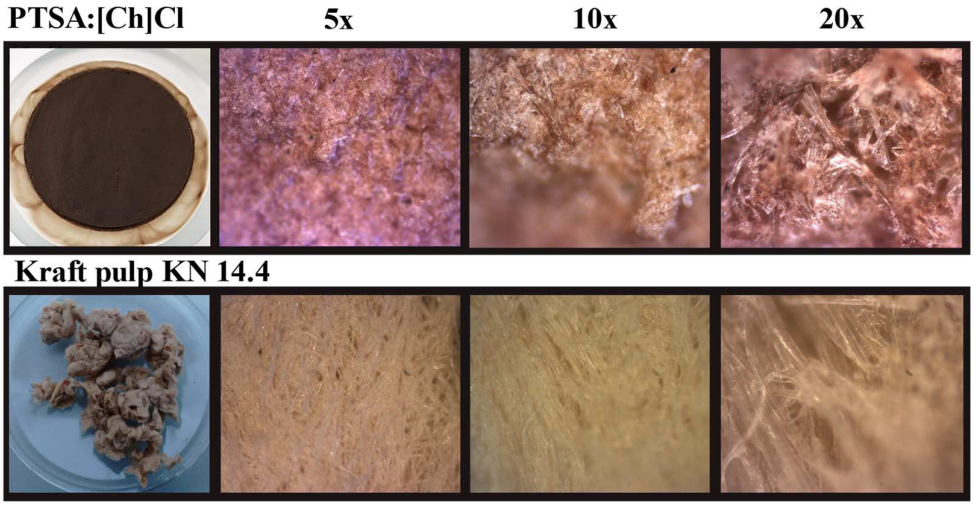

Figure 45. Optical microscopy images of *E. globulus* solid fraction-PTSA:[Ch]Cl and conventional kraft pulp from *E. globulus* wood with kappa number 14.4. Magnification 5x, 10x and 20x.

The precipitated lignin-PTSA:[Ch]Cl (1:1) was characterized by FTIR spectroscopy (Figure 46, see more details in Table S5.3, SI) and elemental analysis (Table S5.4, SI). The absorption bands were assigned according to literature[110,112,114,120] and details are presented in Table S5.3 (SI).

The results show that lignin is the main component of this fraction, and present some chemical structural changes, when compared to technical lignins (kraft and dioxane lignins). Furthermore, partial contamination with hemicelluloses was observed.

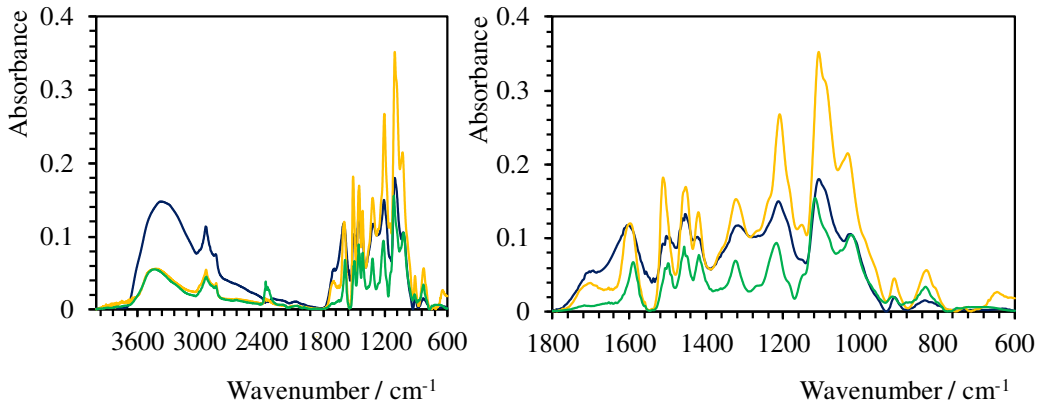

Figure 46. Normalized FTIR spectra of precipitated lignin-PTSA:[Ch] (blue), kraft lignin (yellow) and dioxane lignin (green).

2. Effect of acid catalyst in wood delignification using eutectic solvents aqueous solutions

The results with PTSA:[Ch]Cl (1:1) reported above show the importance of acidic conditions for ESs wood delignification. In this context, it would be logical to infer that the delignification efficiency of any ES media could be improved with the adequate amount of an acid catalyst. Therefore, in order to improve the *E. globulus* wood delignification using LA:[Ch]Cl (10:1), PA:U (2:1) and U:[Ch]Cl (2:1) aqueous solutions, mineral and organic acids, such as hydrochloric acid (HCl), sulfuric acid (H_2SO_4) and PTSA were added as catalysts to ESs aqueous solutions until a pH of 0.5 was achieved. The effects of acid catalysts in ESs aqueous solutions on *E. globulus* wood delignification are shown in Figure 47. The detailed solid fraction and precipitated lignin yields values and the respective standard deviations, are reported in Table S5.6 (SI).

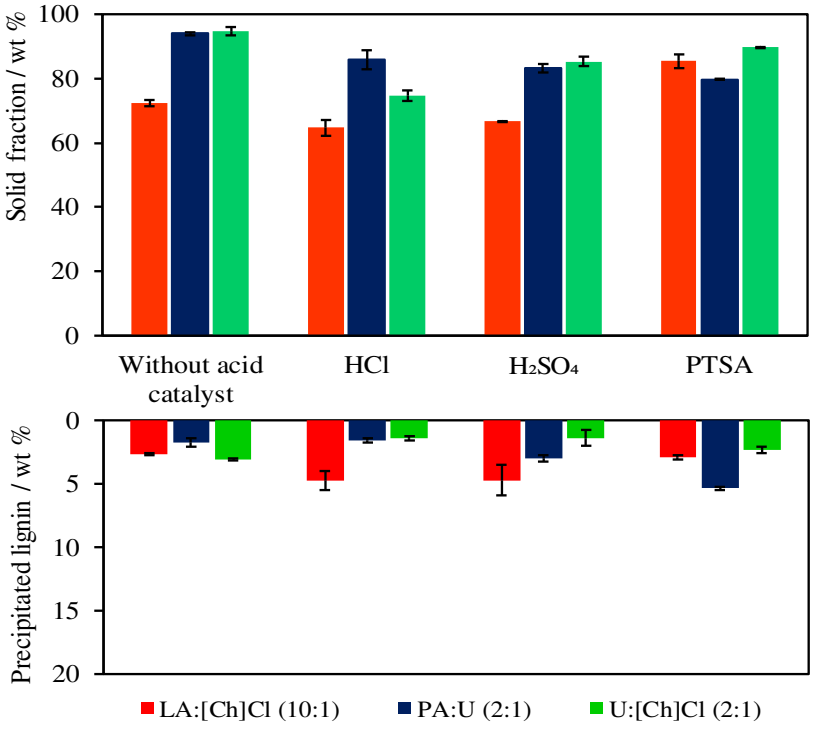

Figure 47. Effect of acid catalyst on *E. globulus* wood delignification (8 h, wood/liquid ratio of 0.5/10 w/w, 300 rpm and 363.15 K), in terms of solid fraction and precipitated lignin yields at constant pH of 0.5.

As observed in Figure 47, this approach allowed to achieve partial wood delignification using LA:[Ch]Cl (10:1) in presence of HCl and H_2SO_4; and PA:U (2:1) in the presence of H_2SO_4 and PTSA (see solid fractions images in Figure 48). The best results regarding of the solid fraction yield combined with the maximum precipitated lignin yield, were achieved with LA:[Ch]Cl (10:1) assisted by H_2SO_4 (solid fraction yield of 66.72 ± 0.23 wt % containing a residual Klason lignin of 7.46 ± 1.56 wt % and precipitated lignin yield of 4.71 ± 1.21 wt %) and PA:U (2:1) in the presence of PTSA (solid fraction of 79.76 ± 0.26 wt % and precipitated lignin of 5.33 ± 0.12 wt %). As expected, the addition of an acid catalyst demonstrated to have a positive effect on wood delignification, improving the lignin removal significantly (from 13.14 to 23.62 wt % and from 8.7 to 26.73 wt %, respectively). These results are in accordance with the lignin removal yields reported in literature (see Table 9)[75] and the results presented above for neat LA:[Ch]Cl (10:1). Despite the good performance of U:[Ch]Cl on hemicelluloses extraction from wood,[62] a weak performance on wood delignification was observed, even under acidic conditions.

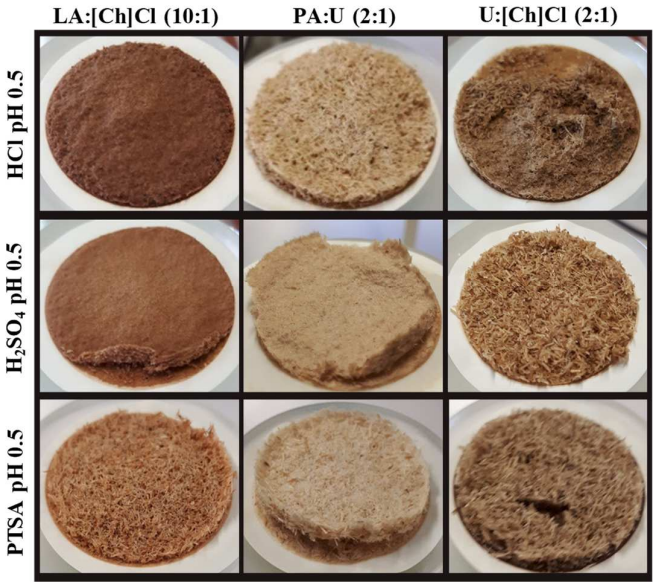

Figure 48. Optical microscopy images of *E. globulus* solid fraction-LA:[Ch]Cl, solid fraction-PA:U and solid fraction-U:[Ch]Cl, obtained after delignification with ESs aqueous solutions in the presence of HCl, H_2SO_4 and PTSA at constant pH value of 0.5, 363.15 K, 8 h and atmospheric pressure.

Although a complete wood delignification was not achieved, the cellulose fibers in the solid fraction-LA:[Ch]Cl+H_2SO_4 and solid fraction-PA:U+PTSA were assessed by optical microscopy, while the chemical structural changes in precipitated lignins were assessed by FTIR spectroscopy. The absorption bands were assigned according to literature.[110,112,114,120]

2.1 Characterization of solid fraction from LA:[Ch]Cl+H_2SO_4 and PA:U+PTSA systems

The optical mycroscopy images of fibers in solid fraction-LA:[Ch]Cl+H_2SO_4 revealed morphological changes when compared with kraft pulp fibers (Figure 50). The fibers in solid fraction-LA:[Ch]Cl+H_2SO_4 are less fragmented than both fibers in solid fraction-PTSA:[Ch]Cl (Figure 45) and in solid fraction-neat LA:[Ch]Cl (10:1) (see Figure 49). However, the brownish color, also observed in the fibers surface of solid fraction-LA:[Ch]Cl+H_2SO_4, suggests the occurrence of lignin condensation reactions, although to a smaller extent than that observed in solid fraction-PTSA:[Ch]Cl fibers, discussed before. On the contrary, the fibers from solid fraction-PA:U+PTSA show more morphological similarity with the kraft pulp fibers. No major differences were observed in fibers produced with ES and kraft pulp fibers.

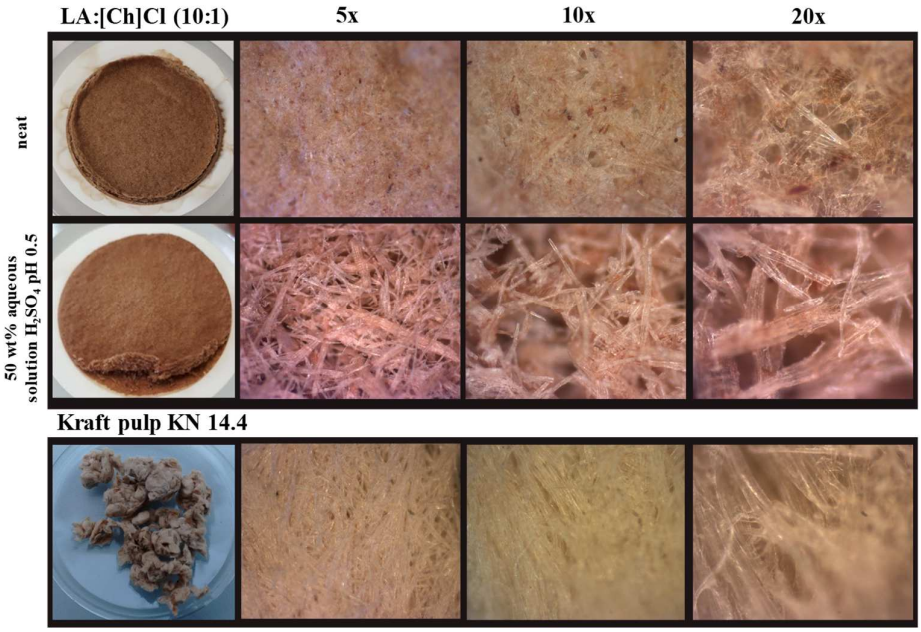

Figure 49. Optical microscopy images of *E. globulus* solid fraction from LA:[Ch]Cl systems, obtained after delignification with neat ESs or ESs aqueous solutions in the presence of H_2SO_4 as catalyst, respectively, at 363.15 K, 8 h and atmospheric pressure. Conventional kraft pulp from *E. globulus* wood with kappa number 14.4. Magnification of 5x, 10x and 20x.

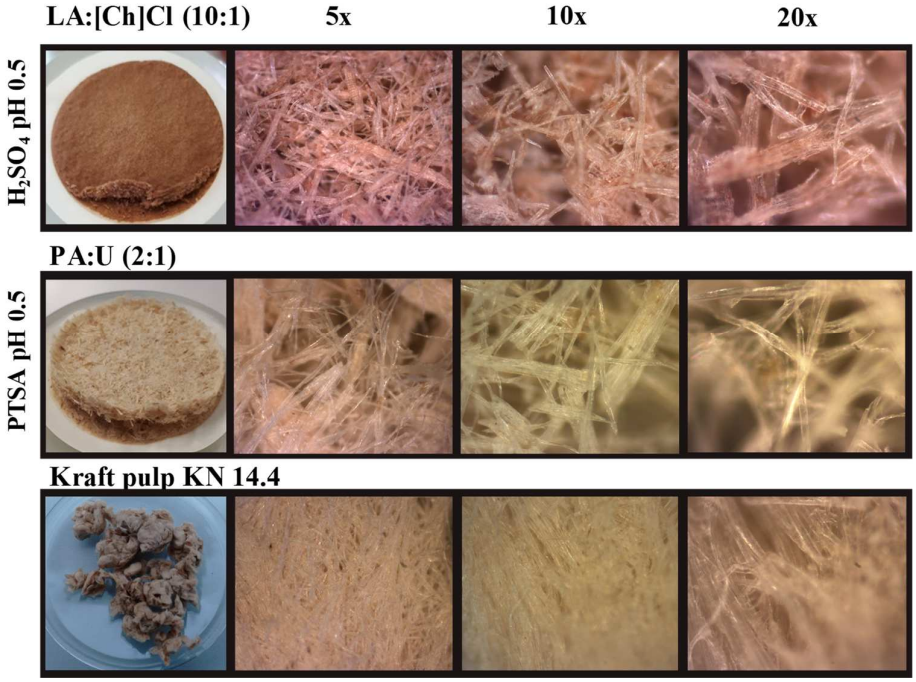

Figure 50. Optical microscopy images of *E. globulus* solid fraction from LA:[Ch]Cl and PA:U systems, obtained after delignification with ESs aqueous solutions in the presence of H_2SO_4 and PTSA as catalysts, respectively at constant pH of 0.5, 363.15 K, 8 h and atmospheric pressure. Conventional kraft pulp from *E. globulus* wood with kappa number 14.4. Magnification of 5x, 10x and 20x.

2.2 Characterization of precipitated lignin from LA:[Ch]Cl+H_2SO_4 and PA:U+PTSA systems

The precipitated lignin-LA:[Ch]Cl+H_2SO_4 show a similar FTIR profile (Figure 51) to dioxane lignin. However, the absorption band that arise at 1734 cm^{-1}, associated with unconjugated ketones (C=O stretching vibrations),[110–112] can be explained by the formation of Hibbert's ketones, characteristic products from wood delignification in acidic media.[5] The mechanisms behind the wood delignification mediated by ESs were investigated by Alvarez-Vasco *et al.*[74] in a preliminary study of a β-*O*-4 linkage lignin dimeric model compound (guaiacylglycerol-β-guaiacyl ether) treated by neat LA:[Ch]Cl under 418.15 K. The authors[74] concluded that this reaction mechanism was similar to lignin acidolysis catalyzed by HCl (dioxane lignin), producing guaiacol and Hibbert's ketones. Recently, Rodriguez *et al.*[113] reported the occurrence of esterification reaction on carboxylic acid-[Ch]Cl based ES, between the acid and the hydroxyl group of choline chloride, promoted by temperature. Furthermore, the authors[113] suggested a less extent esterification reaction occurrence in presence of ES aqueous solutions. In this sense, the presence of C=O stretching vibrations observed in lignin-LA:[Ch]Cl (10:1)+H_2SO_4 FTIR spectrum, can also be explained by the possible occurrence of esterification reaction between the lactic acid from ES and hydroxyl groups in the lignin structure, promoted by temperature and the strong acidity of the medium. Moreover, the presence of a carbonyl group stretching vibration at 1734 cm^{-1}, associated to the occurrence of esterification reactions was also observed in the FTIR spectra of lignin isolated from neat LA:[Ch]Cl (10:1) and 50 wt % aqueous solution of LA:[Ch]Cl (10:1) (Figure 52). No evidences of ES components as contaminants in precipitated lignin were observed, when compared with LA:[Ch]Cl (10:1) 50 wt % aqueous solution FTIR spectrum (Figure 53). However, the precise roles of ES constituents may play in the lignin depolymerization still require further investigation.

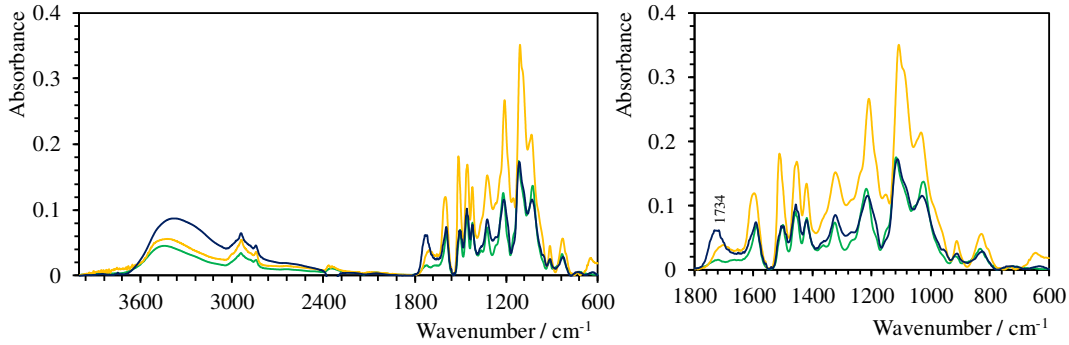

Figure 51. Normalized FTIR spectra of precipitated lignin-LA:[Ch]Cl+H_2SO_4 (blue), kraft lignin (yellow) and dioxane lignin (green).

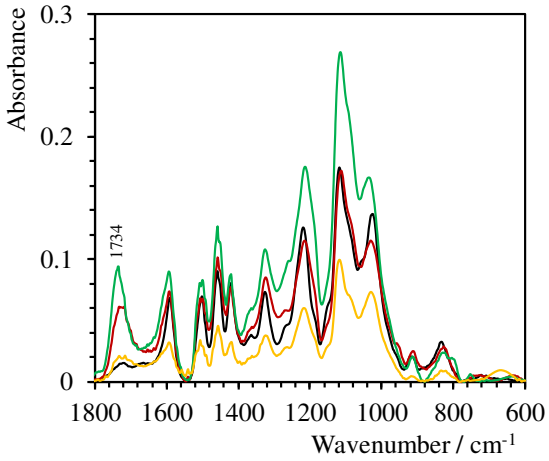

Figure 52. Normalized FTIR spectra of precipitated lignin-LA:[Ch]Cl: neat (green), 50 wt % aqueous solution (yellow), 50 wt % aqueous solution with H_2SO_4 as acid catalyst at pH 0.5 (red) and dioxane lignin (black).

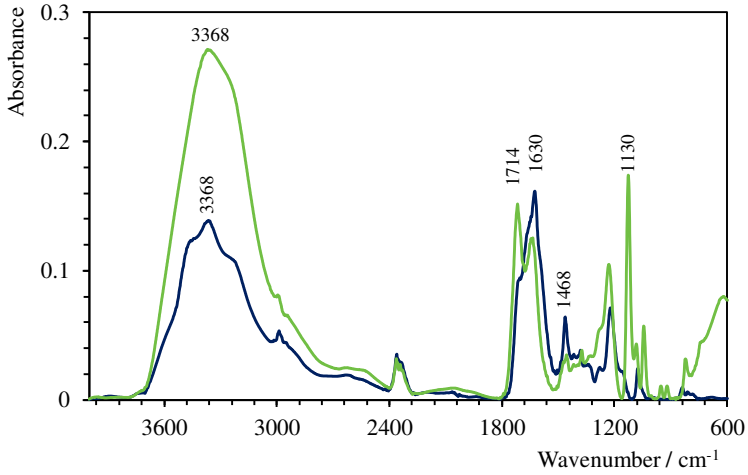

Figure 53. FTIR normalized spectra of ESs aqueous solutions at 50 wt %: PA:U (2:1) (blue) and LA:[Ch]Cl (10:1) (green).

The FTIR spectrum (Figure 54) of the precipitated lignin-PA:U+PTSA also shows a similar profile to dioxane lignin. However, the absorption band at 1706 cm^{-1} associated with unconjugated carbonyl/carboxyl C=O stretching, may be associated to the presence of carbohydrate contaminants.[114] Furthermore, the appearance of absorption bands at 3380 and 1638 cm^{-1}, suggest the presence of ES components as impurities (see the characteristic absorption band of PA:U (2:1) 50 wt % aqueous solution in Figure 53). No evidence of esterification reactions, discussed above, were observed in this system.

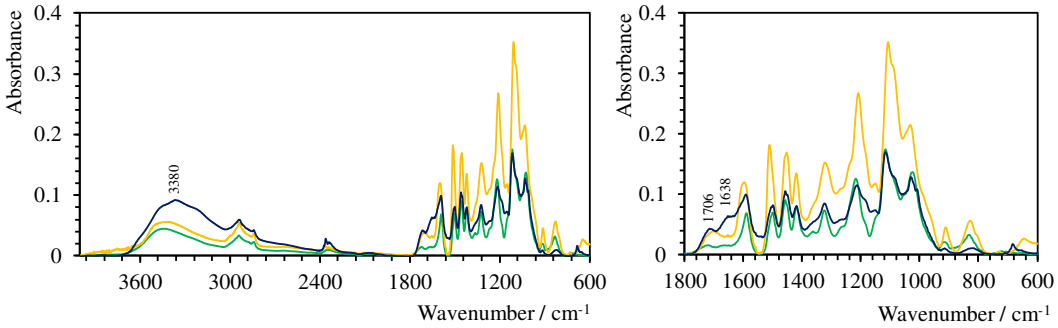

Figure 54. Normalized FTIR spectra of precipitated lignin-PA:U+PTSA (blue), kraft lignin (yellow) and dioxane lignin (green).

These results allowed to conclude that wood delignification using ESs at mild conditions, require the addition of an acid catalyst to enhance lignin depolymerization. The best system, in terms of preserving cellulose fibers and apparently, reduced chemical changes in precipitated lignin structures was PA:U (2:1) aqueous solution assisted by PTSA. However, to achieve a more extensive wood delignification using this system, the process variables would have to be optimized, namely the amount of acid catalyst, temperature, time and ES concentration.

3. Wood delignification using PA:U (2:1) aqueous solution catalyzed with PTSA

To achieve a successful wood delignification with PA:U(2:1)+PTSA system, by obtaining a solid fraction yield close to 50 wt % (preserving cellulose fibers) and maximum amount of precipitated lignin, the amount of PTSA, temperature, time and ES concentration were optimized. In the first place, the effect of pH on wood delignification induced by PTSA

content in PA:U (2:1) aqueous solution at three different levels (13, 17 and 25 wt % of PTSA) was investigated (Figure 55). The detailed solid fraction, precipitated lignin yields and the pH value of aqueous solutions and the respective standard deviations, are reported in Table S5.7 (SI).

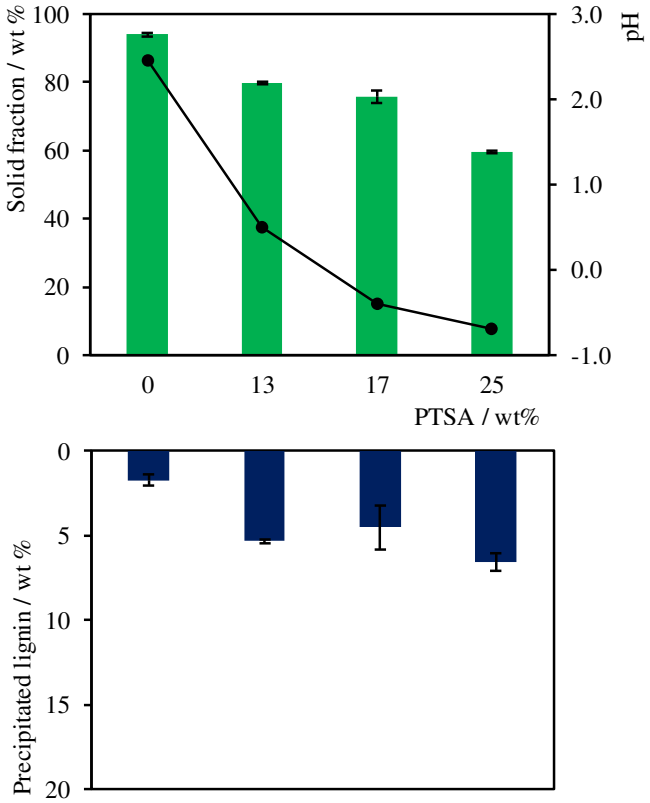

Figure 55. Effect of PTSA content in PA:U (2:1) aqueous solution at 50 wt % on *E. globulus* wood delignification (8 h, wood/liquid ratio of 0.5/10 w/w, 300 rpm and 363.15 K), based on solid fraction (green) and precipitated lignin (blue) yields. The pH values of the ESs aqueous solutions in the presence of PTSA are represented in black dots.

These results show significant improvements on wood delignification (from 79.76 ± 0.26 to 59.50 ± 0.51 wt % of solid fraction) promoted by the increase of PTSA content (from 13 to 25 wt %) in PA:U (2:1) 50 wt % aqueous solution, while only a slight increase in the precipitated lignin yield (from 5.33 ± 0.12 wt % to 6.55 ± 0.50 wt %) was observed. Furthermore, the cellulose fibers in solid fraction-PA:U(2:1)+25PTSA were preserved, as corroborated by the optical microscopy images shown in Figure 56.

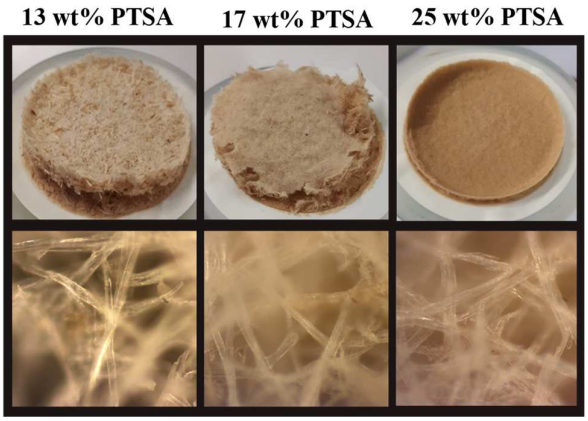

Figure 56. Optical microscopy images of *E. globulus* solid fraction from PA:U (2:1) systems, obtained after delignification with ESs aqueous solutions in the presence of PTSA at three different levels (13, 17 and 25 wt %), 363.15 K, 8 h and atmospheric pressure. Magnification of 20x.

Based on these results, the optimization of process variables, such as temperature, time and ES concentration, was developed using a Box-Behnken design method. This strategy allowed to know the role of each process parameters on wood delignification, based on the solid fraction and precipitated lignin yields (see experimental design matrix and response results on Table S5.8, SI). ANOVA was used to fit a quadratic model for solid fraction and precipitated lignin experimental data (see Table S5.9, SI). The results suggested that the quadratic model effectively adjusted the solid fraction experimental data with a correlation square coefficient (R^2) of 0.8974. Furthermore, the process parameter with higher effect on solid fraction yield was ES concentration, followed by Temperature, the interactions Temperature x ES concentration and Time. On the other hand, the interactions Temperature x Time, Time x ES concentration, Temperature^2, Time^2 and ES concentration^2, were considered not significant model terms, with *p*-value > 0.05. Regarding the precipitated lignin, a quadratic model effectively adjusted the experimental data with a R^2 of 0.9474. Furthermore, Temperature was the most significant model term, followed by ES concentration, the interaction Temperature x ES concentration, Time and Temperature^2. The interactions Temperature x Time, Time x ES concentration, Time^2 and ES concentration^2 were considered not significant model terms, with *p*-value > 0.05.

Thus, experimental results were fitted according to quadratic model for solid fraction yield and precipitated lignin yield responses in Box-Behnken design:

Solid fraction yield = – 162.22 + 2.58 x Temperature – 3.48 x Time – 3.71 x ES concentration – 5.39E-03 x Temperature x Time + 1.31E-02 x Temperature x ES concentration + 4.03E-02 x Time x ES concentration – 5.52E-03 x Temperature^2 +1.10E-01 x Time^2 – 5.06E-03 x ES concentration^2

Precipitated lignin yield = 126.67 – 8.63E-01 x Temperature – 1.24 x Time + 5.07E-01 x ES concentration + 5.07E-03 x Temperature x Time – 1.49E-03 x Temperature x ES concentration – 3.71E-03 x Time x ES concentration + 1.44E-03 x Temperature^2 – 8.06E-03 x Time^2 – 5.00E-05 x ES concentration^2

The residual analysis confirmed the normality of the error distribution (Figure 57).

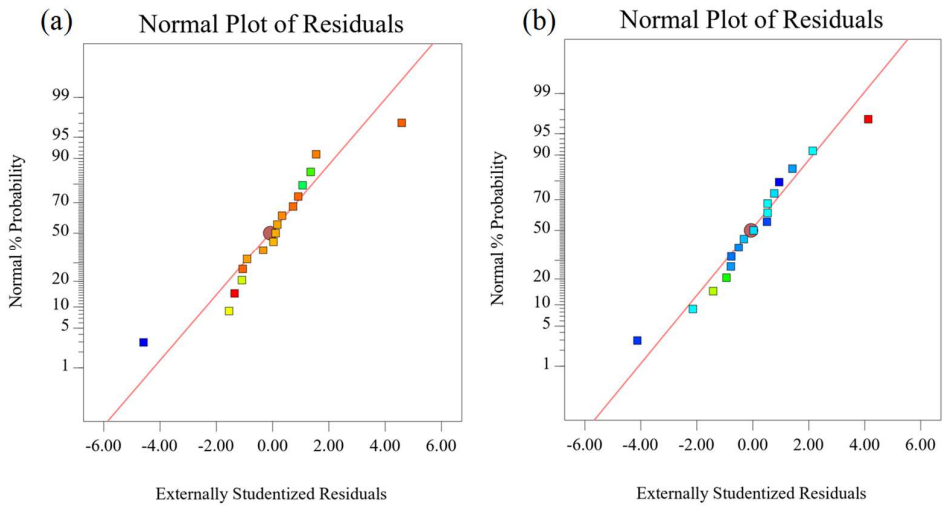

Figure 57. Residual analysis for quadratic model of solid fraction (a) and precipitated lignin (b).

Based on the models developed above, it was possible to obtain the 3D surface plots for solid fraction and precipitated lignin yields responses (Figure 58), where a significant effect of ES concentration on *E. globulus* wood delignification, was observed. The results show that the best process conditions to maximize lignin extraction without loss of cellulose, while preserving the fibers quality, were 363.15 K, 8 h and 50 wt % aqueous solution of PA:U (2:1), in the presence of 25 wt % of PTSA at atmospheric pressure. Under these conditions, a solid fraction yield of 65.85 wt % and precipitated lignin yield of 4.95 wt % were predicted by quadratic models.

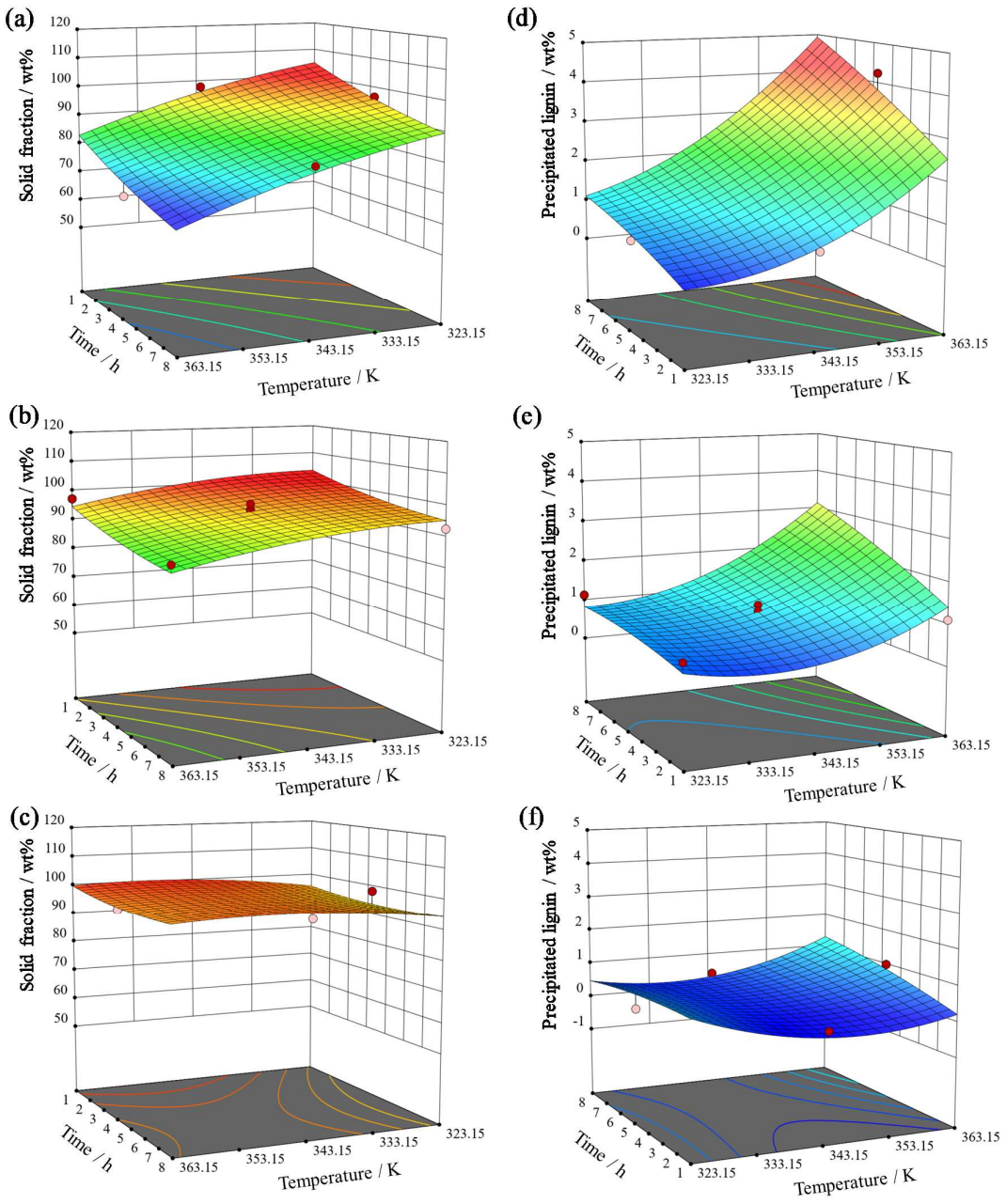

Figure 58. Effects of process variables (temperature, time and ES concentration) on *E. globulus* wood delignification with PA:U (2:1) in the presence of 25 wt % of PTSA. Solid fraction yield response (left) affected by ES concentration of 50 wt % (a), 75 wt % (b) and 100 wt % (c). Precipitated lignin yield response (right) affected by ES concentration of 50 wt % (d), 75 wt % (e) and 100 wt % (f). Minimal (blue) and maximal (red).

To validate the proposed models for solid fraction and precipitated lignin responses, the best process conditions (363.15 K, 8h and 50 wt % aqueous solution of PA:U (2:1), in the presence of 25 wt % of PTSA) were applied on *E. globulus* wood delignification. These conditions allowed to produce a solid fraction yield of 59.50 ± 0.51 wt % containing a

residual Klason lignin of 3.86 ± 0.10 wt %. These results are in accordance with a typical pulp yield obtained by conventional kraft pulping of *E. globulus* wood (55 wt % containing a residual Klason lignin of 2 wt %).[45] Furthermore, it was possible to remove 80.64 wt % of lignin from *E. globulus* wood at mild conditions and to recover 40.73 wt % of lignin (6.55 ± 0.50 wt % of precipitated lignin) from ES liquor. Although, some differences were observed between the experimental and predicted responses, they are within the experimental error. Finally, the solid fraction and precipitated lignin obtained at the best process conditions were characterized by FTIR and NMR spectroscopy, optical microscopy and elemental analysis to assess the cellulose fibers and the chemical structure changes on precipitated lignin induced by this new process.

3.1 Characterization of solid fraction from PA:U(2:1)+25PTSA system at optimal conditions

The solid fraction-PA:U(2:1)+25PTSA was assessed by FTIR spectroscopy and compared with a conventional *E. globulus* kraft pulp with kappa number 14.4 (Figure 59). The absorption bands were assigned following the literature[117–119] and details are presented in Table S5.2 (SI). It is possible to conclude that cellulose is the main component of this fraction. These results are also corroborated by solid-state ^{13}C NMR analysis (Figure 60 and for more details see Table S5.10, SI) in which a characteristic solid-state ^{13}C NMR of cellulose can be observed. Furthermore, the solid-state ^{13}C NMR of solid fraction also shows that the crystalline structure of cellulose was not affected (see Figure 60). Moreover, optical microscopy analysis (Figure 61) revealed that the cellulose fiber quality is preserved in this system.

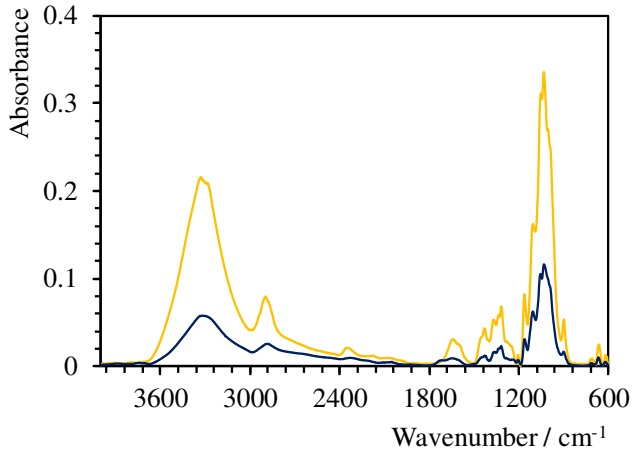

Figure 59. Normalized FTIR spectra of solid fraction-PA:U(2:1)+25PTSA (blue) and the conventional kraft pulp from *E. globulus* wood with kappa number 14.4 (yellow).

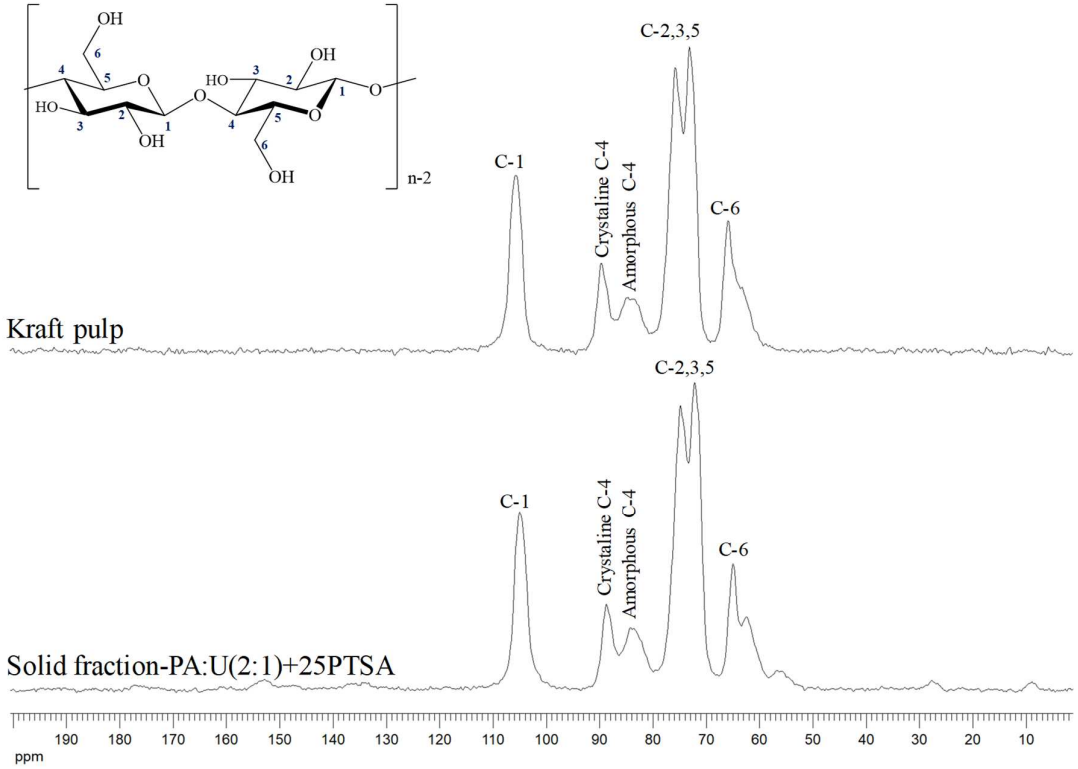

Figure 60. Solid-state ^{13}C CP-MAS NMR spectra of cellulose from solid fraction-PA:U(2:1)+25PTSA and from conventional kraft pulp from *E. globulus* wood with kappa number 14.4. The chemical structure of cellulose is shown above.[6]

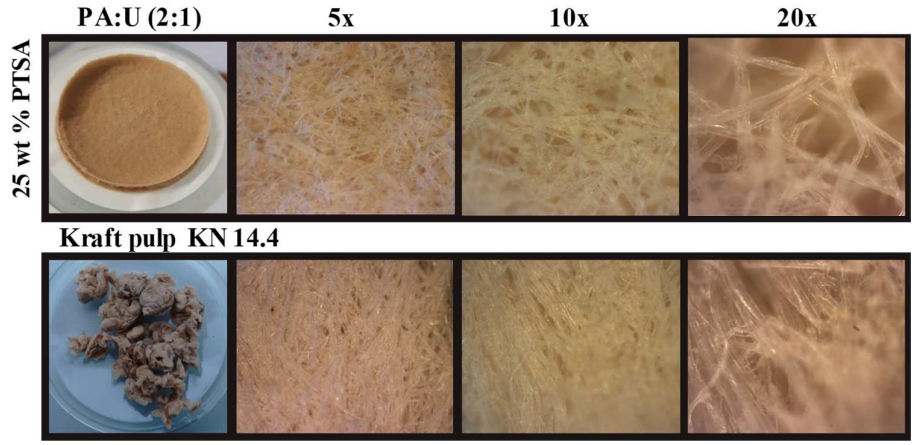

Figure 61. Optical microscopy images of *E. globulu*s solid fraction from PA:U (2:1) systems, obtained after delignification with ESs aqueous solutions in the presence of 25 wt % of PTSA at 363.15 K, 8 h and atmospheric pressure. Conventional kraft pulp from *E. globulus* wood with kappa number 14.4. Magnification of 5x, 10x and 20x.

3.2 Characterization of precipitated lignin from PA:U(2:1)+25PTSA system at optimal conditions

Lignin is the main component present in the fraction obtained from PAU(2:1)+25PTSA system, as revealed by the FTIR analysis (Figure 62). The absorption bands were assigned according to literature.[110,112,114,120] Furthermore, absorption bands characteristic of PA:U (2:1)+25PTSA aqueous solution (3388, 2930 and 1662 cm^{-1}) were also observed (see the characteristic absorption band of PA:U (2:1) 50 wt % aqueous solution in Figure 53). This was corroborated by elemental analysis and ^{1}H NMR spectroscopy. The elemental analysis revealed the presence of 4.05 ± 0.02 wt % of nitrogen in lignin composition (Table S5.4, SI) and the resonance peak characteristic of urea (δ_H, 5.7 ppm) and PTSA (δ_H, 7.6 and 6.9 ppm) were observed in the ^{1}H NMR spectrum (see Figure 63). Moreover, the presence of carbonyl groups were also observed in the FTIR spectra of lignin isolated from PA:U (2:1)+25PTSA system at 1728 cm^{-1} (Figure 62), possibly due to the occurrence of esterification reactions, as discussed above. Finally, the absence of an absorption band at 635 cm^{-1}, assigned to the C-S stretching vibration in lignin-PA:U (2:1)+25PTSA spectra suggests that sulfur-free lignin was produced, without contamination of PTSA. This result was further confirmed by the absence of sulfur content in elemental analysis (see Table S5.4, SI).

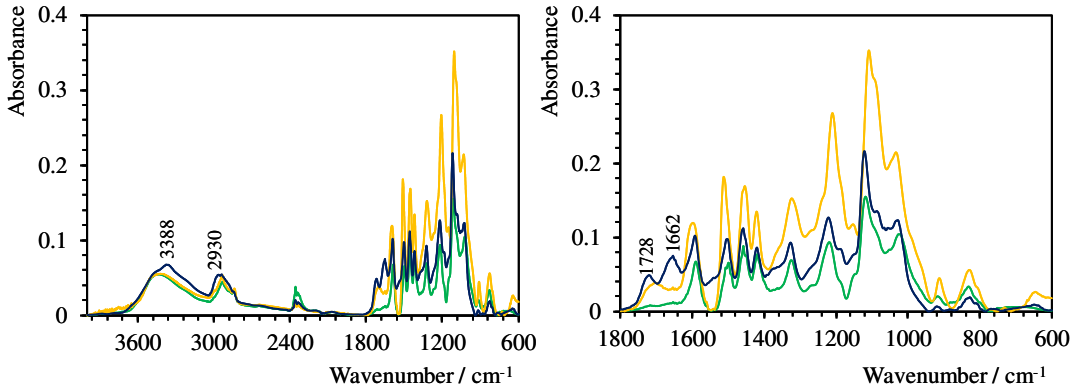

Figure 62. Normalized FTIR spectra of lignin-PA:U(2:1)+25PTSA (blue), kraft lignin (yellow) and dioxane lignin (green).

The main changes induced in lignin-PA:U (2:1)+25PTSA, were assessed in more detail employing ^{1}H and ^{13}C NMR spectroscopy analysis (semi-quantitative and quantitative, correspondingly). The ^{1}H and ^{13}C NMR spectra of lignin-PA:U (2:1)+25PTSA and the technical lignins (kraft and dioxane lignins) are presented in Figure 63 and Figure 64, respectively. The resonance assignments were attributed according to literature[27,111,112,115,116] as shown in Table S5.11 and S5.12, (SI).

The ^{1}H and ^{13}C NMR spectroscopy analysis revealed that aliphatic hydroxyl groups in lignin-PA:U(2:1)+25PTSA presents the lowest content (2.27/C_9) compared to kraft lignin (2.86/C_9) and dioxane lignin (3.61/C_9). For phenolic hydroxyl groups, lignin-PA:U(2:1)+25PTSA (1.15/C_9) presents higher value than dioxane lignin (0.74/C_9) but lower than kraft lignin (1.98/C_9). When compared to chemical structure of precipitated lignin from LA:[Ch]Cl system reported by Alvarez-Vasco *et al.*[74] the lignin-PA:U(2:1)+25PTSA presented lower content of aliphatic hydroxyl groups, phenolic hydroxyl groups and methoxyl groups (see Table 10). Furthermore, the lignin-PA:U(2:1)+25PTSA and kraft lignin presented a lower content of β-*O*-4 structures than dioxane lignin (0.15/C_9, 0.12/C_9 and 0.41/C_9, respectively). Some authors[74,79] reported the absence of β-*O*-4 structures on precipitated lignin obtained from wood delignification using neat LA:[Ch]Cl, at harsh conditions (393.15 – 418.15 K and 6 – 24h). However, lignin-PA:U(2:1)+25PTSA presented higher content of β-*O*-4 structures, when compared with lignin-LA:[Ch]Cl reported by Alvarez-Vasco *et al.*[74] even at mild conditions. The decrease of β-*O*-4 structures content in lignin structure during PA:U(2:1)+25PTSA and kraft processes is a consequence of the

cleavage of aryl-ether structures, one of the main reactions occurring in the delignification process that lead to important changes in lignin structure,[4] like the increase of phenolic hydroxyl groups. Furthermore, these results suggests that PA:U(2:1)+25PTSA system induced less structural changes in lignin, than the kraft process or even the LA:[Ch]Cl system proposed by Alvarez-Vasco *et al.*[74]

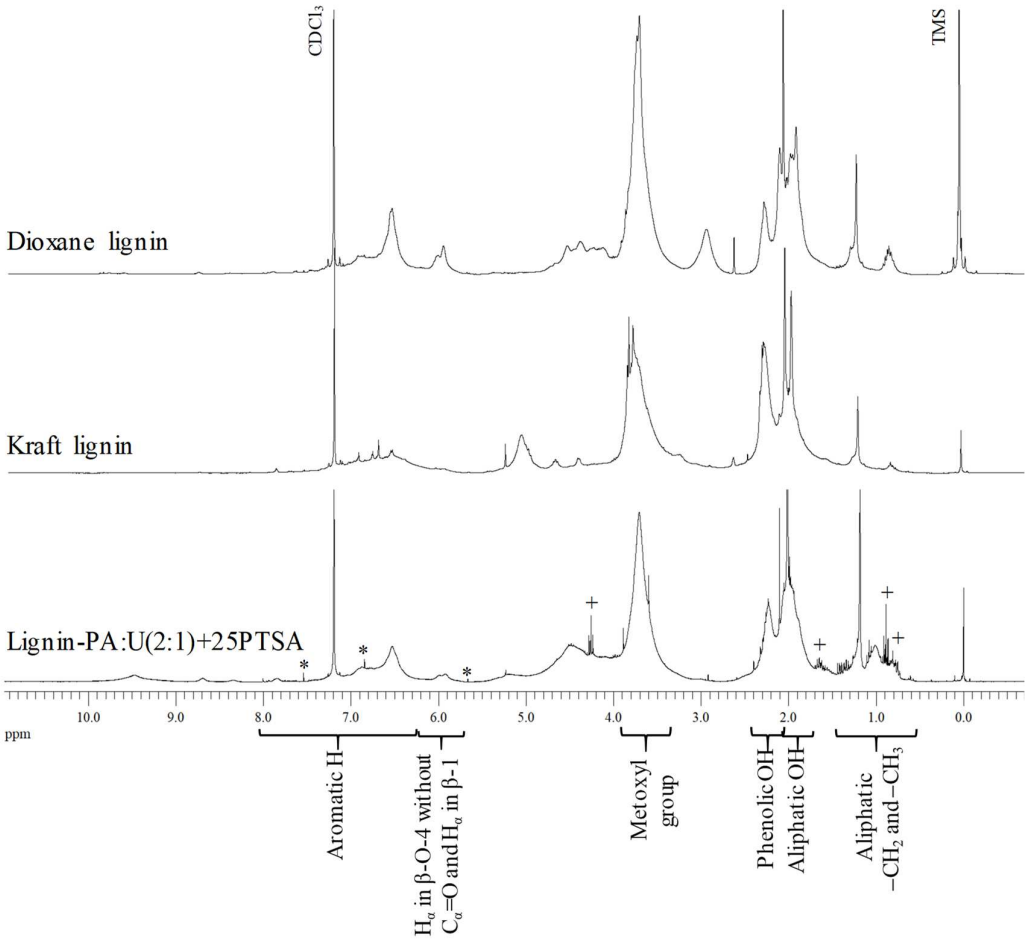

Figure 63. ^{1}H NMR spectra ($CDCl_3$) of acetylated *E. globulus lignins* (dioxane, kraft and PA:U(2:1)+25PTSA). (*) Urea and PTSA contaminants. (+) Solvent contaminant.

The ^{1}H NMR spectrum also shows a lower content of protons in aromatic ring moieties for lignin-PA:U(2:1)+25PTSA (1.15/C_9) and kraft lignin (1.25/C_9) than dioxane lignin (1.63/C_9). The ^{13}C NMR analysis allowed to quantify the content of methoxyl groups/C_6 in lignin structure and the results show that the lowest content was found for

lignin-PA:U(2:1)+25PTSA (1.23/C_6) comparatively to kraft lignin (1.38/C_6) and dioxane lignin (1.73/C_6). Moreover, the S:G:H ratio obtained was 68:32:0 for lignin-PA:U(2:1)+PTSA, 73:25:2 for kraft lignin and 81:18:1 for dioxane lignin, which are in good agreement with the ratio reported in literature for kraft and dioxane *E. globulus* lignins (see Table 5 and Table 6).[27,43] Finally, the degree of condensation (DC) was assessed by ^{13}C NMR spectroscopy and the results revealed that lignin-PA:U(2:1)+25PTSA and kraft lignin presented more condensed structures (31 % and 30 %, respectively) than dioxane lignin (15 %). These results showed that PA:U(2:1)+25PTSA system led to a considerable lost of syringyl propane units in lignin structure, when compared to kraft and dioxane lignins, which leads to the decrease of methoxyl groups observed. On the other hand, the higher degree of condensation in lignin-PA:U(2:1)+25PTSA and kraft lignin, comparatively to dioxane lignin, are possible related with the presence of higher content of guaiacyl propane units, which have an aromatic carbon in C-5 position available to be involved in condensed structures.

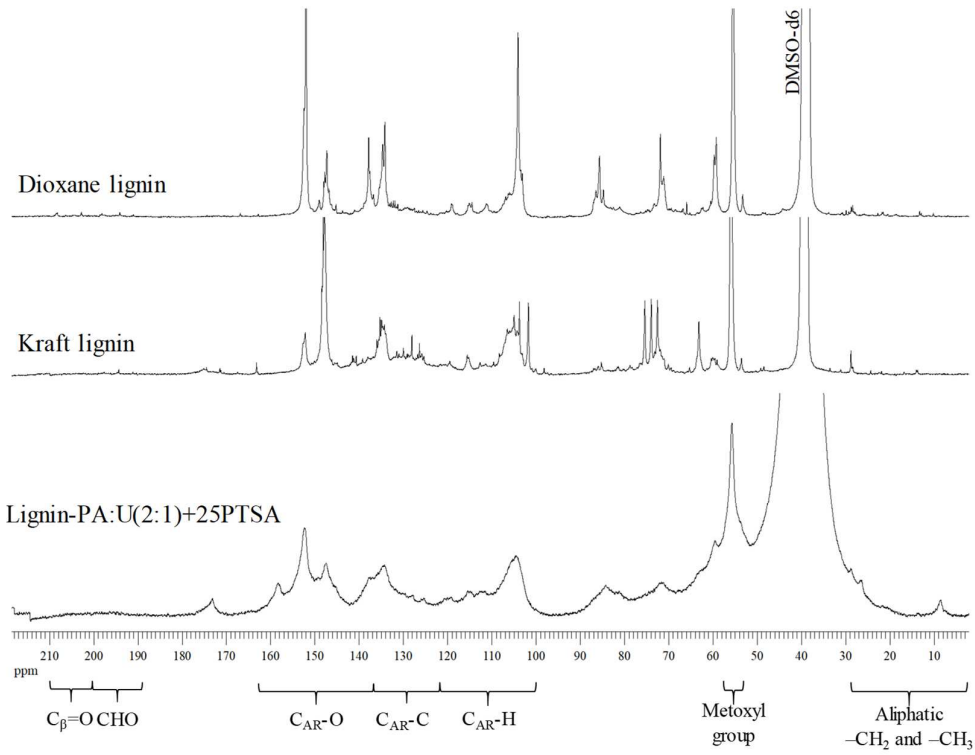

Figure 64. Quantitative ^{13}C NMR spectra (DMSO-d_6) of *E. globulus* lignins (dioxane, kraft and PA:U(2:1)+25PTSA).

In summary, the analysis performed to the final products (solid fraction and precipitated lignin) suggested that PA:U(2:1)+25PTSA aqueous solution system used in *E. globulus* wood delignification process at mild conditions, preserve the cellulose fiber (compared with kraft pulp fibers), while a minor chemical modifications on precipitated lignin were observed (compared to kraft process and the LA:[Ch]Cl system reported in literature[74]).

4. In the PATH of process scale-up – Preliminary study using PA:U(2:1)+25PTSA system

Encouraged by the excellent performance of PA:U(2:1)+25PTSA 50 wt % aqueous solution as solvent on *E. globulus* wood delignification at milder conditions, preliminary studies using a 300 ml PARR Stirred reactor, were performed. This study attempts to replicate the optimized bench scale process (from 0.5/10 (w/w) in glass reaction tubes to 6/120 (w/w) in PARR Stirred reactor) in order to assess its reproducibility at a different scale and to identify a set of best practices for future pilot scale studies.

After wood delignification using the abovementioned system in a reactor, A solid fraction yield of 63.95 wt % was produced containing a residual Klason lignin of 13.07 ± 1.65 wt %. Furthermore, 40.73 wt % of lignin (7.18 ± 0.47 wt % of precipitated lignin) was possible to recover from ES liquor. Higher solid fraction yield and residual Klason lignin were achieved, comparatively to those obtained from ES wood delignification in tubes. The high amount of non-delignified wood present in the solid fraction, as observed in Figure 65, may be the responsible for the increase of residual Klason lignin content in the solid fraction. Despite these results, the optical microscopy analysis (Figure 65) shown that the cellulose fiber is preserved in this system, independently of the used bench scale. Furthermore, the FTIR spectra of precipitated lignin, illustrated in Figure 66, show a similar FTIR profile to lignin-PA:U(2:1)+25PTSA obtained from wood delignification in tubes.

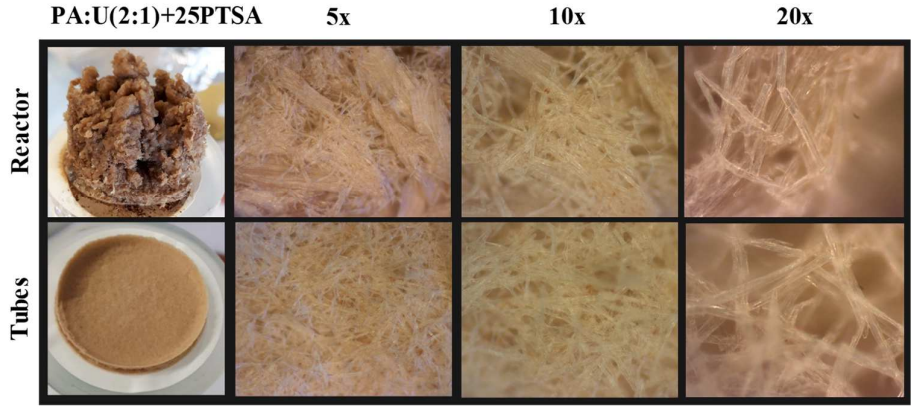

Figure 65. Optical microscopy images of *E. globulus* solid fraction from PA:U (2:1) systems, obtained after delignification with ESs aqueous solutions in the presence of 25 wt % of PTSA at 363.15 K, 8 h and atmospheric pressure at different scales, in tube (0.5 g of wood) and reactor (6 g of wood). Magnification of 5x, 10x and 20x.

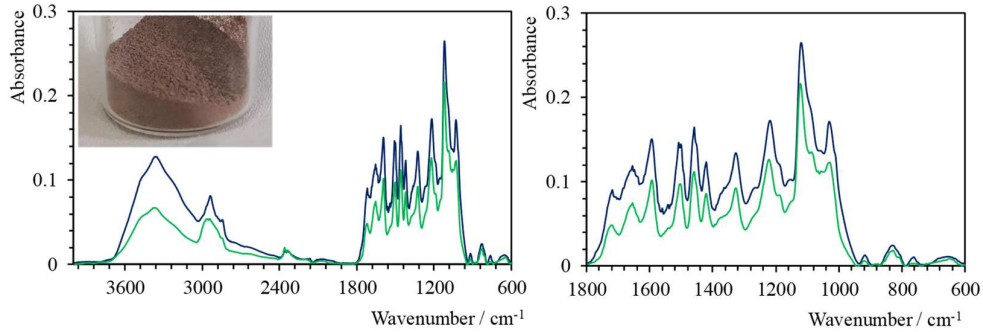

Figure 66. Normalized FTIR spectra of lignin-PA:U(2:1)+25PTSA from reactor (blue) and tubes (green).

These preliminary results highlighted once again the great performance of PA:U(2:1)+25PTSA 50 wt % aqueous solution system on *E. globulus* wood delignification at mild conditions, independently of the bench scale used (glass reaction tubes or PARR Stirred reactor). However, to achieve a more extensive wood delignification using this scale, the process variables would have to be scrutinized and optimized.

CONCLUSIONS

This work reports wood delignification with eutectic solvents aqueous solution at mild conditions and their impact on solid fractions and chemical structure of precipitated lignins. Despite the apparent potential of PTSA:[Ch]Cl (1:1) at 50 wt % aqueous solution to delignify *E. globulus* wood at mild conditions (363.15 K and 8 h, at atmospheric pressure),

the solid fraction containing a residual Klason lignin of 10.69 ± 0.16 wt %, presented degradation comparatively to *E. globulus* kraft pulp. Furthermore, the precipitated lignin (15.38 ± 0.59 wt %) presented significant chemical changes when compared with *E. globulus* technical lignins. The results here reported also showed that wood delignification at mild conditions requires an acid catalyst, particularly when LA:[Ch]Cl (10:1) and PA:U (2:1) are applied as delignification solvents. An experimental design was used to establish the optimal conditions for *E. globulus* wood delignification with a 50 wt % aqueous solution of PA:U (2:1)+25 wt % PTSA. At mild conditions (363.15 K and 8 h, at atmospheric pressure) a solid fraction rich in cellulose (59.50 ± 0.51 wt %, yield) containing a residual Klason lignin of 3.86 ± 0.10 wt % was produced. Furthermore, this optimized process led to a removal lignin of 80.64 wt % from *E. globulus* wood and to recover 40.73 wt % of sulfur-free lignin (6.55 ± 0.50 wt % of precipitated lignin) from eutectic solvent liquor. Moreover, an extensive chemical structure analysis of precipitated lignin and cellulose fibers revealed that fewer transformations are induced by PA:U(2:1)+25PTSA system, as compared to kraft process and the LA:[Ch]Cl system reported in literature. Finally, promising preliminary results on scale-up the eutectic solvent wood delignification process were achieved. This work provides an important contribution to the understanding of the potential of eutectic solvent aqueous solutions on wood delignification process, opening the pathway for a future low-carbon strategy for pulp and paper industry.

Chapter IV

Improvements on wood Delignification with Ternary Eutectic Solvents

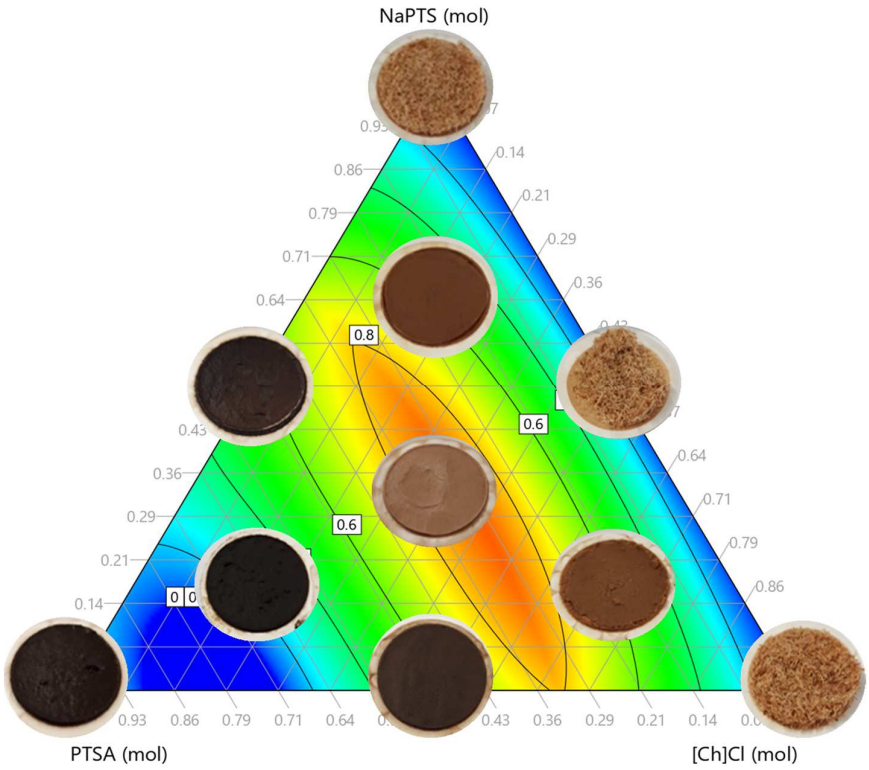

Wood delignification using ternary eutectic solvents aqueous solutions at milder conditions, to produce a preserved cellulose fibers and sulfur-free lignin fraction.

Adapted from:

Belinda Soares; Armando J. D. Silvestre; Paula C. R. Pinto; Carmen S. R. Freire and João A. P. Coutinho. **2019**. *Improvements on wood delignification with ternary deep eutectic solvents.* Under preparation.

ABSTRACT

A new strategy to improve *Eucalyptus globulus* wood delignification process with eutectic solvents was here investigated. Sodium *p*-toluenesulfonate was used as partial substitute of *p*-toluenesulfonic acid in PTSA:[Ch]Cl delignification process, to control the medium acidity in order to preserve the cellulose fibers and to produce a sulfur-free lignin. To prepare and optimize this ternary eutectic solvent system a simplex-centroid design was implemented. This methodology allowed to access the impact of the different components of the ternary eutectic solvent (NaPTS, PTSA and [Ch]Cl) on wood delignification, specifically on the obtained solid fraction and the precipitated lignin yields. The optimization results shown that a 50 wt % aqueous solution of the ternary eutectic solvent (NaPTS:PTSA:[Ch]Cl) at molar proportion of (0.393:0.376:0.232) used as solvent on wood delignification process at mild conditions (3 h, 363 K and atmospheric pressure) produced a cellulose rich fraction (46.60 ± 2.701 wt %) containing a residual Klason lignin of 2.74 ± 0.08 wt %. This new strategy led to a lignin removal of 86.26 wt % from *E. globulus* wood. Furthermore, it was possible to recover 61.68 wt % of the lignin (12.30 ± 1.90 wt % of precipitated lignin yield) from the eutectic solvent liquor by addition of water. The obtained solid fraction and precipitated lignin were characterized in order to evaluate the cellulose fiber and the structural changes on the precipitated lignin, induced by the proposed process.

MAIN GOAL & STRATEGY

In our previous study (Chapter III) the *E. globulus* wood delignification under mild conditions (363.15 K and 8 h, at atmospheric pressure) using an aqueous solution of PTSA:[Ch]Cl (1:1) at 50 wt %, was investigated. However, the obtained solid fraction presented degradations comparatively to *E. globulus* kraft pulp and the precipitated lignin presented significant chemical structural changes when compared with *E. globulus* technical lignins (kraft and dioxane lignins). To improve the final products, sodium *p*-toluenesulfonate was used as partial substitute of *p*-toluenesulfonic acid to control the medium acidity. The success of the wood delignification was evaluated not only in terms of solid fraction and precipitated lignin yields but more importantly, in terms of the cellulose fibers morphology and the structural characteristic of precipitated lignin.

RESULTS & DISCUSSION

1. Optimization of ternary eutectic solvents (NaPTS:PTSA:[Ch]Cl) aqueous solution

To optimize the composition of NaPTS:PTSA:[Ch]Cl system at 50 wt % aqueous solution as solvent on wood delignification process, an experimental design for the ternary mixture NaPTS:PTSA:[Ch]Cl was developed using a simplex-centroid design method. This strategy allowed identifying the role of each components on wood delignification, using the obtained solid fraction and precipitated lignin (isolated from ternary ES liquor) yields as outputs of the process, as shown in Figure 67. The detailed solid fraction and precipitated yields values and the respective standard deviations, are reported in Table S6.1 (SI).

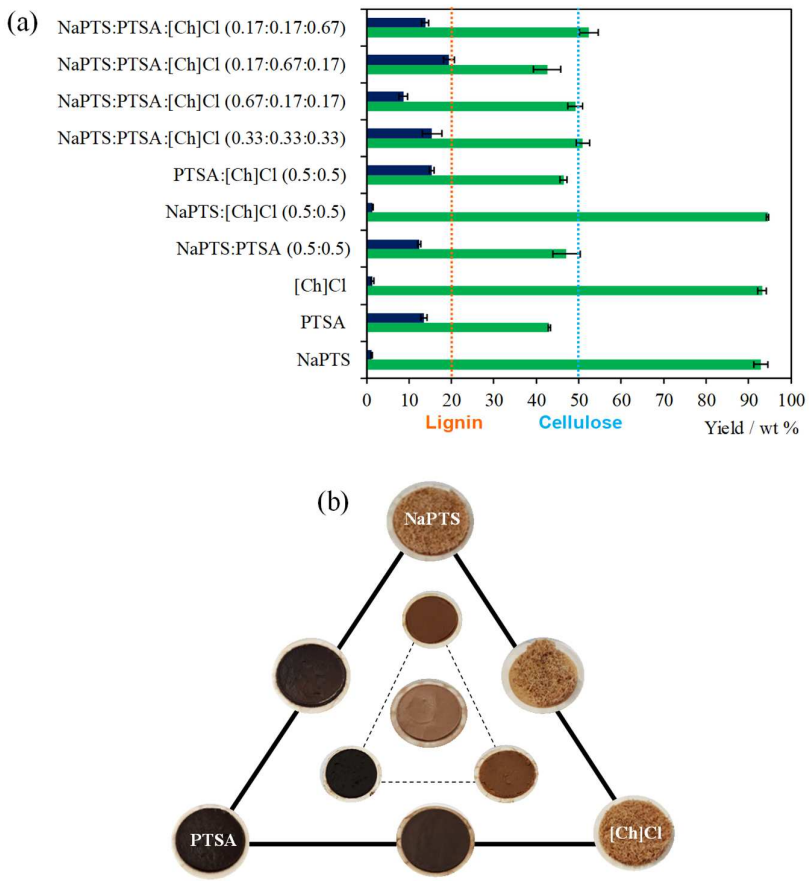

Figure 67. Mixture design of NaPTS:PTSA:[Ch]Cl aqueous solution at 50 wt % used as solvent for *E. globulus* wood delignification (8 h, wood/liquid ratio of 0.5/10 w/w, 300 rpm and 363.15 K), based on the solid fraction (green) and precipitated lignin (blue) yields (a) and simplex-centroid mixture design with solid fractions images (b).

Poor delignification [high solid fraction (92.95 ± 1.64, 93.23 ± 1.04 and 94.50 ± 0.26 wt %) and low precipitated lignin yields (1.16 ± 0.21, 1.37 ± 0.37 and 1.33 ± 0.02 wt %)] were obtained with aqueous solutions of the individual components (NaPTS and [Ch]Cl) and the binary system (NaPTS:[Ch]Cl) (Figure 67, a). Delignification of *E. globulus* wood was only achieved using aqueous solutions containing PTSA, either as an individual component, or in binary (NaPTS:PTSA and PTSA:[Ch]Cl) or ternary mixture (NaPTS:PTSA:[Ch]Cl) with a solid fraction in the range of 43 – 52 wt % and lignin recovery of 9 – 19 wt %. However, as observed in Figure 67 (b), high amounts of PTSA in aqueous solution, as individual component or in mixture, promoted lignin condensation reactions inducing the production of a dark pulps, as shown in our previous work (Chapter III). Furthermore, it was possible to observe that each mixture component seems to play an important role on wood delignification. Indeed, considering the solid fraction yield, precipitated lignin yield and the images of the solid fraction, the best results were obtained for aqueous solution of ternary ES (NaPTS:PTSA:[Ch]Cl), particularly for central point (CP), as observed in Figure 67, (b).

The 50 wt % aqueous solution of ternary ES at CP (0.333:0.333:0.333) used as solvent in *E. globulus* wood delignification at mild conditions, produced a solid fraction of 50.98 ± 1.53 wt %, containing a residual Klason lignin of 2.07 ± 0.63 wt %. This media led to a lignin removal of 89.61 wt % from *E. globulus* wood at mild conditions. Furthermore, it was possible to recover 77.23 wt % of lignin (15.40 ± 2.31 wt % of precipitated lignin yield) from ES liquor. This approach led to better results in term of solid fraction, lignin removal and precipitated lignin yields than PTSA:[Ch]Cl system (46.41 ± 0.88 wt %, 46.39 w % and 15.38 ± 0.59 wt %, respectively), and the neat LA:[Ch]Cl (10:1) system discussed in Chapter III (62.51 ± 1.37 wt %, 39.57 wt % and 4.42 ± 0.37 wt %, respectively) or even those reported in literature (23.95 wt %[74] and 17.98 wt %[75]) from wood delignification under mild conditions (see Table 9).

2. Ternary eutectic solvent – statistical analysis and optimization

ANOVA was used to fit a quadratic model for solid fraction experimental data and special cubic model for precipitated lignin experimental data (Table S6.1 and S6.2, SI). The results suggested that a quadratic model with power transformation (lambda of -2.2)

effectively adjusted the solid fraction experimental data with a correlation square coefficient (R^2) of 0.9371. Furthermore, the terms linear mixture, NaPTS:PTSA and PTSA:[Ch]Cl are significant, with *p*-value < 0.05. Regarding the precipitated lignin, a special cubic model effectively adjusted the experimental data with a R^2 of 0.9696. Furthermore, the terms linear mixture, PTSA:[Ch]Cl and NaPTS:PTSA:[Ch]Cl are significant, with *p*-value < 0.05. Thus, experimental results were fitted according to quadratic model for solid fraction yield response and special cubic model for precipitated lignin yield response in simplex-centroid design:

$$(Solid\ fraction\ yield)^{-2.2} = 4.46E\text{-}05 \times NaPTS + 2.14E\text{-}04 \times PTSA + 4.16E\text{-}05 \times [Ch]Cl + 2.60E\text{-}04 \times NaPTS \times PTSA + 7.50E\text{-}05 \times NaPTS \times [Ch]Cl + 2.65E\text{-}04 \times PTSA \times [Ch]Cl$$

$$Precipitated\ lignin\ yield = 1.09 \times NaPTS + 13.65 \times PTSA + 2.13 \times [Ch]Cl + 19.24 \times NaPTS \times PTSA + 4.09E\text{-}01 \times NaPTS \times [Ch]Cl + 33.78 \times PTSA \times [Ch]Cl + 150.36 \times NaPTS \times PTSA \times [Ch]Cl$$

The residual analysis confirmed the normality of the error distribution (Figure 68).

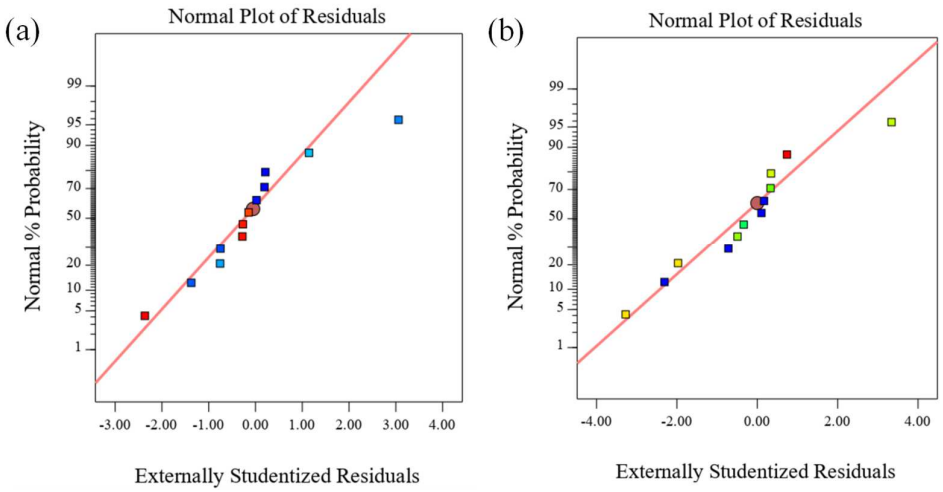

Figure 68. Residual analysis for quadratic model of solid fraction with power transformation (a) and for special cubic model of precipitated lignin (b).

The main goal was to optimize the ternary ES aqueous solution that maximize the extraction of lignin, preserving cellulose fibers (solid fraction not lower than 50 wt %).

Based on the models developed above, it was possible to build ternary contour plots indicating the ternary mixture region where, the target of 50 wt % of solid fraction yield (Figure 69, a) and the maximal lignin extraction (Figure 69, b), were achieved. Combining these two contour plots it was possible to observe the desirable region (Figure 69, c), where both criteria (solid fraction target 50 wt % and maximal lignin extraction) were met and the optimal ternary mixture (NaPTS:PTSA:[Ch]Cl) aqueous solution in molar composition (0.393:0.376:0.232) was found.

In order to confirm this optimal point (OP), an aqueous solution of ternary ES at OP (0.393:0.376:0.232) was tested as solvent in *E. globulus* wood delignification at mild conditions, in duplicate. This process produced a solid fraction yield of 40.86 ± 2.95 wt %, containing a residual Klason lignin of 2.45 ± 0.56 wt %. The optimal ternary ES aqueous solution led to a removal lignin of 87.71 wt % from *E. globulus* wood. Furthermore, it was possible to recover 57.02 wt % of lignin (11.37 ± 0.18 wt % of precipitated lignin yield) from the liquid fraction. These results are in agreement with the results obtained for ternary ES aqueous solution at CP, in terms of lignin removal. However, it was possible to observe a decrease in solid fraction yield, that can be related with the loss of cellulose and the decrease of precipitated lignin yield that can be explained by an inefficient isolation method. Both ternary ES, CP and OP aqueous solutions, presented lower solid fraction and precipitated lignin yields than the predicted responses. A solid fraction yield of 52.65 ± 0.58 wt % and precipitated lignin yield of 17.05 ± 1.74 wt %, were expected for CP ternary ES. Similar results, solid fraction yield of 51.24 ± 0.50 wt % and precipitated lignin yield of 16.99 ± 1.74 wt % for OP ternary ES. The solid fractions and lignins obtained with CP and OP ternary ES systems were characterized by FTIR and ^{1}H NMR spectroscopy and optical microscopy.

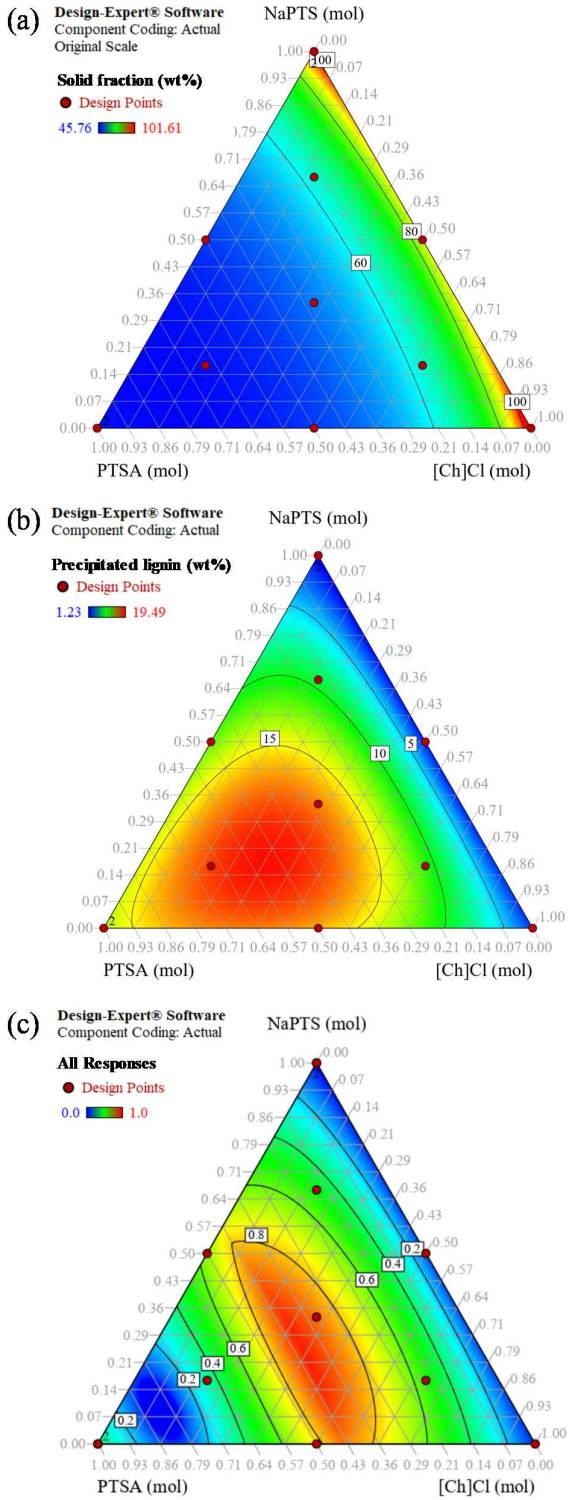

Figure 69. Contour plots of ternary mixture optimization (NaPTS:PTSA:[Ch]Cl) based on solid fraction yield (a), precipitated lignin yield (b) and desirability (c).

2.1 Characterization of solid fraction from CP and OP ternary eutectic solvents

The solid fraction after wood delignification with CP or OP was assessed by FTIR spectroscopy (Figure 70). A standard kraft pulp was also analyzed for comparative purposes. The absorption bands were assigned following the literature[117–119] and details are presented in Table S6.3 (SI).

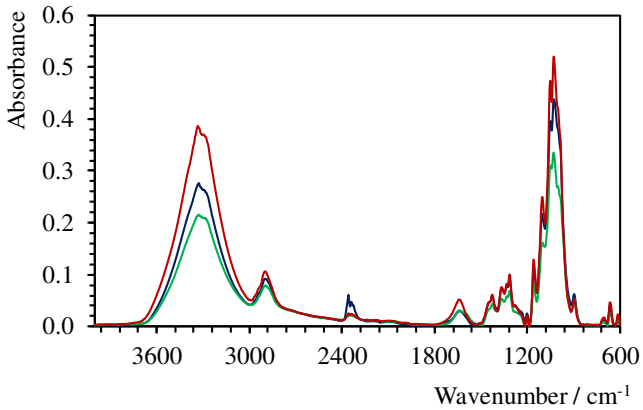

Figure 70. Normalized FTIR spectra of solid fraction-CP (red), solid fraction-OP (blue) and the standard kraft pulp with kappa number 14.4 (green).

Similar FTIR spectra were observed for both solid fractions (CP and OP), and both comparing well with kraft pulp, indicating that these fractions are mainly composed of cellulose. However, optical microscopy images of solid fractions- of CP and OP fibers revealed substantial morphological differences when compared with kraft pulp fibers (Figure 71). The fibers in CP and OP solid fractions- are more fragmented and aggregated, as previously observed in the solid fraction obtained with the PTSA:[Ch]Cl system (Figure 45). Moreover, the brownish color in the fibers surface, particularly observed in solid fraction-OP, can be associated with the occurrence of lignin condensation reactions, but to a smaller extent than observed in solid-fraction-PTSA:[Ch]Cl (Chapter III). These results suggest that experimental conditions allow to preserve the cellulose against the negative effect of PTSA. Based on these results we concluded that, the operational conditions could be adjusted, particularly the time, in order to avoid the cellulose fibers degradation.

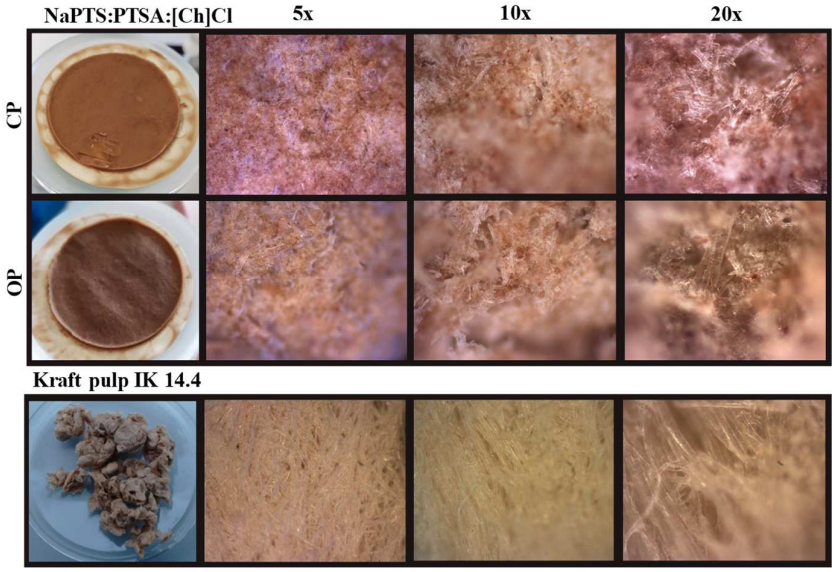

Figure 71. Optical microscopy images of *E. globulus* solid fraction-(CP and OP) obtained after ternary ES delignification process at 363.15 K, 8 h and atmospheric pressure and kraft pulp. Magnification 5x, 10x and 20x.

2.2 Characterization of precipitated lignin from CP and OP ternary eutectic solvent

The chemical features of lignins obtained from CP or OP were assessed by FTIR and ^{1}H NMR spectroscopy (Figure 73). Kraft and dioxane lignins (from alkaline and mild acidic conditions, respectively), were also analyzed for comparative purposes. The absorption bands were assigned according to literature[110,112,114,120] and details are presented in Table S6.4 (SI).

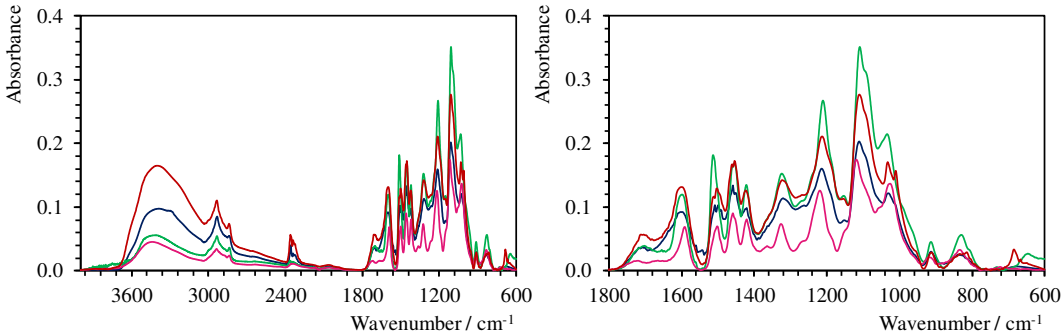

Figure 72. Normalized FTIR spectra of lignin-(CP and OP) obtained after ternary ES delignification process at 363.15 K, 8 h and atmospheric pressure (red and blue, respectively) and technical lignins (kraft (green) and dioxane (pink)).

The FTIR spectra of CP and OP lignins, presented in Figure 72, show typical bands assigned to lignin. However, significant differences when compared with the FTIR profile of technical lignins, were observed, being the spectra of CP and OP lignins more similar to dioxane lignin spectrum. The increase of the peaks at 3410, 3424 cm^{-1} and 2942, 2900 cm^{-1} region, on the spectra of these lignins, can be related with the increase of hydroxyl groups in phenolic structures of precipitated lignins, a consequence of lignin depolymerization induced by this ternary ES. Furthermore, in the carbonyl/carboxyl region, the absorption bands around 1710 – 1716 cm^{-1} originating from unconjugated carbonyl/carboxyl C=O stretching, can be associated to the presence of carbohydrate contaminats[110] (more intense in lignin-CP than lignin-OP), as observed in kraft lignin and lignin-PTSA:[Ch]Cl (1:1) spectra (Figure 44). Moreover, the absence of the peak at 635 cm^{-1} assigned to the stretching vibration of C-S, [110] confirms that sulfur-free lignin is obtained using these ternary ES (CP and OP). This result was corroborated by elemental analysis. A low amount of sulfur (0.42 ± 0.07 wt % was founded in lignin-CP (Table S6.5, SI).

The qualitative ^{1}H NMR spectroscopy analysis of lignin-(CP and OP) (Figure 73 and Table S6.6, SI) showed that for the CP and OP samples the ternary ES induces less changes on precipitated lignin than the PTSA:[Ch]Cl (1:1) system, particularly preserving the β-*O*-4 structures. The increase on phenolic hydroxyl groups content, the decrease of aliphatic phenolic groups, β-*O*-4 structures and protons in aromatic ring contents were observed, comparatively to dioxane lignins.

These results demonstrate the success of this new approach on *E. globulus* wood delignification at mild conditions, using NaPTS:PTSA:[Ch]Cl ternary ES at 0.393:0.376:0.232 molar composition, instead of PTSA:[Ch]Cl system, at 50 wt % aqueous solution as solvent. However, the solid fraction and precipitated lignin characterizations reveal that operational conditions, particularly time, could be adjusted in order to achieve a high extraction of sulfur-free lignin and preserving the cellulose fibers.

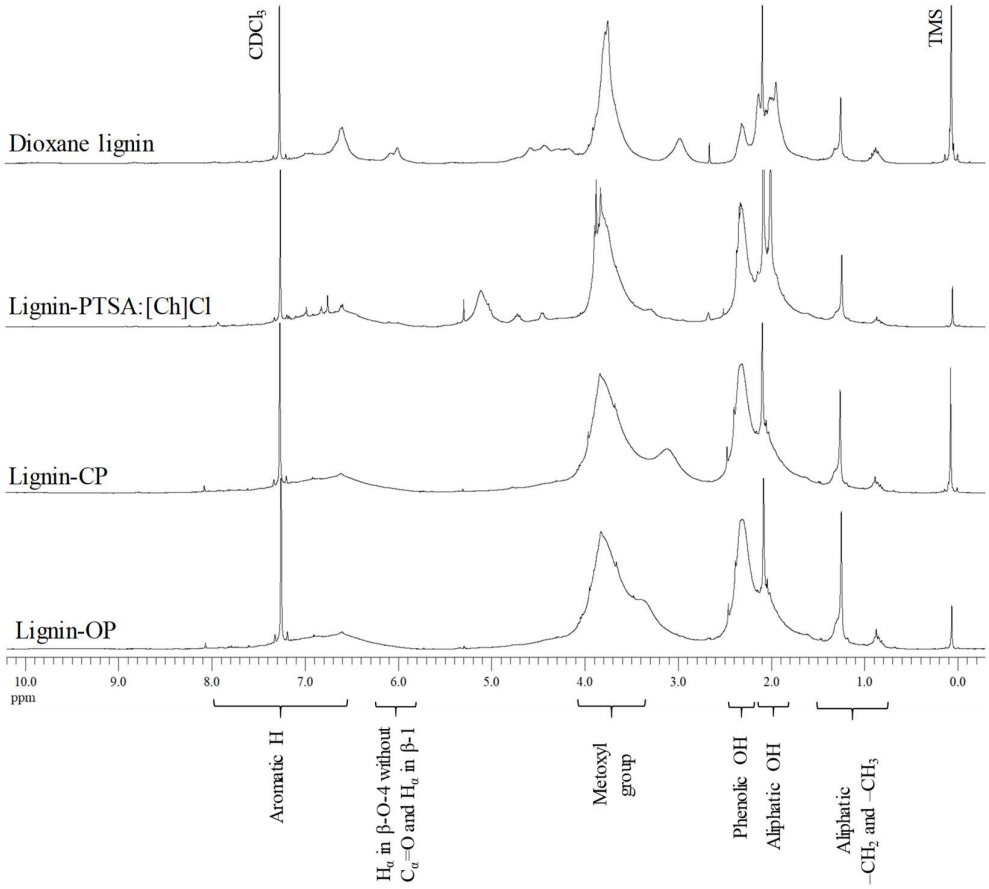

Figure 73. ^{1}H NMR spectra ($CDCl_3$) of acetylated *E. globulus* lignins (dioxane, PTSA:[Ch]Cl, CP-central point and OP-optimal point).

3. Effect of time on wood delignification using optimal ternary eutectic solvent

To improve the final products (cellulose fibers and precipitated lignin) obtained from wood delignification at mild conditions, using the optimal ternary ES (NaPTS:PTSA:[Ch]Cl) at 0.396:0.376:0.232 molar composition and a 50 wt % of aqueous solution as solvent, the effect of delignification time was investigated (Figure 74). The detailed solid fraction and precipitated lignin yields values are reported in Table S6.7 (SI).

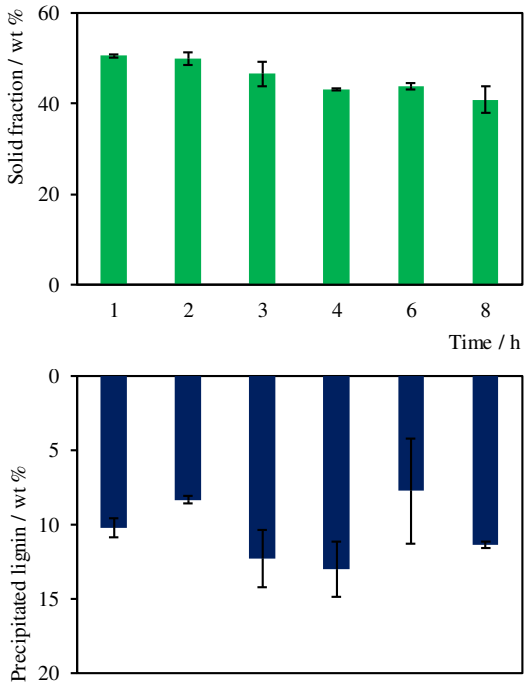

Figure 74. Effect of time on *E. globulus* wood delignification using optimal ternary ES (wood/liquid ratio of 0.5/10 w/w, 300 rpm and 363.15 K), based on solid fraction (green) and precipitated lignin (blue).

As observed in Figure 74, time promotes the loss of 10 wt % in solid fraction yield after 8 h of wood delignification (50.56 ± 0.32 to 40.86 ± 2.95 wt % from 1 to 8 h, respectively). Furthermore, a maximum precipitated lignin yield was observed at the end of 3 h (12.30 ± 1.90 wt %). The effect of delignification time on cellulose fibers was more evident by optical microscopy analysis (Figure 75).

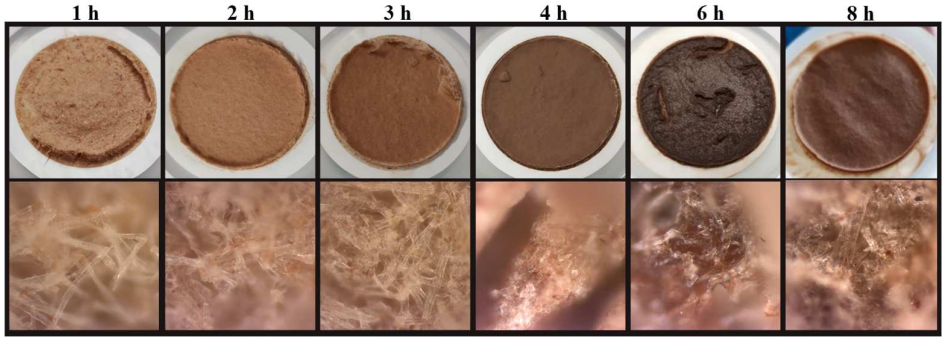

Figure 75. Optical microscopy images of *E. globulus* solid fraction-OP, effect of delignification time at 363.15 K, and atmospheric pressure on cellulose fiber. Magnification of 20x.

After 3 h it was possible to produce a solid fraction yield of 46.60 ± 2.70 wt % (3.40 wt % of cellulose lost) containing a residual Klason lignin of 2.74 ± 0.08 wt %. This new approach at milder condition led to a removal lignin of 86.26 wt % from *E. globulus* wood. Furthermore, it was possible to recover 61.68 wt % of lignin (12.30 ± 1.90 wt % of precipitated lignin yield) from the liquid fraction. This condition led to produce cellulose fibers less fragmented and aggregated when compared to those obtained after 4 h. Furthermore, the occurrence of lignin condensation reactions that lead the production of dark pulps, discussed above, were observed for delignification time above 3 h (see Figure 75). These results are in agreement with the FTIR analysis (Figure 76), where significant changes in solid fractions FTIR spectra with delignification times are observed. Longer delignification times (from 4 to 8 h) promote a significant decrease of the relative absorbance at 1032 cm^{-1} attributed to the C-O stretching vibration in cellulose spectra. Differences in FTIR spectra profiles of lignin-OP induced by delignification time, were not observed (see Figure 77).

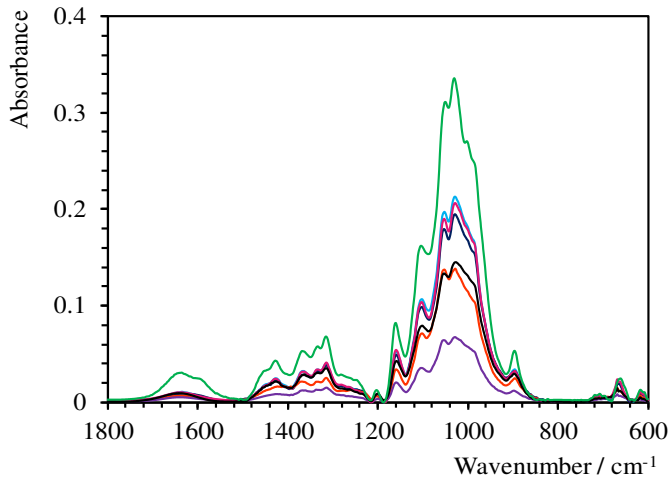

Figure 76. Normalized FTIR spectra of solid fraction-OP at different wood delignification times, 1h (blue), 2h (dark blue), 3h (orange), 4h (purple), 6h (pink), 8h (black) and kraft pulp (green).

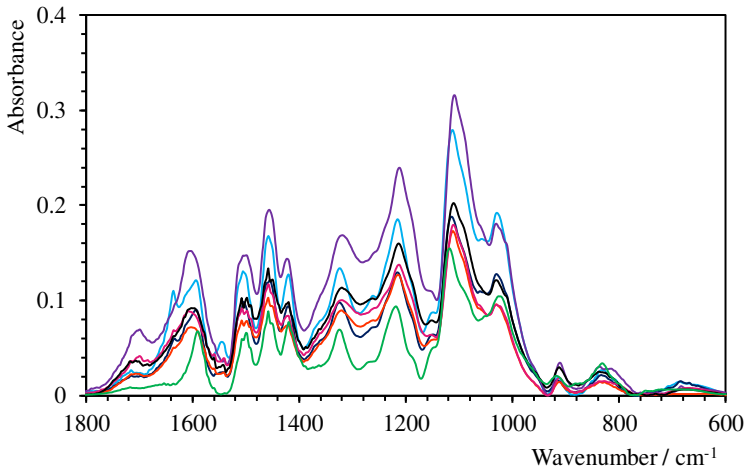

Figure 77. Normalized FTIR spectra of lignin-OP at different wood delignification times, 1h (blue), 2h (dark blue), 3h (orange), 4h (purple), 6h (pink), 8h (black) and dioxane lignin (green).

Given the excellent performance of the 50 wt % aqueous solution of the ternary ES (NaPTS:PTSA:[Ch]Cl) at optimal molar composition (0.393:0.376:0.232) on *E. globulus* wood delignification at milder conditions (363.15 K, 3 h and atmospheric pressure), the final products (solid fraction and precipitated lignin) were characterized in more detail as discussed before.

3.1 Characterization of solid fraction-OP3h

The FTIR spectra of solid fraction-OP3h, revealed that cellulose is the main component on this fraction, comparing with the conventional kraft pulp (Figure 78). Furthermore, the cellulose fibers were assessed by optical microscopy images (Figure 79) and solid-state ^{13}C NMR spectroscopy (Figure 80), using kraft pulp as benchmark. Although, fiber fragmentation continues to be observed, a significant improvement on preserving cellulose fibers was achieved using this optimal ternary ES at 50 wt % aqueous solution, combined with optimal conditions of delignification time, comparatively with the cellulose fibers obtained after 8 h of wood delignification, or even when PTSA:[Ch]Cl system[121] was used as delignification medium. These results are corroborated by the solid-state ^{13}C NMR spectra of solid fraction-OP3h, where it is possible to observe the profile similarity between the solid fraction-OP3h and kraft pulp spectra, as shown in Figure 80, in which carbon resonance were assigned following literature[122–124] (see Table S8, SI). Furthermore, the

solid-state ^{13}C NMR of solid fraction also shows that the crystalline structure of cellulose was not affected (see Figure 80).

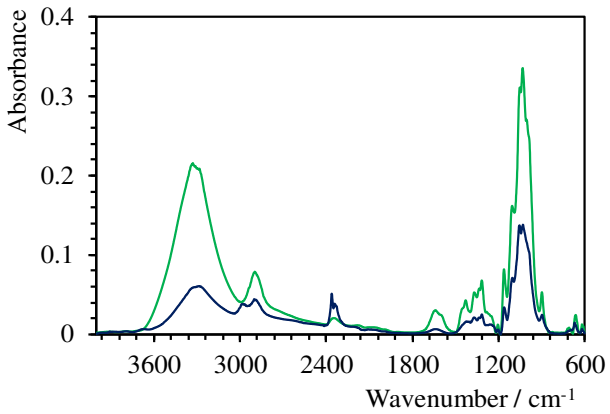

Figure 78. Normalized FTIR spectra of solid fraction-OP3h (blue) and the standard kraft pulp with kappa number 14.4 (green).

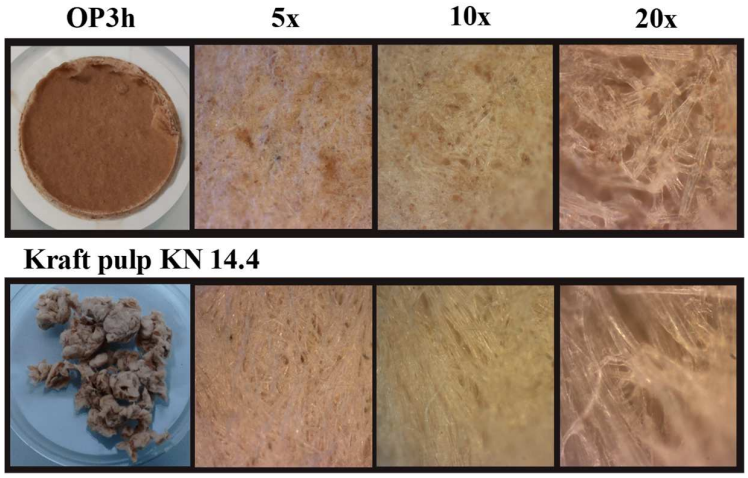

Figure 79. Optical microscopy images of *E. globulus* solid fraction from OP3h systems, obtained after delignification with ternary ES aqueous solutions at 363.15 K, 3 h and atmospheric pressure. Conventional kraft pulp from *E. globulus* wood with kappa number 14.4. Magnification of 5x, 10x and 20x.

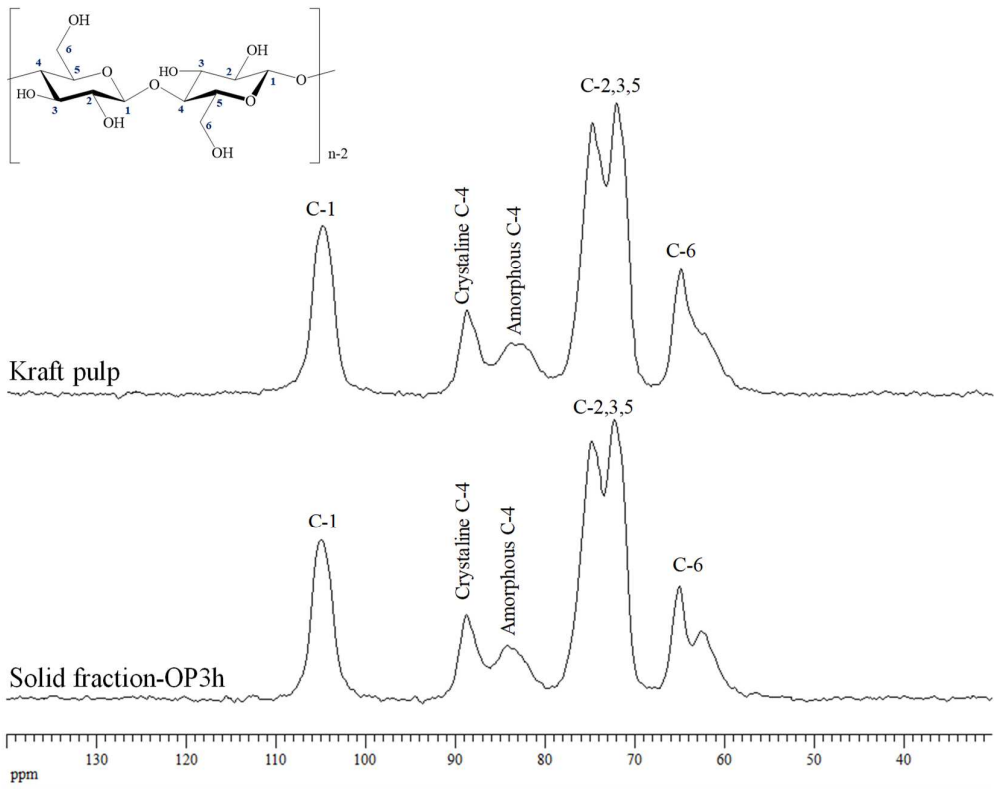

Figure 80. Solid-state ^{13}C CP-MAS NMR spectra of cellulose from solid fraction-OP3h and from conventional kraft pulp from *E. globulus* wood with kappa number 14.4. The chemical structure of cellulose is shown above.[6]

3.2 Characterization of lignin-OP3h

The FTIR analysis of lignin-OP3h confirmed that this fraction is composed mostly of lignin (Figure 81). Although no evidence of ternary ES contamination was found by FTIR analysis, ^{1}H NMR revealed the presence of ternary ES as contaminants in this precipitated lignin. Characteristic resonances of PTSA (δ_H, 7.6 and 6.9 ppm) and [Ch]Cl (δ_H, 4.07 and 3.65 ppm), were observed in spectra in Figure 82. Furthermore, the absence of absorption band at 635 cm^{-1} assigned to the C-S stretching vibration in lignin-OP3h spectra suggest that sulfur-free lignin was produced. This result was corroborated by the absence of sulfur detectable in elemental analysis (see Table S6.5, SI).

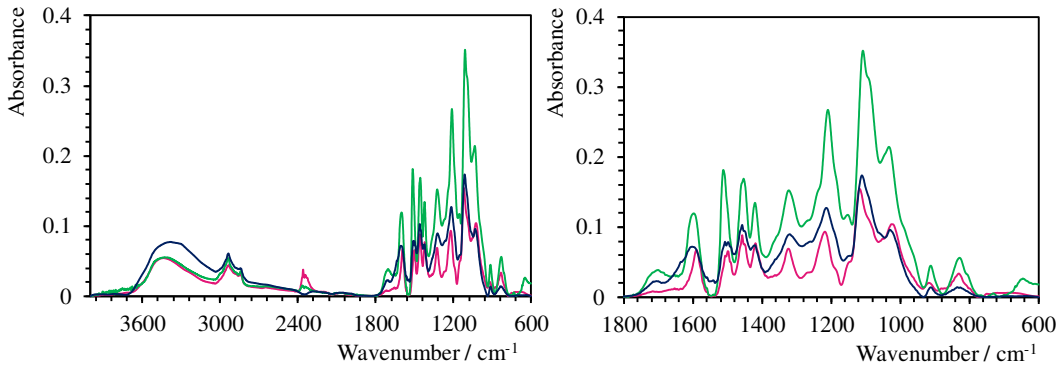

Figure 81. Normalized FTIR spectra of lignin-OP3h (blue), kraft lignin (green) and dioxane lignin (pink).

Finally, the ^{1}H and ^{13}C NMR analysis of lignin-OP3h allowed to highlight the modifications that occurred on the lignin structure induced by this new delignification process (Figure 82 andFigure **83**, respectively). The resonance assignments were performed according to literature[27,111,112,115,116] and the details resonance of lignin-OP3h and lignin-PTSA:[Ch]Cl as shown in Tables S6.9 and S6.10, SI. The detailed resonances assignments of dioxane lignin was used as benchmark and reported in Table S5.12, SI.

The detailed analysis of ^{1}H and ^{13}C NMR spectra from lignin-OP3h (acetylated and not acetylated sample, respectively) show a decrease of aliphatic OH groups (from 3.61/C_9 to 1.41/C_9) and β-*O*-4 structures contents (from 0.41/C_9 to 0.13/C_9) and an increase of phenolic OH groups content (from 0.74/C_9 to 1.87/C_9), when compared to dioxane lignin. However, it shows a higher content of aliphatic OH groups and β-*O*-4 structures when compared to lignin-PTSA:[Ch]Cl (0.91/C_9 and 0.02/C_9, respectively). These results shows that OP3h system led to an improvement on lignin structure, preserving the aryl-ether bonds between phenylpropane units in lignin, comparatively to PTSA:[Ch]Cl system. When compared to literature (lignin-LA:[Ch]Cl system, see Table 10),[74] lignin-OP3h presented a lower content of aliphatic OH groups, phenolic OH groups and methoxyl groups, and higher content of β-*O*-4 structures. These results indicated that OP3h system induced less chemical changes on lignin structure, than LA:[Ch]Cl system proposed in literature for wood delignification at mild conditions. Furthermore, the ^{1}H NMR spectrum of lignin-OP3h also shows a lower content of protons in aromatic moieties, comparatively to dioxane lignin (1.28/C_9 and 1.63/C_9 respectively) and higher content when compared to PTSA:[Ch]Cl system (0.44/C_9). Regarding the content of methoxyl groups/C6 in lignin structure, the

analysis showed that methoxyl groups are preserved in lignin-OP3h compared to lignin-PTSA:[Ch]Cl (1.42/C6 and 0.89/C6, respectively), which are related with the presence of more syringyl propane units in lignin structure than guaiacyl propane units, as corroborated by the quantification of S:G:H ratio on both lignin-OP3h and lignin-PTSA:[Ch]Cl of 71:29:0 and 67:33:1, respectively. Finally, it was possible to determine the degree of condensation and the results revealed that lignin-PTSA:[Ch]Cl (82 %) and lignin-OP3h (82 %), has more condensed structures comparatively to dioxane lignin (15 %).[121]

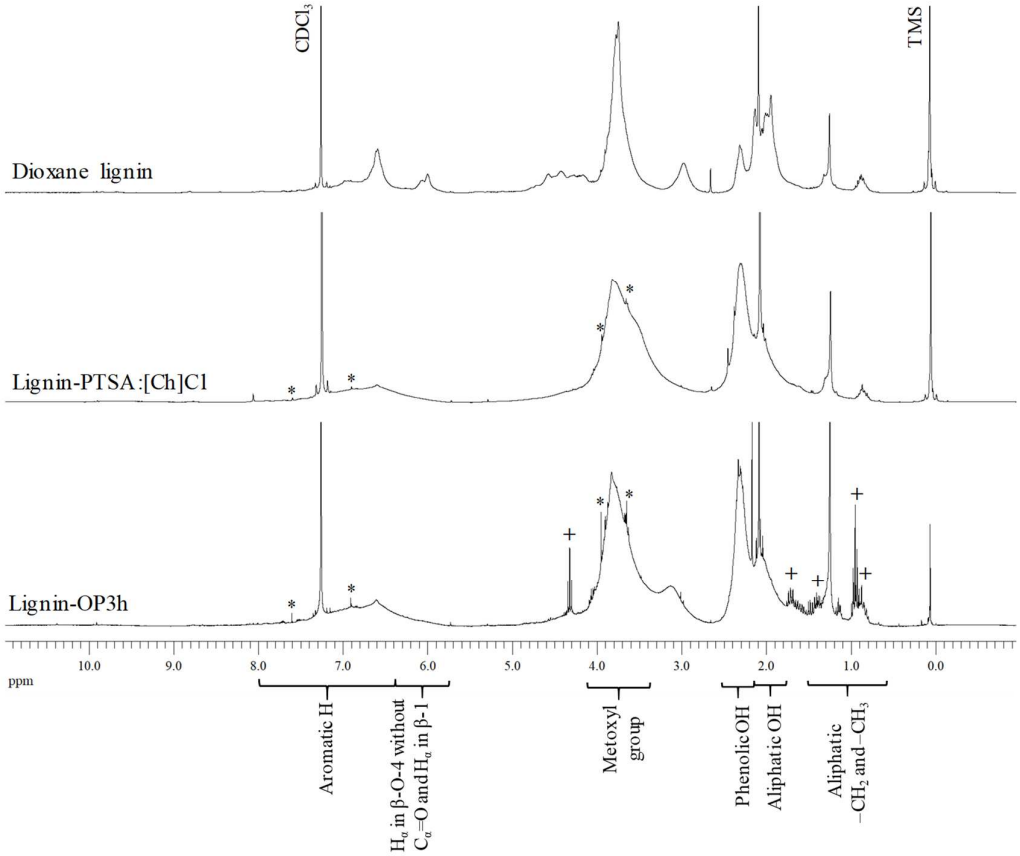

Figure 82. ^{1}H NMR spectra ($CDCl_3$) of acetylated *E. globulus* lignins (dioxane, PTSA:[Ch]Cl and OP3h). (*) PTSA and [Ch]Cl contaminants. (+) Solvent contaminant.

The analysis performed to the final products (cellulose fibers and precipitated lignin) demonstrated the success of this new approach, using NaPTS to control the performance of PTSA:[Ch]Cl system as delignification solvent for *E. globulus* wood at milder conditions, preserving the cellulose fibers and inducing a minor chemical structure changes on precipitated lignin, comparatively to PTSA:[Ch]Cl system.

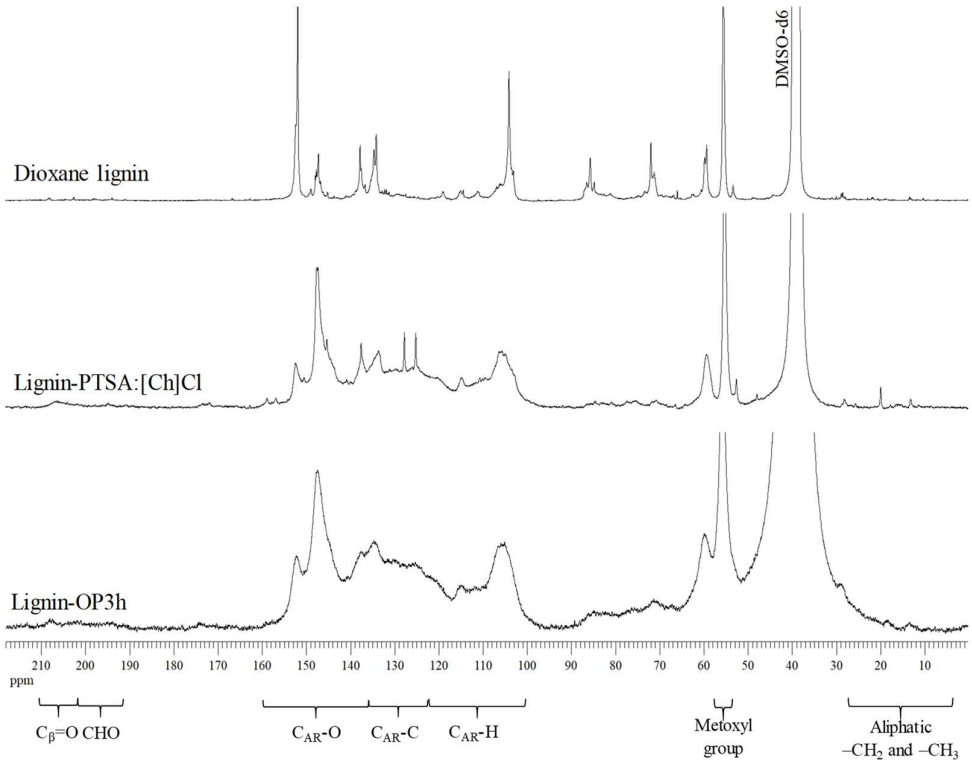

Figure 83. Quantitative ^{13}C NMR spectra (DMSO-d_6) of *E. globulus* lignins (dioxane, PTSA:[Ch]Cl and OP3h).

4. In the PATH of process scale-up – Preliminary study using ternary eutectic solvents

Following the same strategy presented above (Chapter III), to investigate the feasibility on scaling the ternary ES wood delignification process (from 0.5 g to 6 g of wood), preliminary tests were also performed in PARR Stirred reactor with 300 ml of capacity.

After ternary ES wood delignification in reactor, 58.11 wt % of cellulose rich solid fraction was produced with an excellent residual Klason lignin of 1.29 ± 0.02 wt %. This means that 93.53 wt % of lignin was removed from *E. globulus* wood. Furthermore, it was possible to recover 58.0 wt % of sulfur-free lignin (10.83 wt % of precipitated lignin yield) from soluble fraction. These promising results are in accordance with those achieved from OP wood delignification in tubes, which demonstrate the reproducibility of ternary ES delignification process at different scales. Additionally, the optical microscopy analysis of the solid fraction (Figure 84) and the FTIR spectra of precipitated lignin (Figure 85) shown similar characteristics to those achieved in tubes.

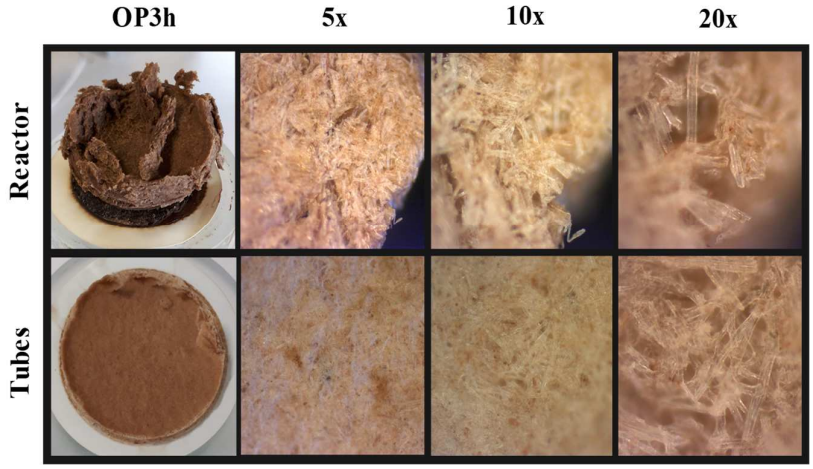

Figure 84. Optical microscopy images of *E. globulu*s solid fraction from OP systems, obtained after delignification with ternary ES aqueous solutions at 363.15 K, 3 h and atmospheric pressure at different scales, in tube (0.5 g of wood) and reactor (6 g of wood). Magnification of 5x, 10x and 20x.

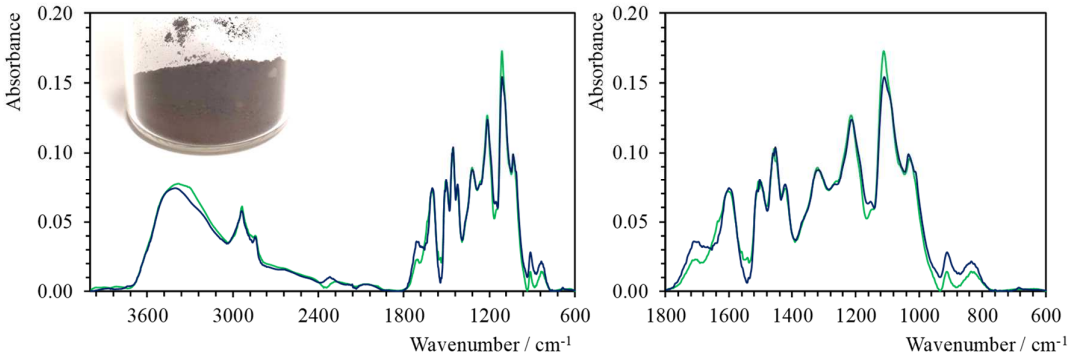

Figure 85. Normalized FTIR spectra of lignin-OP3h from reactor (blue) and tubes (green).

CONCLUSIONS

A new approach for wood delignification using a process at mild conditions based on ternary ES aqueous solutions was here investigated. This study proposed the partial replacement of PTSA on PTSA:[Ch]Cl system using NaPTS to control the medium acidity, in order to improve the properties of the final products. To achieve this goal, a ternary ES (NaPTS:PTSA:[Ch]Cl) was designed, following a simplex-centroid design method. The results highlighted the influence of each ternary ES components on *E. globul*us wood delignification and demonstrated the potential of NaPTS:PTSA:[Ch]Cl ternary mixture at 50

wt % aqueous solution with an optimal molar ration of (0.393:0.376:0.232), as solvent for wood delignification. This new approach for ternary ES delignification operates at mild conditions (3 h, 363.15 K and atmospheric pressure), allowing to produce a preserved cellulose rich solid fraction (46.60 ± 2.70 wt %) containing a residual Klason lignin of 2.74 ± 0.08 wt %. Furthermore, 86.26 wt % of lignin was removed from *E. globulus* wood and 61.68 wt % of sulfur-free lignin (12.30 ± 1.90 wt % of precipitated lignin yield) was recover from the ternary ES liquor. The characterization performed on the final products allowed to access the impact of ternary ES delignification process on their chemical structures. Furthermore, it was possible to confirm the improvements achieved on preserving cellulose fibers and on reducing changes in lignin chemical structure, comparatively to PTSA:[Ch]Cl system. Finally, promising preliminary results on scale-up of the ternary ES wood delignification process were also achieved. This work provided a successful and innovative strategy that led to the development of a breakthrough delignification technology for the production of wood-based materials which involve lignin and cellulose separation.

FINAL REMARKS & FUTURE WORK

The development of a new wood delignification process using eutectic mixtures as solvents, to produce cellulose fibers and sulfur-free lignin at mild conditions, was here reported. A fundamental study followed by a proof of concept were the two strategies drawn to achieve this purpose.

The fundamental study (Chapter I and II) was focused on screening and designing of eutectic solvents (ES) for the selective extraction of lignin from *Eucalyptus globulus* wood. However, bearing in mind the complexity of lignin, the solubilities of lignin monomer model compounds (LMMCs) such as syringaldehyde, and vanillic, syringic and ferulic acids, in ES (neat and their aqueous solutions) were performed. The influence of ES components (hydrogen bond donors and acceptors), chemical structure, molar ratio, concentration and temperature on LMMCs solubility were investigated and the results show that both hydrogen bond donors and acceptors, play a significant role in the solubilization of these LMMCs with a possible synergistic effect between the two ES components. Furthermore, the solubility studies allowed, through the evaluation of LMMCs in several ESs, not only to predict the performance of ESs on the technical lignin solubilization but also to demonstrate the mechanisms that rule their solubilization. Two main solubilization mechanisms were observed, hydrotropy and cosolvency. The results show that the capability of ESs to act as hydrotropes or cosolvents, selectively enhancing the solubility of poorly soluble solute depending on the ES components and solute hydrophobicity. Maximum solubilization of LMMCs (syringaldehyde, and syringic, vanillic and ferulic acids), was achieved using EG:[P_{4444}]Cl (2:1) aqueous solution at 50 or 75 wt % of concentration and 323.15 K [(34.9 ± 6.7)-, (116.6 ± 1.6)-, (58.6 ± 0.4)- and (202.5 ± 16.9)-fold, respectively] driven by hydrotropy mechanism, with the dispersive interactions being the main reason for the good performance of ESs dissolution ability. Regarding the kraft and organosolv lignins solubilities in ESs, a remarkably similar behavior to that obtained for LMMCs was observed. The great performance of PA:U (2:1) aqueous solution at 50 wt % or 75 wt % to solubilize kraft and organosolv lignins at 353.15 K [(228.3 ± 8.2)- and (474.7 ± 2.7)-fold, respectively], driven by hydrotropy solubilization mechanism, was here observed. These studies allowed to select the best candidates to perform the wood delignification as the proof of concept.

The proof of concept (Chapter III and IV) was focused on evaluating the performance of some ESs for *E. globulus* wood delignification at mild conditions and accessing their impact on the chemical structure of cellulose fibers and precipitated lignin. Aqueous solutions of PA:U (2:1) and PTSA:[Ch]Cl (1:1) were selected for these studies (Chapter III). LA:[Ch]Cl (10:1) and U:[Ch]Cl (2:1) were used for comparative purposes. The successful wood delignification was achieved with PTSA:[Ch]Cl system (solid fraction yield of 46.41 ± 0.88 wt %, containing a residual Klason lignin of 10.69 ± 0.16 wt %), however cellulose fiber degradation and significant changes in precipitated lignin were observed, when compared with *E. globulus* kraft and dioxane lignins. The results also show that wood delignification at mild conditions requires an acid catalyst, particularly when LA:[Ch]Cl (10:1) and PA:U (2:1) are used as delignification solvents. After the optimization process, the 50 wt % aqueous solution of PA:U (2:1) in the presence of 25 wt % of PTSA as catalyst was identified as the best system to delignify *E. globulus* wood under mild conditions (8 h, 363.15 K and atmospheric pressure). This system led to produce a solid fraction yield of 59.50 ± 0.51 wt %, containing a residual Klason lignin of 3.86 ± 0.10 wt % with preserved cellulose fibers, when compared to conventional *E. globulus* kraft pulp. The extensive chemical structural analysis of precipitated lignin revealed that fewer transformations are induced by this system, when compared with *E. globulus* kraft and dioxane lignins, and LA:[Ch]Cl (10:1) system reported in literature. In the Chapter IV, a new approach to improve the final products obtained from PTSA:[Ch]Cl wood delignification process, was performed. The NaPTS was used as partial substitute of PTSA to control the medium acidity. Therefore, the 50 wt % aqueous solution of ternary ES (NaPTS:PTSA:[Ch]Cl) was designed and their molar composition optimized to achieve this goal. The results showed that the optimal molar ratio of (0.393:0.376:0.232) allowed to produce 46.60 ± 2.70 wt % of solid fraction, containing a residual Klason lignin of 2.74 ± 0.08 wt % under milder conditions (3 h, 363.15 K and atmospheric pressure). The success of this new approach was confirmed by the characterization of precipitated lignin and cellulose fibers. Finally, promising preliminary results shows the feasibility for scaling the ES wood delignification process using the both proposed ES aqueous solutions systems (PA:U(2:1)+25PTSA and ternary mixture NaPTS:PTSA:[Ch]Cl).

The work developed in the field of ESs based wood delignification technology provided a new insight on the mechanisms that rule the lignin solubilization in ESs aqueous solutions and an important contribution to the understanding of the use of ESs aqueous solutions on wood delignification process. Furthermore, this work shown that ESs are promising solvents to apply in biomass processing, as well as novel solvents for the selective extraction of aromatic compounds present in black liquor, aiming at their future valorization. Apart from the work developed some new contributions should be achieved in order to bring this laboratory technology towards the next stage:

- Development a comprehensive study regarding the mechanisms behind the wood delignification mediated by ESs, in order to access the role that the ESs constituents play in the lignin depolymerization;
- Optimization of process variables (temperature, time, ES concentration and solid/liquid ratio) in wood delignification performed at reactor scale;
- Perform further characterization of final products to evaluate the impact of ES delignification technology on chemical structure of cellulose fibers and lignin;
  - *Solid fraction*: FTIR and solid-state ^{13}C NMR spectroscopy (to assess some chemical structure modifications in cellulose fibers), optical microscopy analysis and scanning electron microscope (to evaluate the fibers morphology), kappa number (to determine the residual lignin content) and viscosity (indirect measure of degree of polymerization of cellulose chains in fibers)
  - *Precipitated lignin*: FTIR and (^{1}H and ^{13}C) NMR spectroscopy (to assess some chemical structure modifications induced by this new technology), elemental analysis (to confirm the isolation of sulfur-free lignin) and the molecular weight by Size Exclusion Chromatography (to understand the reactivity and physicochemical properties of lignin);
- Characterization of the liquid fraction, after lignin isolation, in order to develop efficient methodologies for hemicelluloses, extractive and ESs recovery;
- Perform pilot experiments and viability study;
- Economic-financial analysis.

REFERENCES

(1) Bernstein, L.; Bosch, P.; Canziani, O.; Chen, Z.; Christ, R.; Davidson, O.; Hare, W.; Huq, S.; Karoly, D.; Kattsov, V.; et al. Intergovernmental Panel on Climate Change Fourth Assessment Report- Climate Change 2007: Synthesis Report. **2007**, No. November, 52.

(2) European Commission. *A Roadmap for Moving to a Competitive Low Carbon Economy in 2050*; **2011**. https://ec.europa.eu/clima/sites/clima/files/strategies/2050/docs/roadmap_fact_sheet_en.pdf (acessed, 18 July 2019).

(3) Bajpai, P. *Pulp and Paper Industry: Energy Conservation*; Elsevier B.V., **2016**. DOI:10.1016/B978-0-12-803411-8.00001-9.

(4) Sixta, H. *Handbook of Pulp*, 1st ed.; Sixta, H., Ed.; Wiley-VCH, **2006**. DOI:10.1002/9783527619887.

(5) Smook, G. A. *Handbook for Pulp and Paper Technologists*, 2nd ed.; Angus Wilde Publications Inc: Vancouver, **1992**.

(6) Sjöström, E. *Wood Chemistry. Fundamentals and Applications*, 2nd ed.; Academic Press, Inc: New York, **1993**.

(7) CEPI. *The Forest Fibre Industry: 2050 Roadmap to a Low-Carbon Bio-Economy*; **2011**. https://vnp.nl/wp-content/uploads/2013/05/Unfold-the-future.pdf (acessed, 29 September 2014).

(8) CEPI. *Unfold the Future, The Two Team Project Report*; **2013**. http://www.cepi.org/system/files/public/documents/publications/innovation/2013/finaltwoteamprojectreport_website_updated.pdf (acessed, 29 September 2014).

(9) PROVIDES. *Deep Eutectic Solvents in the Paper Industry*; **2018**. https://www.providespaper.eu/media/Brochure-Provides-ISTP_FINAL.pdf (acessed, 18 July 2019).

(10) CELPA. Boletim Estatístico Da CELPA - 2017. **2017**, 92. http://www.celpa.pt/wp-content/uploads/2018/10/Boletim_WEB-2.pdf (acessed, 18 July 2019).

(11) Patt, R.; Kordsachia, O.; Fehr, J. European Hardwoods versus *Eucalyptus Globulus* as a Raw Material for Pulping. *Wood Sci. Technol.* **2005**, *40* (1), 39–48. DOI:10.1007/s00226-005-0042-9.

(12) *The Navigator Company - Annual Report 2018*; **2018**. http://en.thenavigatorcompany.com/var/ezdemo_site/storage/original/application/38ef39d34a1057e888f2f4bedfe81a47.PDF (acessed, 18 July 2019).

(13) Evtuguin, D. V.; Neto, C. P. Recent Advances in Eucalyptus Wood Chemistry: Structural Features through the Prism of Technological Response. In *3th International colloquium on eucalyptus pulp. Belo Horizonte, Brasil*; **2007**.

(14) Rana, V.; Singh, S. P.; Gupta, P. K. Eucalypts in Pulp and Paper Industry. **2011**, 470–506.

(15) Nishimura, H.; Kamiya, A.; Nagata, T.; Katahira, M.; Watanabe, T. Direct Evidence for α Ether Linkage between Lignin and Carbohydrates in Wood Cell Walls. *Sci. Rep.* **2018**, *8* (1), 1–11. DOI:10.1038/s41598-018-24328-9.

(16) Lachenal, D. Kraft Pulping. In *Lignocellulosic Fibers and Wood Handbook*; Belgacem, N., Pizzi, A., Eds.; Scrivener Publishing LLC, **2016**; pp 207–223.

(17) Bajpai, P. Wood and Fiber Fundamentals. In *Biermann's Handbook of Pulp and Paper*; Elsiever Inc., **2018**; pp 19–74. DOI:10.1016/b978-0-12-814240-0.00002-1.

(18) Shrotri, A.; Kobayashi, H.; Fukuoka, A. *Catalytic Conversion of Structural Carbohydrates and Lignin to Chemicals*, 1st ed.; Elsevier Inc., **2017**; Vol. 60. DOI:10.1016/bs.acat.2017.09.002.

(19) Belgacem, M. N.; Gandini, A. Production, Chemistry and Properties of Cellulose-Based Materials. In *Biopolymers - New Materials for Sustainable Films and Coatings.*; Plackett, D., Ed.; John Wiley & Sons, **2011**; pp 151–178. DOI:10.1002/9781119994312.ch8.

(20) Fengel, D.; Wegener, G. *Wood: Chemistry, Ultrastructure, Reactions*; Walter de Gruyter: Berlin. New York, **1989**. DOI:10.1007/BF02608943.

(21) Klemm, D.; Philipp, B.; Heinze, T.; Heinze, U.; Wagenknecht, W. General Considerations on Structure and Reactivity of Cellulose. In *Comprehensive cellulose chemistry: fundamentals and analytical methods*; Wiley-VCH Verlag GmbH, **1998**; pp 9–29. DOI:10.1002/3527601929.

(22) Stevanoic, T. Chemical Composition and Properties of Wood. In *Lignocellulosic Fibers and Wood Handbook*; Naceur, B., Pizzi, A., Eds.; Scrivener Publishing LLC, **2016**; pp 49–106. DOI:10.1016/b978-0-444-89355-0.50006-5.

(23) Gírio, F. M.; Fonseca, C.; Carvalheiro, F.; Duarte, L. C.; Marques, S.; Bogel-Łukasik,

R. Hemicelluloses for Fuel Ethanol: A Review. *Bioresour. Technol.* **2010**, *101* (13), 4775–4800. DOI:10.1016/j.biortech.2010.01.088.

(24) Santos, R. B.; Hart, P. W.; Jameel, H.; Chang, H.-M. Important Reactions of Lignin. *BioResources* **2013**, *8* (1), 1456–1477.

(25) Berlin, A.; Balakshin, M. Industrial Lignins: Analysis, Properties, and Applications. In *Bioenergy Research: Advances and Applications*; Elsevier, 2014; pp 315–336. DOI:10.1016/B978-0-444-59561-4.00018-8.

(26) Heitner, C.; Dimmel, D. R.; Schmidt, J. A. *Lignin and Lignans: Advances in Chemistry*; Heitner, C., Dimmel, D. R., Schmidt, J. A., Eds.; Taylor & Francis Group: London, **2010**.

(27) Evtuguin, D. V.; Neto, C. P.; Silva, A. M. S.; Domingues, P. M.; Amado, F. M. L.; Robert, D.; Faix, O. Comprehensive Study on the Chemical Structure of Dioxane Lignin from Plantation Eucalyptus Globulus Wood. *J. Agric. Food Chem.* **2001**, *49* (9), 4252–4261. DOI:10.1021/jf010315d.

(28) Pinto, P. C.; Evtuguin, D. V.; Neto, C. P. Effect of Structural Features of Wood Biopolymers on Hardwood Pulping and Bleaching Performance. *Ind. Eng. Chem. Res.* **2005**, *44* (26), 9777–9784. DOI:10.1021/ie050760o.

(29) Adler, E. Lignin Chemistry: Past, Present and Future. *Wood Sci. Technol.* **1977**, *8* (11), 169–2018. DOI:10.1007/BF00365615.

(30) Rodrigues Pinto, P. C.; Borges Da Silva, E. A.; Rodrigues, A. E. Insights into Oxidative Conversion of Lignin to High-Added-Value Phenolic Aldehydes. *Ind. Eng. Chem. Res.* **2011**, *50* (2), 741–748. DOI:10.1021/ie102132a.

(31) Tarasov, D.; Leitch, M.; Fatehi, P. Lignin-Carbohydrate Complexes: Properties, Applications, Analyses, and Methods of Extraction: A Review. *Biotechnol. Biofuels* **2018**, *11* (1), 1–28. DOI:10.1186/s13068-018-1262-1.

(32) Balakshin, M. Y.; Capanema, E. A.; Chang, H. M. MWL Fraction with a High Concentration of Lignin-Carbohydrate Linkages: Isolation and 2D NMR Spectroscopic Analysis. *Holzforschung* **2007**, *61* (1), 1–7. DOI:10.1515/HF.2007.001.

(33) Rodrigues Pinto, P. C.; Borges Da Silva, E. A.; Rodrigues, A. E. Lignin as Source of Fine Chemicals: Vanillin and Syringaldehyde. *Biomass Convers. Interface Biotechnol. Chem. Mater. Sci.* **2012**, 381–420. DOI:10.1007/978-3-642-28418-2_12.

(34) Evtuguin, D. V. Sulphite Pulping. *Lignocellul. Fibers Wood Handb. Renew. Mater. Today's Environ.* **2016**, 225–244. DOI:10.1002/9781118773727.ch8.

(35) Pereira, S. R.; Portugal-Nunes, D. J.; Evtuguin, D. V.; Serafim, L. S.; Xavier, A. M. R. B. Advances in Ethanol Production from Hardwood Spent Sulphite Liquors. *Process Biochem.* **2013**, *48* (2), 272–282. DOI:10.1016/j.procbio.2012.12.004.

(36) Rueda, C.; Calvo, P. A.; Moncali??n, G.; Ruiz, G.; Coz, A. Biorefinery Options to Valorize the Spent Liquor from Sulfite Pulping. *J. Chem. Technol. Biotechnol.* **2015**, *90* (12), 2218–2226. DOI:10.1002/jctb.4536.

(37) Magina, S.; Marques, A. P.; Evtuguin, D. V. Study on the Residual Lignin in Eucalyptus Globulus Sulphite Pulp. *Holzforschung* **2015**, *69* (5), 513–522. DOI:10.1515/hf-2014-0218.

(38) Marques, A. P.; Evtuguin, D. V.; Magina, S.; Amado, F. M. L.; Prates, A. Structure of Lignosulphonates from Acidic Magnesium-Based Sulphite Pulping of Eucalyptus Globulus. *J. Wood Chem. Technol.* **2009**, *29* (4), 337–357. DOI:10.1080/02773810903207762.

(39) Macfarlane, A. L.; Mai, M.; Kadla, J. F. *Bio-Based Chemicals from Biorefining: Lignin Conversion and Utilisation*; **2014**. DOI:10.1533/9780857097385.2.659.

(40) Johansson, A.; Aaltonen, O.; Ylinen, P. Organosolv Pulping - Methods and Pulp Properties. *Biomass* **1987**, *13* (1), 45–65. DOI:10.1016/0144-4565(87)90071-0.

(41) McDonough, T. J. The Chemistry of Organosolv Delignification. *Tappi J.* **1993**, *76* (8).

(42) Sannigrahi, P.; Ragauskas, A. J. Fundamentals of Biomass Pretreatment by Fractionation. *Aqueous Pretreat. Plant Biomass Biol. Chem. Convers. to Fuels Chem.* **2013**, 201–222. DOI:10.1002/9780470975831.ch10.

(43) Costa, C. A. E.; Pinto, P. C. R.; Rodrigues, A. E. Evaluation of Chemical Processing Impact on E. Globulus Wood Lignin and Comparison with Bark Lignin. *Ind. Crops Prod.* **2014**, *61*, 479–491. DOI:10.1016/j.indcrop.2014.07.045.

(44) Neiva, D.; Fernandes, L.; Araújo, S.; Lourenço, A.; Gominho, J.; Simões, R.; Pereira, H. Chemical Composition and Kraft Pulping Potential of 12 Eucalypt Species. *Ind. Crops Prod.* **2015**, *66*, 30–30. DOI:10.1016/j.indcrop.2014.12.016.

(45) Mendes, C. V. T.; Carvalho, M. G. V. S.; Baptista, C. M. S. G.; Rocha, J. M. S.; Soares, B. I. G.; Sousa, G. D. A. Valorisation of Hardwood Hemicelluloses in the

Kraft Pulping Process by Using an Integrated Biorefinery Concept. *Food Bioprod. Process.* **2009**, *87* (3). DOI:10.1016/j.fbp.2009.06.004.

(46) Francisco, M.; van den Bruinhorst, A.; Kroon, M. C. New Natural and Renewable Low Transition Temperature Mixtures (LTTMs): Screening as Solvents for Lignocellulosic Biomass Processing. *Green Chem.* **2012**, *14* (8), 2153. DOI:10.1039/c2gc35660k.

(47) Abbott, A. P.; Capper, G.; Davies, D. L.; Rasheed, R. K.; Tambyrajah, V. Novel Solvent Properties of Choline Chloride/Urea Mixtures. *Chem. Commun. (Camb).* **2003**, *1*, 70–71. DOI:10.1039/B210714G.

(48) Smith, E. L.; Abbott, A. P.; Ryder, K. S. Deep Eutectic Solvents (DESs) and Their Applications. *Chem. Rev.* **2014**, *114* (21), 11060–11082. DOI:10.1021/cr300162p.

(49) Martins, M. A. R.; Pinho, S. P.; Coutinho, J. A. P. Insights into the Nature of Eutectic and Deep Eutectic Mixtures. *J. Solution Chem.* **2018**, 1–3. DOI:10.1007/s10953-018-0793-1.

(50) Van Osch, D. J. G. P.; Zubeir, L. F.; Van Den Bruinhorst, A.; Rocha, M. A. A.; Kroon, M. C. Hydrophobic Deep Eutectic Solvents as Water-Immiscible Extractants. *Green Chem.* **2015**, *17* (9), 4518–4521. DOI:10.1039/c5gc01451d.

(51) Zubeir, L. F.; Lacroix, M. H. M.; Kroon, M. C. Low Transition Temperature Mixtures as Innovative and Sustainable CO2 Capture Solvents. *J. Phys. Chem. B* **2014**, *118* (49), 14429–14441. DOI:10.1021/jp5089004.

(52) García, G.; Aparicio, S.; Ullah, R.; Atilhan, M. Deep Eutectic Solvents: Physicochemical Properties and Gas Separation Applications. *Energy and Fuels* **2015**, *29* (4), 2616–2644. DOI:10.1021/ef5028873.

(53) Florindo, C.; Oliveira, F. S.; Rebelo, L. P. N.; Fernandes, A. M.; Marrucho, I. M. Insights into the Synthesis and Properties of Deep Eutectic Solvents Based on Cholinium Chloride and Carboxylic Acids. *ACS Sustain. Chem. Eng.* **2014**, *2* (10), 2416–2425. DOI:10.1021/sc500439w.

(54) Martins, M. A. R.; Crespo, E. A.; Pontes, P. V. A.; Silva, L. P.; Bülow, M.; Maximo, G. J.; Batista, E. A. C.; Held, C.; Pinho, S. P.; Coutinho, J. A. P. Tunable Hydrophobic Eutectic Solvents Based on Terpenes and Monocarboxylic Acids. *ACS Sustain. Chem. Eng.* **2018**, *6* (7), 8836–8846. DOI:10.1021/acssuschemeng.8b01203.

(55) Zhang, Q.; De Oliveira Vigier, K.; Royer, S.; Jérôme, F. Deep Eutectic Solvents:

Syntheses, Properties and Applications. *Chem. Soc. Rev.* **2012**, *41* (21), 7108–7146. DOI:10.1039/c2cs35178a.

(56) Tang, B.; Row, K. H. Recent Developments in Deep Eutectic Solvents in Chemical Sciences. *Monatshefte fur Chemie* **2013**, *144* (10), 1427–1454. DOI:10.1007/s00706-013-1050-3.

(57) Zhang, Q. H.; Vigier, K. D.; Royer, S.; Jerome, F. Deep Eutectic Solvents: Syntheses, Properties and Applications. *Chem. Soc. Rev.* **2012**, *41* (21), 7108–7146. DOI:10.1039/C2cs35178a.

(58) Francisco, M.; van den Bruinhorst, A.; Kroon, M. C. Low-Transition-Temperature Mixtures (LTTMs): A New Generation of Designer Solvents. *Angew. Chem. Int. Ed. Engl.* **2013**, *52* (11), 3074–3085. DOI:10.1002/anie.201207548.

(59) Kumar, A. K.; Parikh, B. S.; Pravakar, M. Natural Deep Eutectic Solvent Mediated Pretreatment of Rice Straw: Bioanalytical Characterization of Lignin Extract and Enzymatic Hydrolysis of Pretreated Biomass Residue. *Environ. Sci. Pollut. Res.* **2016**, *23* (10), 9265–9275. DOI:10.1007/s11356-015-4780-4.

(60) Lynam, J. G.; Kumar, N.; Wong, M. J. Deep Eutectic Solvents' Ability to Solubilize Lignin, Cellulose, and Hemicellulose; Thermal Stability; and Density. *Bioresour. Technol.* **2017**, *238*, 684–689. DOI:10.1016/j.biortech.2017.04.079.

(61) Chen, L.; Dou, J.; Ma, Q.; Li, N.; Wu, R.; Bian, H.; Yelle, D. J.; Vuorinen, T.; Fu, S.; Pan, X.; et al. Rapid and Near-Complete Dissolution of Wood Lignin at ≤80°C by a Recyclable Acid Hydrotrope. *Sci. Adv.* **2017**, *3* (9). DOI:10.1126/sciadv.1701735.

(62) Morais, E. S.; Freire, C. S. R.; Freire, M. G.; Coelho, J. F. J.; Silvestre, A. J. D.; Mendonça, P. V.; Coutinho, J. A. P. Deep Eutectic Solvent Aqueous Solutions as Efficient Media for the Solubilization of Hardwood Xylans. *ChemSusChem* **2018**, *11* (4), 753–762. DOI:10.1002/cssc.201702007.

(63) Jouyban, A. *Handbook of Solubility Data for Pharmaceuticals*, 1st ed.; Jouyban, A., Ed.; CRC Press, **2010**.

(64) Kumar, A. K.; Parikh, B. S.; Pravakar, M. Natural Deep Eutectic Solvent Mediated Pretreatment of Rice Straw: Bioanalytical Characterization of Lignin Extract and Enzymatic Hydrolysis of Pretreated Biomass Residue. *Environ. Sci. Pollut. Res.* **2016**, *23* (10), 9265–9275. DOI:10.1007/s11356-015-4780-4.

(65) Balasubramanian, D.; Srinivas, V.; Gaikar, V. G.; Sharma, M. M. Aggregation

Behavior of Hydrotropic Compounds in Aqueous Solution. *J. Phys. Chem.* **1989**, *93* (9), 3865–3870. DOI:10.1002/app.11093.

(66) Shimizu, S.; Matubayasi, N. The Origin of Cooperative Solubilisation by Hydrotropes. *Phys. Chem. Chem. Phys.* **2016**, *18* (36), 25621–25628. DOI:10.1039/C6CP04823D.

(67) Subbarao, C. V.; Chakravarthy, I. P. K.; Sai Bharadwaj, A. V. S. L.; Prasad, K. M. M. Functions of Hydrotropes in Solutions. *Chem. Eng. Technol.* **2012**, *35* (2), 225–237. DOI:10.1002/ceat.201100484.

(68) Millard, J. W.; Alvarez-Núñez, F. A.; Yalkowsky, S. H. Solubilization by Cosolvents: Establishing Useful Constants for the Log-Linear Model. *Int. J. Pharm.* **2002**, *245* (1–2), 153–166. DOI:10.1016/S0378-5173(02)00334-4.

(69) Padmawar, A. R.; Bhadoriya, U. Glycol and Glycerin: Pivotal Role in Herbal Industry as Solvent/Co-Soolvent. *Bioresour. Technol. J. Pharm. Med. Res.* **2018**, *4* (5), 153–155.

(70) Gabov, K.; Fardim, P.; da Silva Júnior, F. G. Hydrotropic Fractionation of Birch Wood into Cellulose and Lignin: A New Step towards Green Biorefinery. *BioResources* **2013**, *8* (3), 3518–3531. DOI:10.15376/biores.8.3.3518-3531.

(71) Meng, X.; Parikh, A.; Seemala, B.; Kumar, R.; Pu, Y.; Christopher, P.; Wyman, C. E.; Cai, C. M.; Ragauskas, A. J. Chemical Transformations of Poplar Lignin during Cosolvent Enhanced Lignocellulosic Fractionation Process. *ACS Sustain. Chem. Eng.* **2018**, *6* (7), 8711–8718. DOI:10.1021/acssuschemeng.8b01028.

(72) Chen, Y.; Mu, T. Application of Deep Eutectic Solvents in Biomass Pretreatment and Conversion. *Green Energy Environ.* **2019**, *4* (2), 95–115. DOI:10.1016/j.gee.2019.01.012.

(73) Zainal-Abidin, M. H.; Hayyan, M.; Hayyan, A.; Jayakumar, N. S. New Horizons in the Extraction of Bioactive Compounds Using Deep Eutectic Solvents: A Review. *Anal. Chim. Acta* **2017**, *979*, 1–23. DOI:10.1016/j.aca.2017.05.012.

(74) Alvarez-Vasco, C.; Ma, R.; Quintero, M.; Guo, M.; Geleynse, S.; Ramasamy, K. K.; Wolcott, M.; Zhang, X. Unique Low-Molecular-Weight Lignin with High Purity Extracted from Wood by Deep Eutectic Solvents (DES): A Source of Lignin for Valorization. *Green Chem.* **2016**, *20*, 1–33. DOI:10.1039/C6GC01007E.

(75) Mei, Q.-Q.; Chen, X.; Shen, X.-J.; Yuan, T.-Q.; Wen, J.-L.; Sun, R.-C.; Sun, D. Facile

Fractionation of Lignocelluloses by Biomass-Derived Deep Eutectic Solvent (DES) Pretreatment for Cellulose Enzymatic Hydrolysis and Lignin Valorization. *Green Chem.* **2018**, *21* (2), 275–283. DOI:10.1039/c8gc03064b.

(76) Chen, W.; Liu, Y.; Li, J.; Wang, Q.; Xia, Q.; Liu, Y.; Yu, H.; Guo, B.; Liu, S. Efficient Cleavage of Lignin-Carbohydrate Complexes and Ultrafast Extraction of Lignin Oligomers from Wood Biomass by Microwave-Assisted Treatment with Deep Eutectic Solvent. *ChemSusChem* **2017**, *10* (8), 1857–1857. DOI:10.1002/cssc.201700552.

(77) Mamilla, J. L. K.; Novak, U.; Grilc, M.; Likozar, B. Natural Deep Eutectic Solvents (DES) for Fractionation of Waste Lignocellulosic Biomass and Its Cascade Conversion to Value-Added Bio-Based Chemicals. *Biomass and Bioenergy* **2019**, *120* (December 2018), 417–425. DOI:10.1016/j.biombioe.2018.12.002.

(78) Jablonsky, M.; Haz, A.; Majova, V. Assessing the Opportunities for Applying Deep Eutectic Solvents for Fractionation of Beech Wood and Wheat Straw. *Cellulose* **2019.** DOI:10.1007/s10570-019-02629-0.

(79) Lyu, G.; Li, T.; Ji, X.; Yang, G.; Liu, Y.; Lucia, L. A.; Chen, J. Characterization of Lignin Extracted from Willow by Deep Eutectic Solvent Treatments. *Polymers (Basel).* **2018**, *10* (8), 1–11. DOI:10.3390/polym10080869.

(80) Ashworth, C. R.; Matthews, R. P.; Welton, T.; Hunt, P. A. Doubly Ionic Hydrogen Bond Interactions within the Choline Chloride-Urea Deep Eutectic Solvent. *Phys. Chem. Chem. Phys.* **2016**, *18* (27), 18145–18160. DOI:10.1039/C6CP02815B.

(81) Fache, M.; Boutevin, B.; Caillol, S. Vanillin Production from Lignin and Its Use as a Renewable Chemical. *ACS Sustain. Chem. Eng.* **2016**, *4* (1), 35–46. DOI:10.1021/acssuschemeng.5b01344.

(82) Pinto, P. C. R.; da Silva, E. A. B.; Rodrigues, A. E. Comparative Study of Solid-Phase Extraction and Liquid–Liquid Extraction for the Reliable Quantification of High Value Added Compounds from Oxidation Processes of Wood-Derived Lignin. *Ind. Eng. Chem. Res.* **2010**, *49* (23), 12311–12318. DOI:10.1021/ie101680s.

(83) Pinto, P. C. R.; Oliveira, C.; Costa, C. A.; Gaspar, A.; Faria, T.; Ataíde, J.; Rodrigues, A. E. Kraft Delignification of Energy Crops in View of Pulp Production and Lignin Valorization. *Ind. Crops Prod.* **2015**, *71*, 153–162. DOI:10.1016/j.indcrop.2015.03.069.

(84) Abbott, A. P.; Boothby, D.; Capper, G.; Davies, D. L.; Rasheed, R. Deep Eutectic Solvents Formed Between Choline Chloride and Carboxylic Acids. *J. Am. Chem. Soc* **2004**, *126* (9), 9142. DOI:10.1021/ja048266j.

(85) Myers, R. H.; Montgomery, D. .; Anderson-Cook, C. M. *Response Surface Methodology: Process and Products Optimization Using Designed Experiments*, 3rd ed.; John Wiley & Sons, Inc.: New Jersey, **2009**.

(86) Cornell, J. A. *Experiments with Mixtures: Designs, Models and the Analysis of Mixture Data*, 3rd ed.; John Wiley & Sons: New York, USA, **2002**.

(87) Tappi Standards. T 211 Om-02 Ash in Wood , Pulp , Paper and Paperboard : Combustion at 525 ° C. *TAPPI-Technical Assoc. Pulp Pap. Ind.* **2007**, *T 211*, 1–7.

(88) Tappi. Acid-Insoluble Lignin in Wood and Pulp T222om-02 2002. **2002**, 3–7.

(89) Zakis, G. F. Hydroxyl Groups. In *Functional analysis of lignins and their derivatives*; TAPPI PRESS: Atlanta, G.A, **1994**; pp 13–60.

(90) De Morais, P.; Gonçalves, F.; Coutinho, J. A. P.; Ventura, S. P. M. Ecotoxicity of Cholinium-Based Deep Eutectic Solvents. *ACS Sustain. Chem. Eng.* **2015**, *3* (12), 3398–3404. DOI:10.1021/acssuschemeng.5b01124.

(91) Wang, Y.; Hou, Y.; Wu, W.; Liu, D.; Ji, Y.; Ren, S. Roles of a Hydrogen Bond Donor and a Hydrogen Bond Acceptor in the Extraction of Toluene from N-Heptane Using Deep Eutectic Solvents. *Green Chem.* **2016**, *18* (10), 3089–3097. DOI:10.1039/C5GC02909K.

(92) Dai, Y.; van Spronsen, J.; Witkamp, G.-J.; Verpoorte, R.; Choi, Y. H. Natural Deep Eutectic Solvents as New Potential Media for Green Technology. *Anal. Chim. Acta* **2013**, *766*, 61–68. DOI:10.1016/j.aca.2012.12.019.

(93) Cláudio, A. F. M.; Neves, M. C.; Shimizu, K.; Canongia Lopes, J. N.; Freire, M. G.; Coutinho, J. A. P. The Magic of Aqueous Solutions of Ionic Liquids: Ionic Liquids as a Powerful Class of Catanionic Hydrotropes. *Green Chem.* **2015**, *17* (7), 3948–3963. DOI:10.1039/C5GC00712G.

(94) Xu, C.; Arneil, R.; Arancon, D.; Labidi, J.; Luque, R. Lignin Depolymerisation Strategies: Towards Valuable Chemicals and Fuels. *Chem. Soc. Rev. Chem. Soc. Rev* **2014**, *43* (43), 7485–7500. DOI:10.1039/c4cs00235k.

(95) Cláudio, A. F. M.; Neves, M. C.; Shimizu, K.; Canongia Lopes, J. N.; Freire, M. G.; Coutinho, J. A. P. The Magic of Aqueous Solutions of Ionic Liquids: Ionic Liquids

as a Powerful Class of Catanionic Hydrotropes. *Green Chem.* **2015**, *17* (7), 3948–3963. DOI:10.1039/c5gc00712g.

(96) Evstigneev, E. I. Specific Features of Lignin Dissolution in Aqueous and Aqueous-Organic Media. *Russ. J. Appl. Chem.* **2010**, *83* (3), 509–513. DOI:10.1134/S1070427210030250.

(97) Zhang, C. W.; Xia, S. Q.; Ma, P. S. Facile Pretreatment of Lignocellulosic Biomass Using Deep Eutectic Solvents. *Bioresour. Technol.* **2016**, *219* (July), 1–5. DOI:10.1016/j.biortech.2016.07.026.

(98) Glas, D.; Van Doorslaer, C.; Depuydt, D.; Liebner, F.; Rosenau, T.; Binnemans, K.; De Vos, D. E. Lignin Solubility in Non-Imidazolium Ionic Liquids. *J. Chem. Technol. Biotechnol.* **2015**, *90* (10), 1821–1826. DOI:10.1002/jctb.4492.

(99) Soares, B.; Tavares, D. J. P.; Amaral, J. L.; Silvestre, A. J. D.; Freire, C. S. R.; Coutinho, J. A. P. Enhanced Solubility of Lignin Monomeric Model Compounds and Technical Lignins in Aqueous Solutions of Deep Eutectic Solvents. *ACS Sustain. Chem. Eng.* **2017**, *5* (5), 4056–4065. DOI:10.1021/acssuschemeng.7b00053.

(100) Bauduin, P.; Renoncourt, A.; Kopf, A.; Touraud, D.; Kunz, W. Unified Concept of Solubilization in Water by Hydrotropes and Cosolvents. *Langmuir* **2005**, *21* (15), 6769–6775. DOI:10.1021/la050554l.

(101) Nayak, A. K.; Panigrahi, P. P. Solubility Enhancement of Etoricoxib by Cosolvency Approach. *ISRN Phys. Chem.* **2012**, *2012*, 1–5. DOI:10.5402/2012/820653.

(102) Xu, C.; Arancon, R. A. D.; Labidi, J.; Luque, R. Lignin Depolymerisation Strategies: Towards Valuable Chemicals and Fuels. *Chem. Soc. Rev.* **2014**, *43* (22), 7485–7500. DOI:10.1039/c4cs00235k.

(103) C. J., A. *Equilibrium Thermodynamics*, Third.; McGraw-Hill Book Company: London, **1968**.

(104) Liu, M. J.; Fu, H. L.; Yin, D. P.; Zhang, Y. L.; Lu, C. C.; Cao, H.; Zhou, J. Y. Measurement and Correlation of the Solubility of Enrofloxacin in Different Solvents from (303.15 to 321.05) K. *J. Chem. Eng. Data* **2014**, *59* (6), 2070–2074. DOI:10.1021/je5002158.

(105) Perlovich, G. L.; Kurkov, S. V.; Bauer-Brandl, A. Thermodynamics of Solutions: II. Flurbiprofen and Diflunisal as Models for Studying Solvation of Drug Substances. *Eur. J. Pharm. Sci.* **2003**, *19* (5), 423–432. DOI:10.1016/S0928-0987(03)00145-3.

(106) Francisco, M.; Bruinhorst, A.; Kroon, M. New Natural and Renewable Low Transition Temperature Mixtures (LTTMs): Screening as Solvents for Lignocellulosic Biomass Processing. *Green Chem.* **2012**, *14*, 2153–2157. DOI:10.1039/C2GC35660K.

(107) Zhang, C. W.; Xia, S. Q.; Ma, P. S. Facile Pretreatment of Lignocellulosic Biomass Using Deep Eutectic Solvents. *Bioresour. Technol.* **2016**, *219*, 1–5. DOI:10.1016/j.biortech.2016.07.026.

(108) Jablonsky, M.; Skulcova, A.; Kamenská, L.; Vrska, M.; Sima, J. Deep Eutectic Solvents:Fractionation of Wheat Straw. *BioResources* **2015**, *10* (4), 8039–8047.

(109) Lide, D. R. *CRC Handbook of Chemistry and Physics*, 85th ed.; Lide, D. R., Ed.; CRC Press LLCC, **2005**.

(110) Sarkanen, K. V.; Ludwig, C. H. *Lignins: Occurrence, Formation, Structure and Reactions*; Wiley-Interscience, Ed.; John Wiley & Sons, Inc.: New York, **1971**.

(111) Lin, S. Y.; Dence, C. W. *Methods in Lignin Chemistry*; Timell, T. E., Ed.; Springer-Verlag New York, **1993**.

(112) Sakakibara, A.; Sano, Y. Chemistry of Lignin. In *Wood and Cellulosic chemistry: Second editon, revised and expanded*; N.-S, D., Nobuo Shiraishi, Eds.; Marcel Dekker, Inc.: New York, **2001**.

(113) Rodriguez, N. R.; Bruinhorst, A. Van Den. Degradation of Deep-Eutectic Solvents Based on Choline Chloride and Carboxylic Acids. **2019**. DOI:10.1021/acssuschemeng.9b01378.

(114) Faix, O. Fourier Transform Infrared Spectroscopy. In *Methods in Lignin Chemistry*; Lin, S. Y., Dence, C. W., Eds.; Springer Series in Wood Science, **1992**; pp 83–109.

(115) Ralph, S.; Ralph, J. NMR Database of Lignin and Cell Wall Model Compounds. **1996**.

(116) Capanema, E. A.; Balakshin, M. Y.; Kadla, J. F. Quantitative Characterization of a Hardwood Milled Wood Lignin by Nuclear Magnetic Resonance Spectroscopy. *J. Agric. Food Chem.* **2005**, *53* (25), 9639–9649. DOI:10.1021/jf0515330.

(117) Klemm, D.; Philipp, B.; Heinze, T.; Heinze, U.; Wagenknecht, W. Application of Spectroscopic Analysis in Cellulose Chemistry. In *Comprehensive Cellulose Chemistry: Fundaments and Analytical Methods*; Wiley-VCH Verlag GmbH, **2004**; pp 181–195. DOI:10.1002/3527601929.

(118) Poletto, M.; Ornaghi Júnior, H. L.; Zattera, A. J. Native Cellulose: Structure,

Characterization and Thermal Properties. *Materials (Basel).* **2014**, *7*, 6105–6119. DOI:10.3390/ma7096105.

(119) Hospodarova, V.; Singovszka, E.; Stevulova, N. Characterization of Cellulosic Fibers by FTIR Spectroscopy for Their Further Implementation to Building Materials. *Am. J. Anal. Chem.* **2018**, *9*, 303–310. DOI:10.4236/ajac.2018.96023.

(120) Dawy, M.; Shabaka, A. A.; Nada, A. M. A. Molecular Structure and Dielectric Properties of Some Treated Lignins. *Polym. Degrad. Stab.* **2002**, *62* (3), 455–462. DOI:10.1016/s0141-3910(98)00026-3.

(121) Soares, B.; Silvestre, A. J. D.; Pinto, P. C. R.; Freire, C. S. R.; Coutinho, J. A. P. Wood Delignification with Deep Eutectic Solvents. *ACS Sustain. Chem. Eng.* **2019**. Under preparation.

(122) Liitiä, T.; Maunu, S. L.; Hortling, B. Solid State NMR Studies on Cellulose Crystallinity in Fines and Bulk Fibres Separated from Refined Kraft Pulp. *Holzforschung* **2000**, *54* (6), 618–624. DOI:10.1515/HF.2000.104.

(123) Maciel, G. E.; Kolodziejski, W. L.; Bertran, M. S.; Dale, B. E.; Maciel, G. E.; Kolodziejski, W. L.; Bertran, M. S.; Dale, B. E. 13C NMR and Order in Cellulose. *Macromolecules* **1982**, *15* (2), 686–687. DOI:10.1021/ma00230a097.

(124) Gil, A. M.; Neto, C. P. *Solid-State NMR Studies of Wood and Other Lignocellulosic Materials*; **1999**; Vol. 37. DOI:10.1016/S0066-4103(08)60014-9.

(125) Stone, D.; Ellis, J. Calibration and Linear Regression Analysis: A Self-Guided Tutorial. *CHM314 Instrum. Anal.* **2001**, 1–7.

(126) Vicki, B. Preparation of Calibration Curves - a Guide to the Best Prastice. *Setting Stand. Anal. Sci.* **2003**, 1–27.

(127) Atalla, R. H.; Gast, J. C.; Sindorf, D. W.; Bartuska, V. J.; Maciel, G. E. Carbon-13 NMR Spectra of Cellulose Polymorphs. *J. Am. Chem. Soc.* **1980**, *102* (9), 3249–3251. DOI:10.1021/ja00529a063.

SUPPORTING INFORMATION

S1. Calibration curves for LMMCs solubility and alkali lignin solubility determined by Ultraviolet-visible spectroscopy.

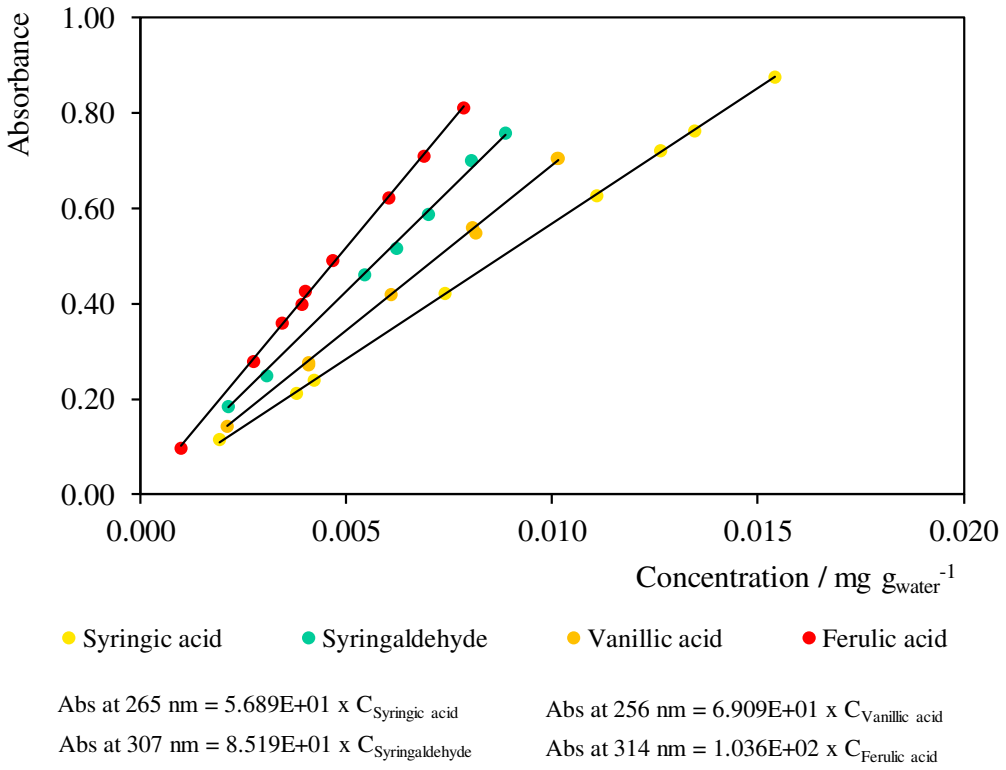

Figure S1.1. Calibration curves of LMMCs in water at 298.15 K. Abs, absorbance and C, concentration of LMMCs (used in chapter 1). The results of the regression analysis (slope, correlation coefficient and residual standard deviation) are presented in Table A1.1.

Table S1.1. Regression analysis of LMMCs calibration curves (used in Chapter I).

	m/g_{water} mg^{-1}	σ	CI_m	R	R^2	*t Stat*	*p*-value
Syringic acid	5.69E+01	2.12E-01	1.41E-02	1.00E+00	9.99E-01	4.79E+02	4.54E-17
Syringaldehyde	8.52E+01	1.29E+00	5.21E-02	9.99E-01	9.99E-01	1.45E+02	1.94E-13
Vanillic acid	6.91E+01	6.84E-01	3.28E-02	9.99E-01	9.99E-01	2.17E+02	2.25E-16
Ferulic acid	1.04E+02	1.13E+00	3.86E-02	9.99E-01	9.99E-01	2.32E+02	2.58E-18

m, slope; σ, standard deviation (error) of the gradient; CI_m, confidence interval (95 %) of the gradient; R, correlation coefficient and R^2, correlation coefficient square.

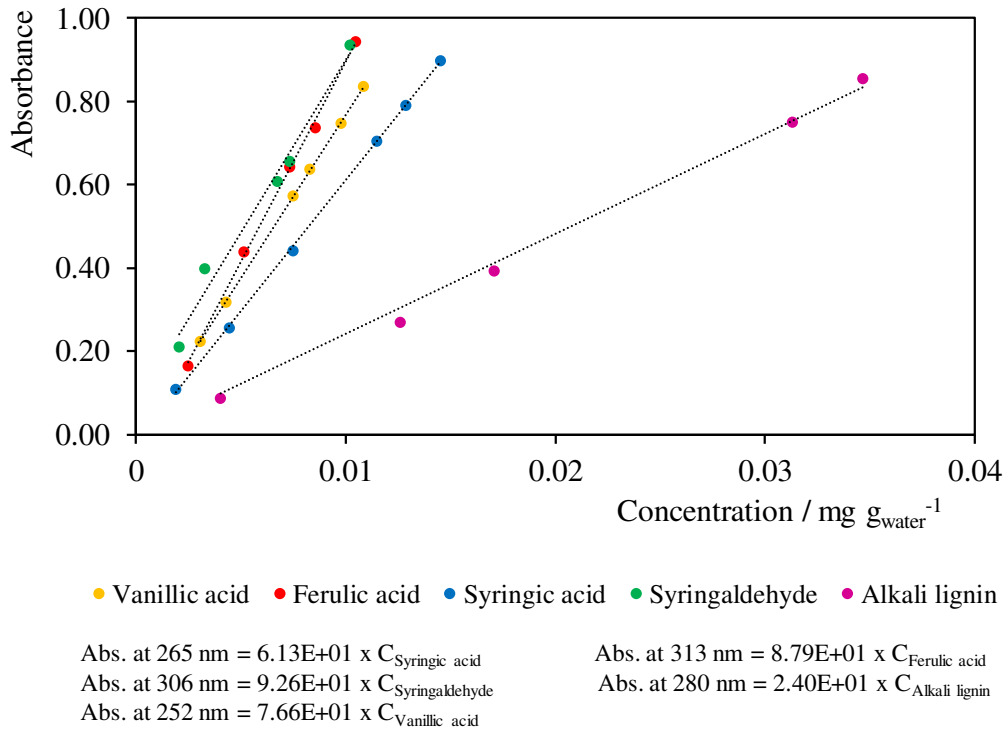

Figure S1.2. Calibration curves of LMMCs and alkali lignin in water at 298.15 K, obtained by UV-vis spectroscopy. Abs, absorbance and C, concentration of lignin monomer model compounds or Alkali lignin (used in chapter 2). The results of the regression analysis (slope, correlation coefficient and residual standard deviation) are presented in Table A1.2.

Table S1.2. Regression analysis of LMMCs and alkali lignin calibration curves (used in Chapter II).

	m/g_{water} mg^{-1}	σ	CI_m	R	R^2	*t-statistic*	*p*-value
Syringic acid	6.13E+01	8.27E-01	5.16E-02	9.99E-01	9.99E-01	140.80	3.43E-10
Syringaldehyde	9.26E+01	5.92E+00	2.43E-01	9.93E-01	9.86E-01	96.32	6.96E-08
Vanillic acid	7.66E+01	7.98E-01	3.92E-02	9.99E-01	9.99E-01	234.86	2.66E-11
Ferulic acid	8.79E+01	3.27E+00	1.49E-01	9.98E-01	9.97E-01	93.39	7.88E-08
Alkali lignin	2.40E+01	7.07E-01	1.01E-01	9.99E-01	9.98E-01	56.98	5.68E-07

m, slope; σ, standard deviation (error) of the gradient; CI_m, confidence interval (95 %) of the gradient; R, correlation coefficient and R^2, correlation coefficient square.

S2. New method to quantify the technical lignins (kraft and organosolv lignins) solubility in eutectic solvents, calibration curve determined by Fourier-transform infrared spectroscopy.

The most conventional analytical method for the quantification of dissolved technical lignins is Ultraviolet-visible (UV-vis) spectroscopy at 280 nm, where the lignin absorbance follows the Beer-Lambert Law.[111] This method require a solids free samples with low concentration of analyte. However, in the technical lignin solubility assays, after reach the saturation in both neat eutectic solvents (ESs) and in aqueous solution, due to the dark color

and the high viscosity of the solutions it was not possible to filtrate or centrifuge the samples in order to separate the two phases. Therefore, this condition precludes the analysis and quantification of lignin solubility in ESs by UV-vis spectroscopy. To overcome this limitation, the Fourier-transform infrared (FTIR) spectroscopy emerge as another analytical technique, that has been shown to be a powerful tool for quantitative lignin analysis in solutions.[111] This technique allow the fast analysis of liquid or solid using an attenuated total reflection (ATR) accessory. In that sense, three technical lignins obtained from different delignification processes (kraft, organosolv and alkali lignins) were selected and analyzed by FTIR spectroscopy accoupled with ATR cell. The FTIR spectra are depicted in Figure S2.1. The absorption bands were assigned as suggested by O. Faix.[114]

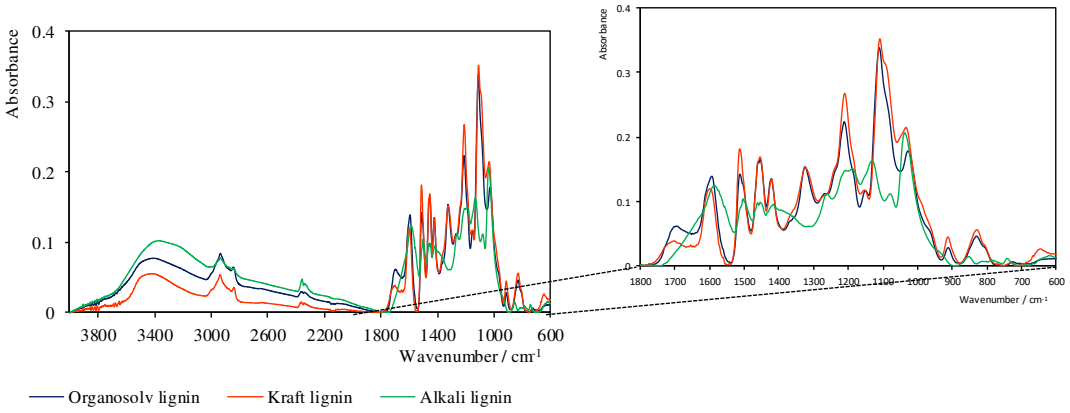

Figure S2.1. Normalized FTIR spectra of technical lignins obtained from different delignification processes of *Eucalyptus globulus* wood.

Figure S2.1, shows the FTIR spectra of some typical technical lignins. Commom features as well as particular vibrations, specific of each lignin, are found in the spectra. In the case of the technical lignins selected for this study, the FTIR spectra show a broad band at 3400 cm^{-1} attributed to the hydroxyl groups in phenolic and aliphatic structures (O-H stretching), and the bands centred around 2930 and 2830 cm^{-1}, predominantly arising from C-H stretching in methyl and methylene groups. In the carbonyl/carboxyl region, a bands is observed at 1710 cm^{-1}, originating from unconjugated carbonyl/carboxyl C=O stretching (this band was absent in the spectra of alkali lignin). Aromatic skeletal vibration at 1594, 1510 and 1424 cm^{-1} and the C-H deformation combined with aromatic ring vibration at 1460 cm^{-1}, are commom for all lignins, although the intensity of the bands may differ.

The spectral region below 1400 cm^{-1} is more difficult to analyse, since most bands are complex, with contribution from various vibration modes. The spectra of kraft and organosolv lignins show a band at 1316 cm^{-1}, which is characteristic for syringyl (S) ring plus (G) ring condensed and at 1269 cm^{-1} for guaiacyl (G) ring plus C=O stretching, observed for all lignins spectra. A strong vibration at 1214 cm^{-1}, only observed for kraft and organosolv lignins spectra, can be associated with C-C plus C-O plus C=O stretching. A shoulder at 1145 cm^{-1} assigned to the aromatic C-H in-plane deformation guaiacyl-type and a strong band at 1107 cm^{-1} characteristic of C-O deformation in secondary alcohols and aliphatic ethers. The spectra of all lignin samples show at 1035 cm^{-1} assigned to the aromatic C-H in-plane deformation, plus C-O deformation in primary alcohols and plus C=O stretch. Finally, the bands at 918 and 822 cm^{-1} are associated with the aromatic C-H out-of-plane deformation, only observed in kraft and organosolv lignin FTIR spectra.

Considering that all technical lignins showed the band at 1510 cm^{-1}, characteristic of aromatic skeletal vibrations in FTIR spectra, a new methodology was implemented to quantify their solubility in ES (neat and in aqueos solution) at this specific band. This band is the most convenient in the region of 1500 – 600 cm^{-1}. The 1594 cm^{-1} lignin band is difficult to use because of water band interference at 1625 cm^{-1} and the interference of carboxyl band at 1698 cm^{-1} from carboxylic acid-based ES.

Therefore, it was possible to build the calibration cuves using the three technical lignins dissolved in different neat ES at 353.15 K and different lignin concentrations (until 42 wt % for organosolv and 13 wt % for kraft and alkali lignins, to avoid the saturation point). The neat ES, EG:[Ch]Cl (2:1), EG:[N_{2222}]Cl (2:1) and EG:[N_{4444}]Cl (2:1) were selected because negligible absorbance, correspondig to the water content in neat ES, were observed in their FTIR spectra in the especific range of 1600 – 1500 cm^{-1} (see Figure S2.2). Furthermore, considering the good performance of PA:U (2:1) on technical lignin solubilization, demonstrated in Chapter I, we decide to introduce the correlation of different kraft lignin concentration dissolved in PA:U (2:1) at 353.15 K with their respective absorbance after FTIR analysis. The objective was to evaluate their influence on the calibration curve, taken into account that PA:U (2:1) present an significant absorbance in the range of 1800 – 1500 cm^{-1}, as observed in their FTIR spectra (see Figure S2.2), associated with the stretching vibration of carboxyl group from propionic acid (PA).

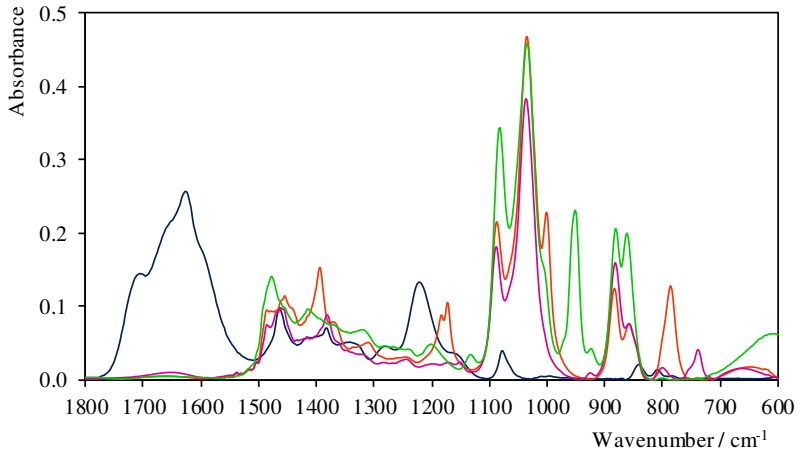

Figure S2.2. Normalized FTIR spectra of neat ES, EG:[Ch]Cl (2:1) (green), EG:[N_{2222}]Cl (2:1) (orange), EG:[N_{4444}]Cl (2:1) (pink) and PA:U (2:1) (blue).

Figure S2.3 (left), ilustrates the correlation between technical lignins concentrations in four different neat ESs and the respective absorbance obtained from FTIR spectroscopy analysis at 1510 cm^{-1}. In the case of polyols-based ESs, these results shows that independently of the HBA used to prepare ESs (with EG as common HBD), no significant influences were observed in the curve, at the same conditions. The sligth data dispersion observed below 15 wt % of technical lignin dissolved in ESs, are possibly related to the different technical lignins chemical structures, associated with the different isolation procces, affecting consequently their solubilization. In the case of kraft lignin disssolved in carboxylic acid-based ESs, the results showed an slight increase of absorbance, when compared with the kraft lignin dissolved in polyols-based ESs. These differences can be associated with the interference of carboxyl group absorbance in the region of our analysis (1600 – 1500 cm^{-1}), as observed in Figure S2.2. Nevertheless, it was possible to obtain a good linearity with high statistical significance at the 95 % confidence level, considering all data (see Figure S2.3, right).

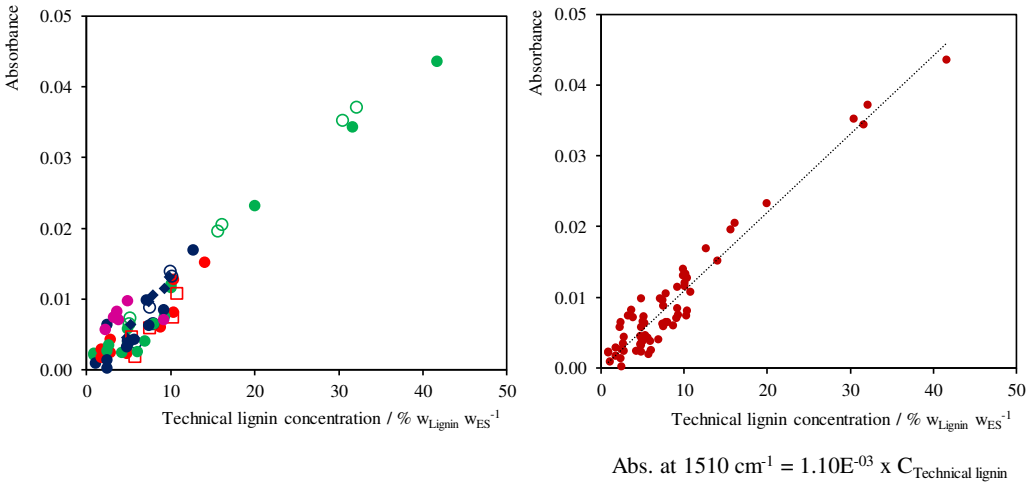

Figure S2.3. Correlation between technical lignins concentration (alkali lignin – red, organosolv lignin – green and kraft lignin – blue) dissolved in different neat ES (EG:[Ch]Cl (2:1) – dot; EG:[N_{4444}]Cl (2:1) – circle; EG:[N_{2222}]Cl (2:1) – square, and PA:U (2:1) – pink dot) at 353.15 K and the respective absorbance, analyzed by FTIR spectroscopy at 1510 cm^{-1} (left) and Calibration curve of technical lignins in these neat ESs at 353.15 K, considering all data (right).

The regression coefficient, their uncertainty associated, correlation coefficient, and the ANOVA analysis are reported in Table S2.1.

Table S2.1 Regression analysis of technical lignins calibration curve, analyzed by FTIR spectroscopy at 1510 cm^{-1}.

m / % w_{ES} w_{Lignin}^{-1}	σ	CI_m	R	Predicted R^2	Adjusted R^2	*t*-statistic	*p*-value
1.10E-03	3.76E-05	6.89E-03	9.83E-01	9.67E-01	9.51E-01	4.34E+01	3.47E-49

m, slope; σ, standard deviation (error) of the gradient; CI_m, confidence interval (95 %) of the gradient; R, correlation coefficient and R^2, correlation coefficient square.

The correlation coeficient (R) or Pearson *R* value[125,126] (R=0.983) provides a measure of the degree to which the values of lignin concentration and the absorbance of lignin dissolved in ESs are lineary correlated. The parameters related to R are the predicted R^2 and the adjusted R^2. The predicted R^2 describe the fraction of the total variance in the data which is contributed by the fitted regression line.[126] In this study, a predicted R^2 of 0.967 means that the data are well-correlated and the best-fit line describes the data. The adjusted R^2 is useful for assessing the effect of adding additional terms to the equation of the fitted line.[126] In this case, the adjusted R^2 of 0.951 is in agreement with the predicted R^2 of 0.967, than we concluded that it is no needed additional terms. Finally, the confidence limitis for

the slope are 1.10E-03 ± 3.76E-05, this represent the extremes of the value that the slope could take, at the 95 % confidence level. Regarding the ANOVA analysis, the *t*-statistic value of 43.4 implies the model is significant and the *p*-value less than 0.05 (in this case, 3.47E-49) indicate that the model terms are also significant.

Regarding the residual analysis, their assumptions: independence (lack of correlation) of error, homoscedasticity (constant variance) of erros and normality of the error distribution, are depicted in Figure S2.4. The residuals normal distributions can be observed in the predicted versus experimental absorbance plot and the normal probability plot, because in a normal distribution the residual are in a straight line. Moreover, the residual plot (residual versus lignin concentration) show that the erro have constant variance, with the residulas scatteres randomly around zero, so assuming that the erros terms have a mean of zero is reasonable. In that sense, we concluded that all the assumptions were successfully verified.

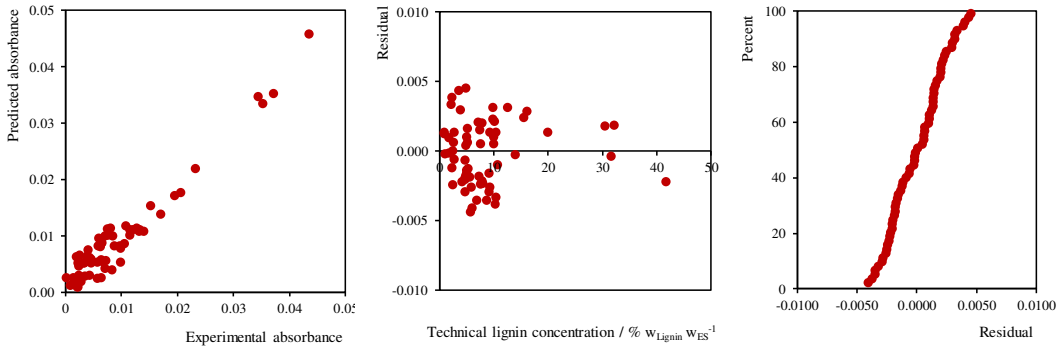

Figure S2.4. Regression analysis of dissolved technical lignins in neat ES: correlation between the predicted and experimental absorbance (left), residual plot (center) and normal probability plot (right).

The calibration curve validation with two test samples. The validation of analytical methods is a requirement for the quality and comparability of analytical results. For this purpose, two different samples of kraft lignin at two different concentrations (a) 5 wt % and (b) 7 wt % dissolved in neat EG:[Ch]Cl (2:1) at 353.15 K, were prepared and analyzed by two different methodologies (FTIR spectroscopy and gravimetrical techniques) to quantify the lignin concentration, in order to validate the calibration curve.

Regarding the methodologies used, the FTIR analysis was carried out following the same procedure previously described. The gravimetrical analyses, after reach the total solubilization of lignin in ES at 353.15 K, the sample was filtrated to separate some solid

residue from the liquid phase (this solid was dried until constant weight). After that, the lignin was isolated from the liquid phase adding cool water overnight, to promote the precipitation of dissolved lignin. The lignin isolated, was collected after filtration and dried at 303.15 K in an oven with vacuum, until constant weight. The lignin that remain in liquid phase was quantified by UV-vis spectroscopy, using an alkali lignin calibration curve in water, because is the lignin more soluble in water when compared with organosolv and kraft lignins (see Figure S1.2 and Table S1.2). The detail values of lignin concentration obtained from each methodology, are reported in Table S2.2.

As observed in Table S2.2, it was possible to determine the lignin concentration dissolved in neat ES by two different methodologies, with a difference between them of 0.05 wt % for (a) sample and 0.43 wt % for (b) sample. Furthermore, around 20 wt % of lignin remain insoluble, as demonstrated by the gravimetrical analysis. Despite this fact, these results proved that the FTIR spectroscopy technique can be a powerful tool for quantitative lignin analysis in solutions. Finally, the lignin concentration dissolved in ES was successfully predicted by the proposed calibration curve with statistical significance at 95 % confidence level.

Table S2.2. Experimental lignin concentration obtained from FTIR spectroscopy at 1510 cm^{-1} and gravimetrical analysis.

FTIR analysis							
Sample	ES / g	Lignin / g	Lignin concentration / % w_{Lignin} w_{ES}^{-1}	Absorbance at 1510 cm^{-1}	Lignin concentration from calibration curve / % w_{Lignin} w_{ES}^{-1}		
a	0.5246	0.0261	4.98	0.00384	**3.49**		
b	0.5334	0.0392	7.35	0.00623	**5.66**		
Gravimetrical analysis (GA)							
Sample	ES / g	Lignin / g	Lignin concentration / % w_{Lignin} w_{ES}^{-1}	Residue / g	Isolated Lignin / g	Lignin in liquid phase by UV-vis / g	Lignin concentration from GA / % w_{Lignin} w_{ES}^{-1}
a	2.0300	0.1007	4.96	0.02	0.0589	0.0109	**3.44**
b	2.0620	0.1528	7.41	0.03	0.0938	0.0141	**5.23**

S3. Experimental data – Chapter I

Table S3.1. Experimental solubilities of syringic acid in 25 wt % aqueous solutions of ESs at 303.15 K.

ESs	Solubility ± σ / mg g^{-1}	$S/S_0 \pm \sigma$	pH ± σ
FA:[Ch]Cl (2:1)	2.96 ± 0.08	2.31 ± 0.06	1.37 ± 0.01
AA:[Ch]Cl (2:1)	4.76 ± 0.03	3.72 ± 0.02	1.98 ± 0.01
PA:[Ch]Cl (2:1)	7.06 ± 0.14	5.51 ± 0.11	2.10 ± 0.03
LA:[Ch]Cl (2:1)	3.21 ± 0.07	2.50 ± 0.06	1.50 ± 0.04
GlyA:[Ch]Cl (3:1)	3.04 ± 0.04	2.37 ± 0.03	1.35 ± 0.01
MA:[Ch]Cl (2:1)	2.73 ± 0.04	2.13 ± 0.03	1.39 ± 0.01
PTSA:[Ch]Cl (1:1)	6.27 ± 0.14	4.89 ± 0.11	0.45 ± 0.00
G:[Ch]Cl (2:1)	2.17 ± 0.06	1.69 ± 0.05	6.19 ± 0.05
EG:[Ch]Cl (2:1)	2.25 ± 0.12	1.76 ± 0.09	4.93 ± 0.02
Glu:[Ch]Cl (1:1)	2.20 ± 0.15	1.72 ± 0.12	4.58 ± 0.01
Xyl:[Ch]Cl (2:1)	2.16 ± 0.15	1.68 ± 0.12	4.13 ± 0.03
Fru:[Ch]Cl (1:1)	2.79 ± 0.01	2.17 ± 0.01	4.06 ± 0.00
U:[Ch]Cl (2:1)	4.13 ± 0.01	3.23 ± 0.01	6.55 ± 0.07
LA:Pro (2:1)	4.09 ± 0.01	3.19 ± 0.01	2.65 ± 0.01
LA:Bet (2:1)	5.22 ± 0.01	4.07 ± 0.01	2.65 ± 0.01
LA:U (2:1)	4.41 ± 0.21	3.44 ± 0.17	1.87 ± 0.02
AA:Pro (2:1)	5.75 ± 0.02	4.49 ± 0.01	3.22 ± 0.01
AA:Bet (2:1)	7.02 ± 0.06	5.47 ± 0.04	3.30 ± 0.08
AA:U (2:1)	8.68 ± 0.28	6.77 ± 0.22	2.19 ± 0.01
PA:Pro (2:1)	9.01 ± 0.21	7.03 ± 0.17	3.35 ± 0.00
PA:Bet (2:1)	9.69 ± 0.26	7.56 ± 0.21	3.37 ± 0.02
PA:U (2:1)	12.31 ± 0.25	9.61 ± 0.20	2.45 ± 0.10
PA:[Ch]Cl (4:1)	8.66 ± 0.20	6.75 ± 0.16	2.04 ± 0.01
PA:[Ch]Cl (3:1)	8.19 ± 0.38	6.39 ± 0.29	2.07 ± 0.00
PA:[Ch]Cl (1:1)	5.50 ± 0.23	4.29 ± 0.18	2.22 ± 0.03
PA:[Ch]Cl (1:2)	4.00 ± 0.10	3.12 ± 0.08	2.34 ± 0.01
PA:[Ch]Cl (1:3)	3.71 ± 0.17	2.90 ± 0.13	2.39 ± 0.01
PA:[Ch]Cl (1:4)	3.35 ± 0.18	2.61 ± 0.14	2.50 ± 0.00
LA:[Ch]Cl (1:2)	2.60 ± 0.02	2.03 ± 0.01	1.75 ± 0.04
GlyA:Pro (3:1)	3.09 ± 0.05	2.41 ± 0.04	2.44 ± 0.00
GlyA:Pro (2:1)	3.13 ± 0.05	2.45 ± 0.04	2.40 ± 0.00
GlyA:Pro (1:1)	3.11 ± 0.07	2.42 ± 0.05	2.87 ± 0.01
PA:U (4:1)	13.80 ± 1.07	10.77 ± 0.84	2.34 ± 0.00
PA:U (1:1)	10.70 ± 0.25	8.35 ± 0.20	2.65 ± 0.00
PA:U (1:2)	8.88 ± 0.06	6.93 ± 0.05	2.85 ± 0.00
PA:U (1:4)	4.76 ± 0.16	3.71 ± 0.13	3.25 ± 0.00

σ, standard deviation; S, the solubility of syringic acid in the aqueous solutions of ESs; S_0, the solubility of syringic acid in pure water.

Table S3.2. Experimental solubilities of lignin monomer model compounds in 25 wt % aqueous solutions of ESs at 303.15 K.

LMMCs	Syringaldehyde		Vanillic acid		Ferulic acid	
	Solubility ± σ / mg g^{-1}	$S/S_0 \pm \sigma$	Solubility ± σ / mg g^{-1}	$S/S_0 \pm \sigma$	Solubility ± σ / mg g^{-1}	$S/S_0 \pm \sigma$
ES						
PA:U (4:1)	36.29 ± 0.63	12.43 ± 0.22	13.01 ± 0.21	7.19 ± 0.12	8.20 ± 0.13	13.03 ± 0.20
PA:U (2:1)	26.74 ± 1.84	9.16 ± 0.63	11.46 ± 0.65	6.33 ± 0.36	6.96 ± 0.04	11.06 ± 0.07
PA:U (1:1)	28.36 ± 0.34	9.71 ± 0.12	9.92 ± 0.71	5.48 ± 0.39	3.39 ± 0.23	5.38 ± 0.37
PA:U (1:2)	21.55 ± 0.24	7.38 ± 0.08	5.47 ± 0.28	3.02 ± 0.15	1.36 ± 0.36	2.16 ± 0.57
PA:U (1:4)	13.18 ± 0.62	4.51 ± 0.21	3.86 ± 0.32	2.13 ± 0.18	0.75 ± 0.01	1.18 ± 0.02

σ, standard deviation; S, the solubility of lignin monomer model compounds in the aqueous solutions of ESs; S_0, the solubility of lignin monomer model compounds in pure water.

Table S3.3. Experimental solubilities of lignin monomer model compounds in PA:U (2:1) aqueous solutions at three different temperatures.

LMMCs	Syringic acid		Syringaldehyde		Vanillic acid		Ferulic acid	
	Solubility ± σ / mg g^{-1}	$S/S_0 \pm \sigma$	Solubility ± σ / mg g^{-1}	$S/S_0 \pm \sigma$	Solubility ± σ / mg g^{-1}	$S/S_0 \pm \sigma$	Solubility ± σ / mg g^{-1}	$S/S_0 \pm \sigma$
Temperature / K				***303.15***				
wt % of ES								
0	1.28 ± 0.01	-	2.92 ± 0.01	-	1.83 ± 0.06	-	0.63 ± 0.06	-
25	12.31 ± 0.25	9.61 ± 0.20	26.74 ± 1.84	9.16 ± 0.63	11.46 ± 0.65	6.33 ± 0.36	6.96 ± 0.04	11.06 ± 0.07
50	37.59 ± 0.34	29.32 ± 0.27	104.04 ± 2.80	35.63 ± 0.96	23.56 ± 0.56	12.85 ± 0.31	21.09 ± 0.41	33.52 ± 0.65
75	33.06 ± 1.37	25.79 ± 1.07	106.01 ± 2.58	36.30 ± 088	24.04 ± 0.42	13.11 ± 0.23	13.85 ± 1.40	22.01 ± 2.22
95	8.80 ± 1.32	6.87 ± 1.03	23.57 ± 2.92	8.07 ± 1.00	15.92 ± 1.21	8.68 ± 0.66	6.85 ± 0.12	10.89 ± 0.18
100	5.18 ± 1.75	4.04 ± 1.36	4.21 ± 0.19	1.44 ± 0.07	8.56 ± 0.18	4.67 ± 0.10	4.13 ± 0.10	6.56 ± 0.17
				313.15				
0	1.60 ± 0.03	-	4.41 ± 0.10	-	2.93 ± 0.06	-	0.82 ± 0.03	-
25	16.17 ± 0.74	10.10 ± 0.46	56.77 ± 2.87	12.88 ± 0.65	15.15 ± 0.19	5.18 ± 0.07	9.04 ± 0.96	10.96 ± 1.16
50	42.98 ± 2.07	26.88 ± 1.29	167.20 ± 1.17	37.93 ± 0.26	34.17 ± 0.71	11.68 ± 0.24	42.10 ± 0.89	51.06 ± 1.08
75	49.64 ± 4.23	31.04 ± 2.65	184.67 ± 3.63	41.89 ± 0.82	31.03 ± 2.99	10.61 ± 1.02	27.10 ± 2.79	32.87 ± 3.39
95	12.66 ± 1.14	7.92 ± 0.71	34.21 ± 3.24	7.76 ± 0.74	16.13 ± 0.41	5.52 ± 0.14	6.77 ± 0.30	8.22 ± 0.36
100	6.06 ± 0.20	3.79 ± 0.13	8.82 ± 0.00	1.32 ± 0.00	12.76 ± 2.08	4.36 ± 0.71	5.69 ± 0.14	6.91 ± 0.17
				323.15				

0	1.87 ± 0.08	-	7.91 ± 0.76	-	3.24 ± 0.11	-	1.53 ± 0.05	-
25	16.94 ± 1.66	9.08 ± 0.89	86.40 ± 3.11	10.93 ± 0.39	20.31 ± 1.57	6.27 ± 0.48	17.60 ± 1.20	11.48 ± 0.79
50	58.02 ± 1.83	36.52 ± 0.59	91.29 ± 2.25	11.54 ± 0.28	51.64 ± 1.99	15.96 ± 0.61	68.99 ± 0.35	45.02 ± 0.23
75	88.37 ± 3.55	47.38 ± 1.90	189.63 ± 2.93	23.98 ± 0.37	52.14 ± 2.20	16.11 ± 0.68	43.50 ± 1.35	28.38 ± 0.88
95	15.86 ± 0.32	8.51 ± 0.17	81.72 ± 0.08	10.33 ± 0.01	35.98 ± 1.55	11.12 ± 0.48	13.69 ± 0.93	8.93 ± 0.61
100	11.27 ± 3.11	6.03 ± 1.67	6.95 ± 1.01	0.88 ± 0.13	19.05 ± 0.48	5.89 ± 0.15	8.18 ± 0.00	5.34 ± 0.00

σ, standard deviation; S, the solubility of lignin monomer model compounds in the aqueous solutions of ES; S_0, the solubility of lignin monomer model compounds in pure water.

Table S3.4. Experimental solubilities of technical lignins in PA:U (2:1) aqueous solutions at two different temperatures.

Temperature / K	***313.15***		***323.15***	
wt % of ES	Solubility ± σ / wt %	$S/S_0 \pm \sigma$	Solubility ± σ / wt %	$S/S_0 \pm \sigma$
Organosolv lignin				
0	0.09 ± 0.02	-	0.11 ± 0.02	-
25	3.06 ± 0.59	35.20 ± 6.80	2.21 ± 0.37	21.34 ± 3.54
50	20.00 ± 1.33	230.29 ± 15.34	13.98 ± 2.38	135.29 ± 22.99
75	31.64 ± 3.09	364.41 ± 35.62	48.90 ± 2.85	473.21 ± 27.61
100	22.94 ± 1.11	264.14 ± 12.73	29.67 ± 3.41	287.11 ± 32.96
Kraft lignin				
0	0.06 ± 0.002	-	0.08 ± 0.003	-
25	1.64 ± 0.01	25.95 ± 0.22	5.71 ± 0.65	74.16 ± 8.44
50	20.30 ± 0.78	321.66 ± 12.23	17.54 ± 0.96	227.75 ± 12.50
75	12.52 ± 2.20	198.43 ± 34.92	3.88 ± 0.1	50.34 ± 1.30
100	7.91 ± 2.10	125.28 ± 33.28	1.67 ± 0.43	21.63 ± 5.58

σ, standard deviation; S, the solubility of technical lignins in the aqueous solutions of ES; S_0, the solubility of technical lignins in pure water.

Table S3.5. Experimental solubilities of technical lignins and lignin monomer model compounds in NaOH aqueous solutions with pH 10 at different temperatures.

Temperature / K	***303.15***		***313.15***		***323.15***	
	Solubility ± σ / wt %	$S/S_0 \pm \sigma$	Solubility ± σ / wt %	$S/S_0 \pm \sigma$	Solubility ± σ / wt %	$S/S_0 \pm \sigma$
Kraft lignin	-	-	5.04 ± 1.14	126.78 ± 30.16	5.47 ± 0.89	71.00 ± 11.27
LMMCs	Solubility ± σ / mg g^{-1}	$S/S_0 \pm \sigma$	Solubility ± σ / mg g^{-1}	$S/S_0 \pm \sigma$	Solubility ± σ / mg g^{-1}	$S/S_0 \pm \sigma$
Syringic acid	1.39 ± 0.03	1.08 ± 0.02	1.73 ± 0.08	1.09 ± 0.05	2.38 ± 0.01	1.28 ± 0.001
Syringaldehyde	3.84 ± 0.03	1.31 ± 0.001	5.28 ± 0.16	1.20 ± 0.04	7.88 ± 0.14	0.99 ± 0.02
Vanillic acid	1.97 ± 0.08	1.08 ± 0.04	2.51 ± 0.02	0.86 ± 0.01	3.70 ± 0.002	1.14 ± 0.00
Ferulic acid	0.71 ± 0.02	1.13 ± 0.02	0.85 ± 0.05	1.03 ± 0.06	1.26 ± 0.03	0.82 ± 0.02

σ, standard deviation; S, the solubility of technical lignin sand lignin monomer model compounds in the aqueous solutions of NaOH at pH 10; S_0, the solubility of technical lignins and lignin monomer model compounds in pure water.

Table S3.6. Experimental nanoaggregate size present in the saturated aqueous solutions of technical lignins and lignin monomer model compounds in PA:U (2:1) at 50 wt % and 323.15 K, analyzed by dynamic light scattering based on intensity, volume and number particle size distribution

Samples	Intensity / %	Size ± σ / d.nm	Volume / %	Size ± σ / d.nm	Number / %	Size ± σ / d.nm
PA:U (2:1) 50 wt % + kraft lignin	73.61	10.43 ± 0.83	96.64	2.43 ± 0.18	99.85	1.73 ± 0.16
PA:U (2:1) 50 wt % + organosolv lignin	96.38	15.31 ± 1.68	78.05	4.80 ± 1.93	100.00	3.21 ± 1.353
PA:U (2:1) 50 wt % + syringaldehyde	96.05	2.38 ± 0.55	97.22	1.24 ± 0.12	100.00	0.86 ± 0.07
PA:U (2:1) 50 wt % + ferulic acid	97.21	1.93 ± 0.43	100.00	1.19 ± 0.23	100.00	0.92 ± 0.19

σ, standard deviation.

S4. Experimental data – Chapter II

Table S4.1. Experimental solubilities of lignin monomer model compounds in different ESs aqueous solutions at 323.15 K, obtained from UV-vis spectroscopy.

LMMCs	Syringic acid		Syringaldehyde		Vanillic acid		Ferulic acid	
	Solubility ± σ / mg g^{-1}	$S/S_0 \pm \sigma$	Solubility ± σ / mg g^{-1}	$S/S_0 \pm \sigma$	Solubility ± σ / mg g^{-1}	$S/S_0 \pm \sigma$	Solubility ± σ / mg g^{-1}	$S/S_0 \pm \sigma$
ES	***FA:[Ch]Cl (2:1)***							
wt % of ES								
0	1.87 ± 0.08	1.00 ± 0.00	7.91 ± 0.76	1.00 ± 0.00	3.24 ± 0.11	1.00 ± 0.00	1.53 ± 0.05	1.00 ± 0.00
25	6.13 ± 0.68	3.28 ± 0.36	18.36 ± 0.98	2.32 ± 0.12	8.95 ± 0.36	2.77 ± 0.11	5.25 ± 0.39	3.43 ± 0.25
50	10.85 ± 0.41	5.82 ± 0.22	34.46 ± 1.22	4.36 ± 0.15	15.91 ± 0.32	4.92 ± 0.10	15.10 ± 0.22	9.87 ± 0.15
75	17.24 ± 0.12	9.24 ± 0.06	57.30 ± 3.14	7.25 ± 0.40	28.72 ± 0.32	8.88 ± 0.10	30.54 ± 0.22	19.96 ± 0.15
95	25.75 ± 1.25	13.81 ± 0.67	89.68 ± 2.08	11.34 ± 0.26	42.64 ± 0.75	13.18 ± 0.23	51.88 ± 2.20	33.91 ± 1.44
100	27.22 ± 0.50	14.59 ± 0.27	85.33 ± 0.38	10.79 ± 0.05	51.77 ± 1.56	16.00 ± 0.48	73.97 ± 0.55	48.35 ± 0.36
	LA:[Ch]Cl (10:1)							
0	1.87 ± 0.08	1.00 ± 0.00	7.91 ± 0.76	1.00 ± 0.00	3.24 ± 0.11	1.00 ± 0.00	0.82 ± 0.03	1.00 ± 0.00
25	6.76 ± 0.48	3.62 ± 0.26	22.21 ± 3.69	2.81 ± 0.47	6.64 ± 1.39	2.05 ± 0.43	4.23 ± 0.57	2.76 ± 0.37
50	9.80 ± 2.47	5.26 ± 1.32	50.32 ± 4.13	6.36 ± 0.52	13.32 ± 2.53	4.12 ± 0.78	12.07 ± 1.56	7.88 ± 1.02
75	13.28 ± 2.45	7.12 ± 1.32	67.12 ± 1.30	8.49 ± 0.16	18.67 ± 1.04	5.77 ± 0.32	16.55 ± 2.33	10.80 ± 1.52
95	15.16 ± 2.89	8.13 ± 1.55	94.42 ± 4.73	11.94 ± 0.60	19.95 ± 0.80	6.16 ± 0.25	27.82 ± 1.61	18.15 ± 1.05
100	16.87 ± 1.96	9.67 ± 1.27	87.83 ± 6.27	11.11 ± 0.79	19.50 ± 2.56	6.03 ± 0.79	26.17 ± 0.82	17.08 ± 0.53
	PA:[Ch]Cl (2:1)							
0	1.87 ± 0.08	1.00 ± 0.00	7.91 ± 0.76	1.00 ± 0.00	3.24 ± 0.11	1.00 ± 0.00	0.82 ± 0.03	1.00 ± 0.00
25	9.89 ± 1.70	5.30 ± 0.91	56.54 ± 1.71	7.15 ± 0.22	15.61 ± 0.30	4.82 ± 0.09	10.59 ± 0.57	6.91 ± 0.37
50	13.20 ± 0.93	7.08 ± 0.50	80.58 ± 0.02	10.19 ± 0.00	38.61 ± 0.22	11.93 ± 0.07	41.10 ± 0.84	26.82 ± 0.55
75	31.50 ± 1.41	16.89 ± 0.76	178.22 ± 40.0	22.54 ± 5.10	63.86 ± 1.39	19.73 ± 0.43	84.54 ± 1.42	55.16 ± 0.92
95	60.47 ± 0.62	32.42 ± 0.33	121.14 ± 10.95	15.32 ± 1.38	85.32 ± 0.73	26.36 ± 0.23	114.97 ± 4.88	75.02 ± 3.19
100	57.23 ± 1.33	30.69 ± 0.71	107.98 ± 6.00	13.65 ± 0.76	95.77 ± 0.19	29.59 ± 0.06	130.89 ± 1.20	85.41 ± 0.78
	PA:U (2:1)							
0	1.87 ± 0.08	1.00 ± 0.00	7.91 ± 0.76	1.00 ± 0.00	3.24 ± 0.11	1.00 ± 0.00	1.53 ± 0.05	1.00 ± 0.00
25	16.94 ± 1.66	9.08 ± 0.89	86.40 ± 3.11	10.93 ± 0.39	20.31 ± 1.57	6.27 ± 0.48	17.60 ± 1.20	11.48 ± 0.79
50	58.02 ± 1.83	36.52 ± 0.59	91.29 ± 2.25	11.54 ± 0.28	51.64 ± 1.99	15.96 ± 0.61	68.99 ± 0.35	45.02 ± 0.23
75	88.37 ± 3.55	47.38 ± 1.90	189.63 ± 2.93	23.98 ± 0.37	52.14 ± 2.20	16.11 ± 0.68	43.50 ± 1.35	28.38 ± 0.88

95	15.86 ± 0.32	8.51 ± 0.17	81.72 ±0.08	10.33 ± 0.01	35.98 ± 1.55	11.12 ± 0.48	13.69 ± 0.93	8.93 ± 0.61
100	11.27 ± 3.11	6.03 ± 1.67	6.95 ± 1.01	0.88 ± 0.13	19.05 ± 0.48	5.89 ± 0.15	8.18 ± 0.00	5.34 ± 0.00
				PTSA:[Ch]Cl (1:1)				
0	1.87 ± 0.08	1.00 ± 0.00	7.91 ± 0.76	1.00 ± 0.00	3.24 ± 0.11	1.00 ± 0.00	0.82 ± 0.03	1.00 ± 0.00
25	8.05 ± 1.10	4.32 ± 0.59	29.93 ± 3.92	3.78 ± 0.50	11.84 ± 0.48	3.66 ± 0.15	4.50 ± 0.52	2.94 ± 0.34
50	13.07 ± 1.18	7.01 ± 0.63	53.62 ± 3.54	6.78 ± 0.45	16.13 ± 0.04	4.98 ± 0.01	7.35 ± 0.11	4.80 ± 0.07
75	15.82 ± 1.6	8.48 ± 0.89	64.09 ± 4.47	8.10 ± 0.57	19.49 ± 1.11	6.02 ± 0.34	18.82 ± 1.09	12.28 ± 0.71
95	24.93 ± 1.06	13.37 ± 0.57	63.60 ± 0.00	8.04 ± 0.00	34.72 ± 4.85	10.73 ± 1.50	17.88 ± 0.94	11.66 ± 0.61
100	33.80 ± 1.50	18.12 ± 0.80	78.99 ± 0.00	9.99 ± 0.00	45.19 ± 0.00	13.96 ± 0.00	16.75 ± 0.19	10.93 ± 0.12
				EG:[Ch]Cl (2:1)				
0	1.87 ± 0.08	1.00 ± 0.00	7.91 ± 0.76	1.00 ± 0.00	3.24 ± 0.11	1.00 ± 0.00	1.53 ± 0.05	1.00 ± 0.00
25	3.78 ± 0.11	2.03 ± 0.06	14.05 ± 0.88	1.78 ± 0.11	7.17 ± 0.30	2.21 ± 0.09	3.64 ± 0.26	2.38 ± 0.17
50	7.37 ± 0.15	3.95 ± 0.08	17.74 ± 0.64	2.24 ± 0.08	14.47 ± 1.31	4.47 ± 0.41	9.55 ± 0.52	6.23 ± 0.34
75	15.71 ± 0.18	8.43 ± 0.10	31.37 ± 0.83	3.97 ± 0.11	35.99 ± 0.71	11.12 ± 0.22	31.18 ± 0.05	20.34 ± 0.03
95	34.49 ± 0.17	18.49 ± 0.09	51.95 ± 1.46	6.57 ± 0.18	78.69 ± 1.25	24.32 ± 0.39	94.81 ± 5.94	61.86 ± 3.88
100	52.81 ± 3.75	28.31 ± 2.01	93.28 ± 4.68	11.80 ± 0.59	86.61 ± 2.89	26.76 ± 0.89	125.70 ± 3.19	82.02 ± 2.08
				EG:[P_{4444}]Cl (2:1)				
0	1.87 ± 0.08	1.00 ± 0.00	7.91 ± 0.76	1.00 ± 0.00	3.24 ± 0.11	1.00 ± 0.00	0.82 ± 0.03	1.00 ± 0.00
25	39.98 ± 0.09	26.09 ± 0.06	113.37 ± 9.14	14.34 ± 1.16	57.85 ± 8.62	17.87 ± 2.66	192.71 ± 4.72	125.74 ± 3.08
50	115.39 ± 0.66	75.29 ± 0.43	200.07 ± 32.51	25.30 ± 4.11	116.85 ± 3.36	36.11 ± 1.04	310.32 ± 25.82	202.48 ± 16.85
75	178.74 ± 2.51	116.63 ± 1.64	275.84 ± 53.11	34.88 ± 6.72	189.77 ± 1.47	58.64 ± 0.45	287.35 ± 2.37	187.50 ± 1.54
95	166.98 ± 0.00	94.31 ± 0.00	264.46 ± 58.55	33.44 ± 7.40	192.07 ± 8.19	59.35 ± 2.53	211.30 ± 22.60	137.87 ± 14.75
100	165.27 ± 6.79	88.62 ± 3.64	218.79 ± 31.67	27.67 ± 4.00	195.97 ± 6.60	60.55 ± 2.04	*	*
				U:[Ch]Cl (2:1)				
0	1.87 ± 0.08	1.00 ± 0.00	7.91 ± 0.76	1.00 ± 0.00	3.24 ± 0.11	1.00 ± 0.00	0.82 ± 0.03	1.00 ± 0.00
25	11.77 ± 0.46	6.31 ± 0.25	19.52 ± 1.68	2.47 ± 0.21	11.21 ± 0.77	3.46 ± 0.24	15.76 ± 0.95	10.28 ± 0.62
50	19.52 ± 1.81	10.47 ± 0.97	27.31 ± 4.52	3.45 ± 0.57	18.23 ± 0.67	5.63 ± 0.21	14.13 ± 0.65	13.69 ± 1.42
75	14.13 ± 0.65	7.58 ± 0.35	5.51 ± 0.89	0.70 ± 0.11	26.28 ± 1.01	8.12 ± 0.31	14.30 ± 1.51	9.33 ± 0.99
95	9.74 ± 0.08	5.22 ± 0.04	4.05 ± 0.18	0.51 ± 0.02	24.30 ± 0.28	7.51 ± 0.09	9.51 ± 0.45	6.20 ± 0.30
100	10.17 ± 0.13	5.45 ± 0.07	1.60 ± 0.47	0.20 ± 0.06	*	*	6.66 ± 1.74	4.34 ± 1.14

σ, standard deviation; S, the solubility of lignin monomer model compounds in the aqueous solutions of ESs; S_0, the solubility of lignin monomer model compounds in pure water; *, the high viscosity of sample hampers the filtration and consequently the analysis.

Table S4.2. Experimental solubilities of lignin monomer model compounds in FA:[Ch]Cl (2:1) aqueous solutions at three different temperatures, obtained from UV-vis spectroscopy.

LMMCs	Syringic acid		Syringaldehyde		Vanillic acid		Ferulic acid	
Temperature / K **wt % of ES**	Solubility ± σ / mg g^{-1}	$S/S_0 \pm \sigma$	Solubility ± σ / mg g^{-1}	$S/S_0 \pm \sigma$	Solubility ± σ / mg g^{-1}	$S/S_0 \pm \sigma$	Solubility ± σ / mg g^{-1}	$S/S_0 \pm \sigma$
				303.15				
0	1.28 ± 0.01	1.00 ± 0.00	2.92 ± 0.01	1.00 ± 0.00	1.83 ± 0.06	1.00 ± 0.00	0.63 ± 0.06	1.00 ± 0.00
25	2.96 ± 0.08	2.31 ± 0.06	8.88 ± 0.12	3.04 ± 0.04	4.35 ± 0.05	2.37 ± 0.03	2.18 ± 0.10	3.47 ± 0.17
50	5.54 ± 0.18	4.32 ± 0.14	19.09 ± 1.43	6.54 ± 0.49	13.08 ± 1.77	7.14 ± 0.97	5.43 ± 0.54	8.62 ± 0.86
75	9.25 ± 0.48	7.22 ± 0.38	33.83 ± 2.58	11.58 ± 0.88	16.49 ± 0.11	9.00 ± 0.06	16.28 ± 1.67	25.87 ± 2.65
100	19.37 ± 0.25	15.11 ± 0.20	49.07 ± 0.59	16.81 ± 0.20	42.04 ± 2.34	22.93 ± 1.27	42.40 ± 0.68	67.37 ± 1.08
				313.15				
0	1.60 ± 0.03	1.00 ± 0.00	4.41 ± 0.10	1.00 ± 0.00	2.93 ± 0.06	1.00 ± 0.00	0.82 ± 0.03	1.00 ± 0.00
25	4.51 ± 0.09	2.82 ± 0.06	8.42 ± 0.17	1.91 ± 0.04	6.88 ± 1.05	2.35 ± 0.36	2.83 ± 0.06	3.45 ± 0.07
50	8.87 ± 0.46	5.55 ± 0.29	16.96 ± 0.07	3.85 ± 0.02	11.94 ± 0.34	4.08 ± 0.11	9.82 ± 0.06	11.98 ± 0.08
75	14.72 ± 0.03	9.21 ± 0.02	28.08 v 0.08	6.37 ± 0.02	21.80 ± 0.49	7.45 ± 0.17	19.56 ± 1.13	23.85 ± 1.38
100	26.21 ± 0.80	16.39 ± 0.50	42.01 ± 0.28	9.53 ± 0.06	33.94 ± 0.60	11.60 ± 0.20	77.60 ± 2.06	94.64 ± 2.51
				323.15				
0	1.87 ± 0.08	1.00 ± 0.00	7.91 ± 0.76	1.00 ± 0.00	3.24 ± 0.11	1.00 ± 0.00	1.53 ± 0.05	1.00 ± 0.00
25	6.13 ± 0.68	3.28 ± 0.36	18.36 ± 0.98	2.32 ± 0.12	8.95 ± 0.36	2.77 ± 0.11	5.25 ± 0.39	3.43 ± 0.25
50	10.85 ± 0.41	5.82 ± 0.22	34.46 ± 1.22	4.36 ± 0.15	15.91 ± 0.32	4.92 ± 0.10	15.10 ± 0.22	9.87 ± 0.15
75	17.24 ± 0.12	9.24 ± 0.06	57.30 ± 3.14	7.25 ± 0.40	28.72 ± 0.32	8.88 ± 0.10	30.54 ± 0.22	19.96 ± 0.15
100	27.22 ± 0.50	14.59 ± 0.27	85.33 ± 0.38	10.79 ± 0.05	51.77 ± 1.56	16.00 ± 0.48	73.97 ± 0.55	48.35 ± 0.36

σ, standard deviation; S, the solubility of lignin monomer model compounds in the aqueous solutions of ES; S_0, the solubility of lignin monomer model compounds in pure water.

Table S4.3. Experimental solubilities of lignin monomer model compounds in EG:[Ch]Cl (2:1) aqueous solutions at three different temperatures, obtained from UV-vis spectroscopy.

LMMCs	Syringic acid		Syringaldehyde		Vanillic acid		Ferulic acid	
	Solubility ± σ / mg g^{-1}	$S/S_0 \pm \sigma$	Solubility ± σ / mg g^{-1}	$S/S_0 \pm \sigma$	Solubility ± σ / mg g^{-1}	$S/S_0 \pm \sigma$	Solubility ± σ / mg g^{-1}	$S/S_0 \pm \sigma$
Temperature / K	***303.15***							
wt % of ES								
0	1.28 ± 0.01	1.00 ± 0.00	2.92 ± 0.01	1.00 ± 0.00	1.83 ± 0.06	1.00 ± 0.00	0.63 ± 0.06	1.00 ± 0.00
25	2.25 ± 0.12	1.76 ± 0.09	5.12 ± 0.42	1.75 ± 0.14	3.44 ± 0.12	1.88 ± 0.07	1.68 ± 0.02	2.67 ± 0.03
50	4.43 ± 0.11	3.46 ± 0.09	7.24 ± 0.42	2.48 ± 0.14	6.82 ± 0.20	3.72 ± 0.11	6.11 ± 0.13	9.71 ± 0.21
75	10.35 ± 0.04	8.07 ± 0.03	13.06 ± 0.18	4.47 ± 0.06	19.04 ± 0.02	10.39 ± 0.01	9.56 ± 0.30	15.20 ± 0.48
100	38.11 ± 0.43	29.73 ± 0.34	53.94 ± 0.76	18.47 ± 0.26	83.71 ± 2.43	45.66 ± 1.32	98.09 ± 2.96	155.85 ± 4.70
	313.15							
0	1.60 ± 0.03	1.00 ± 0.00	4.41 ± 0.10	1.00 ± 0.00	2.93 ± 0.06	1.00 ± 0.00	0.82 ± 0.03	1.00 ± 0.00
25	3.12 ± 0.22	1.95 ± 0.14	8.16 ± 0.08	1.85 ± 0.02	3.17 ± 0.39	1.08 ± 0.13	2.58 ± 0.24	3.13 ± 0.30
50	5.08 ± 0.01	3.18 ± 0.01	12.72 ± 0.82	2.89 ± 0.19	20.81 ± 0.06	7.11 ± 0.02	5.78 ± 0.14	7.01 ± 0.16
75	14.81 ± 1.19	9.26 ± 0.74	20.58 ± 1.09	4.67 ± 0.25	26.09 ± 0.41	8.92 ± 0.14	23.26 ± 0.40	28.22 ± 0.48
100	55.54 ± 1.03	34.74 ± 0.65	69.68 ± 1.53	15.81 ± 0.35	92.52 ± 0.69	31.62 ± 0.24	109.28 ± 1.60	132.54 ± 1.93
	323.15							
0	1.87 ± 0.08	1.00 ± 0.00	7.91 ± 0.76	1.00 ± 0.00	3.24 ± 0.11	1.00 ± 0.00	1.53 ± 0.05	1.00 ± 0.00
25	3.78 ± 0.11	2.03 ± 0.06	14.05 ± 0.88	1.78 ± 0.11	7.17 ± 0.30	2.21 ± 0.09	3.64 ± 0.26	2.38 ± 0.17
50	7.37 ± 0.15	3.95 ± 0.08	17.74 ± 0.64	2.24 ± 0.08	14.47 ± 1.31	4.47 ± 0.41	9.55 ± 0.52	6.23 ± 0.34
75	15.71 ± 0.18	8.43 ± 0.10	31.37 ± 0.83	3.97 ± 0.11	35.99 ± 0.71	11.12 ± 0.22	31.18 ± 0.05	20.34 ± 0.03
100	52.81 ± 3.75	28.31 ± 2.01	93.28 ± 4.68	11.80 ± 0.59	86.61 ± 2.89	26.76 ± 0.89	125.70 ± 3.19	82.02 ± 2.08

σ, standard deviation; S, the solubility of lignin monomer model compounds in the aqueous solutions of ES; S_0, the solubility of lignin monomer model compounds in pure water.

Table S4.4. Experimental solubilities of technical lignins in different neat ES at 353.15 K, obtained from FTIR spectroscopy at 1510 cm^{-1}.

Technical lignins	kraft lignin	organosolv lignin
	Solubility ± σ / % w_{Lignin} w_{ES}^{-1}	Solubility ± σ / % w_{Lignin} w_{ES}^{-1}
ES		
FA:[Ch]Cl (2:1)	8.10 ± 1.28	37.81 ± 0.88
LA:[Ch]Cl (10:1)	8.59 ± 0.51	*
PA:[Ch]Cl (2:1)	6.00 ± 0.00	28.68 ± 2.96
PA:U (2:1)	23.86 ± 1.03	31.04 ± 0.85
BA:U (2:1)	4.21 ± 0.44	13.27 ± 0.13
PPA:[Ch]Cl (2:1)	7.47 ± 0.51	15.07 ± 1.99
PTSA:[Ch]Cl (1:1)	7.46 ± 0.51	*
EG:[Ch]Cl (2:1)	12.56 ± 0.76	25.74 ± 3.33
G:[Ch]Cl (2:1)	9.54 ± 0.79	5.13 ± 1.16
EG:[N_{1111}]Cl (2:1)	12.96 ± 0.21	18.07 ± 2.30
EG:[N_{2222}]Cl (2:1)	16.54 ± 0.66	31.07 ± 0.45
EG:[N_{3333}]Cl (2:1)	19.80 ± 1.96	20.61 ± 0.89
EG:[N_{4444}]Cl (2:1)	14.12 ± 2.62	28.10 ± 0.40
EG:[P_{4444}]Cl (2:1)	23.40 ± 0.37	28.93 ± 0.61
U:[Ch]Cl (2:1)	7.01 ± 1.26	1.18 ± 0.23

σ, standard deviation; *, insufficient organosolv lignin to make the solubility test.

Table S4.5. Experimental solubilities of technical lignins in different ESs aqueous solutions at 353.15 K, obtained from FTIR spectroscopy at 1510 cm^{-1}.

Technical lignins	kraft lignin		organosolv lignin	
	Solubility ± σ / % w_{Lignin} w_{ES}^{-1}	S/S_0 ± σ	Solubility ± σ / % w_{Lignin} w_{ES}^{-1}	S/S_0 ± σ
ESs	***FA:[Ch]Cl (2:1)***			
wt % of ESs				
0	0.12 ± 0.01	1.00 ± 0.00	0.10 ± 0.00[a]	1.00 ± 0.00[a]
25	2.20 ± 0.93	18.12 ± 7.70	*	*
50	4.82 ± 0.54	39.72 ± 4.47	1.52 ± 0.34[a]	14.71 ± 3.29[a]
75	6.89 ± 1.85	56.79 ± 15.25	6.68 ± 1.32[a]	64.64 ± 12.74[a]
100	8.10 ± 1.28	66.70 ± 10.52	19.72 ± 2.38[a]	190.80 ± 23.05[a]
	LA:[Ch]Cl (10:1)			
0	0.12 ± 0.01	1.00 ± 0.00	0.15 ± 0.02	1.00 ± 0.00

25	0.61 ± 0.19	4.98 ± 1.92	*	*
50	1.07 ± 0.03	8.84 ± 0.28	*	*
75	3.47 ± 0.96	28.54 ± 7.89	*	*
100	8.59 ± 0.51	70.76 ± 4.23	*	*
	PA:[Ch]Cl (2:1)			
0	0.12 ± 0.01	1.00 ± 0.00	0.15 ± 0.02	1.00 ± 0.00
25	1.13 ± 0.39	9.30 ± 3.23	*	*
50	8.41 ± 0.74	72.98 ± 6.42	*	*
75	12.19 ± 0.39	100.42 ± 3.19	*	*
100	6.00 ± 0.00	49.41 ± 0.04	28.68 ± 2.96	192.51 ± 19.86
	PA:U (2:1)			
0	0.12 ± 0.01	1.00 ± 0.00	0.10 ± 0.00[a]	1.00 ± 0.00[a]
25	2.25 ± 0.68	18.50 ± 5.59	2.24 ± 0.28[a]	21.69 ± 2.74[a]
50	27.73 ± 1.00	228.28 ± 8.24	15.06 ± 2.34[a]	145.70 ± 22.66[a]
75	20.37 ± 1.00	167.71 ± 8.26	49.06 ± 0.28[a]	474.74 ± 2.69[a]
100	+	+	+	+
	BA:U (2:1)			
0	0.12 ± 0.01	1.00 ± 0.00	0.15 ± 0.02	1.00 ± 0.00
25	5.41 ± 0.76	44.54 ± 6.27	9.36 ± 0.15	62.79 ± 0.98
50	20.97 ± 3.37	172.65 ± 27.72	15.71 ± 0.52	105.47 ± 3.47
75	15.09 ± 0.31	124.22 ± 2.57	11.52 ± 1.16	77.30 ± 7.79
100	4.21 ± 0.44	34.69 ± 3.62	13.27 ± 0.13	89.05 ± 0.86
	PTSA:[Ch]Cl (1:1)			
0	0.12 ± 0.01	1.00 ± 0.00	0.15 ± 0.02	1.00 ± 0.00
25	1.58 ± 0.33	13.08 ± 2.71	*	*
50	3.72 ± 0.87	30.63 ± 7.18	*	*
75	4.13 ± 0.38	33.99 ± 3.15	*	*
100	10.64 ± 1.98	87.59 ± 16.30	*	*
	EG:[Ch]Cl (2:1)			
0	0.12 ± 0.01	1.00 ± 0.00	0.15 ± 0.02	1.00 ± 0.00
25	1.12 ± 0.18	9.19 ± 1.47	1.91± 0.70	12.82 ± 4.72
50	1.60 ± 0.50	13.16 ± 4.14	1.23 ± 0.13	8.27 ± 0.86
75	7.51 ± 0.69	61.82 ± 5.71	4.63 ± 0.24	31.07 ± 1.61

100	12.56 ± 0.76	103.38 ± 6.30	25.75 ± 3.33	172.78 ± 22.36
	EG:[N$_{3333}$]Cl (2:1)			
0	0.12 ± 0.01	1.00 ± 0.00	0.15 ± 0.02	1.00 ± 0.00
25	2.86 ± 0.66	23.52 ± 5.47	2.40 ± 0.68	16.08 ± 5.40
50	6.60 ± 1.32	54.37 ± 10.89	13.42 ± 2.82	90.04 ± 10.55
75	9.87 ± 0.67	81.26 ± 5.49	12.41 ± 1.08	83.32 ± 24.35
100	19.80 ± 1.96	163.03 ± 16.12	20.61 ± 1.03	138.32 ± 5.98
	EG:[P$_{4444}$]Cl (2:1)			
0	0.12 ± 0.01	1.00 ± 0.00	0.15 ± 0.02	1.00 ± 0.00
25	1.39 ± 0.22	11.50 ± 1.82	2.39 ± 0.81	16.08 ± 5.40
50	12.68 ± 0.19	104.41 ± 1.58	8.83 ± 1.60	59.26 ± 10.73
75	15.48 ± 0.10	127.10 ± 1.02	15.13 ± 3.33	101.54 ± 22.34
100	13.77 ± 0.20	113.40 ± 1.00	28.93 ± 0.61	194.17 ± 4.12
	U:[Ch]Cl (2:1)			
0	0.12 ± 0.01	1.00 ± 0.00	0.15 ± 0.02	1.00 ± 0.00
25	1.62 ± 0.73	14.06 ± 6.36	*	*
50	5.66 ± 0.55	46.64 ± 4.54	*	*
75	10.92 ± 0.12	89.87 ± 0.99	*	*
100	7.02 ± 1.26	57.76 ± 10.40	1.18 ± 0.23	7.94 ± 1.53

σ, standard deviation; S, the solubility of technical lignins in the aqueous solutions of ESs; S_0, the solubility of technical lignins in pure water; *, insufficient organosolv lignin to make the solubility test; [a], data obtained at 323.15 K; [+], the high viscosity of sample hampers the filtration and consequently the analysis.

Table S4.6. Experimental solubilities of organosolv lignin in FA:[Ch]Cl (2:1), EG:[Ch]Cl (2:1) and PA:U (2:1) aqueous solutions at three different temperatures, obtained from FTIR spectroscopy at 1510 cm^{-1}.

ES	FA:[Ch]Cl (2:1)		EG:[Ch]Cl (2:1)		PA:U (2:1)	
	Solubility ± σ / % $w_{Lignin}\, w_{ES}^{-1}$	$S/S_0 \pm \sigma$	Solubility ± σ / % $w_{Lignin}\, w_{ES}^{-1}$	$S/S_0 \pm \sigma$	Solubility ± σ / % $w_{Lignin}\, w_{ES}^{-1}$	$S/S_0 \pm \sigma$
Temperature / K			***313.15***			
wt % of ES						
0	0.09 ± 0.00	1.00 ± 0.00	0.09 ± 0.00	1.00 ± 0.00	0.09 ± 0.00	1.00 ± 0.00
25	*	*	*	*	3.06 ± 0.60	35.20 ± 6.80
50	1.56 ± 0.39	18.00 ± 4.50	1.49 ± 0.08	17.21 ± 0.97	19.20 ± 1.33	230.29 ± 15.34
75	1.85 ± 0.63	21.29 ± 7.30	1.60 ± 0.15	17.33 ± 1.76	31.64 ± 3.09	364.41 ± 35.62
100	18.13 ± 2.43	208.80 ± 28.01	15.16 ± 3.57	174.66 ± 41.09	22.94 ± 1.10	264.14 ± 12.73
			323.15			
0	0.10 ± 0.00	1.00 ± 0.00	0.10 ± 0.00	1.00 ± 0.00	0.10 ± 0.00	1.00 ± 0.00
25	*	*	*	*	2.24 ± 0.28	21.69 ± 2.74
50	1.52 ± 0.34	14.71 ± 3.29	3.12 ± 0.41	30.17 ± 4.01	15.06 ± 2.34	145.70 ± 22.66
75	6.68 ± 1.32	64.65 ± 12.74	3.34 ± 0.19	32.35 ± 1.81	49.06 ± 0.28	474.74 ± 2.69
100	19.72 ± 2.38	190.80 ± 23.05	17.60 ± 1.65	170.29 ± 15.98	29.67 ± 3.41	287.11 ± 32.96
			353.15			
0	0.15 ± 0.02	1.00 ± 0.00	0.15 ± 0.02	1.00 ± 0.00	0.15 ± 0.02	1.00 ± 0.00
50	*	*	1.23 ± 0.13	8.27 ± 0.86	*	*
75	*	*	4.63 ± 0.24	31.07 ± 1.61	*	*
100	37.81 ± 0.88	253.77 ± 5.91	25.75 ± 3.33	172.78 ± 22.36	31.04 ± 0.85	206.95 ± 5.68

σ, standard deviation; S, the solubility of organosolv lignin in the aqueous solutions of ESs; S_0, the solubility of organosolv lignin in pure water; *, insufficient organosolv lignin to make the solubility test.

Table S4.7 Experimental solubilities of kraft lignin in PA:U (2:1) aqueous solutions at three different temperatures, obtained from FTIR spectroscopy at 1510 cm^{-1}.

ES	PA:U (2:1)	
	Solubility ± σ / % $w_{Lignin}\, w_{ES}^{-1}$	$S/S_0 \pm \sigma$
Temperature / K	***313.15***	
wt % of ES		
0	0.06 ± 0.00	1.00 ± 0.00
25	1.64 ± 0.01	25.95 ± 0.22
50	20.30 ± 0.77	321.66 ± 12.23
75	12.52 ± 2.20	198.43 ± 34.91
100	7.90 ± 2.10	125.28 ± 33.97
	323.15	
0	0.08 ± 0.00	1.00 ± 0.00
25	1.68 ± 0.65	21.83 ± 8.44
50	17.53 ± 0.96	227.74 ± 12.50
75	3.88 ± 0.1	50.34 ± 1.30
100	1.67 ± 0.43	21.63 ± 5.58
	353.15	
0	0.12 ± 0.00	1.00 ± 0.00
25	2.25 ± 0.68	18.50 ± 5.60
50	27.73 ± 1.00	228.28 ± 8.24
75	20.37 ± 1.00	167.71 ± 8.26
100	23.86 ± 1.03	196.40 ± 8.51

σ, standard deviation; S, the solubility of kraft lignin in the aqueous solutions of PA:U (2:1); S_0, the solubility of kraft lignin in pure water.

Table S4.8. Mole-fraction solubilities of LMMCs (x_{LMMCs}) in ESs at different temperatures.

ESs	$x_{Syringic\ acid}$	$x_{Syringaldehyde}$	$x_{Vanillic\ acid}$	$x_{Ferulic\ acid}$
FA:[Ch]Cl (2:1)				
Temperature / K		303.15		
ES concentration / wt %				
0	1.16E-04	2.88E-04	1.96E-04	5.83E-05
25	3.32E-04	1.08E-03	5.76E-04	2.50E-04
50	8.15E-04	3.05E-03	2.26E-03	8.16E-04
75	1.98E-03	7.81E-03	4.14E-03	3.53E-03
		313.15		
0	1.45E-04	4.35E-04	2.13E-04	7.60E-05
25	5.06E-04	1.03E-03	9.10E-04	3.24E-04
50	1.30E-03	2.71E-03	2.07E-03	1.47E-03
75	3.13E-03	6.50E-03	5.46E-03	4.25E-03
		323.15		
0	1.69E-04	7.81E-04	3.46E-04	1.42E-04
25	6.88E-04	2.23E-03	1.18E-03	6.02E-04
50	1.60E-03	5.49E-03	2.75E-03	2.27E-03
75	3.67E-03	1.31E-02	7.18E-03	6.62E-03
EG:[Ch]Cl (2:1)				
Temperature / K		303.15		
ES concentration / wt %				
0	1.16E-04	2.88E-04	1.96E-04	5.83E-05
25	2.55E-04	6.31E-04	4.59E-04	1.94E-04
50	6.67E-04	1.19E-03	1.21E-03	9.39E-04
75	2.32E-03	3.19E-03	5.02E-03	2.19E-03
		313.15		
0	1.45E-04	4.35E-04	3.13E-04	7.60E-05
25	3.53E-04	1.00E-03	4.23E-04	2.98E-04
50	7.65E-04	2.08E-03	3.68E-03	8.89E-04
75	3.32E-03	5.01E-03	6.87E-03	5.31E-03
		323.15		
0	1.70E-04	7.81E-04	3.47E-04	1.42E-04
25	4.28E-04	1.72E-03	9.57E-04	4.21E-04
50	1.11E-03	2.90E-03	2.56E-03	1.47E-03

75	3.52E-03	7.62E-03	6.85E-03	7.11E-03
PA:U (2:1)				
Temperature / K		303.15		
ES concentration / wt %				
0	1.16E-04	2.88E-04	1.96E-04	5.83E-05
25	1.35E-03	3.14E-03	1.48E-03	7.85E-04
50	5.39E-03	1.61E-02	3.99E-03	3.09E-03
75	6.71E-03	2.30E-02	5.75E-03	2.88E-03
95	3.11E-03	9.00E-03	6.60E-03	2.47E-03
		313.15		
0	1.45E-04	4.34E-04	3.13E-04	7.60E-05
25	1.80E-03	6.84E-03	1.99E-03	1.02E-03
50	6.16E-03	2.55E-02	5.77E-03	6.16E-03
75	1.00E-02	3.94E-02	7.42E-03	5.62E-03
95	3.86E-03	1.13E-02	5.79E-03	2.12E-03
		323.15		
0	1.69E-04	7.81E-04	3.47E-04	1.42E-04
25	1.88E-03	1.04E-02	2.66E-03	1.99E-03
50	8.30E-03	1.41E-02	8.70E-03	1.00E-02
75	1.77E-02	4.04E-02	1.24E-02	8.99E-03
95	4.63E-03	2.14E-02	1.15E-02	4.10E-03

Table S4.9. Values of the Fitting Parameters obtained from equation (4) based on the experimental mole-fraction solubility of LMMCs in ESs.

	A	B / K	$\Delta_{Sol}G_m$ (303.15 K) / kJ mol^{-1}	$\Delta_{Sol}H_m$ (303.15 K) / kJ mol^{-1}	$\Delta_{Sol}S_m$ (303.15 K) / J K^{-1} mol^{-1}	ζ_H / %	ζ_{TS} / %
Syringic acid							
ES concentration / wt %							
FA:[Ch]Cl (2:1)							
0	-2.92	-1859.39	22.84	15.46	-24.33	67.70	32.30
25	2.32	-3103.79	20.19	25.81	18.54	82.12	17.88
50	3.74	-3288.56	17.92	27.34	31.06	74.38	25.62
75	3.9	-3056.20	15.70	25.41	32.04	72.35	27.65

EG:[Ch]Cl (2:1)							
0	-2.92	-1859.39	22.84	15.46	-24.33	67.70	32.30
25	0.14	-2546.45	20.85	21.17	1.05	98.52	1.48
50	0.82	-2477.98	18.43	20.60	7.17	90.46	9.54
75	0.75	-2053.02	15.29	17.07	5.89	90.54	9.46
PA:U (2:1)							
0	-2.92	-1859.39	22.84	15.46	-24.33	67.70	32.30
25	-1.18	-1633.19	16.65	13.58	-10.12	81.57	18.43
50	1.68	-2102.40	13.16	17.48	14.24	80.20	19.80
75	7.62	-3826.81	12.61	31.82	63.35	62.36	37.64
95	1.03	-2061.70	14.55	17.14	8.55	86.87	13.13
Syringaldehyde							
FA:[Ch]Cl (2:1)							
0	7.87	-4868.19	20.54	40.48	65.75	67.01	32.99
25	4.61	-3507.67	17.21	29.16	39.44	70.92	29.08
50	3.71	-2881.00	14.60	23.95	30.85	71.92	28.08
75	3.27	-2507.30	12.23	20.85	28.42	70.76	29.24
EG:[Ch]Cl (2:1)							
0	7.87	-4868.19	20.54	40.48	65.75	67.01	32.99
25	8.89	-4933.45	18.57	41.02	74.05	64.63	35.37
50	10.88	-5341.38	16.98	44.41	90.48	61.82	38.18
75	8.34	-4270.72	14.49	35.51	69.34	62.82	37.18
PA:U (2:1)							
0	7.87	-4868.19	20.54	40.48	65.75	67.01	32.99
25	8.47	-4213.91	14.53	35.04	67.65	63.08	36.92
50	10.42	-4411.57	10.41	36.68	86.65	58.27	41.73
75	5.33	-2760.33	9.51	22.95	44.35	63.06	36.94
95	2.32	-2131.20	11.87	17.72	19.29	75.18	24.82
Vanillic acid							
FA:[Ch]Cl (2:1)							
0	0.81	-2815.70	21.52	23.41	6.24	92.53	7.47
25	1.49	-2658.99	18.80	22.11	10.90	86.99	13.01
50	-3.06	-2897.90	15.35	24.09	28.85	73.37	26.63
75	3.42	-2701.96	13.83	22.46	28.48	72.24	27.76
EG:[Ch]Cl (2:1)							

0	0.81	-2815.70	21.52	23.41	6.24	92.53	7.47
25	4.17	-3594.93	19.37	29.89	34.70	73.97	26.03
50	5.42	-3677.83	16.93	30.58	45.02	69.14	30.86
75	4.51	-2972.79	13.34	24.72	37.52	68.48	31.52
PA:U (2:1)							
0	0.81	-2815.70	21.52	23.41	6.24	92.53	7.47
25	2.92	-2862.12	16.42	23.80	24.34	76.33	23.67
50	7.06	-3817.18	13.92	31.74	58.76	64.05	35.95
75	7.15	-3744.52	13.00	31.13	59.82	63.19	36.81
95	3.65	-2670.40	12.65	22.20	31.51	69.92	30.08
Ferulic acid							
FA:[Ch]Cl (2:1)							
0	4.46	-4325.49	24.57	35.96	37.58	75.94	24.06
25	5.77	-4283.21	20.91	35.61	48.51	70.77	29.23
50	7.36	-4346.10	17.92	36.13	60.07	66.49	33.51
75	4.38	-3051.65	14.22	25.37	36.77	69.48	30.52
EG:[Ch]Cl (2:1)							
0	4.46	-4325.49	24.57	35.96	37.58	75.94	24.06
25	3.96	-3789.22	21.54	31.50	32.87	75.97	24.03
50	9.18	-5075.49	15.43	24.50	29.92	72.99	27.01
75	4.17	-2947.12	7.96	11.18	10.64	77.62	22.38
PA:U (2:1)							
0	4.46	-4325.49	24.57	35.96	37.58	75.94	24.06
25	7.79	-4550.70	18.02	37.84	65.37	65.63	34.37
50	10.74	-4958.40	14.56	41.23	87.95	60.73	39.27
75	10.00	-4754.44	14.74	39.53	81.76	61.46	38.54
95	1.91	-2440.70	15.13	20.29	17.03	79.72	20.28

S5. Experimental data – Chapter III

Table S5.1. *E. globulus* wood delignification with ESs aqueous solution at 363.15 K, 8 h and atmospheric pressure.

Yields / wt %	pH value ± σ	Solid fraction ± σ	Precipitated lignin ± σ
PA:U (2:1) aqueous solution at 50 wt %	2.45 ± 0.10	93.99 ± 0.56	1.74 ± 0.33
LA:[Ch]Cl (10:1) aqueous solution at 50 wt %	1.00 ± 0.04	72.35 ± 0.89	2.62 ± 0.09
LA:[Ch]Cl (10:1) 100 wt %	-0.42 ± 0.02	62.51 ± 1.37	4.42 ± 0.37
PTSA:[Ch]Cl (1:1) aqueous solution at 50 wt %	-0.20 ± 0.00	46.41 ± 0.88	15.38 ± 0.59
U:[Ch]Cl (2:1) aqueous solution at 50 wt %	7.30 ± 0.07	94.77 ± 1.37	3.04 ± 0.05

σ, standard deviation.

Table S5.2. Absorption bands assignment in normalized FTIR spectra of solid fraction-PTSA:[Ch]Cl and kraft pulp.

Kraft pulp / cm^{-1}	PTSA:[Ch]Cl (1:1) / cm^{-1}	Assignment[117–119]
3290	3310	O-H stretching vibration, -OH groups
2928	2902	C-H stretching vibration in methyl and methylene groups
2864	2882	C-H stretching vibration in methyl and methylene groups
1608	1608	vibration of water molecules absorbed in cellulose
1590	ND	aromatic skeletal vibration on lignin
ND	1508	aromatic skeletal vibration on lignin
1412	1418	stretching and bending vibrations of -CH_2 and -CH and -OH bonds in cellulose
1380	1376	stretching and bending vibrations of -CH_2 and -CH and -OH bonds in cellulose
1326	1310	stretching and bending vibrations of -CH_2 and -CH and -OH bonds in cellulose
1184	1172	C-O stretching vibration
1166	1164	C-O stretching vibration
1108	1076	C-O stretching vibration
1056	1014	C-O stretching vibration
1024	1032	C-O stretching vibration
890	890	C-H deformation mode of the glycosidic linkage between the glucose units

ND, not detected.

Table S5.3. Absorption bands assignment in normalized FTIR spectra of lignin-PTSA:[Ch]Cl and technical lignins (kraft and dioxane).

Dioxane / cm^{-1}	Kraft / cm^{-1}	PTSA:[Ch]Cl (1:1) / cm^{-1}	Assignment[110,112,114,120]
3474	3474	3340	O-H stretching vibration, hydroxyl groups in phenolic and aliphatic structures
2932	2932	2926	C-H stretching in methyl, methylene and methoxyl groups -OCH_3
2856	2832	2864	C-H stretching in methoxyl groups -OCH_3
ND	1721	1714	C=O stretching vibration in unconjugated carbonyl/carboxyl group, can be related with the presence of carbohydrate contaminants.
1596	1606	1609	aryl ring stretching, symmetric
1508	1508	1497	aryl ring stretching, asymmetric
1454	1456	1445	C-H bending in O-CH_3 groups, asymmetric
1420	1426	1430	aromatic skeletal vibration coombined with C-H bending in O-CH_3 groups, asymmetric in-plane
1332	1314	1302	syringyl rings breathing with Ar-OCH_3 stretching
1278	1279	1265	guaiacyl rings breathing with Ar-OCH_3 stretching
1212	1210	1206	C-C plus C-O plus C=O stretching
1140	1156	1136	aromatic C-H in-plane deformation guaiacyl-type
1112	1105	1114	aromatic C-H deformation in the syringyl ring
1016	1040	1016	aromatic C-H in-plane deformation in guaiacyl with C-O deformation in the primary alcohols
920	907	920	C-H deformation out-of-plane, aromatic ring
836	836	818	C-H deformation out-of-plane, aromatic ring
ND	635	ND	C-S stretching vibration

ND, not detected.

Table S5.4. Elemental composition of *E. globulus* lignin-PTSA:[Ch]Cl, lignin-PA:U (2:1)+25PTSA and technical lignins (kraft and dioxane).

Lignin samples	C ± σ / %	H ± σ / %	N ± σ / %	S ± σ / %	O ± σ / %
Dioxane	60.34 ± 0.07	5.80 ± 0.07	0.07 ± 0.03	0.00 ± 0.00	33.78 ± 0.02
Kraft	56.48 ± 0.67	5.49 ± 0.12	-	4.77 ± 0.17	33.26 ± 0.65
PTSA:[Ch]Cl	62.48 ± 0.15	5.02 ± 0.29	0.68 ± 0.06	0.00 ± 0.00	31.83 ± 0.38
PA:U (2:1)+25PTSA	54.19 ± 0.06	5.41 ± 0.11	4.05 ± 0.02	0.00 ± 0.00	36.36 ± 0.03

C-carbon, H-hydrogen, N-nitrogen, S-sulfur and O-oxygen, without correction of carbohydrate contaminants; σ, standard deviation.

Table S5.5. Amount of acid catalyst on ESs aqueous solutions.

Acid catalyst	Initial pH	HCl wt %	H_2SO_4 wt %	PTSA wt %	Final pH
PA:U (2:1)	2.6	11.85	2.39	13.24	0.5
LA:[Ch]Cl (10:1)	1.0	1.18	0.91	0.41	0.5
U:[Ch]Cl (2:1)	8.6	13.69	9.61	13.66	0.5

Table S5.6. Effect of acid catalyst in ESs aqueous solution on *E. globulus* wood delignification with at pH of 0.5, 363.15 K, 8 h and atmospheric pressure.

Yields / wt %	Solid fraction ± σ			Precipitated lignin ± σ		
Acid catalysts (pH value 0.5)	HCl	H_2SO_4	PTSA	HCl	H_2SO_4	PTSA
	Aqueous solution at 50 wt %					
PA:U (2:1)	85.94 ± 3.09	83.33 ± 1.30	79.76 ± 0.26	1.52 ± 0.18	2.94 ± 0.26	5.33 ± 0.12
LA:[Ch]Cl (10:1)	64.75 ± 2.51	66.72 ± 0.23	85.47 ± 2.06	4.67 ± 0.75	4.71 ± 1.21	2.87 ± 0.20
U:[Ch]Cl (2:1)	74.75 ± 1.56	85.36 ± 1.53	89.78 ± 0.13	1.41 ± 0.16	1.36 ± 0.61	2.30 ± 0.26

σ, standard deviation.

Table S5.7. Effect of pH on *E. globulus* wood delignification induced by PTSA content in PA:U (2:1) 50 wt % aqueous solution at 363.15 K, 8 h and atmospheric pressure.

Yields / wt %	pH value ± σ	Solid fraction ± σ	Precipitated lignin ± σ
PTSA content in PA:U (2:1) 50 wt % aqueous solution			
0	2.45 ± 0.10	93.99 ± 0.56	1.74 ± 0.33
13	0.50 ± 0.02	79.76 ± 0.26	5.33 ± 0.12
17	-0.44 ± 0.01	75.68 ± 1.85	4.52 ± 1.27
25	-0.70 ± 0.03	59.50 ± 0.51	6.55 ± 0.50

σ, standard deviation.

Table S5.8. Experimental Box-Behnken design matrix and response results for process variables optimization.

Runs	Temperature / K	Time / h	ES concentration / wt %	Solid fraction / wt %	Precipitated lignin / wt %
1	343.15	4.5	75	95.75	1.17
2	363.15	1	75	97.20	1.10
3	343.15	8	100	96.17	0.40
4	343.15	4.5	75	95.47	0.88
5	343.15	1	50	97.99	0.67
6	343.15	8	50	82.03	2.27
7	343.15	4.5	75	95.97	1.17
8	323.15	4.5	50	96.78	0.58
9	323.15	8	75	92.57	1.13
10	363.15	8	75	87.03	2.91
11	343.15	4.5	75	91.68	1.0
12	323.15	4.5	100	98.28	0.32
13	323.15	1	75	101.23	0.74
14	363.15	4.5	50	68.57	4.25
15	343.15	4.5	75	97.93	0.73
16	343.15	1	100	98.02	0.10
17	363.15	4.5	100	96.34	1.00

Table S5.9. ANOVA analysis of Box-Behnken design.

	Sum of Squares	df [a]	Mean Square	*F*-value	*p*-value[b]	R^2	Adjusted R^2
ANOVA for quadratic model of solid fraction response							
Model	894.34	9	99.37	6.80	0.0097	**0.8974**	**0.7655**
Temperature	197.21	1	197.21	13.50	0.0079		
Time	167.81	1	167.81	11.49	0.0116		
ES concentration	235.88	1	235.88	16.15	0.0051		
Temperature x Time	0.5700	1	0.5700	0.0390	0.8490		
Temperature x ES concentration	172.53	1	172.53	11.81	0.0109		
Time x ES concentration	49.77	1	49.77	3.41	0.1074		
$Temperature^2$	20.49	1	20.49	1.40	0.2749		
$Time^2$	7.72	1	7.72	0.5282	0.4909		

ES concentration^2	42.08	1	42.08	2.88	0.1335		
Residual	102.26	7	14.61				
Lack of fit	81.57	3	27.19	5.26	0.0713		
Pure Error	20.68	4	5.17				
Cor Total	996.59	16					
ANOVA for quadratic model of precipitated lignin response							
Model	16.38	9	1.82	14.01	0.0011	**0.9474**	**0.8798**
Temperature	5.27	1	5.27	40.52	0.0004		
Time	2.10	1	2.10	16.17	0.0050		
ES concentration	4.43	1	4.43	34.06	0.0006		
Temperature x Time	0.5041	1	0.5041	3.88	0.0895		
Temperature x ES concentration	2.24	1	2.24	17.20	0.0043		
Time x ES concentration	0.4225	1	0.4225	3.25	0.1143		
Temperature^2	1.41	1	1.41	10.85	0.0132		
Time^2	0.0411	1	0.0411	0.3160	0.5915		
ES concentration^2	0.0041	1	0.0041	0.0316	0.8638		
Residual	0.9095	7	0.1299				
Lack of fit	0.7649	3	0.2550	7.05	0.0448		
Pure Error	0.1446	4	0.0361				
Cor Total	17.29	16					

[a] df- degrees of freedom; [b] *p*-value < 0.0500 indicate model terms are significant.

Table S5.10. Assignments and integration of the Solid-state ^{13}C NMR spectra of solid fraction-PA:U(2:1)+25PTSA and kraft pulp.[122–124,127]

Assignment (spectroscopy range) / ppm	**Integration**	
	Kraft pulp	Solid fraction-PA:U(2:1)+25PTSA
CH$_3$–COO– Carbohydrate (δ_C, 27)	0.24	0.12
Ar–O**C**H$_3$, –O**C**H$_3$ Lignin and carbohydrate (δ_C, 56)	ND[a]	0.13
–**C**H$_2$OH C-6: carbohydrate (δ_C, 62-65)	**0.89**	**0.90**
–**C**HOH– C-2,3,5: carbohydrate (δ_C, 72) –**C**HOH– C-2,3,5: carbohydrate (δ_C, 75)	**2.78**	**2.98**
–**C**$_\beta$–OR Lignin (δ_C, 84)	ND[a]	ND[a]
–**C**HOH– C-4: carbohydrate (δ_C, 84)	**0.47**	**0.51**
–**C**HOH– C-4: carbohydrate (δ_C, 89)	**0.42**	**0.40**
–**C**H– C-1: carbohydrate (δ_C, 105)	1	**1**

–quaternary C S-1 (ne), S-4 (ne), G-1 (e): lignin (δ_C, 134)	ND[a]	0.02
–quaternary C S-1 (e), S-4 (e), G-1 (e): lignin (δ_C, 137)	ND[a]	0.02
–quaternary C S-3 (ne), S-5 (ne), G-1, G-4: lignin (δ_C, 148)	ND[a]	0.02
–quaternary C S-3 (e), S-5 (e): lignin (δ_C, 153)	ND[a]	0.05
–**C**OO–R, CH_3–**C**OO– Carbohydrate (δ_C, 177)	ND[a]	0.01

(e), etherified units in C-4; (ne), non—etherified units in C-4 (phenolic); [a] ND, not detected

Table S5.11. Assignments and quantification (number/C_9) of the linkages and functional groups of acetylated lignin-PA:U(2:1)+25PTSA and technical lignins (kraft and dioxane) identified by ^{1}H NMR spectroscopy in $CDCl_3$.[27,111,112,115]

Assignment (spectroscopy range) / ppm	**Amount / (number/ C_9)**		
	Dioxane lignin	Kraft lignin	lignin-PA:U(2:1)+25PTSA
aliphatic -CH_2 and -CH_3 (δ_H, 0.7-1.5)	0.94	0.66	1.53
aliphatic OH, -$OCOH_3$ aliphatic (δ_H, 1.5-2.2)	**3.61**	**2.86**	**2.27**
phenolic OH, -$OCOH_3$ phenolic (δ_H, 2.2-2.5)	**0.74**	**1.98**	**1.15**
H_β in β-β structures (δ_H, 3.0-3.2)	ND[b]	0.15	0.04
aromatic -OCH_3 (δ_H, 3.2-4.1)	1.73[a]	1.38[a]	1.24[a]
H_α in β-5 structure (phenilcoumaran) and H_α in α-O-4 structures (δ_H, 4.9-5.6)	0.07	ND[b]	0.22
H_α in β-O-4 structures without C_α=O and H_α in β-1structures (δ_H, 5.7-6.2)	**0.41**	**0.12**	**0.15**
H in aromatic ring (δ_H, 6.2-8.0)	**1.63**	**1.25**	**1.15**
H in C_β in non-conjugated aldehyde groups (δ_H, 9.3-9.5)	0.002	ND[b]	0.22
H in carbonyl group in Cɣ and conjugated cinnamaldehyde-type structures (δ_H, 9.5-9.7)	0.005	ND[b]	ND[b]
H in carbonyl group in benzaldehyde-type structures (δ_H, 9.7-10)	0.013	0.003	ND[b]

[a] Data obtained by quantitative ^{13}C NMR spectroscopy (Table S5.12); [b]ND, not detected.

Table S5.12. Assignments and quantification (number/aromatic group C_6) of the linkages and functional groups of lignin-PA:U(2:1)+25PTSA and technical lignins (kraft and dioxane) identified by ^{13}C NMR spectroscopy in DMSO-d_6.[27,111,112,115]

Assignment (spectroscopy range) / ppm	**Amount / (number/aromatic group C_6)**		
	Dioxane lignin	Kraft lignin	lignin-PA:U(2:1)+25PTSA
aliphatic -CH_2 and -CH_3 (δ_C, 10-33)	0.24	0.12	0.08
C_β in tetrahydrofuran structures (δ_C, 46-50.1)	0.06	0.06	ND[a]
C_β in β-5 and β-β structures (δ_C, 52.5-54)	0.11	0.06	ND[a]
aromatic -OCH_3 (δ_C, 54-57)	**1.73**	**1.38**	**1.23**
C_γ in β-*O*-4 structures without C_α=O (δ_C, 58.5-60.8)	**0.61**	**0.22**	**0.60**
C_γ in β-5 and β-*O*-4 structures with C_α=O; C_γ in β-1 (δ_C, 61.6-64.2)	0.10	ND[a]	ND[a]
C_α in β-*O*-4 structures; C_γ in pinoresinol and β-β structures (δ_C, 69-77)	0.78	ND[a]	0.73
C_β in β-*O*-4 structures; C_α in β-5 and β-β structures (δ_C, 79-90)	0.78	ND[a]	0.75
carbohydrate contaminants (δ_C, 61.6-100)	no	yes	no
aromatic C_{Ar}-H (δ_C, 100-120)	2.03	1.95	2.72
aromatic C_{Ar}-C (δ_C, 120-135)	1.26	1.71	1.27
aromatic C_{Ar}-O (δ_C, 135-160)	2.71	2.34	2.01
C in syringyl unit, S in C_2 and C_6 (δ_C, 102-110)	1.51	1.28	1.18
C in guaiacyl unit, G in C_2, C_5 and C_6 (δ_C, 110-122)	0.52	0.67	0.83
C in *p*-hydroxyphenyl unit, H in C_4 (δ_C, 162-163)	0.01	0.02	ND[a]
CHO in benzaldehyde-type structures (δ_C, 190-191.8)	0.01	0.005	ND[a]
CHO in cinnamaldehyde-type structures (δ_C, 193-194.6)	0.02	0.01	ND[a]
CO in aldehyde and ketones, C_α=O/C_β=O (δ_C, 196.5-203.5)	0.04	0.01	ND[a]
CO in cinnamic acid-type structures (δ_C, 166-167)	0.01	0.01	ND[a]
CO C_α=O, carboxyl (δ_C, 207-209.5)	0.02	ND[a]	ND[a]
DC[b] %	**14.84**	**30.08**	**31.23**
S:G:H ratio	**81:18:1**	**73:25:2**	**68:32:0**

[a] ND, not detected; [b]DC, Degree of condensation.[116]

S6. Experimental data – Chapter IV

Table S6.1. Design of 50 wt % aqueous solutions of ternary ES (NaPTS:PTSA:[Ch]Cl) for *E. globulus* wood delignification at 363.15 K, 8 h and atmospheric pressure.

Yields / wt %	Solid fraction ± σ	Precipitated lignin ± σ
Individual components		
NaPTS	92.95 ± 1.64	1.16 ± 0.21
PTSA	43.07 ± 0.24	13.55 ± 0.80
[Ch]Cl	93.23 ± 1.04	1.37 ± 0.37
Binary mixtures		
NaPTS:PTSA (0.5:0.5)	47.12 ± 3.22	12.36 ± 0.37
NaPTS:[Ch]Cl (0.5:0.5)	94.50 ± 0.26	1.33 ± 0.02
PTSA:[Ch]Cl (0.5:0.5)	46.41 ± 0.88	15.38 ± 0.59
Ternary mixtures		
NaPTS:PTSA:[Ch]Cl (0.33:0.33:0.33)[a]	50.98 ± 1.53	15.40 ± 2.31
NaPTS:PTSA:[Ch]Cl (0.66:0.17:0.17)	49.12 ± 1.71	8.70 ± 1.01
NaPTS:PTSA:[Ch]Cl (0.17:0.68:0.17)	42.56 ± 3.26	19.49 ± 1.29
NaPTS:PTSA:[Ch]Cl (0.17:0.17:0.65)	52.40 ± 2.20	13.84 ± 0.87
NaPTS:PTSA:[Ch]Cl (0.393:0.376:0.232)[b]	40.86 ± 2.95	11.37 ± 0.18

σ, standard deviation; [a]Central point (CP); [b]Optimal point (OP).

Table S6.2. ANOVA analysis of ternary mixture design. Data obtained using simplex-centroid design method.

	Sum of Squares	df [a]	Mean Square	*F*-value	*p*-value[b]	R^2	Adjusted R^2
ANOVA for quadratic model of solid fraction response							
Model	5.85E-08	5	1.17E-08	17.87	0.0015	**0.9371**	**0.8846**
Linear Mixture	4.89E-08	2	2.44E-08	37.35	0.0004		
NaPTS:PTSA	4.28E-09	1	4.28E-09	6.54	0.0431		
NaPTS:[Ch]Cl	3.21E-10	1	3.21E-10	0.4906	0.5099		
PTSA:[Ch]Cl	3.95E-09	1	3.95E-09	6.03	0.0494		
Residual	3.92E-09	6	6.54E-10				
Lack of fit	3.91E-09	4	9.79E-10	181.95	0.005		
Pure Error	1.08E-11	2	5.37E-12				
ANOVA for special cubic model of precipitated lignin response							

Model	482.24	6	80.37	26.48	0.0012	**0.9695**	**0.9329**
Linear Mixture	285.93	2	142.97	47.11	0.0006		
NaPTS:PTSA	19.23	1	19.23	6.34	0.0534		
NaPTS:[Ch]Cl	0.0078	1	0.0078	0.0026	0.9615		
PTSA:[Ch]Cl	53.26	1	53.26	17.55	0.0086		
NaPTS:PTSA:[Ch]Cl	22.07	1	22.07	7.27	0.0430		
Residual	15.17	5	3.03				
Lack of fit	14.52	3	4.84	14.80	0.0639		
Pure Error	0.6538	2	0.3269				

[a] df- degrees of freedom; [b] *p*-value < 0.0500 indicate model terms are significant.

Table S6.3. Absorption bands assignment in normalized FTIR spectra of solid fraction-(CP and OP) and kraft pulp.

Kraft pulp / cm^{-1}	CP / cm^{-1}	OP / cm^{-1}	Assignment[117–119]
3316	3324	3334	O-H stretching vibration, -OH groups
2854	2898	2918	C-H stretching vibration in methyl and methylene groups
1650	1646	1646	vibration of water molecules absorbed in cellulose
1590	ND	ND	aromatic skeletal vibration on lignin
1412	1436	1436	stretching and bending vibrations of -CH_2 and -CH and -OH bonds in cellulose
1380	1356	1356	stretching and bending vibrations of -CH_2 and -CH and -OH bonds in cellulose
1346	1322	1322	stretching and bending vibrations of -CH_2 and -CH and -OH bonds in cellulose
1306	1320	1320	stretching and bending vibrations of -CH_2 and -CH and -OH bonds in cellulose
1168	1154	1156	C-O stretching vibration
1118	1106	1112	C-O stretching vibration
1056	1048	1060	C-O stretching vibration
1024	1026	1012	C-O stretching vibration
890	890	890	C-H deformation mode of the glycosidic linkage between the glucose units

ND, not detected; CP-central point; OP-optimal point.

Table S6.4. Absorption bands assignment in normalized FTIR spectra of lignin-(CP and OP) and technical lignins (kraft and dioxane).

Dioxane / cm^{-1}	Kraft pulp / cm^{-1}	CP / cm^{-1}	OP / cm^{-1}	Assignment[110,112,114,120]
3474	3474	3410	3424	O-H stretching vibration, hydroxyl groups in phenolic and aliphatic structures
2932	2932	2942	2900	C-H stretching in methyl, methylene and methoxyl groups -OCH_3
2856	2832	2850	2826	C-H stretching in methoxyl groups -OCH_3
1716	1710	1712	1716	C=O stretching vibration in unconjugated carbonyl/carboxyl group, can be related with the presence of carbohydrate contaminants.
1596	1606	1604	1615	aryl ring stretching, symmetric
1508	1508	1502	1518	aryl ring stretching, asymmetric
1454	1456	1454	1442	C-H bending in O-CH_3 groups, asymmetric
1420	1426	1422	1412	aromatic skeletal vibration coombined with C-H bending in O-CH_3 groups, asymmetric in-plane
1332	1314	1326	1340	syringyl rings breathing with Ar-OCH_3 stretching
1268	1274	1274	1264	guaiacyl rings breathing with Ar-OCH_3 stretching
1212	1210	1216	1234	C-C plus C-O plus C=O stretching
1140	1156	1158	1138	aromatic C-H in-plane deformation guaiacyl-type
1112	1105	1110	1110	aromatic C-H deformation in the syringyl ring
1016	1040	1034	1038	aromatic C-H in-plane deformation in guaiacyl with C-O deformation in the primary alcohols
ND	ND	1012	ND	contamination
920	907	916	916	C-H deformation out-of-plane, aromatic ring
836	836	832	832	C-H deformation out-of-plane, aromatic ring
ND	ND	688	ND	contamination
ND	635	ND	ND	C-S stretching vibration

ND, not detected; CP-central point; OP-optimal point.

Table S6.5. Elemental composition of *E. globulus* lignin-(CP, OP and OP3h).

Lignin samples	C ± σ / %	H ± σ / %	N ± σ / %	S ± σ / %	O ± σ / %
CP	60.82 ± 0.01	5.13 ± 0.22	0.45 ± 0.01	0.42 ± 0.07	33.18 ± 0.31
OP	61.69 ± 0.08	5.23 ± 0.02	0.77 ± 0.04	0.00 ± 0.00	32.32 ± 0.10
OP3h	60.04 ± 0.65	5.38 ± 0.07	0.77 ± 0.01	0.00 ± 0.00	33.81 ± 0.71

C-carbon, H-hydrogen, N-nitrogen, S-sulfur and O-oxygen, without correction of carbohydrate contaminants; σ, standard deviation; CP-central point; OP-optimal point.

Table S6.6. Assignments and qualitative analysis of the linkages and functional groups of acetylated lignin-CP, lignin-OP, lignin-PTSA:[Ch]Cl and dioxane lignin identified by ^{1}H NMR spectroscopy in $CDCl_3$.[27,111,112,115]

Assignment (spectroscopy range) / ppm	**Integral based on C_9**			
	Dioxane lignin	lignin-PTSA:[Ch]Cl (1:1)	lignin-CP	lignin-OP
aliphatic -CH_2 and -CH_3 (δ_H, 0.7-1.5)	0.19	0.10	0.13	0.21
aliphatic OH, -$OCOH_3$ aliphatic (δ_H, 1.5-2.2)	**0.72**	**0.34**	**0.33**	**0.34**
phenolic OH, -$OCOH_3$ phenolic (δ_H, 2.2-2.5)	**0.15**	**0.42**	**0.54**	**0.57**
H_β in β-β structures (δ_H, 3.0-3.2)	ND[a]	ND[a]	ND[a]	ND[a]
aromatic -OCH_3 (δ_H, 3.2-4.1)	1.73[b]	0.89[b]	NQ[c]	NQ[c]
H_α in β-5 structure (phenilcoumaran) and H_α in α-O-4 structures (δ_H, 4.9-5.6)	0.01	0.001	0.01	0.01
H_α in β-O-4 structures without C_α=O and H_α in β-1structures (δ_H, 5.7-6.2)	**0.08**	**0.01**	**0.04**	**0.02**
H in aromatic ring (δ_H, 6.2-8.0)	**0.33**	**0.17**	**0.23**	**0.24**
H in C_β in non-conjugated aldehyde groups (δ_H, 9.3-9.5)	0.0003	ND[a]	0.003	0.001
H in carbonyl group in Cɣ and conjugated cinnamaldehyde-type structures (δ_H, 9.5-9.7)	0.001	ND[a]	0.002	0.001
H in carbonyl group in benzaldehyde-type structures (δ_H, 9.7-10)	0.003	0.001	0.003	0.001

[a] ND, not detected; [b] Data obtained by quantitative ^{13}C NMR spectroscopy (dioxane in Table S5.12 and lignin-PTSA:[Ch]Cl in Table S6.10); [c] NQ, not quantified; CP-central point; OP-optimal point.

Table S6.7. Effect of time on *E. globulus* wood delignification using the optimal ternary mixture aqueous solution at 363.15 K and atmospheric pressure.

Yields / wt %	Solid fraction ± σ	Precipitated lignin ± σ
Time / h		
1	50.56 ± 0.32	10.22 ± 0.65
2	49.84 ± 1.35	8.34 ± 0.26
3	46.60 ± 2.70	12.30 ± 1.90
4	43.11 ± 0.32	13.01 ± 1.88
6	43.78 ± 0.64	7.76 ± 3.51
8	40.86 ± 2.96	11.37 ± 0.18

σ, standard deviation

Table S6.8. Assignments and integration of the Solid-state ^{13}C NMR spectra of solid fraction-OP3h and kraft pulp.[122–124,127]

Assignment (spectroscopy range) / ppm	Integration	
	Kraft pulp	Solid fraction-OP3h
CH_3–COO– Carbohydrate (δ_C, 27)	0.24	ND[a]
Ar–O**C**H_3, –O**C**H_3 Lignin and carbohydrate (δ_C, 56)	ND[a]	ND[a]
–**C**H_2OH C-6: carbohydrate (δ_C, 62-65)	**0.89**	**0.95**
–**C**HOH– C-2,3,5: carbohydrate (δ_C, 72) –**C**HOH– C-2,3,5: carbohydrate (δ_C, 75)	**2.78**	**3.13**
–**C**$_\beta$–OR Lignin (δ_C, 84)	ND[a]	ND[a]
–**C**HOH– C-4: carbohydrate (δ_C, 84)	**0.47**	**0.50**
–**C**HOH– C-4: carbohydrate (δ_C, 89)	**0.42**	**0.47**
–**C**H– C-1: carbohydrate (δ_C, 105)	**1**	**1**

Table S6.9. Assignments and quantification (number/C_9) of the linkages and functional groups of acetylated lignin-PTSA:[Ch]Cl and lignin-OP3h identified by ^1H NMR spectroscopy in $CDCl_3$. [27,111,112,115]

Assignment (spectroscopy range) / ppm	Amount / (number/ C_9)	
	lignin-PTSA:[Ch]Cl	lignin-OP3h
aliphatic -CH_2 and -CH_3 (δ_H, 0.7-1.5)	0.27	1.58
aliphatic OH, -$OCOCH_3$ aliphatic (δ_H, 1.5-2.2)	**0.91**	**1.41**
phenolic OH, -$OCOCH_3$ phenolic (δ_H, 2.2-2.5)	**1.12**	**1.87**
H_β in β-β structures (δ_H, 3.0-3.2)	ND[b]	ND[b]
aromatic -OCH_3 (δ_H, 3.2-4.1)	**0.89**[a]	**1.42**[a]
H_α in β-5 structure (phenilcoumaran) and H_α in α-O-4 structures (δ_H, 4.9-5.6)	0.003	ND[b]
H_α in β-O-4 structures without C_α=O and H_α in β-1structures (δ_H, 5.7-6.2)	**0.02**	**0.13**
H in aromatic ring (δ_H, 6.2-8.0)	**0.44**	**1.28**
H in C_β in non-conjugated aldehyde groups (δ_H, 9.3-9.5)	ND[b]	ND[b]
H in carbonyl group in Cγ and conjugated cinnamaldehyde-type structures (δ_H, 9.5-9.7)	ND[b]	ND[b]
H in carbonyl group in benzaldehyde-type structures (δ_H, 9.7-10)	0.003	ND[b]

[a] Data obtained by quantitative ^{13}C NMR spectroscopy (Table S6.10); [b] ND, not detected.

Table S6.10. Assignments and quantification (number/aromatic group C_6) of the linkages and functional groups of lignin-PTSA:[Ch]Cl and lignin-OP3h identified by ^{13}C NMR spectroscopy in DMSO-d_6. [27,111,112,115]

Assignment (spectroscopy range) / ppm	**Amount / (number/aromatic group C_6)**	
	lignin-PTSA:[Ch]Cl	lignin-OP3h
aliphatic -CH_2 and -CH_3 (δ_C, 10-33)	0.08	0.05
C_β in tetrahydrofuran structures (δ_C, 46-50.1)	0.07	ND[a]
C_β in β-5 and β-β structures (δ_C, 52.5-54)	0.06	ND[a]
aromatic -OCH_3 (δ_C, 54-57)	**0.89**	**1.42**
C_γ in β-*O*-4 structures without C_α=O (δ_C, 58.5-60.8)	**0.37**	**0.73**
C_γ in β-5 and β-*O*-4 structures with C_α=O; C_γ in β-1 (δ_C, 61.6-64.2)	ND[a]	ND[a]
C_α in β-*O*-4 structures; C_γ in pinoresinol and β-β structures (δ_C, 69-77)	ND[a]	0.22
C_β in β-*O*-4 structures; C_α in β-5 and β-β structures (δ_C, 79-90)	ND[a]	0.15
carbohydrate contaminants (δ_C, 61.6-100)	no	no
aromatic C_{Ar}-H (δ_C, 100-120)	1.51	1.47
aromatic C_{Ar}-C (δ_C, 120-135)	2.13	2.08
aromatic C_{Ar}-O (δ_C, 135-160)	2.36	2.45
C in syringyl unit, S in C_2 and C_6 (δ_C, 102-110)	0.87	0.92
C in guaiacyl unit, G in C_2, C_5 and C_6 (δ_C, 110-122)	0.64	0.56
C in *p*-hydroxyphenyl unit, H in C_4 (δ_C, 162-163)	0.002	0.003
CHO in benzaldehyde-type structures (δ_C, 190-191.8)	0.01	ND[a]
CHO in cinnamaldehyde-type structures (δ_C, 193-194.6)	0.02	0.03
CO in aldehyde and ketones, C_α=O/C_β=O (δ_C, 196.5-203.5)	0.02	0.06
CO in cinnamic acid-type structures (δ_C, 166-167)	ND[a]	ND[a]
CO C_α=O, carboxyl (δ_C, 207-209.5)	0.08	ND[a]
S:G:H ratio	**67:33:0**	**71:29:0**
DC[b]	**82.35**	**82.06**

[a] ND, not detected; [b] DC – Degree of condensation.[116]

SCIENTIFIC CONTRIBUTIONS

From 2015 to 2019

ARTICLE

Related to PhD work

(1) **Belinda Soares**, Daniel J.P. Tavares, José L. Amaral, Armando J.D. Silvestre, Carmen S.R. Freire and João A. P. Coutinho. Enhanced solubility of lignin monomeric model compounds and technical lignins in aqueous solutions of deep eutectic solvents. *ACS Sustain Chem Eng*, 5(5), (**2017**), pp. 4056-4065. DOI: 10.1021/acssuschemeng.7b00053.

(2) **Belinda Soares**, Armando J.D. Silvestre, Paula C. Rodrigues Pinto, Carmen S.R. Freire and João A. P. Coutinho. Hydrotropy and cosolvency in lignin solubilization with deep eutectic solvents. *ACS Sustain Chem Eng*, 7 (14), (**2019**), pp. 12485-12493. DOI: 10.1021/acssuschemeng.9b02109.

(3) **Belinda Soares**, André M. da Costa Lopes, Armando J.D. Silvestre, Paula C. Rodrigues Pinto, Carmen S.R. Freire and João A. P. Coutinho. Wood delignification with deep eutectic solvents. *Green Chem.* (**2019**). Submitted 6/9/2019.

(3) **Belinda Soares**, Armando J.D. Silvestre, Paula C. Rodrigues Pinto, Carmen S.R. Freire and João A. P. Coutinho. Improvements on wood delignification with ternary deep eutectic solvents (**2019**). Under preparation.

In collaborations

(1) Catarina F. Araujo, João A.P. Coutinho, Mariela M. Nolasco, S.F. Parker, Paulo J.A. Ribeiro-Claro, S. Rubic, **Belinda Soares** and P.D. Vaz. Ineslastic neutron scattering study of reline: shedding light on the Hydrogen bonding network of deep eutectic solvents. *Phys Chem Phys*, 19(27), (**2017**), pp. 17998-18009. DOI: 10.1039/C7CP01286A.

(2) Emanuel A. Crespo, João M. L. Costa, André M. Palma, **Belinda Soares**, M. Carmen Martín. José J. Segovia, Pedro J. Carvalho, João A. P. Coutinho. Thermodynamic characterization of deep eutectic solvents at high pressures. *Fluid Phase Equilibria*, 500 (**2019**) 112249. DOI: 10.1016/j.fluid.2019.112249.

REVIEW

Belinda Soares, Helena Passos, Carmen S.R. Freire, João A.P. Coutinho, Armando J.D. Silvestre and Mara G. Freire. Ionic liquids in chromatographic and electrophoretic techniques: toward additional improvements on the separation of natural compounds. *Green Chem*, 18 (**2016**), pp. 4582 – 4604. DOI: 10.1039/c6gc01778a.

CONFERENCES

Poster presentation

(1) **Belinda Soares**, Carmen S.R. Freire, José L. Amaral, Mara G. Freire, Armando J.D. Silvestre, João A.P. Coutinho. Solubility of lignin precursors in aqueous solution of deep eutectic solvents. *Iberoamerican Meeting on Ionic Liquids – IMIL*, Madrid, Spain, 2-3 July **2015**. DOI: 10.1055/s-0034-1394529.

(2) **Belinda Soares**, José L. Amaral, Mara G. Freire, Armando J.D. Silvestre, Carmen S.R. Freire, João A.P. Coutinho. Evaluation of deep eutectic solvent potential to selectively extract lignin from *Eucalyptus globulus* wood. *European Workshop on Lignocellulosics and Pulp* -EWLP, Autrans, France, 28 June to 1 July **2016**.

(3) **Belinda Soares**, Paula C.R. Pinto, Armando J.D. Silvestre, Carmen S.R. Freire, João A.P. Coutinho. Remarkable performance of deep eutectic solvents aqueous solutions on lignin solubilization and *Eucalyptus* wood delignification. *CICECO Meeting*, University of Aveiro, Portugal, 11-12th June **2018.**

(4) **Belinda Soares**, André M. da Costa Lopes, Paula C.R. Pinto, Armando J.D. Silvestre, Carmen S.R. Freire, João A.P. Coutinho. Delignification of *Eucalyptus globulus* wood using DES aqueous solutions. *European Workshop on Lignocellulosics and Pulp* -EWLP, Aveiro, Portugal, 26-28 June **2018**.

(5) **Belinda Soares**, André M. da Costa Lopes, Armando J. D. Silvestre, Paula C. Rodrigues Pinto, Carmen S. R. Freire and João A. P. Coutinho. Remarkable performance of deep eutectic solvents aqueous solutions on lignin solubilization and wood delignification. *13th International Chemical and Biological Engineering Conference (CHEMPOR 2018)*, Aveiro, Portugal, 2nd to the 4th of October, **2018**.
(6) **Belinda Soares**, Armando J. D. Silvestre, Paula C. Rodrigues Pinto, Carmen S. R. Freire and João A. P. Coutinho. New wood delignification technology using eutectic solvents. *1st International Meeting on Deep Eutectic Systems*, Lisbon, Portugal. June 24-27, **2019**.

Oral presentation

(1) **Belinda Soares**, José L. Amaral, Armando J.D. Silvestre, Carmen S.R. Freire and João A.P. Coutinho. Remarkable performance of deep eutectic solvents on technical lignin solubilization. *PATH 2nd Edition Spring Workshop Deep Eutectic Solvents*, Meliã Ria Hotel & Spa, Aveiro, Portugal, 8 June **2017**.
(2) **Belinda Soares**, Paula C.R. Pinto, Armando J.D. Silvestre, Carmen S.R. Freire and João A.P. Coutinho. Fractionation of wood using deep eutectic solvents aqueous solutions. *PATH 3nd Edition Spring Workshop Multibiorefinery.* Meliã Ria Hotel & Spa, Aveiro, Portugal, 8 June **2018**.
(3) **Belinda Soares**, Paula C.R. Pinto, Armando J.D. Silvestre, Carmen S.R. Freire and João A.P. Coutinho. Selective biomass fractionation using eutectic solvents. *PATH 4th Edition Spring Workshop Deeping in the Eutectic Mixtures & Polymers.* University of Aveiro, Aveiro, Portugal, April 11th **2019**.
(4) **Belinda Soares**, Paula C.R. Pinto, Armando J.D. Silvestre, Carmen S.R. Freire and João A.P. Coutinho. Development of eutectic solvents for the fractionation of wood. Summit *Research.* University of Aveiro, Aveiro, Portugal. July 3-5, **2019**.

PARTICIPATION IN R&D PROJECTS

(1) PT2020-PTDC/AGR-TEC/1191/2014 project. Natural Deep Eutectic Solvents: A platform to Boost *Eucalyptus globulus* and *Quercus suber* cork integrated Biorefineries (**2016 – 2019**).
(2) POCI-01-0145-FEDER-016403 project. MultiBiorefinery – Multi-purpose strategies for broadband agro-forest and fisheries by-products valorization: a step forward for a truly integrated biorefinery (**2016 – 2019**).
(3) PROVIDES (PROcesses for Value added fibers by Innovative Deep Eutectic Solvents) project. Deep Eutectic Solvents for Sustainable Paper Production (**2015 – 2018**). Coordinated by the Institute for Sustainable Process Technology (ISTP).